

DISS. ETH NO. 21028

**Enantioselective Imine Aziridination with Ru/PNNP Catalysts:
a Breakthrough**

A dissertation submitted to

ETH ZURICH

for the degree of

Doctor of Sciences

presented by

AMATA SCHIRA

Dottoressa Magistrale in Scienze Chimiche, Università de gli Studi di Milano

Born on June 6th, 1985

citizen of Isorno (TI)

accepted on the recommendation of

Prof. Dr. Antonio Mezzetti, examiner
Prof. Dr. Christophe Copéret, co-examiner
Prof. Dr. Antonio Togni, co-examiner

Zurich 2013

Ai miei genitori

e

a Marino S. Falco

*We do not retreat from reality,
we rediscover it.*

C. S. Lewis

Acknowledgments

I would sincerely like to thank all the people who helped me during these years.

First, I thank *Prof. Antonio Mezzetti*, who gave me the possibility of working in his group. Thank you for your encouragement in the hard moments and for teaching me a lot, not just about chemistry but, even more important, about life.

I also thank *Prof. Antonio Togni* for being co-supervisor of my dissertation, for giving me the opportunity to work together with his group, and for broadening my chemistry knowledge and perspective.

Thank to *Professor Christophe Copéret*, for co-supervising my thesis, for the stimulating discussions and suggestions.

Thank to René Verel for his patient assistance at the NMR.

Many thanks to all my labmates of the *Mezzetti Group*. Starting from the beginning, a special thank to Marco, for introducing me into the PNNP world. I would also like to acknowledge Christoph for kind help and for the PNNP complexes. Thanks to my students: Amaia and a particularly Joël for the great contribution to the PNNP research. Thanks to Raphael for his kind help and his helpful presence in the lab and to Martino, with whom I definitively spent the best time in the lab.

Thanks to Tina for her friendship, and for sharing unforgettable Panini lunches

Thanks to all the members of the *Togni Group*: Serena, Jamal, Mihai, Raffael K. Aline, Jan(nino) and Jan(none), Michelle, Raphael A., Raphaël R. Esteban, Barbara, Peter, Katrine, Jonas, Elli, Vaclav, Nico, Remo, Philip, Jolanda, Nathalia, and Alex and the *Cvengros group*: Jan(none) and Raul. In particular: Raphael A. and Elly for the nice time in Toulouse, Barbara and Peter for the nice extra chemistry experience; Rino, Remo, Raul, and Alex for their help.

Un grande grazie a Pietro for his very useful advice, a Francesco for discussion and support (since I was a child), a Luca and soprattutto a Ivano for the great company and fantastic time together.

Many thanks to Huriye, Raphael and Dominikus for being always so kind and supportive.

Last but not least, Eva, with whom I shared hopes in the last unforgettable moments, thanks for fantastic discussions, and for sharing motivation and energies.

Then, I absolutely want to thank all the people who stepped besides me during these four years outside the HCI:

Elisabetta, for introducing me to Zurich, Martino and Africa for the amusing, endless evenings we used to spend together, Michele (Miché) for the discovery of the linguistic world, and all the guys who lived in Funkwiesen (Domenico, Alvaro Marcello, and Marco Barcellini) and the guys who live there now (Zeno, Francesco, Simone, Gioele), Jona and Katrina for their special marriage, Paolo Minelli for his oniric visions and his enthusiasm, Elisa for her kindness and company, especially in the last months, Désirée for her being frank, Franco and the Paninaro for the real food and the warm welcome every time.

The Moresis, Rothembergers, Schellenbergs, Fallitis, Casanovas, Maria, Guido and Raffaella, Duarte, and Perrine.

Pepe, for his precious friendly presence.

Francesca, who, day after day, shared life, chocolate and strengths.

My dear Mari and Mari. Without you my life would have been much sadder, thanks for the abundance of joyful moments.

My dearest Ila, for the sincere friendship, help, and encouragement, even after the Knopfler's curse.

Stefania, for our deep, serious, synesthetic, and yellow discussions.

Finally, my beloved adoptive families: the Beniamini (Marta e Andrea) and the Reggiani (Matteo, Maddalena, and Pietro). Thanks for never, never leaving me alone.

Myriam, Daniel, Lambert and Valentine for your special affection

Marta e Matteo, Adriano, Mara, Caterina, Lucia, Giulia, Konzo, Lucilla, Marco, and Lucia for never letting me go.

To conclude, my family: Vera, Paolo, Teodor and my parents, Mariaceleste e Giorgio for being always at my side, *no time, no space, like a bird in the wire.*

Table of Contents

Abstract.....	5
Riassunto.....	8
1. Introduction.....	11
1.1 Structural Properties.....	11
1.2 Biological Properties.....	12
1.3 Reactivity.....	12
1.3.1 Ring Opening.....	13
1.3.2 Cycloaddition.....	18
1.3.3 Ring Expansion.....	19
1.4 Synthesis of Aziridines.....	20
1.4.1 Catalytic Aziridination by Nitrene Transfer to Olefins.....	21
1.4.2 Carbene Transfer to an Imine.....	28
1.4.2.1 α -Haloenolesters as Carbenoid Sources.....	28
1.4.2.2 Sulfur Ylides as Carbenoid Sources.....	30
1.4.2.3 Diazocompounds as Carbenoid Sources.....	32
1.4.2.3.1 Acidic Activation of the Imine and its Reaction with a Diazoalkane.....	32
1.4.2.3.2 Reaction of a Metal Carbene Intermediate with the Free Imine...37	
1.4.2.4 General Features of Catalytic Imine Aziridination.....	39
1.5 Imine Aziridination with Ru /PNNP Complexes.....	40
1.5.1 Structural Properties of Ruthenium(II) Dichloro PNNP Complexes.....	41
1.5.2 Dicationic Ru/PNNP Complexes.....	42
1.5.3 Monocationic Ru/PNNP Complexes.....	43
1.5.4 Asymmetric Imine Aziridination.....	47
1.5.4.1 Preliminary Studies: Olefin Aziridination.....	47
1.5.4.2 Imine Aziridination.....	49
1.5.4.3 Spectroscopic Studies and Mechanistic Considerations.....	53

1.6	Macrocyclic PNNP Ligands.....	56
1.7	Rationale of the Project	58
2.	Substituted PNNP Ligands for Ru-Catalyzed Imine Aziridination	60
2.1	[RuCl(OEt ₂)(PNNP)]PF ₆ as Catalyst: New Substituted Ligands.....	61
2.1.1	[RuCl ₂ (PNNP)] Complexes	64
2.1.2	Activation of the Dichloro Complexes [RuCl ₂ (1b-1h)] (2b-2h)	66
2.1.2.1	Temperature Effect	69
2.2	Catalyst Optimization with [RuCl(OEt ₂)(1b)]PF ₆ (3bPF₆)	71
2.2.1	<i>Tert</i> -Butyl Diazoacetate as Carbenoid Source.....	72
2.2.2	Temperature Screening	73
2.2.3	Pressure Effect.....	74
2.2.4	Considerations on the Catalytic Activity of [RuCl(OEt ₂)(1b)]PF ₆	76
2.3	Five-Coordinate [RuCl(1b)]PF ₆ (4aPF₆) as Catalyst.....	77
2.3.1	Temperature and Pressure Effects.....	77
2.3.2	<i>Tert</i> -Butyl Diazoacetate as Carbenoid Source.....	80
2.3.3	NMR Spectroscopic Investigations.....	81
2.3.3.1	[RuCl(1b)]PF ₆ (4bPF₆)	81
2.3.3.2	[RuCl(OEt ₂)(1b)]PF ₆ (3bPF₆).....	85
2.4	Conclusion and Outlook	89
3.	Enantioselective Imine Aziridination: a Breakthrough.....	91
3.1	[RuCl(OEt ₂)(1b)] ⁺ (3b) with Nonhydrolyzable Counterions.....	92
3.1.1	Synthesis of the Meerwein Salts.....	92
3.1.2	[RuCl(OEt ₂)(1b)]BF ₄ (3bBF₄)	92
3.1.3	Catalytic Aziridination with [RuCl(OEt ₂)(1b)]BF ₄	94
3.1.3.1	Preliminary Tests	94
3.1.3.2	Optimization of Catalyst 3bBF₄	96
3.1.4	[RuCl(OEt ₂)(1b)]SbF ₆ (3bSbF₆).....	98
3.1.5	[RuCl(OEt ₂)(1a)]X (3aX) (X = BF ₄ , SbF ₆).....	99
3.1.6	Substrate Screening	101

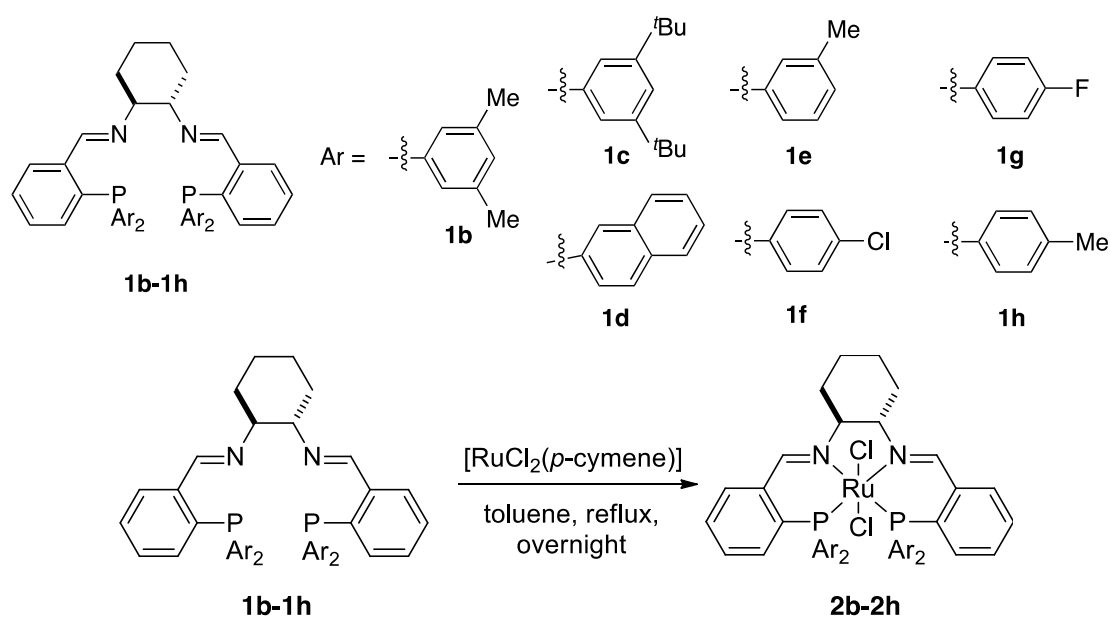
3.2	Mechanistic Investigations	103
3.2.1	Trapping Test with Diethyl Fumarate	103
3.2.2	Competition Experiments with [RuCl(OEt ₂)(1b)]BF ₄ (3b BF ₄)	104
3.2.3	Considerations on the Diazoester Complex	109
3.2.4	The Role of Carbene Nucleophilicity	113
4.	Latest Studies on the Synthesis of New Chiral P ₂ N ₂ Macrocycles of C ₂ -Symmetry	121
4.1.	Introduction	122
4.1.1	P ₂ N ₂ Macrocycles	122
4.1.2	C ₁ -Symmetric PNNP Macrocycles	124
4.1.3	Chiral Phosphines with Stereogenic Phosphorus	125
4.2	C ₂ - Symmetric Macrocycles: New Attempts	133
4.2.1	Cyclization by Condensation	122
4.2.2	Cyclization by Substitution	137
4.2.3	Secondary Diphosphines With a Chiral Backbone	139
4.2.3.1	Cleavage of the P–Ph Bond with Lithium Metal	140
4.2.3.2	Reaction of KPPhH with the Corresponding Tosyl Derivative	142
4.2.3.3	Reaction of the Deprotonated Primary Diphosphine with a Chiral Tosyl Derivative	143
4.2.4	Doubly Bridged Diphosphines	147
4.3	Conclusion and Outlook	148
5.	Conclusion and Outlook	151
6.	Experimental Part	154
6.1	General	154
6.1.1	Techniques and Instrumentation	154
6.2	Catalyst	155
6.2.1	Precursors	155
6.2.2	PNNP Ligands	157
6.2.3	Ru/PNNP Complexes	161
6.3	Ru/PNNP Catalyzed Asymmetric Imine aziridination	164

6.3.1	Imine aziridination	164
6.3.2	Synthesis of Imines	165
6.3.3	NMR experiments.....	174
6.4	PNNP Macrocycles.....	176
7.	References.....	179

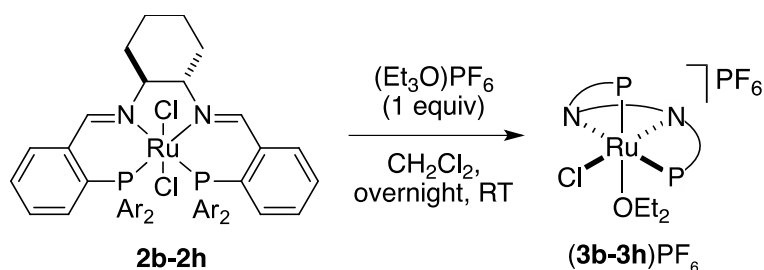
Abstract

This thesis is focused on the asymmetric imine aziridination with open-chain and cyclic Ru/PNNP complexes. On the basis of previous mechanistic studies performed in our group, we investigated the possibility of controlling the chemoselectivity of the reaction by increasing either the steric bulk or the rigidity of the PNNP ligands.

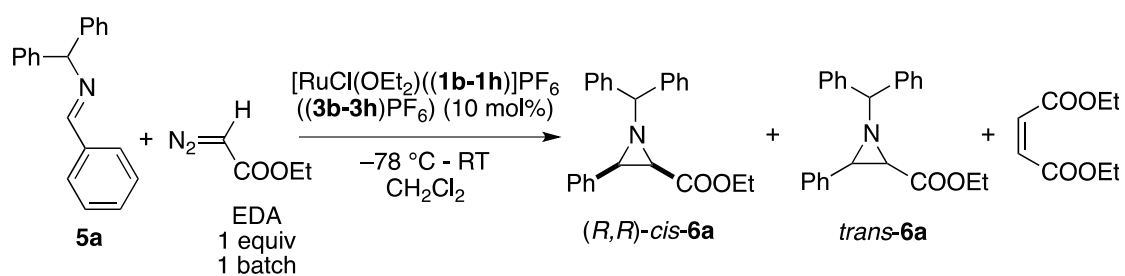
Firstly, a series of new open-chain PNNP ligands with a substitution pattern on the *meta* and *para* positions of the phenyl rings was prepared.



The catalytically active ether adducts $[\text{RuCl}(\text{OEt}_2)(\text{PNNP})]^+$ (**3a-3h**) were obtained by treatment of **2b-2h** with $(\text{Et}_3\text{O})\text{PF}_6$:



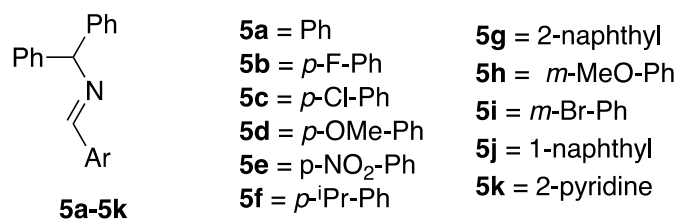
The six-coordinate **(3b-3h)PF₆** were tested in the catalytic aziridination of imine **5a** with ethyl diazoacetate (EDA) under a very strict temperature protocol (-78°C - RT):



In the case of ligand ((1*S*,2*S*)-*N,N'*-bis{2-[bis(3,5-dimethylphenyl)phosphino]-benzylidene}-cyclohexane-1,2-diamine (**1b**), imine **5a** gave aziridine *cis-6a* in a very high yield (80%) but nearly no enantioselectivity (3% ee). It was also observed that complex **3bPF₆** catalyzed the reaction also at constant temperature (0 °C), giving *cis-6a* with 55% yield, but still low enantioselectivity (13% ee). Finally, it was found out that, under the reaction conditions, the PF₆⁻ ion hydrolyzed to give an acid species that catalyzes a nonenantioselective aza-Darzens reaction between imine **5a** and EDA, which explains the high yield and low enantioselectivity.

Hence, chloride scavengers with nonhydrolyzable anions ((Et₃O)BF₄ and (Et₃O)SbF₆) were screened. With $[\text{RuCl}(\text{OEt}_2)(\mathbf{1b})]\text{BF}_4$ (**3bBF₄**) as catalyst under optimized conditions, imine **5a** reacted with an excess of EDA (4 equiv) to give aziridine (R,R) -**6a** with 39% yield and high enantioselectivity (93% ee). To our knowledge, this is the highest enantioselectivity obtained with a transition metal catalyst.

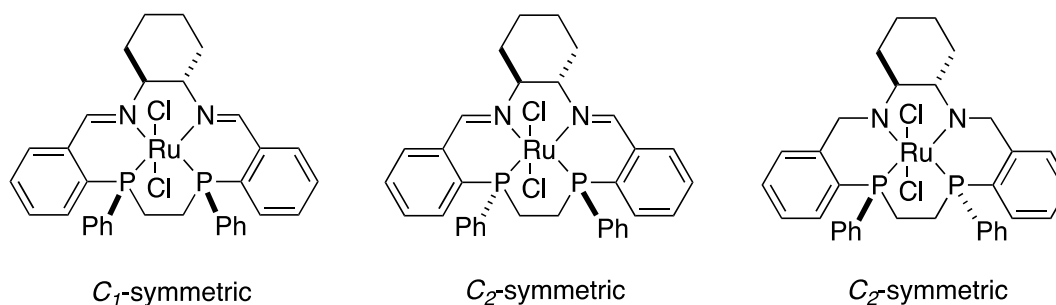
The scope of the catalyst was briefly tested. With all substituted imines **5b-5k**, the enantioselectivity was lower than with **5a** (24 - 0% ee).



Additionally, the electronic effects of substituents were studied with competition experiments performed with 4-substituted-*N*-benzylidene-anilines.

The catalytic activity of the five-coordinate species $[\text{RuCl}(\mathbf{1b})]\text{PF}_6$ ($\mathbf{4bPF}_6$) was also investigated. The catalyst was prepared from chloride abstraction with TlPF_6 (1 equiv) and a complete screening of the reaction conditions was performed, included the use of another carbene source (*tert*-butyl diazoacetate), but generally a low enantioselectivity was observed.

The last chapter describes attempts of preparing chiral C_2 -symmetric PNNP macrocycles. They are potentially interesting for asymmetric aziridination, as they are analogous to open-chain P_2N_2 ligands and are expected to form stable and conformationally rigid complexes. The synthetic targets were C_2 -symmetric analogues of the C_1 -symmetric macrocycle that has been prepared previously in our group.

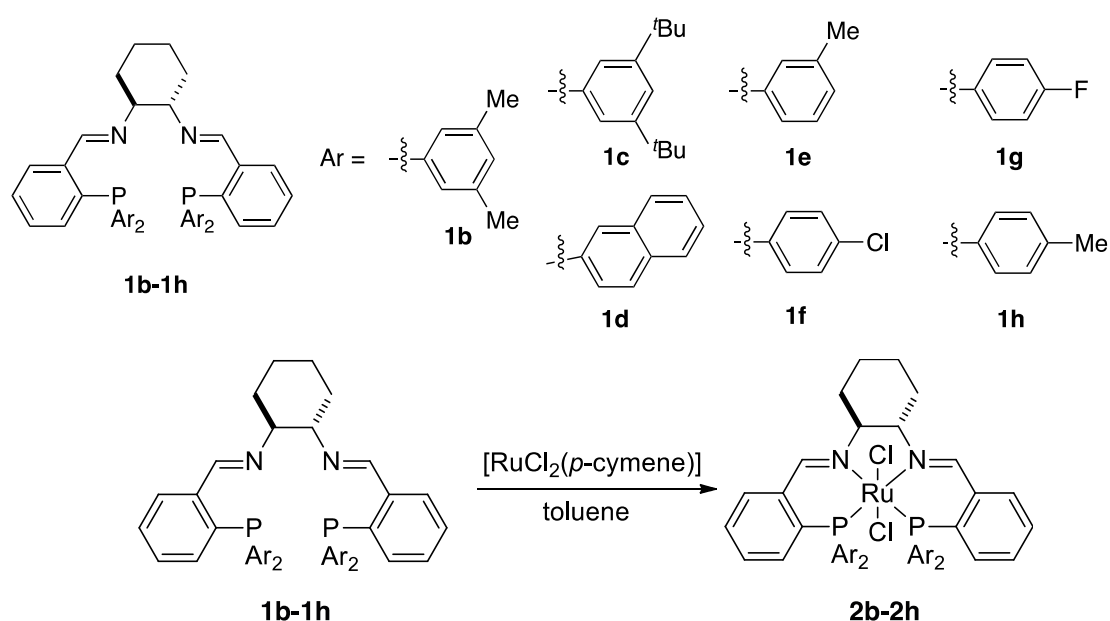


The strategies developed to prepare C_2 -symmetric PNNP macrocycles and the difficulties encountered will be presented. Different approaches to control the stereochemistry at the phosphorus have been tested focusing in introducing stereogenic centers on the molecule before the final cyclization step. However, all the attempts failed, as no selective reaction to give the desired C_2 -symmetric cycle occurred and the C_1 -symmetric isomer was formed predominantly.

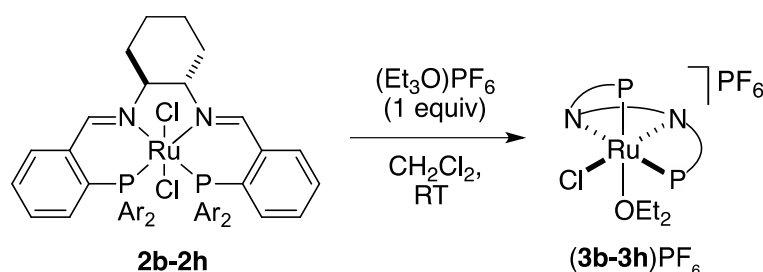
Riassunto

Questa tesi è incentrata sull'aziridinazione asimmetrica di imine con complessi di rutenio con leganti PNNP a catena aperta e ciclici. Sulla base di studi meccanicistici condotti in precedenza nel nostro gruppo di ricerca, abbiamo indagato sulla possibilità di controllare la chemoselettività della reazione aumentando sia l'ingombro sterico, sia la rigidità dei leganti PNNP.

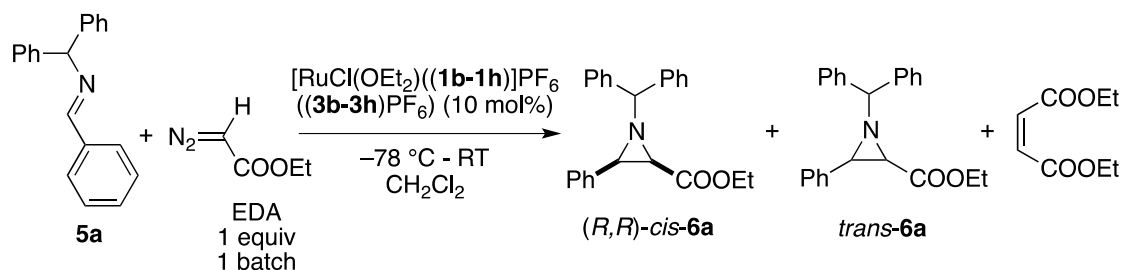
Innanzitutto, si è preparata una serie di nuovi leganti PNNP a catena aperta, che presentano sostituenti nelle posizioni *meta* e *para* degli anelli fenilici.



Gli etere addotti cataliticamente attivi $[RuCl(OEt_2)(PNNP)]^+$ (**3a-3h**) sono stati ottenuti trattando i complessi **2b-2h** con $(Et_3O)PF_6$.



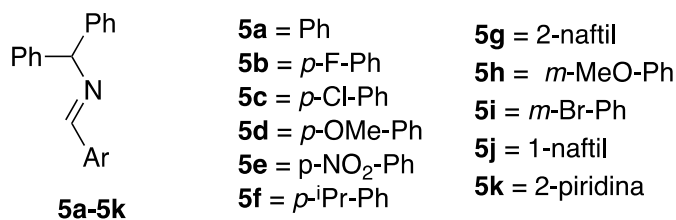
I complessi esacoordinati (**3b-3h**)PF₆ sono stati testati nell'aziridinazione catalitica dell'imina **5a** con etil diazoacetato (EDA), usando condizioni di temperatura strettamente controllate (-78 - RT):



Nel caso del complesso (1*S*,2*S*)-*N,N'*-bis{2-[bis(3,5-dimetilfenil)fosfino]-benzilidene}-cicloesano-1,2-diamina (**1b**), l'imina **5a** dà l'aziridina **6a** in rese molto alte (80%) ma con enantioselettività quasi nulla (3% ee). Si è anche osservato che il complesso **3b**PF₆ catalizza la reazione anche a temperatura costante (0 °C), dando *cis*-**6a** con resa del 55%, ma con enantioselettività ancora bassa (13% ee). Infine, si è scoperto che, sotto le condizioni di reazione descritte, l'anione PF₆⁻ idrolizza a dare una specie acida, la quale catalizza una reazione aza-Darzens non enantioselettiva tra l'imina **5a** e l'EDA, il che spiega l'alta resa e la bassa enantioselettività.

Sono stati, quindi, testati astrattori di cloruro con anioni non idrolizzabili ((Et₃O)BF₄ e (Et₃O)SbF₆). Con [RuCl(OEt₂)(**1b**)]BF₄ (**3b**BF₄) come catalizzatore, in condizioni ottimali, l'imina **5a** reagisce con un eccesso di EDA (4 equiv) a dare l'aziridina (*R,R*)-**6a** con 39% di resa e alta enantioselettività (93% ee). Questa è la più alta enantioselettività mai ottenuta con un catalizzatore basato su un metallo di transizione.

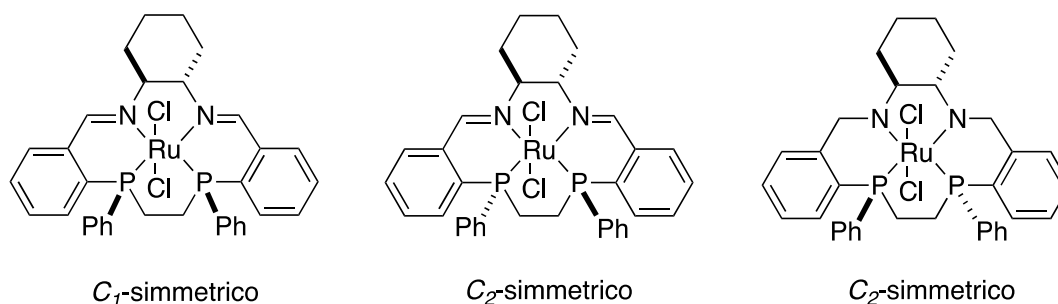
Anche l'ambito di applicazione della reazione è stato testato. Con tutte le imine sostituite (**5b-5k**), l'enantioselettività è più bassa che con **5a** (24 - 0% ee).



Inoltre, gli effetti elettronici dei sostituenti sono stati studiati attraverso esperimenti di competizione effettuati con *N*-benzilidenaniline *para* sostituite.

Si è anche investigata l'attività catalitica del complesso pentacoordinato [RuCl(**1b**)]PF₆ (**4b**PF₆). Il catalizzatore è stato preparato per astrazione di cloruro con TlPF₆ (1 equiv) e uno screening completo delle condizioni di reazione è stato effettuato, incluso l'uso di un'altra fonte di carbene (*tert*-butil diazoacetato). In tutti questi esperimenti è stata osservata una bassa enantioselettività.

L'ultimo capitolo descrive i tentativi di preparare macrocicli PNNP chirali con simmetria C_2 . Tali leganti sono potenzialmente interessanti per l'aziridinazione asimmetrica, poiché sono analoghi ai PNNP a catena aperta e ci si aspetta che formino complessi stabili e conformazionalmente rigidi. Gli obiettivi sintetici sono stati perciò gli analoghi a simmetria C_2 dei macrocicli di simmetria C_1 già preparati precedentemente nel nostro gruppo.



Le strategie sviluppate per preparare tali leganti PNNP macrociclici con simmetria C_2 verranno presentate. Sono stati tentati diversi approcci volti al controllo della stereochimica al fosforo, attraverso l'introduzione di centri stereogenici nella molecola prima del passaggio finale di ciclizzazione. Comunque, tutti i tentativi sono falliti, poiché la reazione di ciclizzazione non è selettiva verso il prodotto di simmetria C_2 desiderato e l'isomero di simmetria C_1 si forma in modo predominante.

1. Introduction

This first chapter is an introduction into the topic of aziridines, starting from their chemical properties and including their reactivity and literature examples of the state of the art of their catalytic synthesis.

Three membered ring heterocycles containing two carbon and one nitrogen atoms are generally called aziridines. They are an interesting synthetic target as precursors for a wide variety of organic molecules, ranging from N-containing cyclic or acyclic amines, to amino acids by ring-opening reactions.¹ Furthermore, it has been shown that they possess antibiotic and antitumor activities.^{2,3}

The structural properties of aziridines, their general reactivity, and their catalytic synthesis will be described in detail in the following paragraphs.

1.1 Structural Properties

The main structural characteristic of aziridines is the presence of a three membered ring, with one amine group and two methylene groups. The internal angle is close to 60°, far away from the 111.3° of the C-N-C bond angle in the open-chain analogous dimethylamine. In comparison with the open-chain analogue, the ethylenimine possesses short C-C bonds with values similar to C-N bonds.^{4,5}

Spectroscopic studies indicate that the barrier to pyramidal inversion of the nitrogen atom of aziridines is considerably higher than in acyclic amines. The barrier for pyramidal inversion in unsubstituted aziridine is around 82 kJ mol⁻¹. More specifically, the activation enthalpy of the *N*-inversion of 2-methylaziridine is approximately 70 kJ mol⁻¹, which is considerably larger than in a typical secondary amine, but still does not prevent racemization at room temperature. If, however, an electronegative substituent is present on the nitrogen, the inversion barrier increases. For instance, 1-chloro-2-methylaziridine, in which the inversion barrier ΔG^\ddagger is 112 kJ mol⁻¹, can be separated into diastereoisomers that are stable at room temperature. The ring-strain energy of aziridine is similar to that of cyclopropane (113 kJ mol⁻¹), reflecting high bond-angle strain (Figure 1.1).

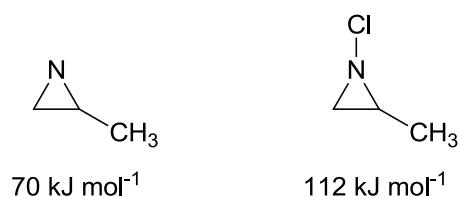


Figure 1.1 Inversion barrier (ΔG^\ddagger) for different substituted aziridines.

The nitrogen lone pair has an increased *s* character, which results in a lower basicity of aziridines in comparison with acyclic amines and in a reduced π donor ability. The conjugate acid of an aziridine has a pK_a value of 7.98, compared to a typical pK_a value of around 11 for the conjugate acid of an acyclic secondary amine.

1.2 Biological Properties

Since aziridines can undergo, for instance, attack from nucleophiles such as the nitrogenous bases of the DNA, they are potentially mutagenic. Therefore, they have been classified as carcinogenic to humans. However, as powerful alkylating agents, aziridines have an inherent *in vivo* potency, often based primarily on toxicity rather than specific activity. Deeper studies identified several classes of aziridine-containing natural products that combine potency with selectivity. The best-known examples thereof are the mitosanes, such as Mitomycin, which has a use as chemotherapeutic agent:^{2,3}

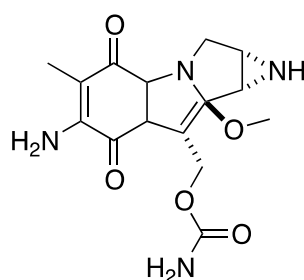


Figure 1.2 Mitomycin C.

1.3 Reactivity

Aziridines are a versatile starting material for a large number of useful applications and many papers and reviews have been published, especially in the last

fifteen years, focusing both on their synthesis and synthetic applications.^{1,6-8}

1.3.1 Ring Opening

Because of the combination of the Bayer ring strain and the electronegativity of the nitrogen atom, aziridines are subject to ring-opening reactions under relatively mild conditions and with a very broad range of substrates.^{1,6-8} The diminished electronegativity of nitrogen as compared to oxygen makes these reactions more difficult than the ring opening of epoxides, but there are still plenty of examples of such chemistry. In the case of aziridines, ring-opening reactions are indeed very useful, since they give access to the regio- and stereoselective installation of different functional groups in a 1,2-relationship to the nitrogen atom.

With respect to ring-opening reactions, aziridines can be classified into two groups, according to the type of substituent present on the nitrogen atom. In the first group, the nitrogen atom is basic, and ring-opening reactions generally occur only after protonation, quaternarization, or formation of a Lewis acid adduct. Therefore, aziridines of this type are considered as ‘nonactivated’:

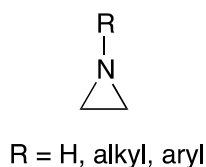


Figure 1.3 Nonactivated aziridines.

On the contrary, the nitrogen atom of ‘activated aziridines’ bears a substituent able to stabilize the negative charge that develops there during the ring opening reaction. Examples of these ‘activated’ aziridines contain carboxylic groups as substituents:

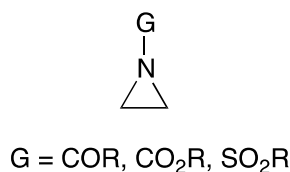
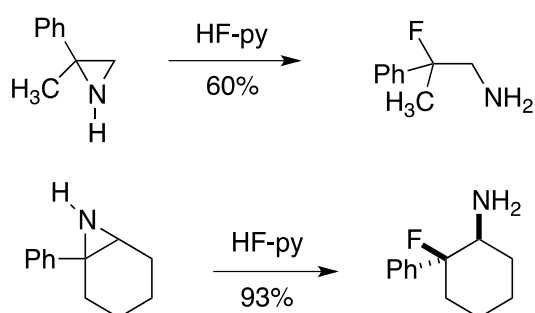


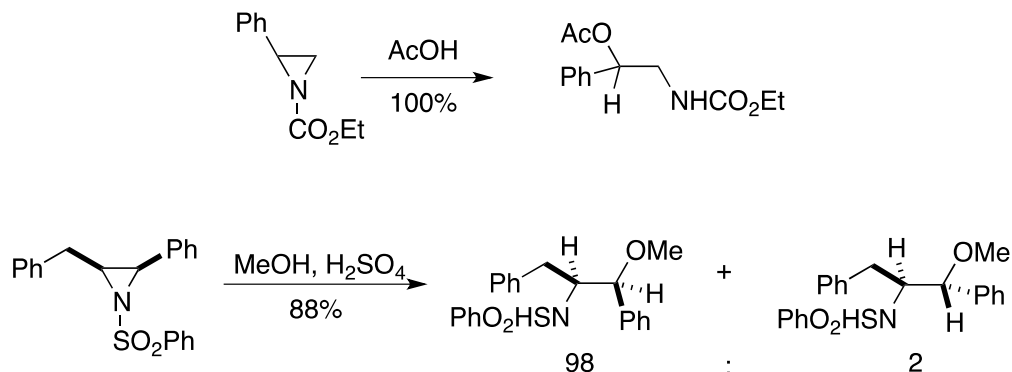
Figure 1.4 Activated aziridines.

N-substitution⁹ increases the ability of the nitrogen atom to function as a leaving group. For instance, Stamm¹⁰ has shown that, in order to carry out the reaction on nonactivated aziridines in the absence of a catalyst, it is imperative that the nucleophile supplies a proton in order to generate a neutral leaving group.

As the detailed mechanism of the acid catalyzed ring-opening reaction of aziridines has been the subject of much debate, we show here only examples both for nonactivated (Scheme 1.1) and activated aziridines (Scheme 1.2).¹¹



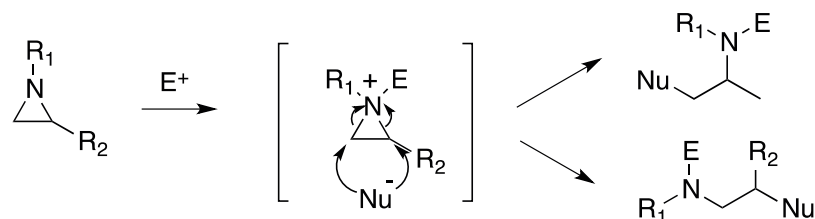
Scheme 1.1 Ring opening reaction for nonactivated aziridines.



Scheme 1.2 Ring opening reaction for activated aziridines.

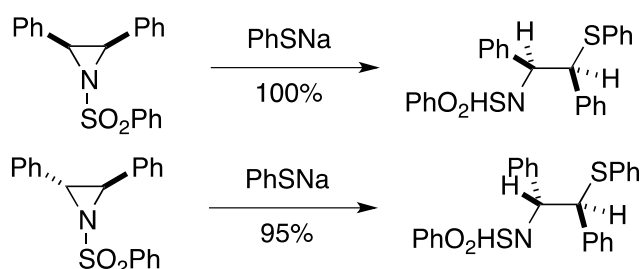
Both protic (HCl, H₂SO₄, TfOH) and Lewis acids (Yb(OTf)₃,^{12,13} cyanocuprates,¹⁴ BF₃(OEt₂),¹⁵⁻¹⁷ tris(pentafluorophenyl)borane)¹⁸ induce the ring opening of activated and nonactivated aziridines, which proceeds regioselectively and in good yields. Nonactivated aziridines have been also reported to undergo ring-opening reactions via aziridinium ions.^{19,20} Common methodologies for this latter approach involve *N*-alkylation, *N*-acylation, *N*-protonation, or *N*-complexation with a

Lewis acid to give a highly electrophilic intermediate, which can be easily opened by different types of nucleophiles:



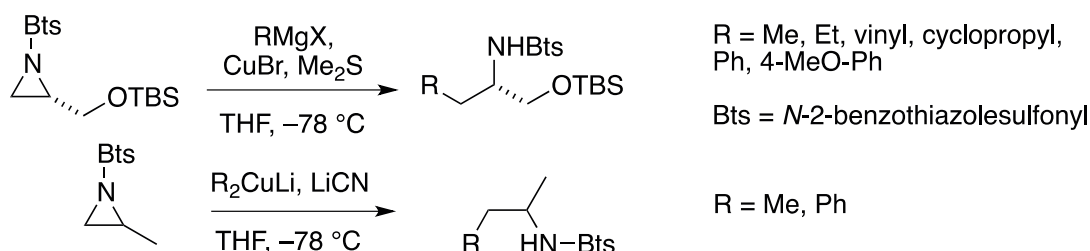
Scheme 1.3 Ring-opening via aziridinium intermediates formation.

The mechanism for the nucleophilic ring opening of activated aziridines bearing an electron-withdrawing group at nitrogen has been studied intensively. As it resulted to be more clear-cut than that for nonactivated species, some generalization can be made. For monocyclic aziridines, nucleophilic attack occurs with an S_N2 -like mechanism involving mainly a Walden inversion of configuration:²¹



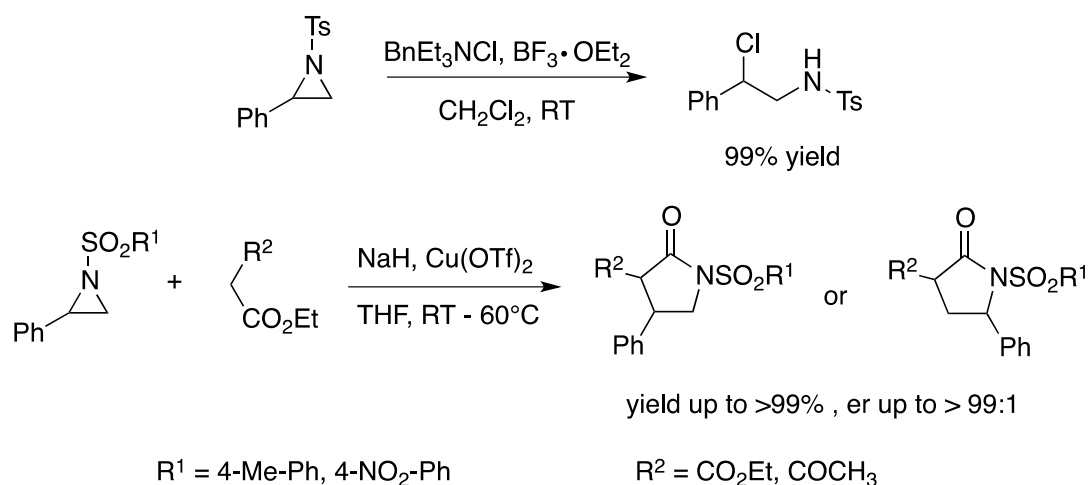
Scheme 1.4 Nucleophilic ring opening reaction.

In most cases, the ring-opening reactions of 2-substituted activated aziridines involves the nucleophilic attack at the less hindered aziridine carbon atom.^{22,23}



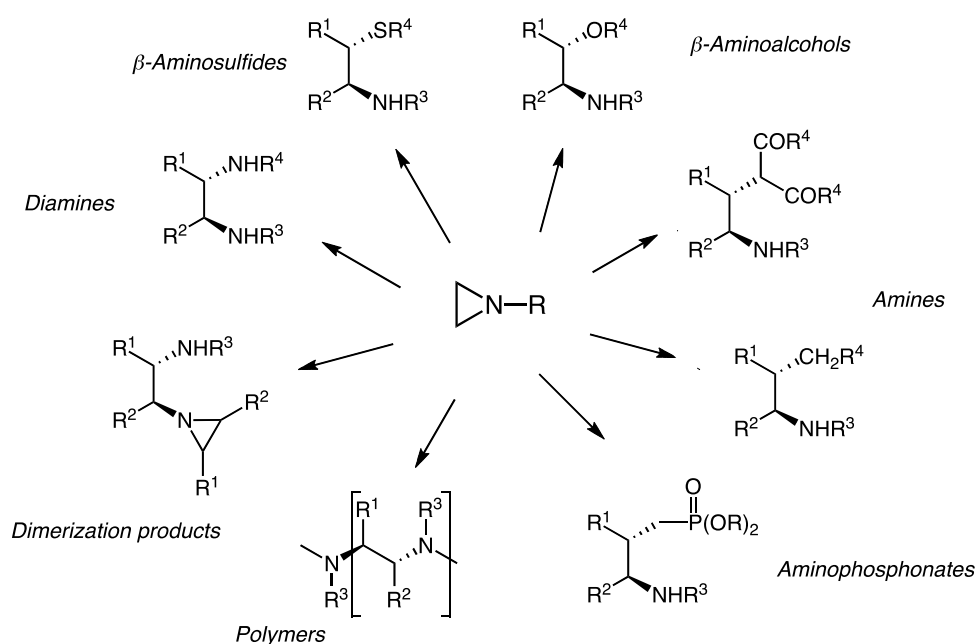
Scheme 1.5 Regioselective nucleophilic ring opening.

In some exceptional cases, the nucleophilic attack involves the sterically disfavored benzylic position of the aziridine moiety.^{24,25}



Scheme 1.6 Nucleophilic attack at the benzylic position.

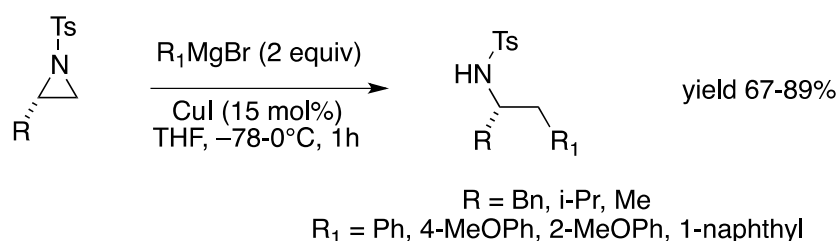
Because regioselective ring-opening reactions of aziridines are a versatile method to prepare a large variety of compounds, different nucleophiles have been used, such as organometallic reagents,²⁶ silyl nucleophiles,²⁷ Wittig reagents,¹³ amines,²⁸ halides,²⁹ and alkenes.¹⁷ The products that can be obtained from ring-opening reactions using different nucleophiles³⁰ are summarized in Scheme 1.7.



Scheme 1.7 Nucleophilic ring-opening reactions.

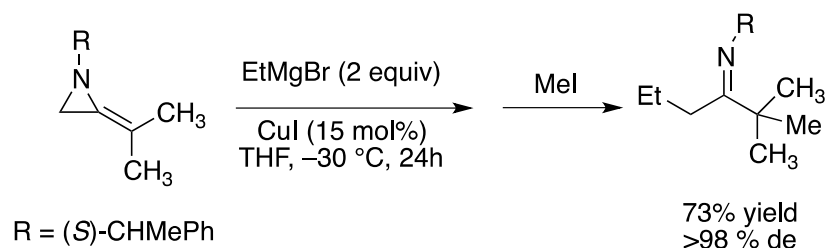
Moreover, Compernolle and co-workers¹⁵ investigated the role of electronic effects. For example, either tosyl aziridine or nosyl aziridine undergo ring opening with the soft nucleophiles malonate and sulfonyl acetonitrile anions in high yields. Harder carbon nucleophiles, such as phenyl and 1,3-dithian-2-yl anions, react with tosyl aziridine relatively faster. Although the nosyl group is considered an excellent activating group that can be more easily removed than the tosyl group, it might not be compatible with strong nucleophiles, which may contribute to the poor chemoselectivity of some reactions.

Most of the reported ring-opening reactions with carbanions require the activation of the aziridine ring by an electron-withdrawing group on the nitrogen. One representative procedure is outlined in Scheme 1.8 using *N*-tosyl aziridines derived from optically active amino acids as effective templates to undergo nucleophilic ring opening by aryl and heteroaryl Grignard reagents. The attack occurs at the unsubstituted ring carbon with high regiocontrol in most examples:³¹



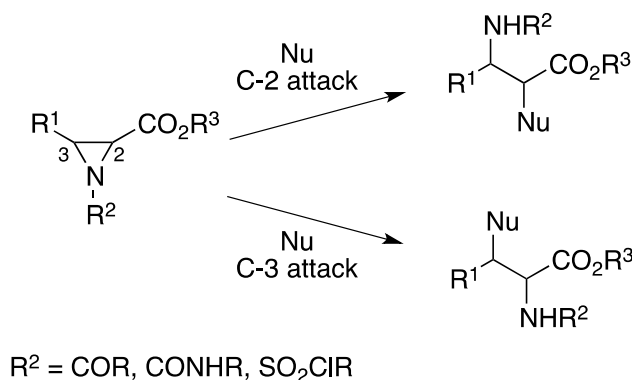
Scheme 1.8 Ring opening reaction of activated aziridines with aryl Grignard reagents.

However, one example was found in the literature describing the ring opening of aziridines without activation, under Grignard nucleophilic addition conditions:³²



Scheme 1.9 Ring opening reaction of nonactivated aziridines with an alkyl Grignard reagent.

Among all the aziridines, aziridine-2-carboxylates are an interesting case, as they can undergo either C-2 attack to give β -amino acid derivatives, or C-3 attack to give α -amino acid derivatives. Their ring opening is promoted by *N*-activation with an electron-withdrawing group (such as acyl, carbamoyl, sulfonyl), Brønsted, or Lewis acids with high stereoselectivity:⁷

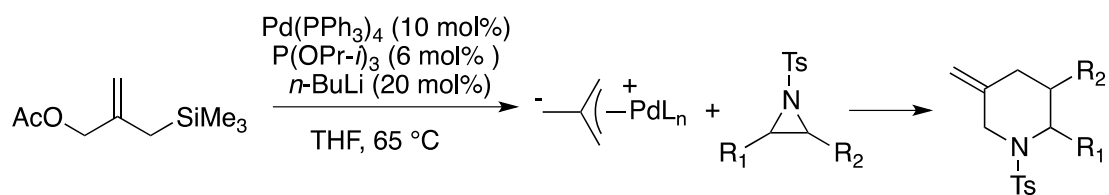


Scheme 1.10 Nucleophilic attack to aziridine-2-carboxylates.

A general preference for the ring opening at the C-3 position was widely observed.⁷ It was proposed that the flexible ester chain protects the C-2 position from the nucleophilic attack. However, when an aryl group is present at the C-2 position, the aziridine undergoes ring opening at the C-2 position, as the cleavage of the benzylic C-N bond is preferred. Moreover, the use of organometallic reagents might be problematic as the competing reaction with the ester moiety reduces the chemoselectivity of the reaction.

1.3.2 Cycloaddition

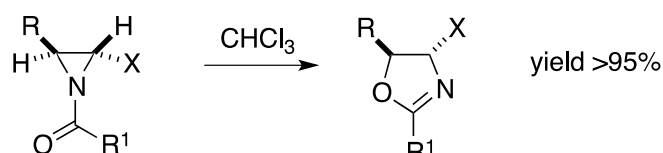
Aziridines are also known to undergo [3+3] cycloaddition reactions. Harrity³³ illustrated the method with a palladium complex of trimethylenemethane (Pd-TMM) generated *in situ*. The enantiomerically pure aziridine undergoes regioselective addition with the Pd-TMM complex at the less hindered site, affording enantiomerically pure piperidine (Scheme 1.11).



Scheme 1.11 Palladium catalyzed [3+3] cycloaddition.

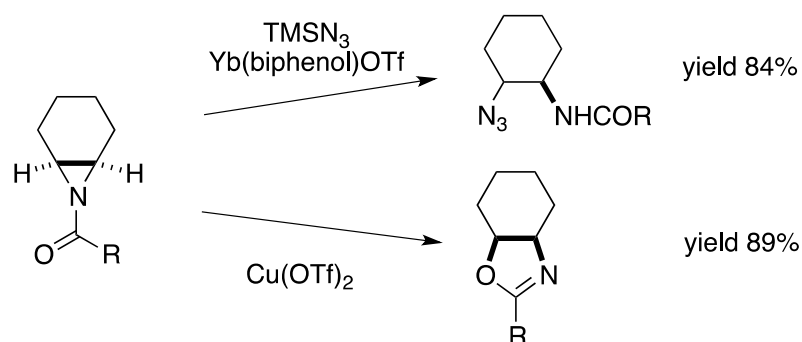
1.3.3 Ring Expansion

Acyl aziridines readily rearrange to oxazolines under thermal, acidic, or nucleophilic conditions,³⁴⁻³⁶ and in some cases with complete regio- and stereocontrol and excellent yields:



Scheme 1.12 Rearrangement of acyl aziridines to oxazolines.

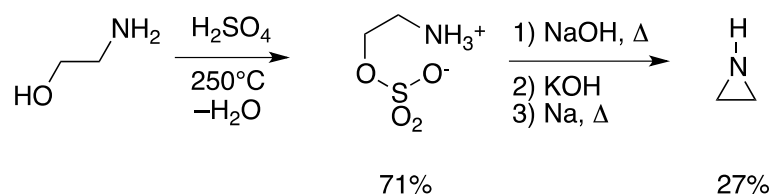
The balance of reactivity between ring opening and rearrangement of acyl-aziridines depends on the nature of the Lewis acid. The oxophilic Lewis acid Y(biphenol)OTf coordinates to the oxygen and activates the aziridine to the nucleophilic attack. On the other hand, the more azaphilic $\text{Cu}(\text{OTf})_2$ is supposed to coordinate to nitrogen and to catalyze the rearrangement to oxazolines:^{37,38}



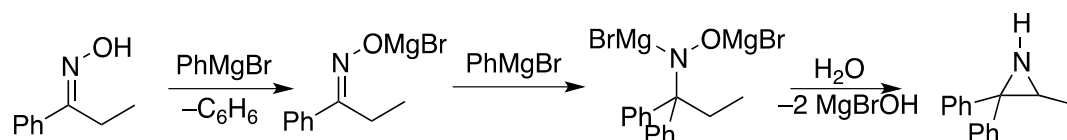
Scheme 1.13 Ring opening reaction with different Lewis acids.

1.4 Synthesis of Aziridines

The first preparation of aziridines dates back to 1888, when Gabriel synthesized the parent member ethyleneimine.³⁹ Since then, Wenker⁴⁰ (Scheme 1.14) and Hoch⁴¹ (Scheme 1.15) have developed many methods to produce racemic aziridines by the ring closing approach.



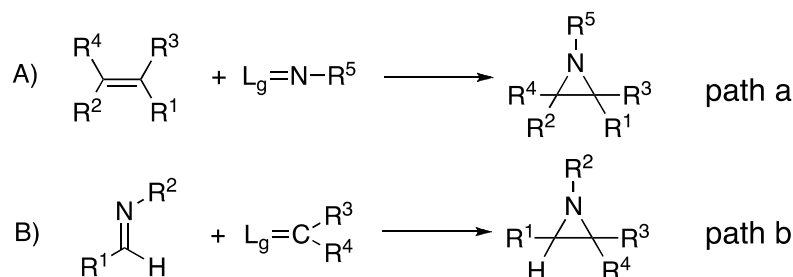
Scheme 1.14 Wenker's synthesis of aziridine.



Scheme 1.15 Hoch's synthesis of aziridine.

Many other ring-closing reactions of 1,2-aminoalcohol derivatives via Mitsunobu type reactions have been explored. Aziridines have been obtained in an enantioselective way^{42,43} by taking advantage of steric, stereoselective, and conformational effects and manipulating regio- and stereoselectively chiral starting materials.

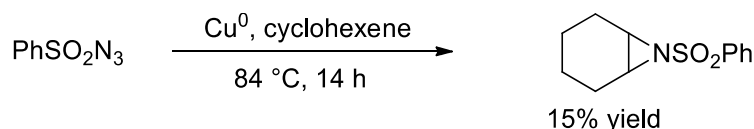
Besides these, two other main transformations directed toward the synthesis of chiral aziridines have been reported, namely nitrene transfer to an olefin or carbene transfer to an imine. In these reactions, homogeneous catalysis plays a major role (Scheme 1.16).



Scheme 1.16 The two main paths of catalytic imine aziridination.

1.4.1 Catalytic Aziridination by Nitrene Transfer to Olefins

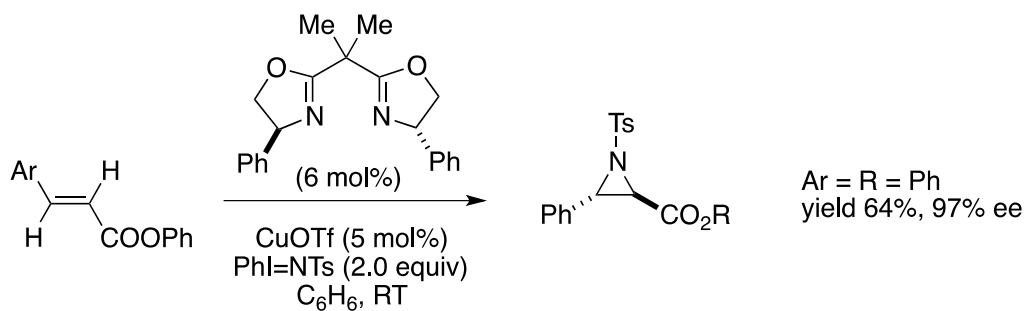
After Oehlschlanger's⁴⁴ discovery of nitrene from the thermal decomposition of sulfonyl azides and its subsequent trapping reaction with bicycle[2.2.1]-2-heptene, Abramovich⁴⁵ studied the reaction of sulfonyl nitrenes with aromatic compounds to give aryl amines through an aziridine intermediate and discovered the singlet nature of the free nitrene intermediate. Kwart and Khan's⁴⁶ reported the first metal-catalyzed nitrene transfer in 1967, demonstrating that copper powder promotes the decomposition of benzenesulfonyl azide when heated in cyclohexene:



Scheme 1.17 Kwart and Khan's aziridination with copper powder.

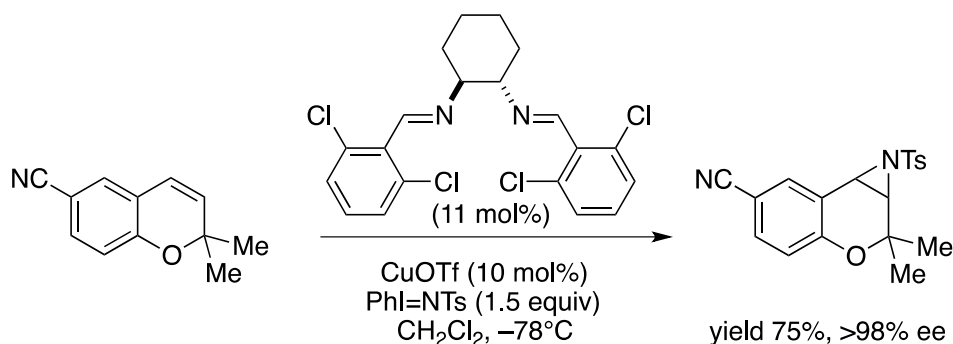
Since then, much effort has been directed toward the development of the enantioselective aziridination of alkenes with a nitrene source. Therefore, catalytic systems based on different ligands will be presented in the next paragraphs.

Highly enantioselective reactions have been developed with copper and bidentate chiral oxazoline ligands as catalyst. In the last two decades, Evans and co-workers⁴⁷⁻⁵⁰ made the crucial discovery that low-valent copper complexes catalyze the aziridination of various types of olefins with *N*-(*p*-tolylsulfonyl)imino)-phenyl-iodinane (PhI=NTs) as nitrene source (Scheme 1.18). This transformation is analogous to the enantioselective cyclopropanation developed independently by Evans,⁴⁷⁻⁵⁰ Masamune,^{51,52} and Pfaltz.⁵³



Scheme 1.18 Evans' copper/bis-oxazolines catalytic system.

Given that both Cu(I) and Cu(II) complexes are capable of mediating alkene aziridination by PhI=NTs, other types of chiral diimino complexes were fruitfully used by Jacobsen⁵⁴ in nitrene transfer to olefins with high yields and enantioselectivity (Scheme 1.19). By analogy with cyclopropanation, a Cu-nitrene intermediate such as [LCu=NTs]⁺ was proposed.⁵⁵

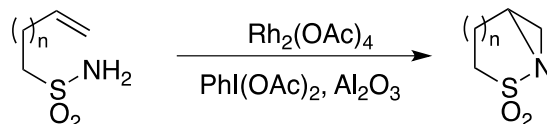


Scheme 1.19 Jacobsen's aziridination by nitrene transfer to olefins with a chiral diimino/copper catalyst.

After that, various other successful approaches were reported for olefin aziridination in the presence of Cu-based catalysts with chiral diimines of different types as ligands.⁵⁶⁻⁶¹

Bidentate chiral ligands were used also in combination with Rh(II). Binuclear Rh(II) catalysts, such as [Rh₂(OAc)₄], are competitive with those based on copper in certain cyclopropanation and CH-insertion reactions, but were found to be inefficient for aziridination with Ph=NTs. An extensive optimization of Rh(II) catalysts for the nitrene transfer indicated PhI=NNs as a very interesting new nitrogen source.⁶² Che reported in 2002⁶³ that achiral dirhodium(II,II) complexes catalyze the asymmetric

intramolecular aziridination of ω -tosylamino-olefins in the presence of $\text{PhI}(\text{OAc})_2$ and Al_2O_3 to give the corresponding aziridines in excellent yield (up to 98%) and with good to excellent conversions (Scheme 1.20). High turnover numbers (up to 1375) were achieved, too.



Scheme 1.20 Intramolecular aziridination of olefins by a dirhodium complex.

With chiral dirhodium(II,II) complexes (Figure 1.5), the asymmetric intramolecular aziridination of unsaturated sulfonamides (Scheme 1.20) and carbamates gave aziridines in good yields (up to 95%) and enantioselectivity (up to 76% ee).⁶⁴

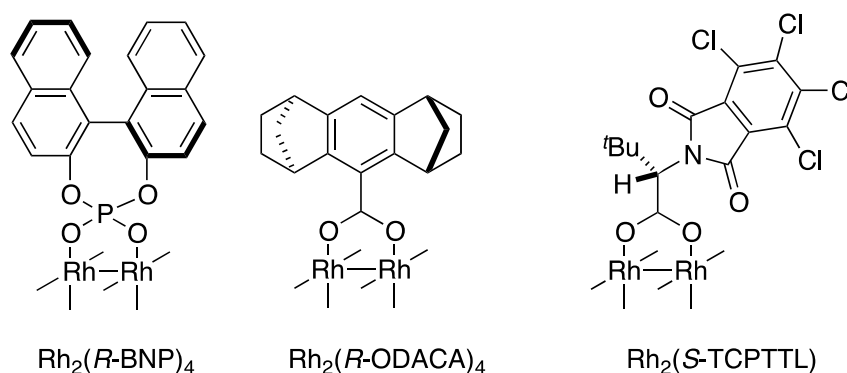
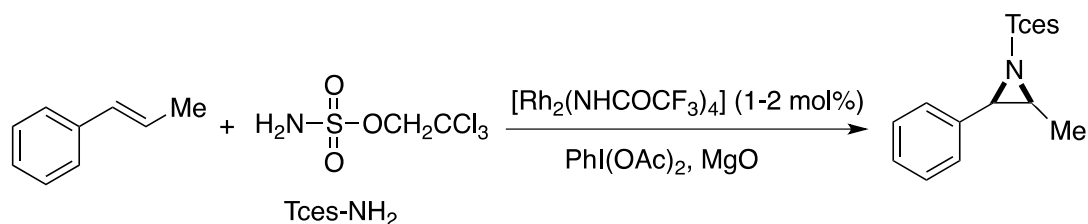


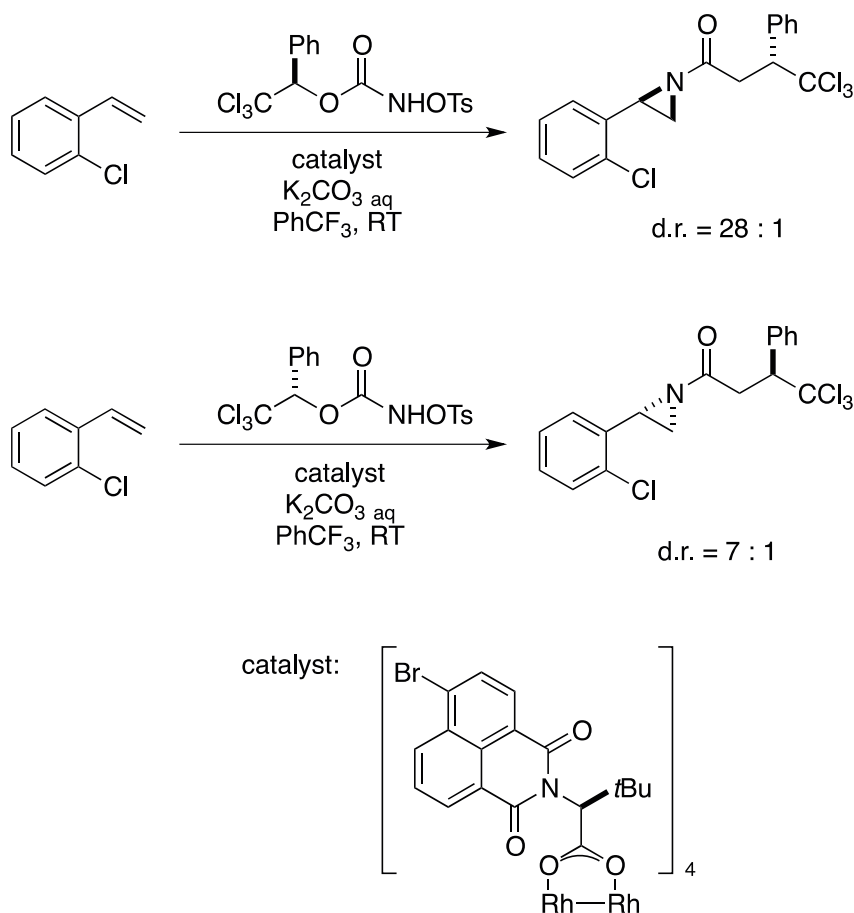
Figure 1.5 Dirhodium chiral complexes.

Du Bois⁶⁵ expanded the substrate scope and identified trichloroethylsulfamate as a novel and markedly effective nitrene source for the intra- and intermolecular aziridination of olefins:



Scheme 1.21 Aziridination with trichloroethylsulfamate.

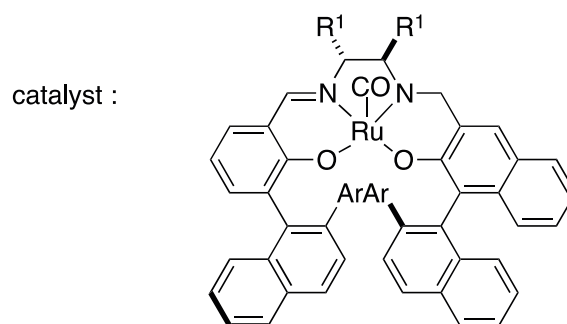
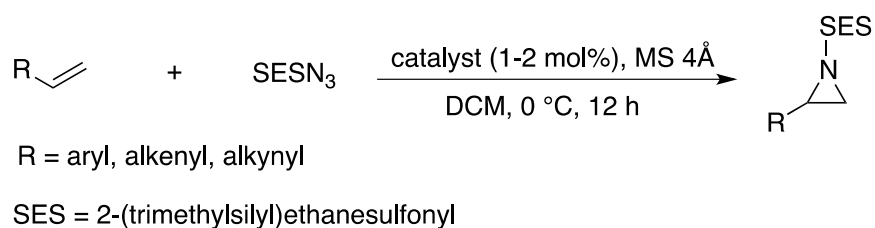
Lebel⁶⁶ recently described the first stereoselective rhodium-catalyzed intermolecular aziridination and C–H amination of alkenes to produce chiral acyl-protected aziridines and allylic amines (Scheme 1.22). Good yields and diastereoselectivities were achieved using a readily available chiral *N*-tosyloxycarbamate and a stoichiometric amount of the alkene substrate. Furthermore, the protecting group was easy to cleave under mild reaction conditions.



Scheme 1.22 Lebel's stereoselective rhodium-catalyzed intermolecular aziridination.

Tetradentate ligands, in particular chiral salen derivatives, have been used in combination with ruthenium to catalyze nitrene transfer to olefins. For instance, chiral $[\text{Ru}(\text{salen})(\text{CO})]$ complexes efficiently decompose azides at room temperature and catalyze asymmetric aziridination. Katsuki^{67,68} successfully expanded the substrate scope and reduced the catalyst load, reporting the highly enantioselective aziridination of conjugated and non conjugated olefins, using a robust novel $[\text{Ru}(\text{salen})(\text{CO})]$ complex as catalyst in the presence of SESN_3 as a nitrene source, with yields up to

99% and enantioselectivity up to >99% ee:



Scheme 1.23 Katsuki's [Ru(salen)(CO)] catalyst for olefin aziridination.

He also reported that manganese salen complexes catalyze the asymmetric aziridination of styrene with moderate yields (up to 76%) and enantioselectivity (up to 74% ee).^{69,70}

Besides salen, porphyrin ligands in combination with different metals (Figure 1.6) were found effective in nitrene transfer to olefins. In the early 1980s, Mansuy⁷¹⁻⁷³ and Breslow and Gellman^{74,75} reported the first examples of aziridination of alkenes and amidation of C–H bonds catalyzed by Fe(III) and Mn(III)-TPP complexes (TPP = tetraphenylporphyrin dianion) with PhI=NTs, respectively. With such metalloporphyrins, Che⁷⁶ was able to extend the diastereoselective aziridination of C–C bonds with different nitrogen sources.

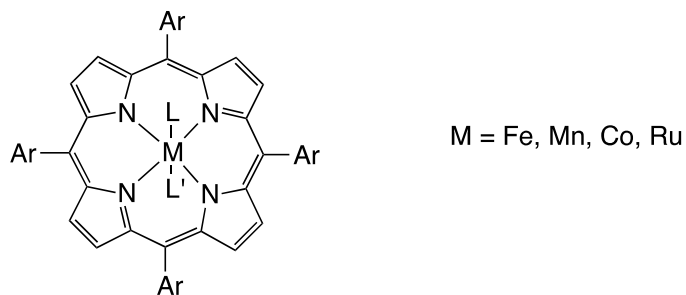


Figure 1.6 General representation of a metalloporphyrin.

$[\text{Mn}^{\text{IV}}(\text{Por}^*)(\text{OH})(\text{MeOH})]$ (Figure 1.7) was the first reported example of a chiral porphyrin as catalyst for asymmetric alkene aziridination. With this complex, Che⁷⁷ described the reaction of aromatic alkenes such as styrenes, *trans*-stilbene, 2-vinylnaphthalene, indene, and 2,2-dimethylchromene with $\text{PhI}=\text{NTs}$ as nitrogen source. The enantioselectivity was moderate (from 43 to 63% ee).

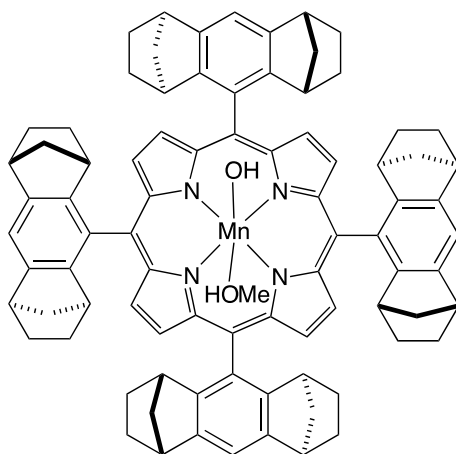
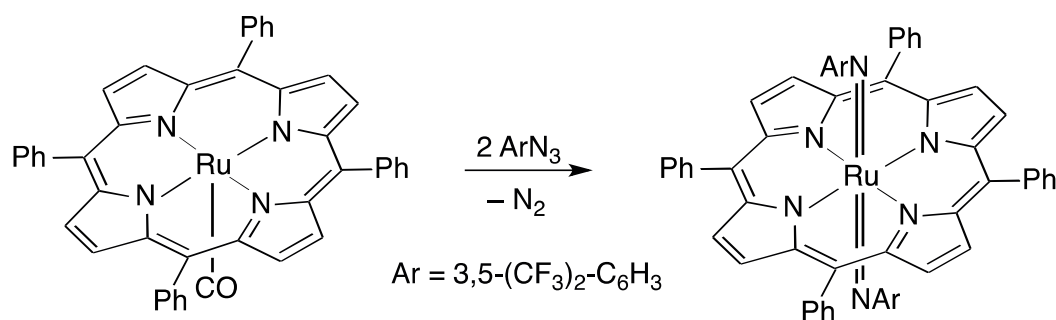


Figure 1.7 $[\text{Mn}^{\text{IV}}(\text{Por}^*)(\text{OH})(\text{MeOH})]$

Metal porphyrins have been tested in nitrene transfer with more economic nitrogen sources, such as aromatic azides. For instance, azides have been used efficiently in combination with ruthenium porphyrins, but with or low or no enantioselectivity.⁷⁸ On the other hand, achiral systems have been vastly applied for mechanistic studies of the nitrene transfer reaction. The scope and limits of the reaction were investigated with different azides, olefins, and $[\text{Ru}(\text{porphyrin})(\text{CO})]$ complexes.⁷⁹ Steric factors were found to strongly affect the reaction, as internally disubstituted olefins exhibited a lower reactivity, and tri- and tetra- substituted olefins did not react at all. In contrast, higher yields and short reaction times were achieved by using terminal olefins and electron-poor aryl azides. In particular, $[\text{Ru}(\text{TPP})(\text{CO})]$ complexes were found to catalyze the direct aziridination of conjugated dienes by aryl azides to provide *N*-aryl-2-vinylaziridines with high chemoselectivity.⁸⁰ Recently, Cenini and co-workers⁸¹ described the synthesis of allylic amines by aromatic azides (ArN_3) catalyzed by $[\text{Ru}(\text{TPP})(\text{CO})]$ with molecular nitrogen as the only stoichiometric byproduct. The bisimido complex $[\text{Ru}(\text{TPP})(\text{ArN})_2]$ ($\text{Ar} = 3,5\text{-(CF}_3)_2\text{C}_6\text{H}_3$) was isolated and found to be active both in stoichiometric and in

catalytic nitrene transfer (Scheme 1.24).



Scheme 1.24 The bisimido complex $[\text{Ru}(\text{TPP})(\text{ArN})_2]$ ($\text{Ar} = 3,5\text{-(CF}_3\text{)}_2\text{C}_6\text{H}_3$).

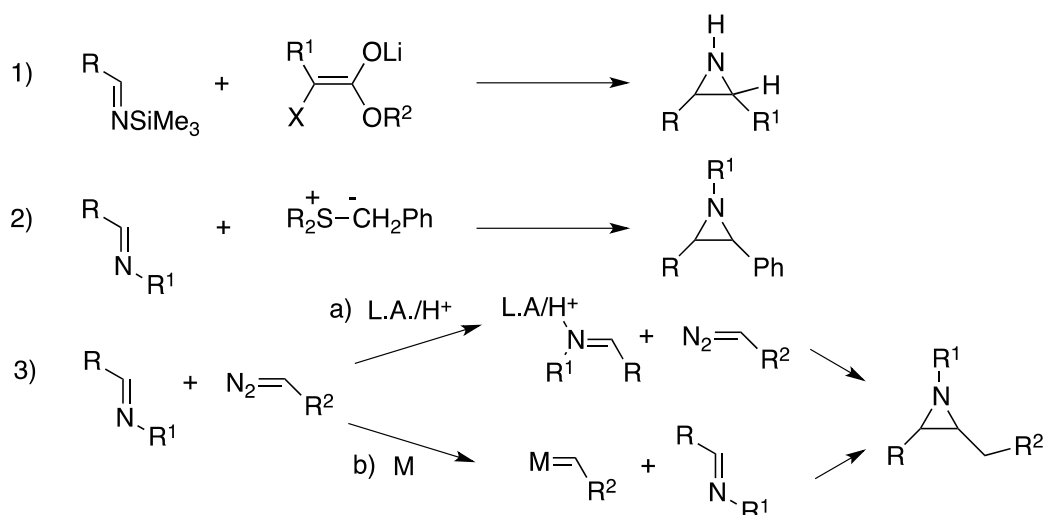
Also Co(II)/TPP complexes catalyze the reaction of aromatic azides with nonactivated olefins to afford aziridines in good yields.⁸² Mechanistic investigations showed that the reaction proceeded by reversible coordination of the aryl azide to the Co(II)-porphyrin complex. Interestingly, a thorough kinetic study showed that the often postulated “nitrene” complex is not an intermediate in the reaction.⁸² Moreover, Zhang^{83,84} reported that Co(II) complexes of D_2 -symmetric porphyrins catalyze the asymmetric aziridination of styrenes. When trichloroethoxysulfonyl azide (TcesN_3) was used as the nitrogen source, very high yields (up to 99%) and enantioselectivities (up to 99% ee) were achieved.⁸⁵ Interestingly, the presented nitrene transfer from RN_3 is analogue to the carbene transfer from coordinate EDA to olefin that is discussed in the next paragraph.

To summarize, catalytic nitrene transfer to olefins is a vastly explored approach for asymmetric aziridination, with, in some cases, very high yields and good enantioselectivity, but also some important drawbacks. For instance, the aziridination reactions using N -arylsulfonyliminophenylidines ($\text{PhI}=\text{NTs}$) or their equivalents as a nitrene source are not atom efficient. Phenylidines are very strong oxidants and, in case of the system reported by Evans,⁴⁷⁻⁵⁰ they require the addition of an excess of the olefin. Therefore, recent studies have been directed toward higher enantioselectivity and higher reactivity, as in the case of Du Bois.⁶⁵ On the other hand, azides are weaker oxidants than phenylidines and produce dinitrogen as the only side product, but they are often unstable and need to be handled with care.⁸⁶ Katsuki's system^{67,68} gives high yields for aryl olefins, like styrene derivatives, but only poor selectivities for aliphatic alkenes. This limited drastically the substrate

scope, although different azides have been developed in order to have substituents on the nitrogen that can be easily removed thereafter. Therefore, the combination of high enantioselectivity with a wide substrate scope still remains a crucial issue in olefin aziridination.

1.4.2 Carbene Transfer to an Imine

An alternative approach that has been developed for catalytic aziridination is the reaction of a carbenoid species with an imine. The following scheme summarizes the possible reactions starting from different sources of carbenoids: 1) Aza-Darzens reaction with α -haloenolesters, 2) carbene transfer from sulfur ylides, and 3) the reaction of a diazoalkane.

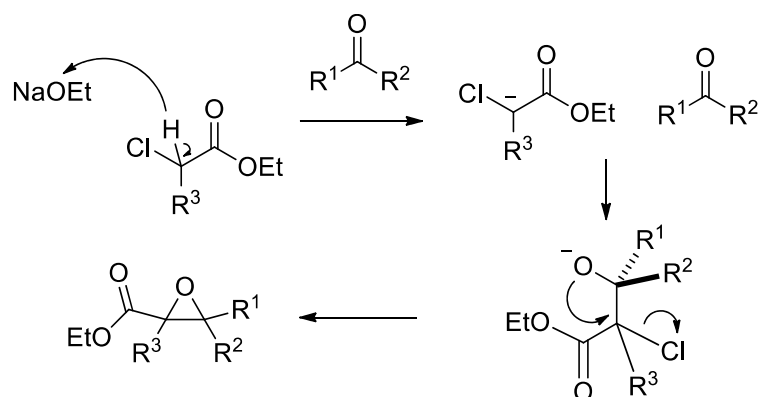


Scheme 1.25 Carbene transfer to imine from different sources of carbenoids.

1.4.2.1 α -Haloenolesters as Carbenoid Sources

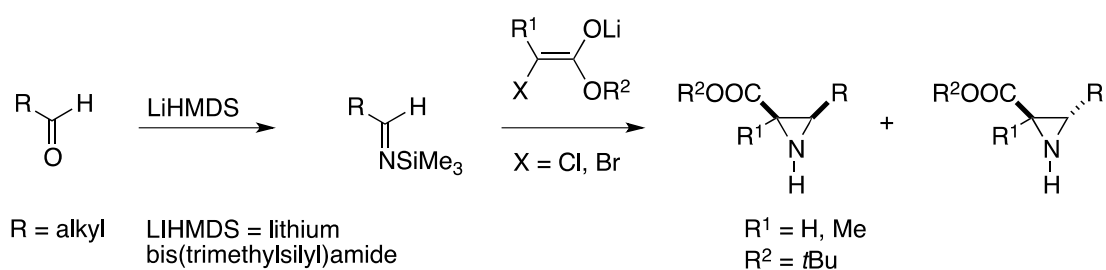
It is well established that aziridines can be prepared by the reaction between imines and the esters of an α -haloenole, which is known as aza-Darzens. Originally, the Darzens reactions were a general class of reactions between an aldehyde and an α -haloester in presence of a base, forming an α,β -epoxy ester (Scheme 1.26).⁸⁷ The role of the base was to form a resonance-stabilized carbanion that then attacked the aldehyde. The final step was the ring closure by nucleophilic attack of the oxygen

atom and the following chloride elimination.



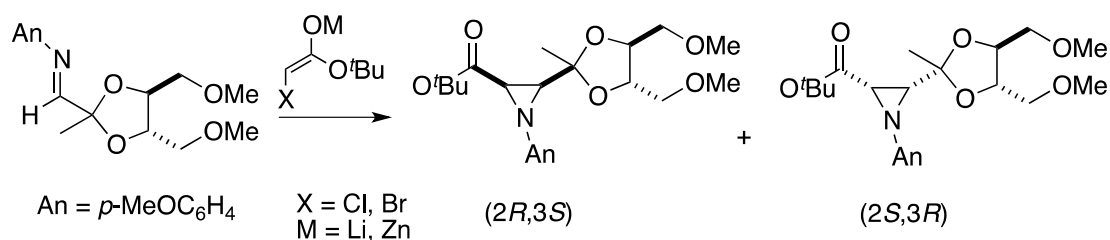
Scheme 1.26 Synthesis of an α,β -epoxy ester by Darzens reaction.

Deyrup⁸⁸ developed a procedure to extend the Darzens synthesis to the preparation of aziridine esters and amides. In 1991, Panunzio, Cainelli, and Giacomini⁸⁹ reported the stereoselective synthesis of aziridines by the Darzens-type reaction of *N*-trimethylsilyl imines with lithium enolates of α -haloesters, with yields of up to 60% and *cis/trans* ratios from 60:40 to 100:0:



Scheme 1.27 Stereoselective synthesis of aziridines by Darzens-type reaction.

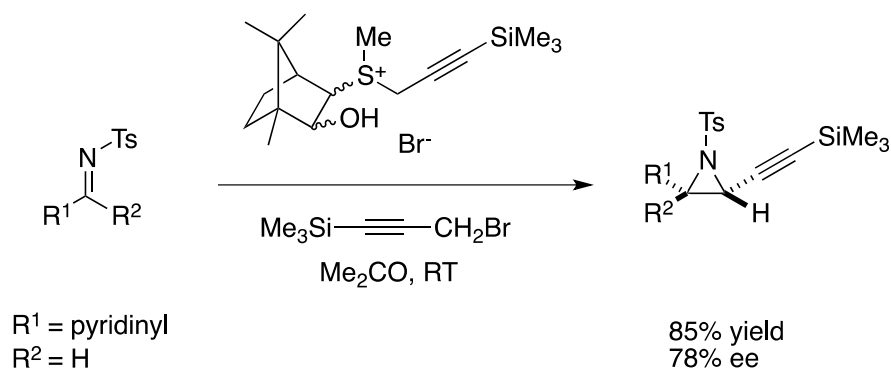
Shimizu⁹⁰ and Reddy^{91,92} reported the diastereoselective synthesis of optically active aziridines by condensation of lithium and zinc enolates of α -haloacetate with chiral imines or sulfonimines, respectively (Scheme 1.28).



Scheme 1.28 Diastereoselective synthesis of aziridines by condensation of lithium and zinc enolates of α -haloacetate.

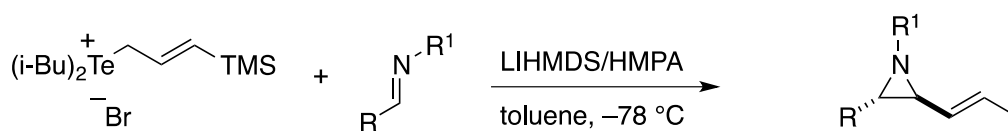
1.4.2.2 Sulfur Ylides as Carbenoid Sources

The Dai and Hou⁹³⁻⁹⁶ groups studied the stoichiometric reactions of sulfonium, arsonium, and telluronium allylic ylides with *N*-sulfonylimines, which give vinylaziridines with low diastereoselectivity. Chiral ylides gave the corresponding aziridines with good yield and enantioselectivity up to 78% ee:⁹⁷



Scheme 1.29 Reaction of a sulfonium allylic ylide with an *N*-sulfonylimine to give a vinylaziridine.

Tang⁹⁸ developed the aziridination of a telluronium allylide with less active imines such as *N*-phenylaldimine and *N*-Boc-aliphatic imines, obtaining the desired product with high stereoselectivity (Scheme 1.30).

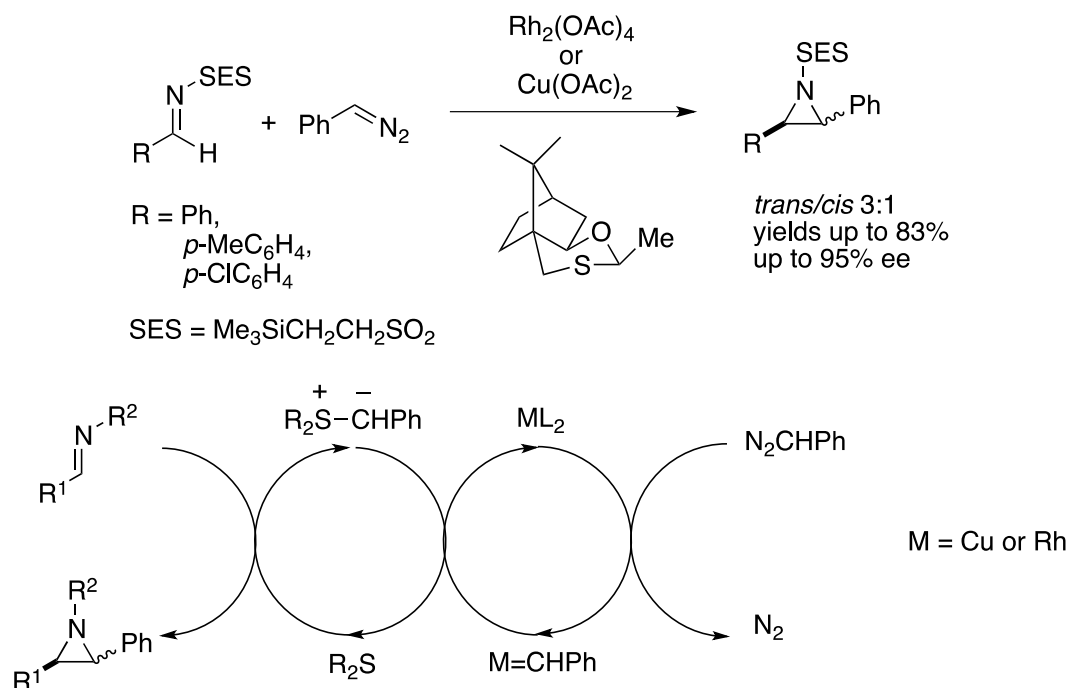


$R^1 = \text{Ph}, R^2 = \text{Ph}$ yield 84%, cis/trans 2/98

$R^1 = (\text{CH}_3)_2\text{CH}, R^2 = \text{Boc}$ yield 77%, cis/trans 91/9

Scheme 1.30 Reaction of a telluronium allylide with an *N*-phenylaldimine to give the corresponding aziridine.

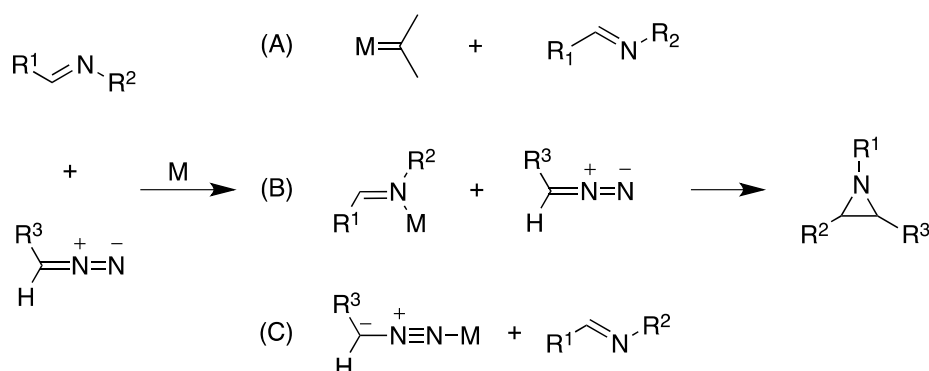
As an extension to his studies on carbene transfer to olefins and ketones,^{99,100} Aggarwal^{101,102} has developed a catalytic approach that exploits sulfur ylides for imine aziridination. Despite the relatively low reactivity of *N*-alkyl- or *N*-arylimines toward the nucleophilic attack of ylides, Aggarwal's successfully reacted silylated sulfur ylides with *N*-sulfonylimines. The corresponding aziridines were afforded and the SES group was easily removed afterwards (Scheme 1.31). A distinctive feature of this system is that the ylide is generated *in situ* by decomposition of PhCHN_2 by the Rh(II) or Cu(II) catalyst:



Scheme 1.31 Reaction of a sulfur ylide with an *N*-sulfonylimine to give the corresponding aziridine in the presence of a Rh(II) or Cu(II) catalyst.

1.4.2.3 Diazocompounds as Carbenoid Sources

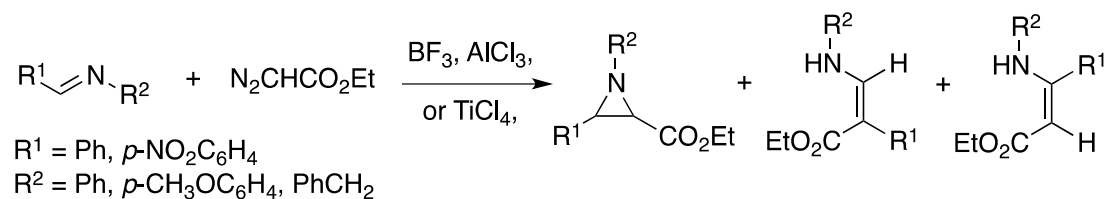
Two mechanisms have been reported for the reaction of an imine with a diazoalkane as carbene precursor (Scheme 1.32): the reaction of the acid activated imine with the diazoalkane (A), or the reaction of a metal carbene intermediate with the free imine (B).^{103,104} Recently, our research group has proposed a third mechanism (C) that involves carbene transfer from a diazoester complex to the free imine.¹⁰⁵



Scheme 1.32 Mechanisms for the reaction of an imine with a diazoalkane.

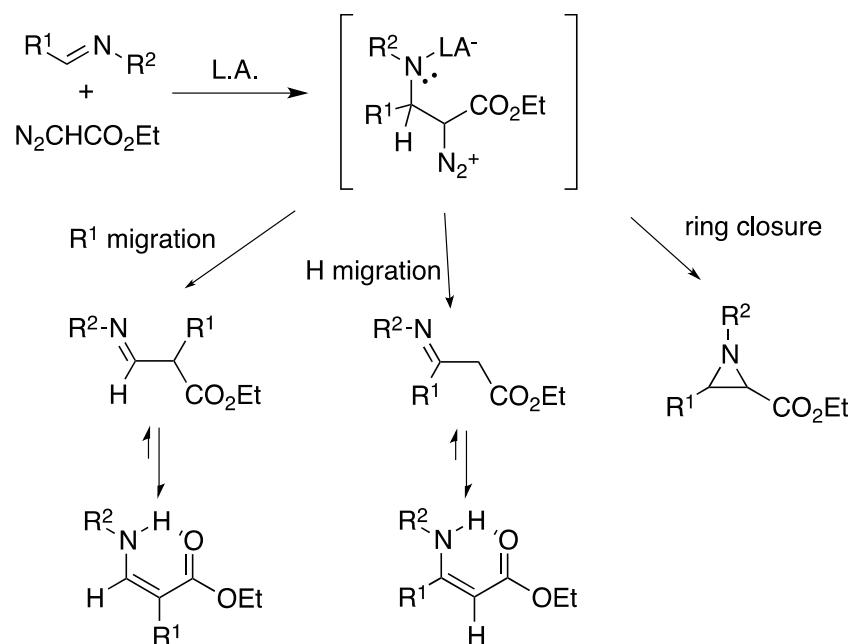
1.4.2.3.1 Acidic Activation of the Imine and its Reaction with a Diazoalkane

Mloston^{106,107} reported the first general preparation of aziridines by reaction of imines with phenyldiazomethane and zinc iodide as catalyst. Yields were moderate, but this method failed with ethyl diazoacetate as the carbene source. Aziridines were also obtained from the reaction of diazopenicillanates with imines in the presence of $BF_3 \cdot Et_2O$.¹⁰⁸ In 1991, Brookhart and Templeton reported a convenient synthesis of *cis*-aziridines from various imines and ethyl diazoacetate (EDA) catalyzed by common Lewis acids, such as BF_3 , $AlCl_3$, and $TiCl_4$.¹⁰⁹



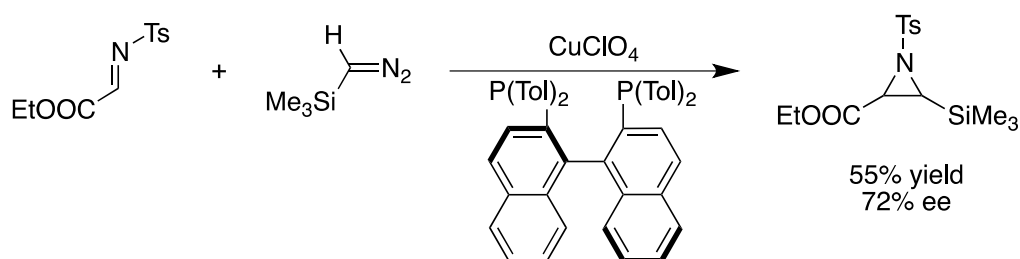
Scheme 1.33 Imine aziridination with EDA in the presence of Lewis acids.

Enaminoesters were found among the reaction products, whereas species deriving from carbene coupling, such as diethylfumarate or maleate, were never detected. This suggested that no metal carbenoid species were involved in the reaction, in agreement with the following proposed mechanism, which involves the nucleophilic attack of the diazoalkane onto the Lewis acid-activated imine:¹⁰⁹



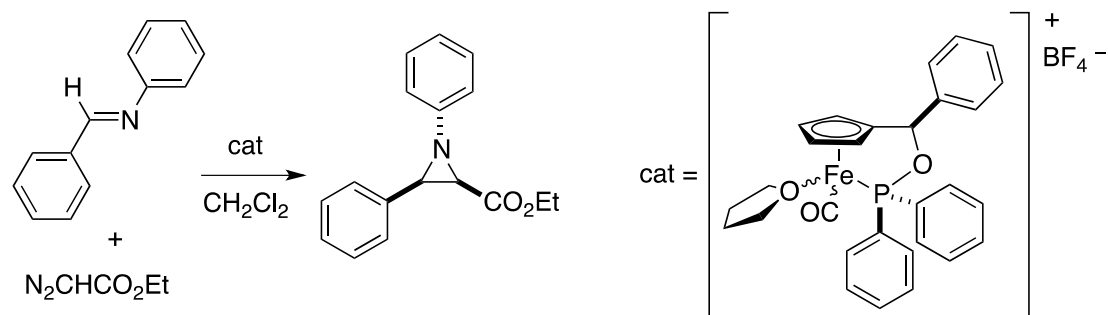
Scheme 1.34 Proposed aziridination mechanism in the presence of Lewis acids.

The first catalytic asymmetric imine aziridination that is thought to involve Lewis acid activation of the imine was reported by Jørgensen in 1999.¹¹⁰ *N*-Tosylaziridines were produced with high *cis*-selectivity by treating ethyl-2-tosyliminoacetate with trimethylsilyldiazomethane in the presence of catalytic amounts of a copper(I)/BINAP complex:



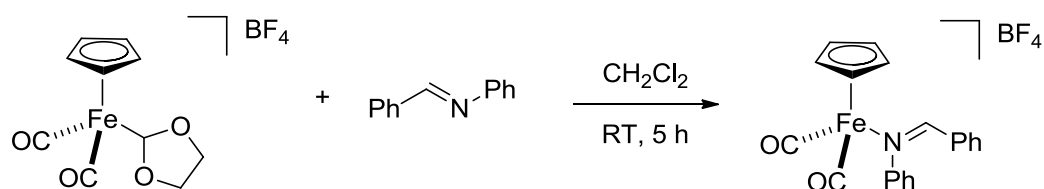
Scheme 1.35 Aziridination as reported by Jørgensen.

Moreover, Hossain developed a rational approach to Lewis acid-catalyzed carbene transfer to imines with $[\text{Fe}(\text{CO})(\text{THF})(\eta^5\text{-}\eta^1\text{-C}_5\text{H}_4\text{CH}(\text{Ph})\text{OPPh}_2)]\text{BF}_4$, which features a diphenylphosphinite tethered to a cyclopentadienyl ring.¹¹¹ This complex was found to be an effective catalyst in the aziridination reaction, but the *cis*-aziridine was formed with low enantioselectivity (5% ee):



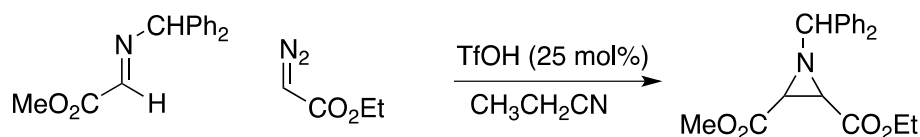
Scheme 1.36 Hossain's imine aziridination with a chiral Lewis acid.

Mayer and Hossain studied the mechanism with the achiral analogue of the complex. In the reaction crude, enaminoesters were detected as side products, which supports the Lewis acid activation path. Besides, they isolated the intermediate imine complex (Scheme 1.37), which was found to be active in the aziridination with the same product distribution.¹¹²



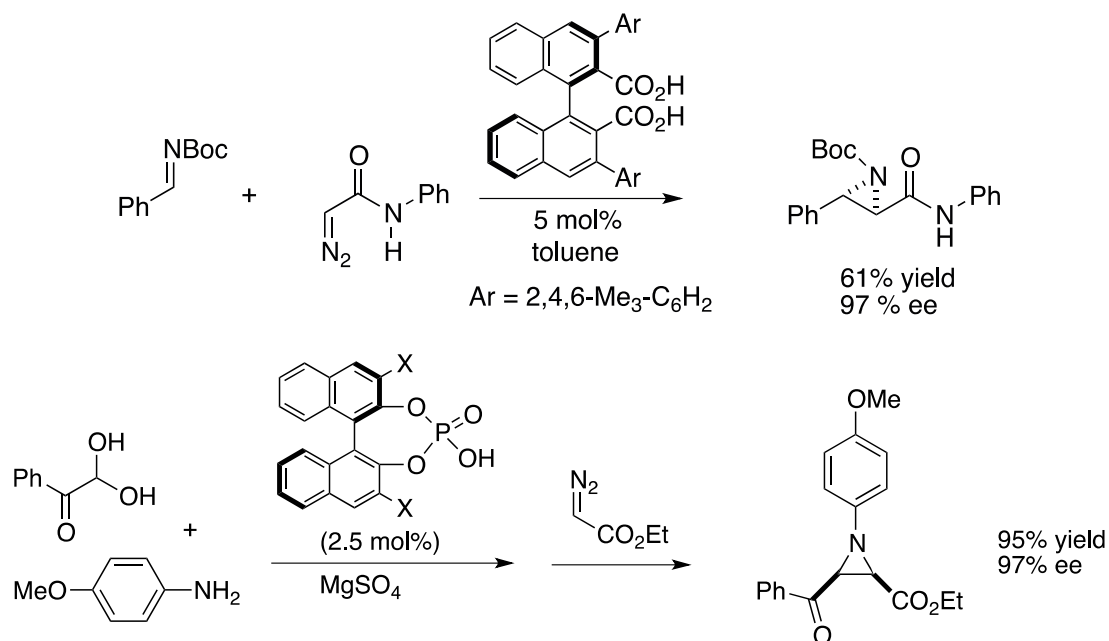
Scheme 1.37 Formation of the imine complex.

Williams and Johnston¹¹³ expanded the aza-Darzens-type aziridination reactions from Lewis to Brønsted acids, among which triflic acid turned out to be the most efficient one (Scheme 1.38).



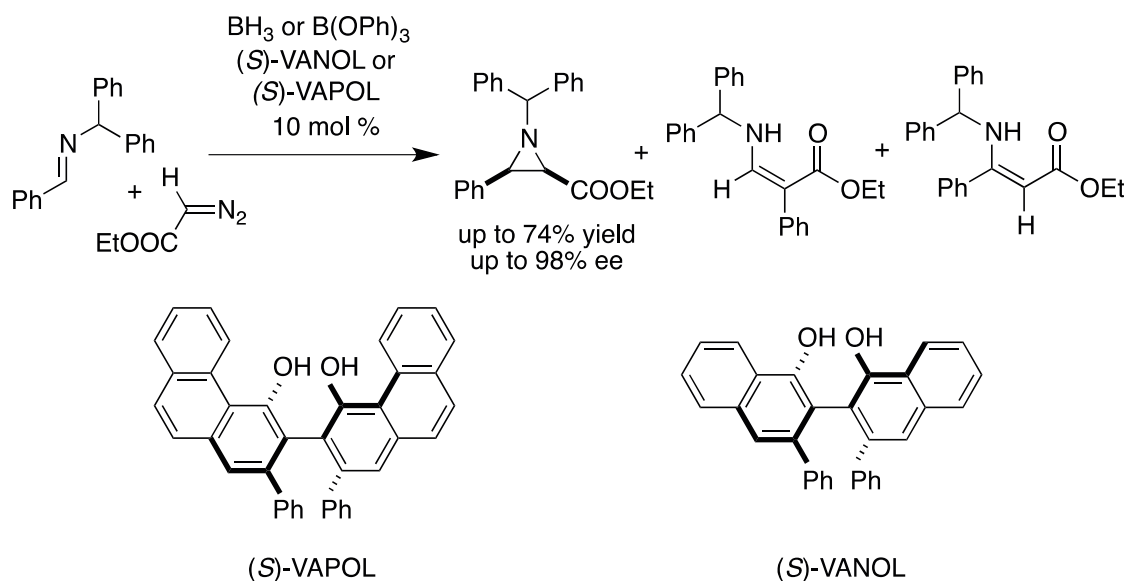
Scheme 1.38 Imine aziridination with TfOH as Brønsted acid.

Recently, several examples of asymmetric imine aziridination catalyzed by chiral Brønsted acids have been reported.¹¹⁴ The optimization of the acid has led to very high yields (up to 95%) and excellent enantioselectivity (up to 97% ee).¹¹⁵



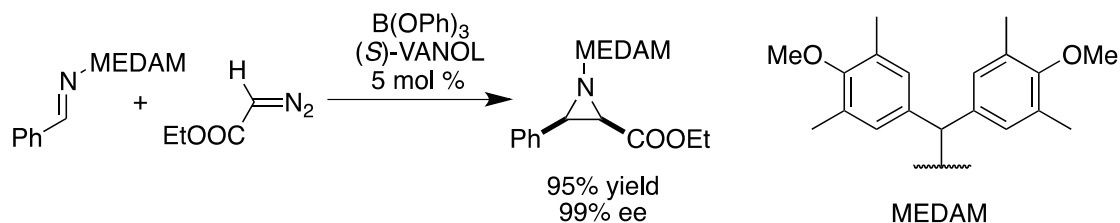
Scheme 1.39 Enantioselective imine aziridination with a chiral Brønsted acid.

Chiral Brønsted acids play an increasing role in asymmetric aziridination also in view of new assessments of existing catalytic systems. In particular, this is the case of Wulff's VANOL- and VAPOL-based boron catalysts, which have been originally proposed to operate via Lewis acid activation of the imine (Scheme 1.40)^{116,117}



Scheme 1.40 Imine aziridination as reported by Wulff.

Recently, Wulff reported¹¹⁸ that, by changing the protection group of the imine to MEDAM, the aziridination reaction was ten times faster than for the diphenylmethyl protecting group, while retaining the excellent enantioselectivity and yield:



Scheme 1.41 Enantioselective aziridination of imine bearing the MEDAM group on the nitrogen.

Wulff's system enabled the successful enantioselective synthesis of L-DOPA, used for treatment of Parkinson's disease, and the synthesis of (–)-chloramphenicol, a broad-spectrum antibiotic.

Initially, it was proposed that the catalyst for this reaction was the boron Lewis acid. After a thorough mechanistic study, Wulff concluded that the actual catalyst is a chiral Brønsted acid generated *in situ* by reaction of the boron precatalyst with adventitious water (Figure 1.8).¹¹⁹

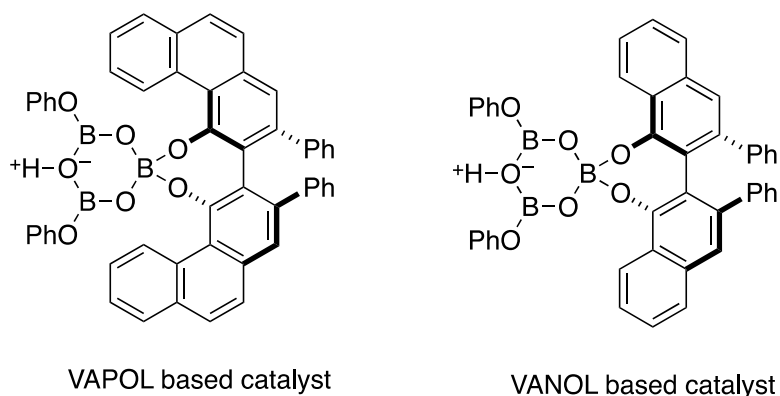
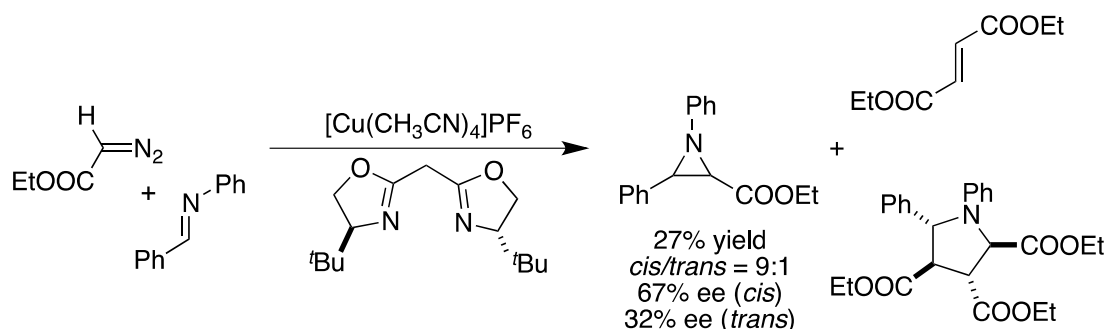


Figure 1.8 Wulff's VAPOL and VANOL based catalysts.

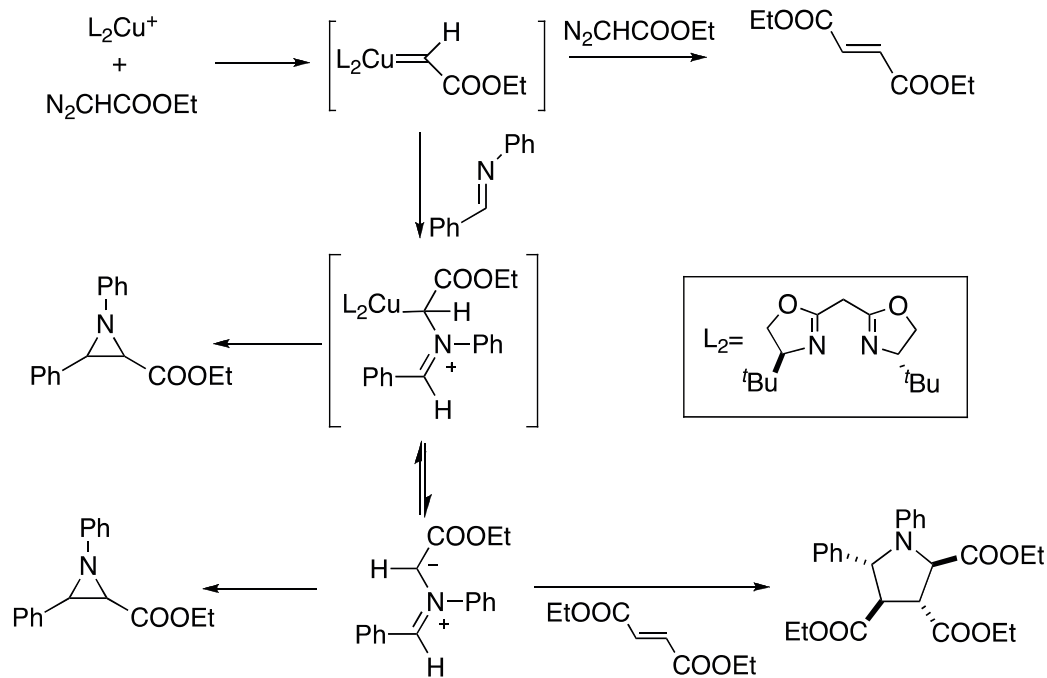
1.4.2.3.2 Reaction of a Metal Carbene Intermediate with the Free Imine

In 1972, Baret reported the first example of stoichiometric carbene transfer to imines, which involved the decomposition of ethyl diazoacetate catalyzed by copper powder to give aziridines.¹²⁰ In 1995, Jacobsen¹²¹ reported the first asymmetric imine aziridination mediated by a metal carbene complex. Catalytic amounts of a Cu(I)-Box complex were used to aziridinate *N*-benzylidenaniline with ethyl diazoacetate to give 2-carboxyaziridine in low yield and moderate enantioselectivity. A major drawback of this system was that it required a phenyl group on the nitrogen, which cannot be removed:



Scheme 1.42 Jacobsen's imine aziridination with a Cu(I)-Box complex.

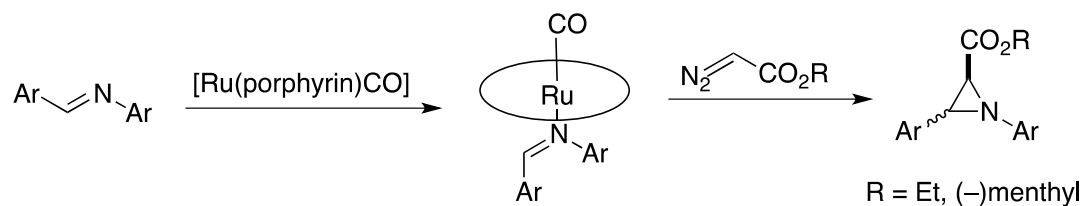
Jacobsen suggested that the formation of the aziridine involved a copper azomethine ylide complex as intermediate, generated by the nucleophilic attack of the imine onto a metal carbene complex (Scheme 1.43).



Scheme 1.43 Jacobsen's mechanism for imine aziridination catalyzed by copper.

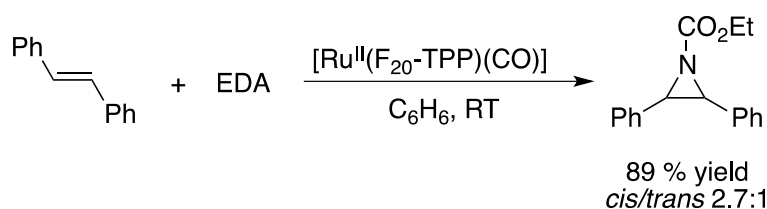
The analysis of the side products of the reaction (maleate, fumarate, pyrrolidine and enaminoesters) led to some important mechanistic considerations. In particular, Jacobsen noticed that, by adding an excess of diethylfumarate to the reaction solution, pyrrolidine was the exclusive product. Moreover, the formation of racemic pyrrolidine indicated that its generation was not mediated by the chiral copper/box system as it was for the aziridine. As ylides are known to arise in absence of transition metals and to react with dipolarophiles, such as diethyl fumarate,^{122,123} he proposed an ylide intermediate for the formation of the pyrrolidine and explained the low enantioselectivity with its dissociation from the chiral complex (Scheme 1.43).

Several transition metal catalysts that are known to form carbene complexes by decomposition of diazoesters, such ruthenium(II) porphyrins, catalyze the aziridination of imines:¹²⁴



Scheme 1.44 Imine aziridination with ruthenium(II) porphyrins.

In particular, Che reported that ruthenium porphyrins, such as $[\text{Ru}(\text{F}_{20}\text{-TPP})(\text{CO})]$, where $(\text{F}_{20}\text{-TPP})$ is the 5,10,15,20-tetrakis(pentafluorophenyl)-porphyrinato dianion, and $[\text{Ru}(\text{Por}^*)(\text{CO})]$, where (Por^*) is the 5,10,15,20-tetrakis[(1*S*,4*R*,5*R*,8*S*)-1,2,3,4,5,6,7,8-octahydro-1,4:5,8-dimethanoanthracen-9-yl]-porphyrinato dianion) are active catalysts albeit in a nonenantioselective way:¹²⁴



Scheme 1.45 Imine aziridination with $[\text{Ru}^{\text{II}}(\text{F}_{20}\text{-TPP})(\text{CO})]$ as catalyst.

A mechanistic study with this catalyst suggested the involvement of an azomethine ylide in aziridine formation. However, as the carbene complex $[\text{Ru}(\text{F}_{20}\text{-TPP})(\text{CHCO}_2\text{Et})]$ failed to react with imines, such as $(p\text{-ClPh})\text{CH}=\text{NPh}$ or $(p\text{-MePh})\text{CH}=\text{NPh}$, the ylide cannot be formed from a carbene intermediate, in contrast to Jacobsen's mechanistic hypothesis with copper catalysts. Therefore, the reaction mechanism remains unclear. We will come back to this issue below.

1.4.2.4 General Features of Catalytic Imine Aziridination

In general, the most significant advantage of imine aziridination is that diazoacetates, such as EDA, are commercially available. Also, the resulting aziridine-2-carboxylate esters are a convenient source for a variety of compounds including unnatural α - and β -aminoacids. To this purpose, Wulff's¹¹⁶⁻¹¹⁸ system is very efficient in terms of yield and enantioselectivity, but presents the disadvantage that the MEDAM group on the nitrogen is not a protecting group and cannot be removed thereafter, still limiting the substrate scope. Finally, Aggarwal's⁹⁹⁻¹⁰² new approach involving ylides allowed to prepare aziridines, such as vinylaziridines, with high selectivity where other methods failed.

On the other hand, the competitive formation of byproducts, in particular carbene dimerization products and enaminoesters, is one of the problems in the

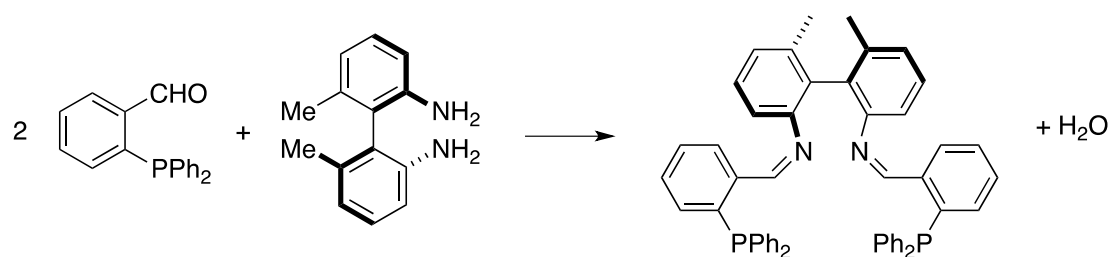
development of the catalytic synthesis of aziridine-2-carboxylate esters from diazocompounds.

Some general observations on the mechanism can be made. The attribution of the corresponding reaction path is not trivial. For instance, the most successful system, which was reported by Wulff, was at first considered to operate via Lewis acid activation, whereas lately it turned out to be Bronsted acid mediated.¹¹⁹ The enantioselectivity is generally low in the case of the carbene transfer by transition metal complexes, but, with the exception of Jacobsen's studies, most mechanisms were not investigated in detail. In addition, Che reported a very unclear mechanism, on the basis of the unprecedented observation that the carbene complex was not reacting with the imine.

In sum, there is still room for further investigations to discover more efficient catalysts and to cast light on mechanistic aspects for transition metal based system.

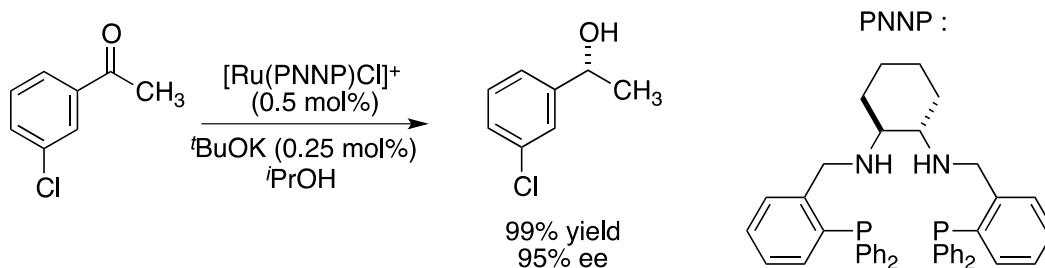
1.5 Imine Aziridination with Ru /PNNP Complexes

Chiral C_2 -symmetric tetradentate ligands with a P_2N_2 donor set were synthesized by Pignolet in 1984.¹²⁵



Scheme 1.46 Pignolet's synthesis of a C_2 -symmetric P_2N_2 ligand.

In 1996, their first application in catalysis in combination with ruthenium was reported by Gao, Ikarya and Noyori¹²⁶ for the transfer hydrogenation of acetophenones. The best results were obtained with the *m*-chloroacetophenone as reagent and the diamino PNNP as ligand (Scheme 1.47).



Scheme 1.47 Transfer hydrogenation of acetophenones catalyzed by Ru/PNNP.

Since then, our group focused on ruthenium complexes with ligand **1a** (Figure 1.9) and their application in various catalytic reactions, including the asymmetric aziridination of imines. The common precursor to the catalytically active species is the dichloro complex *trans*-[RuCl₂(**1a**)] (**2a**).

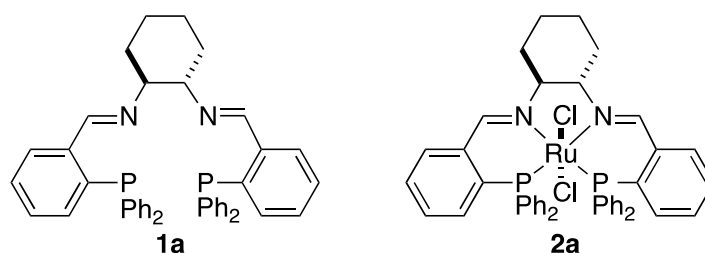


Figure 1.9 *C*₂-symmetric PNNP ligand **1a** and its ruthenium dichloro complex **2a**.

Some general considerations about the structure and the reactivity of Ru/PNNP complexes are necessary to understand the rationale of this project as well as the catalytic results presented in the next paragraphs.

1.5.1 Structural Properties of Ruthenium(II) Dichloro PNNP Complexes

Ruthenium(II) dichloro complexes bearing tetradentate PNNP ligands are 18 electron, coordinatively saturated species.¹²⁷ Because of their low spin *d*⁶ configuration, they are kinetically inert and therefore inactive as catalysts. Their octahedral geometry presents five possible configurations in case of an open-chain PNNP: *trans*, *cis*-β (Λ and Δ), and *cis*-α (Λ and Δ) (Figure 1.10).

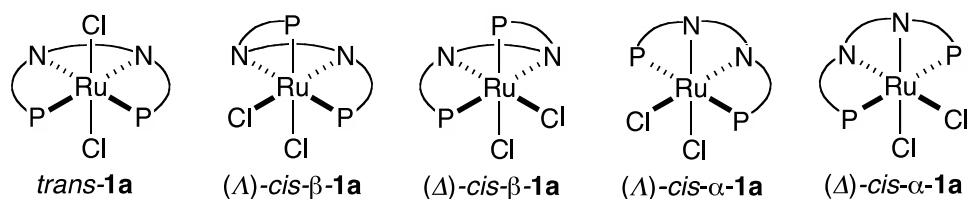


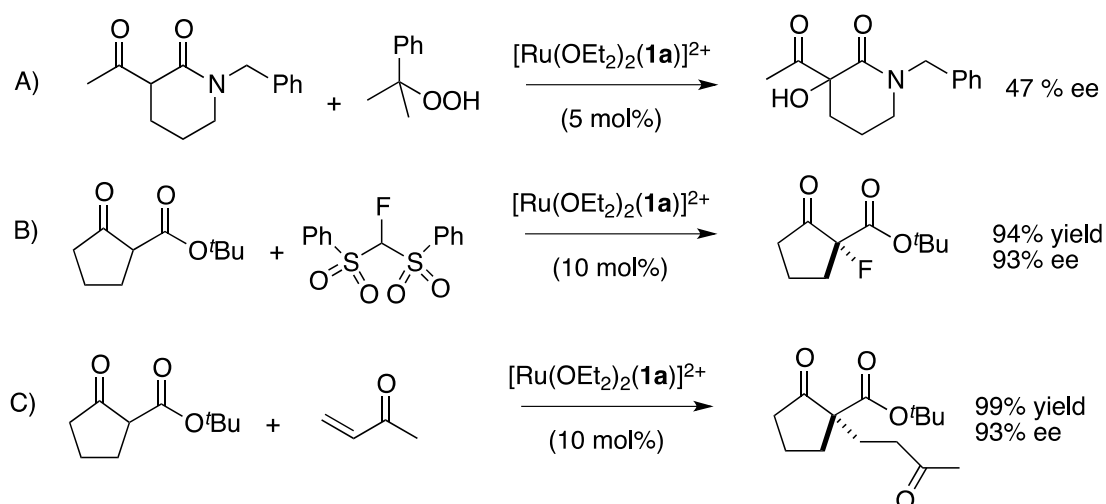
Figure 1.10 The five possible configurations of a ruthenium dichloro complex with a PNNP ligand.

In fact, the *trans* isomer is the most stable one and is generally obtained upon heating. One of the *cis-β* isomers has been observed,¹²⁸ but we never detected the *cis-α* species.

In order to get an active catalytic species, single or double chloride abstraction from **2a** must be performed to form a labile or unsaturated species, as described hereafter.¹²⁷

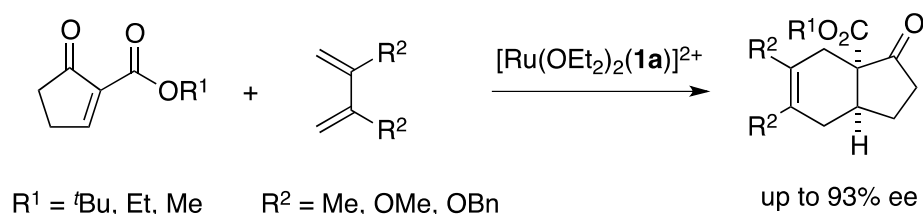
1.5.2 Dicationic Ru/PNNP Complexes

When chloride abstraction is performed with Et_3OPF_6 (2 equiv), a labile bis-ether adduct $[\text{Ru}(\text{OEt}_2)_2(\mathbf{1a})]^{2+}$ is formed, which catalyzes the hydroxylation (A),^{129,130} fluorination (B),¹³¹⁻¹³³ and Michael reaction (C)¹³⁴⁻¹³⁶ of β -ketoesters:

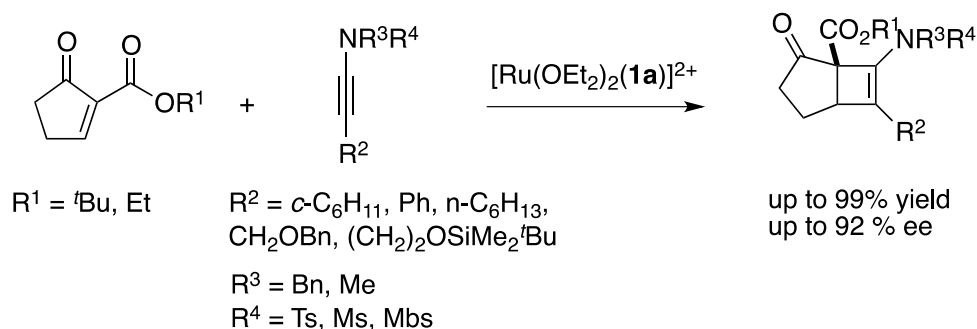


Scheme 1.48 Catalytic activity of the dicationic $[\text{Ru}(\text{OEt}_2)_2(\mathbf{1a})]^{2+}$.

The elusive dicationic complex $[\text{Ru}(\text{OEt}_2)_2(\mathbf{1a})]^{2+}$ has been shown to react with β -ketoesters to form, after deprotonation, the monocationic enolato complex. This species, after hydride abstraction, gives the corresponding alkylidene β -ketoester, which undergoes Diels-Alder reactions with dienes (Scheme 1.49)¹³⁶ and enantioselective Ficini reactions with ynamides (Scheme 1.50).^{137,138}



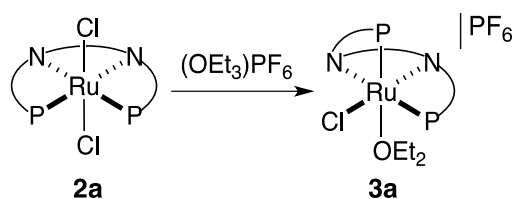
Scheme 1.49 Diels-Alder reaction of β -ketoester with dienes.



Scheme 1.50 Ficini reaction of β -ketoester with dienes.

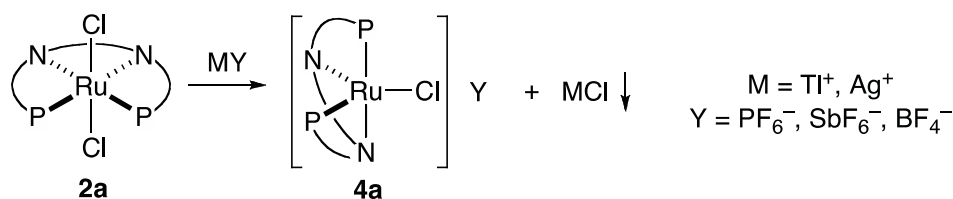
1.5.3 Monocationic Ru/PNNP Complexes

Single chloride abstraction from the dichloro complex $[\text{RuCl}_2(\mathbf{1a})]$ ($\mathbf{2a}$) gives different species, depending on the nature of the chloride scavenger used. The six-coordinated adduct $[\text{RuCl}(\text{OEt}_2)(\mathbf{1a})]^+$ ($\mathbf{3a}$) is formed upon treatment of complex $\mathbf{2a}$ with $(\text{Et}_3\text{O})\text{PF}_6$ (1 equiv) (Scheme 1.51).¹³⁹



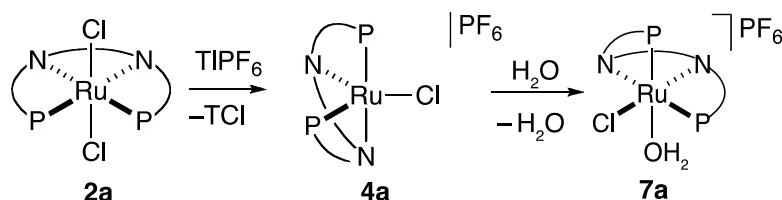
Scheme 1.51

Alternatively, complex **2a** reacts with 1 equiv of thallium(I) or silver(I) salts of noncoordinating anions to form the five-coordinate species $[\text{RuCl}(\mathbf{1a})]^+$ (**4a**).^{129,140}



Scheme 1.52 Activation of **2a** with Tl(I) or Ag(I) salts.

The six-coordinate aqua complex $[\text{RuCl}(\text{OH}_2)(\mathbf{1a})]^+$ (**7a**) was prepared by addition of water to the five-coordinate complex **4a**.^{140,141}



Scheme 1.53 Preparation of **7a** from **2a**.

NMR spectroscopic studies performed by Marco Ranocchiari revealed that the six-coordinate ether adduct $[\text{RuCl}(\text{OEt}_2)(\mathbf{1a})]^+$ is in equilibrium with the five-coordinate complex $[\text{RuCl}(\mathbf{1a})]^+$.^{142,143} The ³¹P NMR spectrum of $[\text{RuCl}(\text{OEt}_2)(\mathbf{1a})]\text{PF}_6$ (**3aPF₆**) at room temperature shows one broad signal at δ 41 ppm and some minor signals of impurities (Figure 1.11).

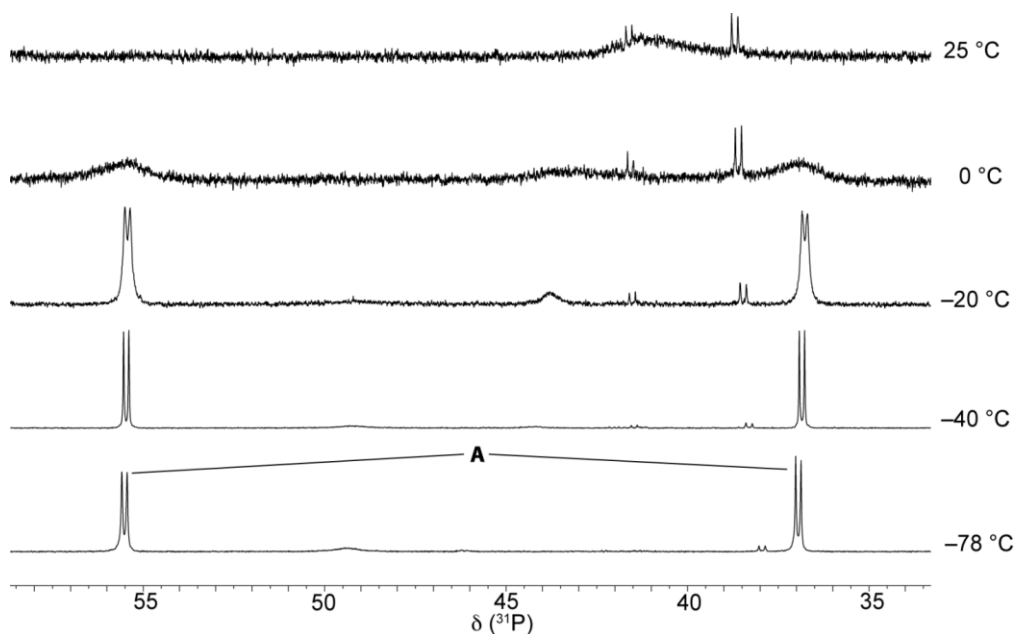
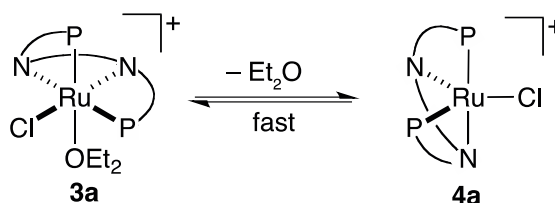


Figure 1.11 ^{31}P NMR spectra of $[\text{RuCl}(\text{OEt}_2)(\mathbf{1a})]\text{PF}_6$ at different temperatures.

Upon cooling the system, the signals resolved, and decoalescence was reached at $-20\text{ }^\circ\text{C}$. At $-78\text{ }^\circ\text{C}$, the sharp signals (A) of an AX pattern (a doublet δ 55.5 and 36.9, $^2J_{\text{P,P}'} = 29.5\text{ Hz}$) were observed (Figure 1.11). This indicated a dynamic equilibrium, probably due to the lability of the ether ligand. By analogy with the six-coordinate aqua complex $[\text{RuCl}(\text{OH}_2)(\mathbf{1a})]\text{PF}_6$ (**7a**), which rapidly dissociate the aqua ligand to give the five-coordinate $[\text{RuCl}(\mathbf{1a})]^+$ (**4a**), it was proposed that the dynamic process is an equilibrium between the ether adduct *cis*- β -**3a** and the five coordinate complex **4a**:

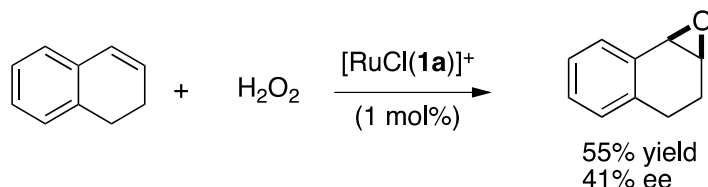


Scheme 1.54 Dynamic process involving **4a** and **3a**.

Our research group has explored the catalytic activity of the monocationic complexes $[\text{RuCl}(\text{L})(\text{PNNP})]^+$, where $\text{L} = \text{nil}, \text{OEt}_2, \text{or OH}_2$, in different reactions, such as the epoxidation and cyclopropanation of olefins. In these complexes, only one coordination site is available, either by ligand addition, as in $[\text{RuCl}(\mathbf{1a})]^+$, or by

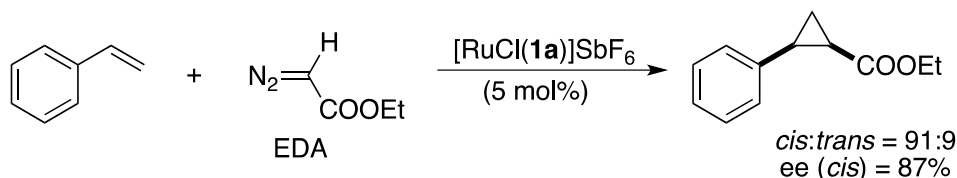
substitution of L, as in $[\text{RuCl}(\text{L})(\mathbf{1a})]^+$ (L = OEt_2 (**3a**) or OH_2 (**7a**)). Therefore, they are suitable to bind a monodentate, reactive ligand and to transfer it to the non-coordinated substrate.

$[\text{RuCl}(\mathbf{1a})]^+$ (**4a**) catalyzes the epoxidation of styrene and different functionalized olefins with H_2O_2 with enantioselectivities up to 41% ee:^{128,140,144}



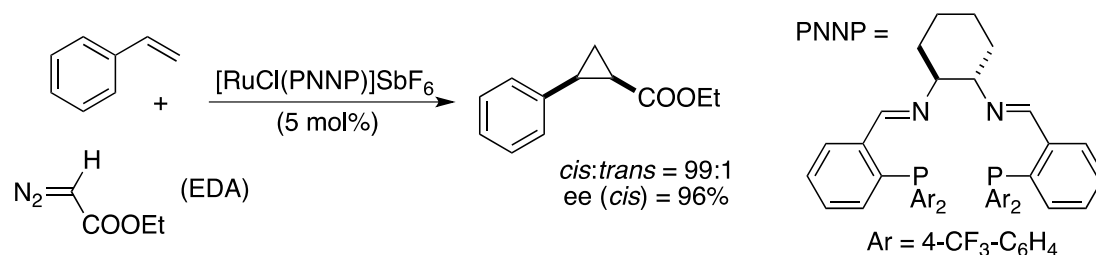
Scheme 1.55 Epoxidation of styrene catalyzed by $[\text{RuCl}(\mathbf{1a})]^+$ (**4a**).

Complex **4a** also catalyzes the selective *cis*-cyclopropanation of olefins with ethyl diazoacetate (EDA) as carbene source (Scheme 1.56).^{145,146}



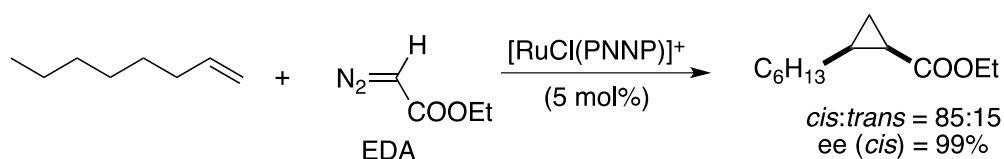
Scheme 1.56 *Cis*-cyclopropanation of styrene catalyzed by **4a**.

On the other hand, six-coordinate monocationic Ru/PNNP complexes, such as $[\text{RuCl}(\text{OH}_2)(\mathbf{1a})]^+$, *cis*- β - $[\text{RuCl}(\text{OEt}_2)(\mathbf{1a})]^+$, and $[\text{RuCl}(\text{PyNO})(\mathbf{1a})]^+$ (pyNO = pyridine-*N*-oxide) are active in the cyclopropanation of olefins with high *cis*-selectivity, but with lower diastereo- and enantioselectivity.^{129,147} Eventually, the best results were obtained with the five-coordinate complex and with a PNNP ligand bearing electron-withdrawing substituents on the phosphorus atoms:^{145,148}



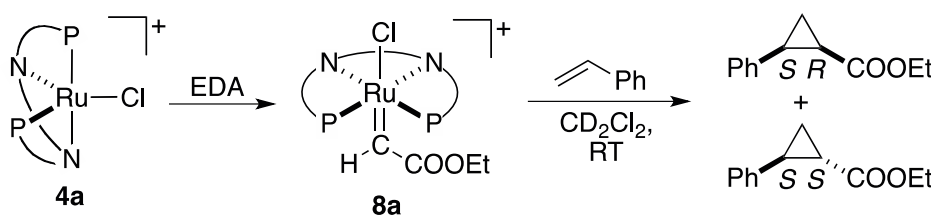
Scheme 1.57 *Cis*-cyclopropanation of styrene catalyzed by $[\text{RuCl}(\text{PNNP})]^+$.

The $[\text{RuCl}(\text{PNNP})]^+$ complex was also able to catalyze the *cis*-selective cyclopropanation of an aliphatic olefin, such as 1-octene, which was considered a difficult substrate for this reaction:¹⁴⁷



Scheme 1.58 *Cis*-cyclopropanation of 1-octene catalyzed by $[\text{RuCl}(\text{PNNP})]^+$ (See Scheme 1.57 for the definition of PNNP).

A carbene complex from the decomposition of EDA in the presence of the $[\text{RuCl}(\text{PNNP})]^+$ was prepared and characterized.¹⁴⁶ It was observed that this carbene species reacted instantaneously with the styrene (1 equiv) to give the corresponding cyclopropane:



Scheme 1.59 Formation of a carbene complex from the decomposition of EDA in the presence of the $[\text{RuCl}(\text{PNNP})]^+$.

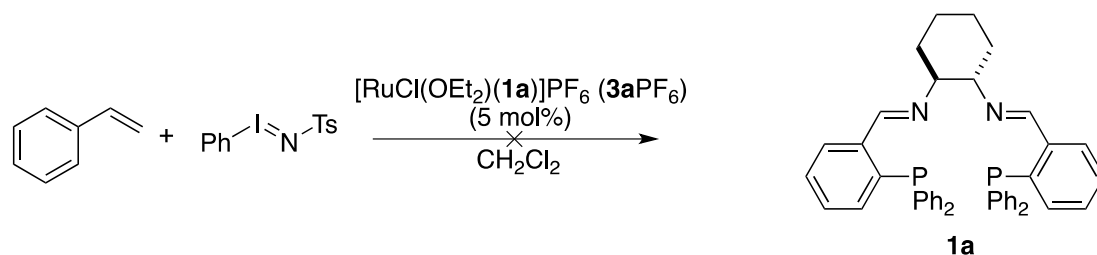
1.5.4 Asymmetric Imine Aziridination

1.5.4.1 Preliminary Studies: Olefin Aziridination

In view of the formal analogy with cyclopropanation by carbene transfer to an olefin, the cationic Ru/PNNP complexes were tested as catalysts in aziridine formation by nitrene transfer to olefins and carbene transfer to imines.¹³⁹

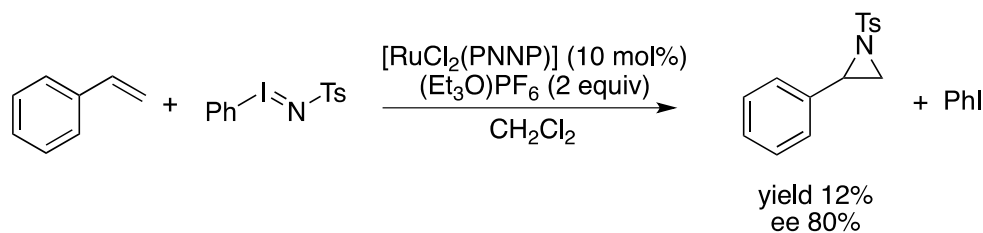
In a preliminary study, Marco Ranocchiaro, a former PhD student in our group, studied the catalytic activity of $[\text{RuCl}_2(\mathbf{1a})]$ ($\mathbf{2a}$) in olefin aziridination after either single or double chloride abstraction and in combination with phenyliodinane, tosyl

azide, and chloramine-T as nitrene sources. The monocationic $[\text{RuCl}(\text{OEt}_2)(\mathbf{1a})]^+$ ($\mathbf{3a}$) was not active in the presence of the highly reactive *N*-((*p*-toluenesulfonyl)imino)-phenyliodinane ($\text{PhI}=\text{NTs}$):



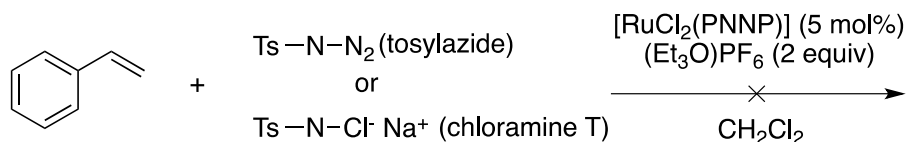
Scheme 1.60 Nitrene transfer to an imine in the presence of $[\text{RuCl}(\text{OEt}_2)(\mathbf{1a})]^+$ ($\mathbf{3a}$).

A first success was obtained with the dicationic complex $[\text{Ru}(\text{OEt}_2)(\text{PNNP})]^{2+}$. Upon double chloride abstraction from $[\text{RuCl}_2(\text{PNNP})]$ ($\mathbf{2a}$) with $(\text{Et}_3\text{O})\text{PF}_6$ (2 equiv), aziridine was formed in 12% yield and 80% ee:



Scheme 1.61 Catalytic aziridination by nitrene transfer from tosyl iodine with $[\text{Ru}(\text{PNNP})]^{2+}$ (See scheme 1.57 for the definition of PNNP).

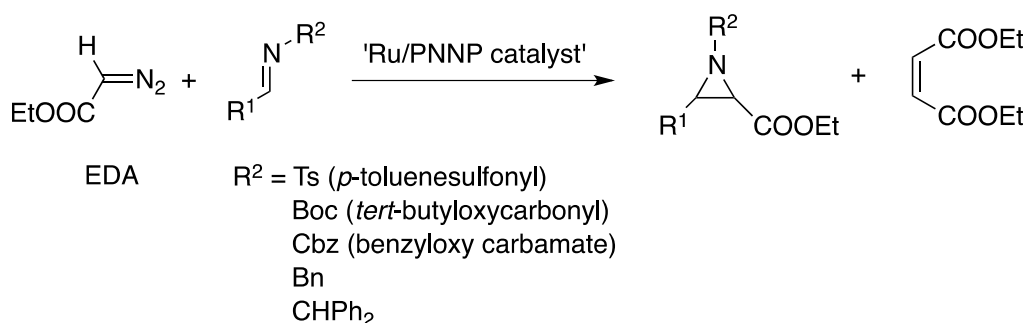
The substrate scope was limited to styrene, however. As for the nitrene source, the milder tosylazide and chloramine-T were ineffective:



Scheme 1.62 Catalytic aziridination by nitrene transfer from tosylazide and chloramines T with $[\text{Ru}(\text{Et}_2\text{O})_2(\text{PNNP})]^{2+}$ (See scheme 1.57 for the definition of PNNP).

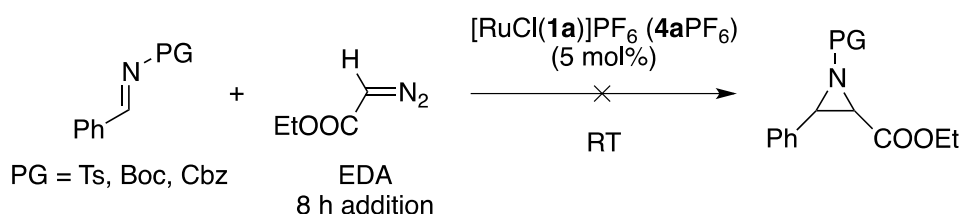
1.5.4.2 Imine Aziridination

The limitations concerning the substrate scope were not surprising, since several systems for nitrene transfer to olefin proved to be not versatile, being ineffective toward aliphatic imines, as already discussed in chapter 1.4.1. Due to these unsuccessful preliminary results, the attention was shifted to the alternative aziridination path, the carbene transfer from ethyl diazoacetate (EDA) to imines. This was a more interesting approach, since it gave access to 2-carboxy-aziridines, which are useful for the synthesis of α - and β - aminoacids. Thus, further efforts were directed to the study of the activity of Ru/PNNP complexes in the catalytic aziridination of imines bearing a very easily removable *N*-protecting group:



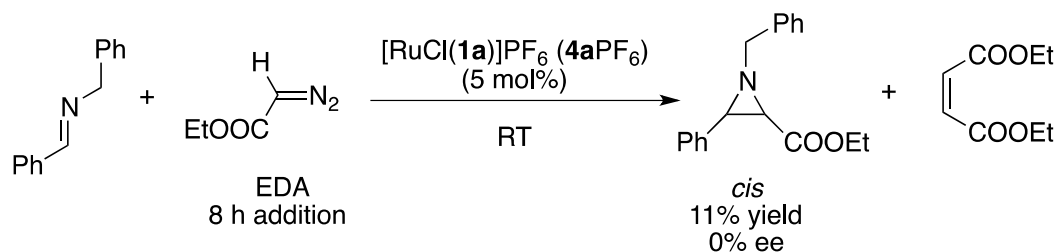
Scheme 1.63 General scheme for imine aziridination with ethyl diazoacetate.

These studies showed that, in the presence of $[\text{RuCl}(\mathbf{1a})]\text{PF}_6$ ($\mathbf{4aPF}_6$), imines bearing the electron-withdrawing groups Ts (*p*-toluenesulfonyl), Cbz (benzyloxy carbamate), and Boc (*tert*-butyloxycarbonyl) did not react to give aziridine:



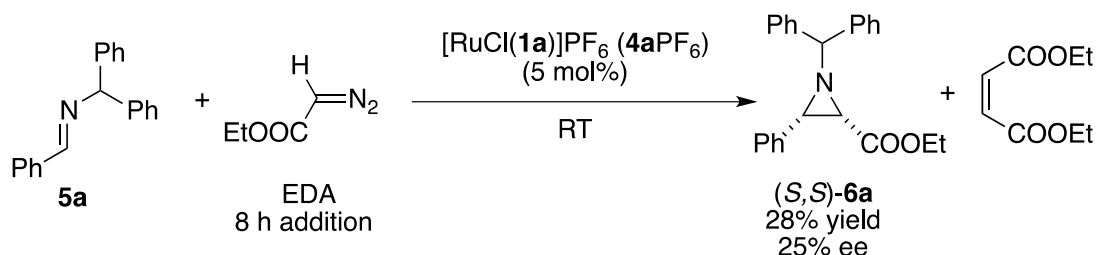
Scheme 1.64 Aziridination of different protected imines with ethyl diazoacetate in the presence of $[\text{RuCl}(\mathbf{1a})]\text{PF}_6$ ($\mathbf{4aPF}_6$).

In contrast, catalytic tests performed in presence of **4a**PF₆ with imines bearing the electron-donating benzyl *N*-protecting group led to the corresponding *cis*-aziridine in 11% yield, although without enantioselectivity:



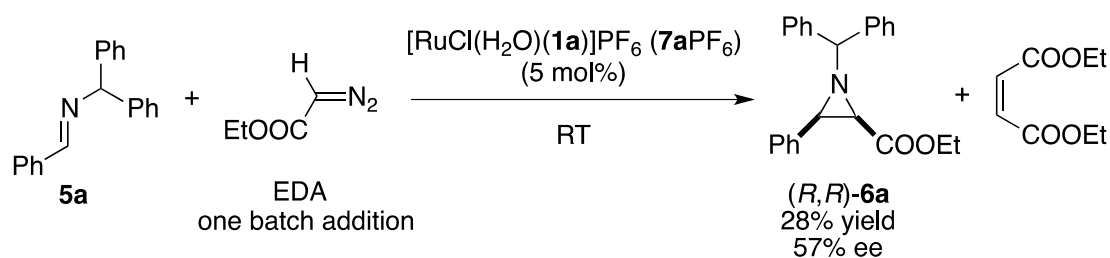
Scheme 1.65 Aziridination of a benzyl protected imine with ethyl diazoacetate in the presence of **4a**.

Finally, benzhydryl *N*-protected imines reacted with EDA to give (*S,S*)-**6a** with 28% yield and 25% ee:



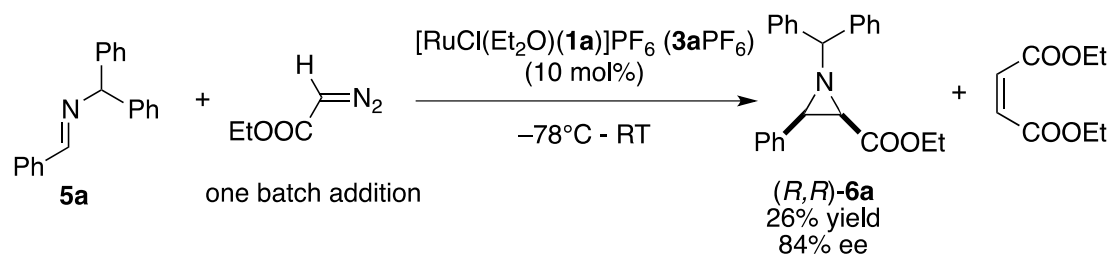
Scheme 1.66 Aziridination of a benzhydryl protected imine with ethyl diazoacetate in the presence of **4a**.

More encouraging results were obtained with the six-coordinate complexes $[\text{RuCl}(\text{L})(\mathbf{1a})]^+$ ($\text{L} = \text{OH}_2, \text{OEt}_2$). The coordination of oxygen donors such as water or diethyl ether is known to modify the catalytic activity and selectivity of the PNNP catalyst. Thus, the addition of water (4.6 equiv) to a solution of the five-coordinate complex **4a** led to increased yield (28%) and enantioselectivity (57% ee) of the (*S,S*)-ethyl-1-benzhydryl-3-phenylaziridine-2-carboxylate ((*S,S*)-**6a**) from *N*-benzylidene-1,1-diphenylmethanamine (**5a**) (Scheme 1.67).



Scheme 1.67 Aziridination of a benzhydryl protected imine with ethyl diazoacetate in the presence of **7a**.

On the other hand, the ether complex $[\text{RuCl}(\text{OEt}_2)(\mathbf{1a})]\text{PF}_6$ (**3aPF₆**), obtained from activation of **2a** with Et_3OPF_6 (1 equiv), catalyzed the aziridination of **5a** to give (*R,R*)-**6a** in 26% yield and 84% ee:



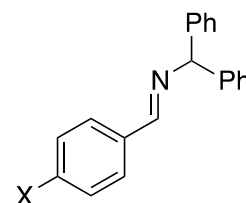
Scheme 1.68 Aziridination of a benzhydryl protected imine with ethyl diazoacetate in the presence of **3a**.

Aziridine *cis*-**6a** was formed only by following a strict temperature protocol. After the overnight activation of the dichloro complex **2a** at room temperature, imine **5a** was added to the reaction mixture at -78°C in an *i*-propanol/dry ice bath. Then, EDA (1 equiv) was added in one batch, and the reaction solution was warmed to room temperature and stirred for 3 h. If any of these temperature conditions was not fulfilled, only ethyl maleate was formed. The role of an addition of an excess of imine, EDA, or Et_2O was investigated, too. It was found that an excess of the reagent (imine and EDA), catalyst, or additive (direct addition of diethylether to the reaction mixture) led either to a reduction of the yield or to a drastic loss of the enantioselectivity. Finally, different imines with *p*-substituents were tested in the

presence of catalyst **3a** (5 mol%) (Table 1.1). No general trend concerning electronic effects was discovered, though.

Table 1.1

X	Aziridine yield (%)	ee (%)
H	25	77
OMe	3	-
F	10	84
CF ₃	11	30
Me	5	-
NMe ₂	0	-



In contrast, the aqua complex $[\text{RuCl}(\text{OH}_2)(\mathbf{1a})]^+$ (**7a**) (5 mol%) gave *cis*-aziridine **6a** with 18% yield and 61% ee. With the five-coordinate species $[\text{RuCl}(\mathbf{1a})]\text{PF}_6$ (**4aPF₆**), the enantioselectivity was also reduced (28% yield, 25% ee). The reaction was highly stereoselective as only *cis*-aziridine was formed. Diethylmaleate was the only byproduct observed in all the experiments. The most important results are summarized in Table 1.2.

Table 1.2 Catalytic Activity of Differently Activated $[\text{RuCl}_2(\mathbf{1a})]$ Complexes

Catalyst	Temperature protocol	Catalyst loading (mol%)	EDA addition	<i>cis</i> - 6a isolated yield (%)	(<i>R,R</i>)- <i>cis</i> - 6a ee (%)
$[\text{RuCl}(\text{OEt}_2)(\mathbf{1a})]^+$ (3a)	-78 °C - RT	5	one batch	25	77
	-78 °C - RT	10	one batch	26	84
	RT	5	one batch	0	-
$[\text{RuCl}(\text{OH}_2)(\mathbf{1a})]^+$ (7a) ^a	RT	5	one batch	25	57
$[\text{RuCl}(\mathbf{1a})]^+$ (4a)	RT	5	8 h	28	-25 ^b

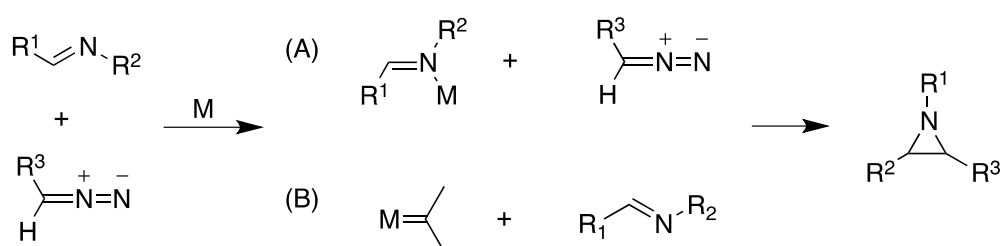
^a Obtained with the addition of an excess of H₂O (4.6 equiv).

^b (*S,S*)-*cis*-**6a** formed instead of (*R,R*)-*cis*-**6a**.

Interestingly, with catalysts **3a**PF₆ and **7a**PF₆, aziridine *cis*-**6a** was formed with the inverse absolute configuration compared to the one obtained with **4a**PF₆. This might be a hint for a possible different mechanism.

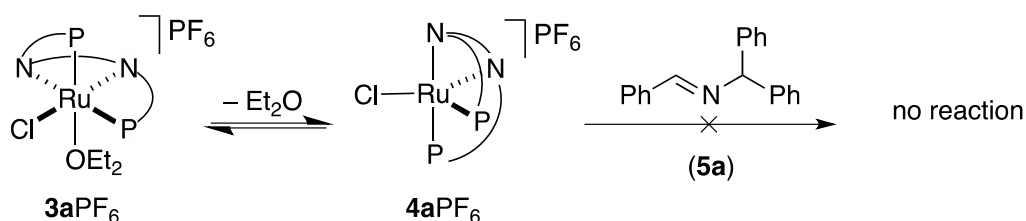
1.5.4.3 Spectroscopic Studies and Mechanistic Considerations

NMR spectroscopic studies were performed in order to get insight into the reaction mechanism.¹³⁹ As mentioned above, two reaction paths have been suggested for carbene transfer to imines:



Scheme 1.69 Two general reaction paths for carbene transfer to imines.

The first path, which is the Lewis-acid activation of the imine, was strongly disfavored by several observations. In particular, imine **5a** did not react with [RuCl(**1a**)]⁺ (**4a**) even at low temperature:

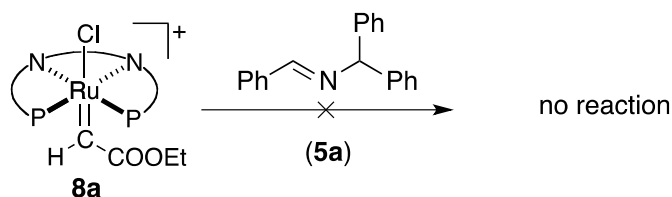


Scheme 1.70 Reaction of imine **5a** with the five-coordinate complex **4a**.

Moreover, no enaminoesters were formed as by-product in the catalytic runs described above, as usually observed in the Lewis-acid catalyzed imine aziridination.¹⁰⁹

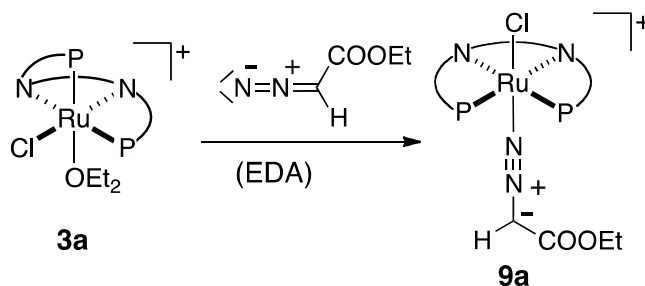
On the other hand, the carbene complex *trans*-[RuCl(CHCOOEt)(**1a**)]⁺ (**8a**),

prepared from **3a**PF₆ and EDA (1 equiv), did not react with imine **5a** to give aziridine **6a**:



Scheme 1.71 Reaction of imine **5a** with the carbene complex **8a**.

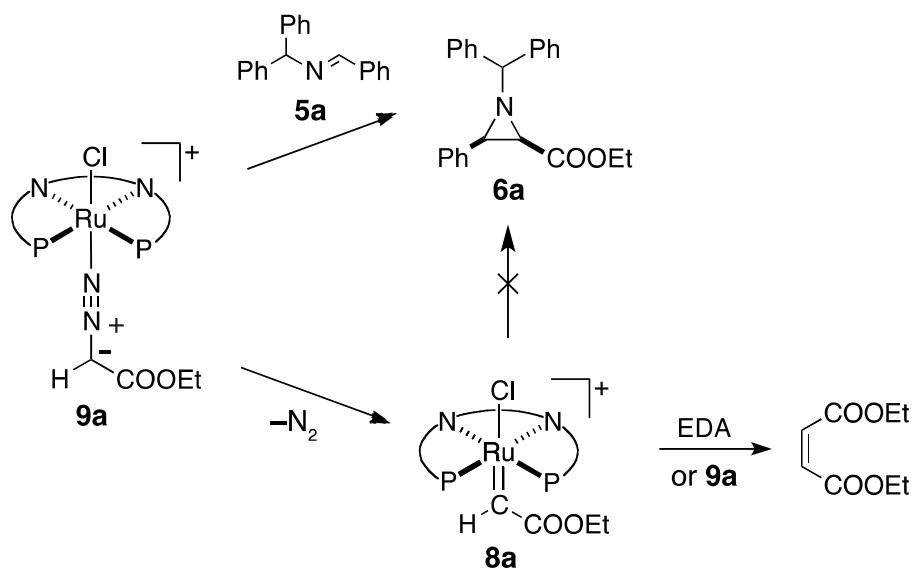
As the above results ruled out both path A (Lewis acid activation of the imine) and path B (reaction of a carbene complex with the free imine), low temperature ¹H, ¹³C, ³¹P, and ¹⁵N NMR spectroscopic studies were performed with the labeled diazoesters N₂¹³C(H)COOEt (2-¹³C-EDA) and ¹⁵NNC(H)COOEt (¹⁵N-EDA). When *cis*-[RuCl(OEt₂)(**1a**)]⁺ (**3a**) was treated with EDA in excess at -78 °C, the EDA complex *trans*-[RuCl(N₂C(H)COOEt)(**1a**)]⁺ (*trans*-**9a**) was formed as the major product:



Scheme 1.72 Formation of a *trans*-diazoester complex **9a**.

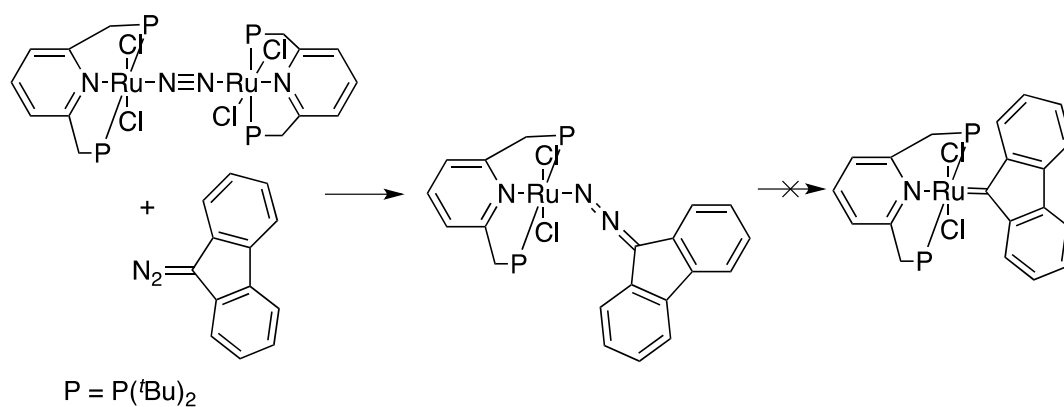
This EDA complex (**9a**) reacts with imine **5a** to give aziridine **6a** as cyclization product. After EDA is consumed, it decomposes to the corresponding carbene complex **8a** (Scheme 1.73). Further experiments showed that the carbene complex **8a** reacts with EDA to give diethyl maleate, which is the only byproduct formed during the catalytic runs. Therefore, the formation of the carbene complex **8a** from **9a** is responsible for the production of maleate and the low aziridine yield. Thus, the chemoselectivity of the reaction is controlled by the difference between the rate of the decay of the EDA complex **9a** to the carbene **8a** and the rate of the reaction of **9a** with the imine. The slower the decay to carbene, the higher is the selectivity for

aziridine:



Scheme 1.73 Reactivity scheme for the diazoester complex **9a**.

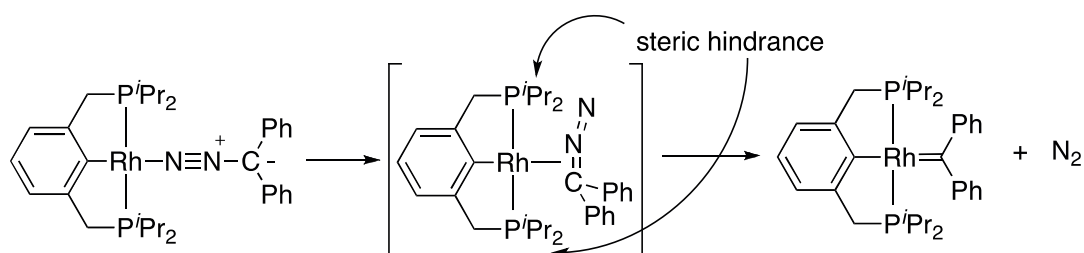
It is well established in the literature that steric factors influence the decay of diazoalkane complexes to the corresponding carbene complexes. Milstein¹⁴⁹ has reported diazoalkane complexes of ruthenium with PNP pincer ligands bearing *tert*-butyl groups on the phosphines :



Scheme 1.74 Formation of stable ruthenium diazocomplexes with bulky PNP pincer ligand.

Calculations suggested that the formation of the carbene complex from the diazoalkane analogue requires the change of the coordination mode of the diazoalkane

from *end-on* to η^2 -N,N and, eventually, to η^2 -N,C. The latter complex undergoes N₂ extrusion and forms the carbene:



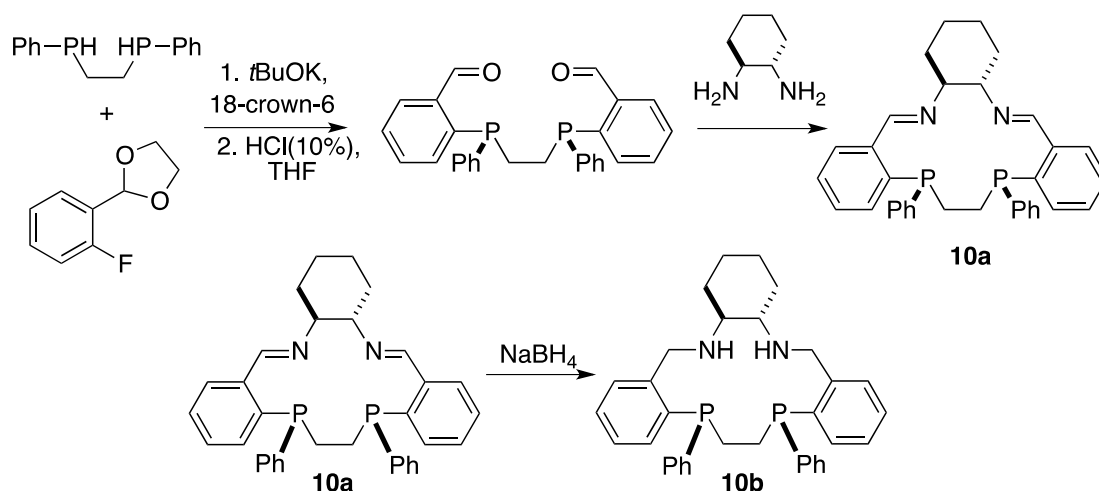
Scheme 1.75 Formation of a carbene complex from the corresponding diazoalkane analogue.

It was concluded that the combined steric bulk of the P^tBu₂ groups and the diazofluorene ligand hinders the η^2 -N,C coordination of the latter and hence the formation of a carbene complex.¹⁵⁰

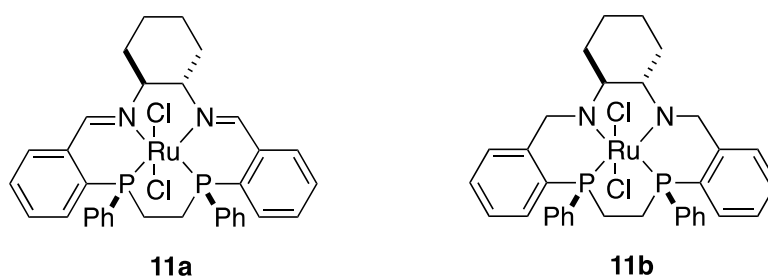
With these results in mind, Marco Ranocchiari suggested that macrocyclic PNNP ligands, because of the higher conformational rigidity than their open chain analogues, might represent a possibility to stabilize the diazoalkane complex **9a**.

1.6 Macrocyclic PNNP Ligands

Chiral macrocyclic ligands containing P and N donors are potentially interesting for asymmetric catalysis as they are expected to form stable and conformationally rigid complexes. Moreover, they are analogous to open-chain P₂N₂ ligands, which have found application in hydroxylation,^{129,130} fluorination,¹³¹⁻¹³³ and Michael reaction¹³⁴⁻¹³⁶ of β -ketoesters, epoxidation^{128,140,144} and cyclopropanation^{145,146} of olefins, and in the transfer hydrogenation of ketones either in combination with ruthenium¹²⁶ or with iron.¹⁵¹ However, owing to the challenges posed by their synthesis, they are still rare.¹⁵² Our group developed a straightforward synthesis to the first chiral macrocyclic PNNP (**10a**), which was easily reduced to its diamino analogue **10b** (Scheme 1.76) and prepared their ruthenium(II) dichloro complexes (**11a**, **11b**) (Scheme 1.77).¹⁵³

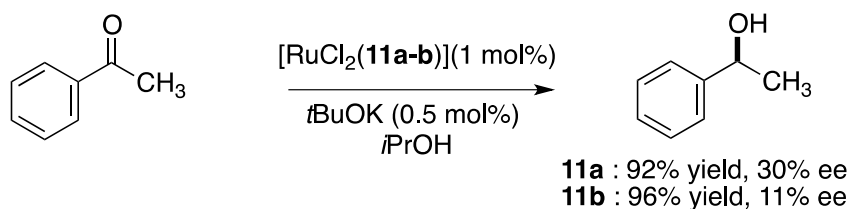


Scheme 1.76 Synthetic method for the preparation of C_1 -symmetric macrocyclic PNNP.



Scheme 1.77 Ruthenium dichloro complexes with C_1 -symmetric macrocyclic PNNP.

The diimino complex **11a** and **11b** catalyze the transfer hydrogenation of acetophenone to 1-phenylethanol with modest enantioselectivity of 30% and 11% ee, respectively:



Scheme 1.78 Transfer hydrogenation of acetophenones catalyzed by **11a** and **11b**.

The low enantioselectivity was not surprising in view of the pseudo *meso* relationship between the P atoms in the C_1 -symmetric diastereoisomer. Therefore, the synthesis of C_2 -symmetric P_2N_2 chiral macrocycles and the use of their ruthenium complexes in asymmetric imine aziridination were set as next goal.

1.7 Rationale of the Project

The above results suggest that, to increase the aziridine yield, the decomposition of the EDA complex must be slowed down as compared to decay of the diazoester complex to carbene. As ruthenium complexes with conformationally rigid macrocyclic ligands seemed to be suitable to this purpose, our primary goal was the synthesis of novel C_2 -symmetric macrocyclic ligands:

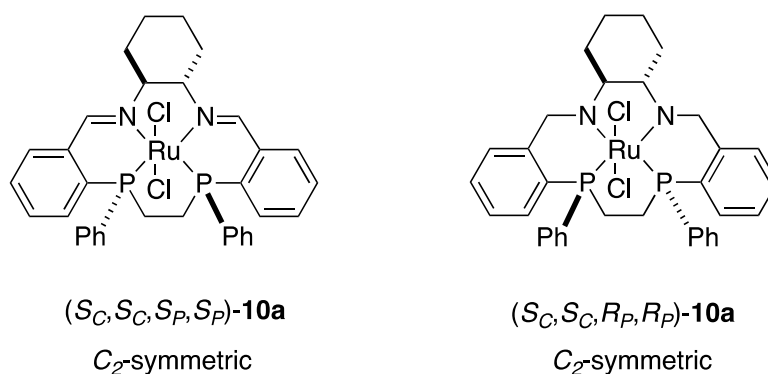


Figure 1.12 C_2 -symmetric macrocyclic PNNP ligands.

The strategies developed to prepare C_2 -symmetric PNNP macrocycles and the difficulties encountered are described in Chapter 4 of this thesis. Eventually, we decided to explore a simpler possibility of stabilizing the diazoester adduct, that is, the use of bulky open-chain PNNP ligands. To this purpose, a new series of open PNNP ligands was prepared, which contain bulky substituents on the phosphine groups (Figure 1.13).

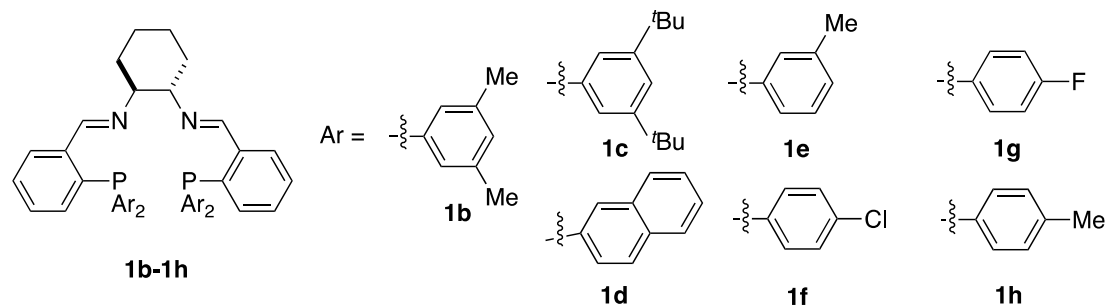
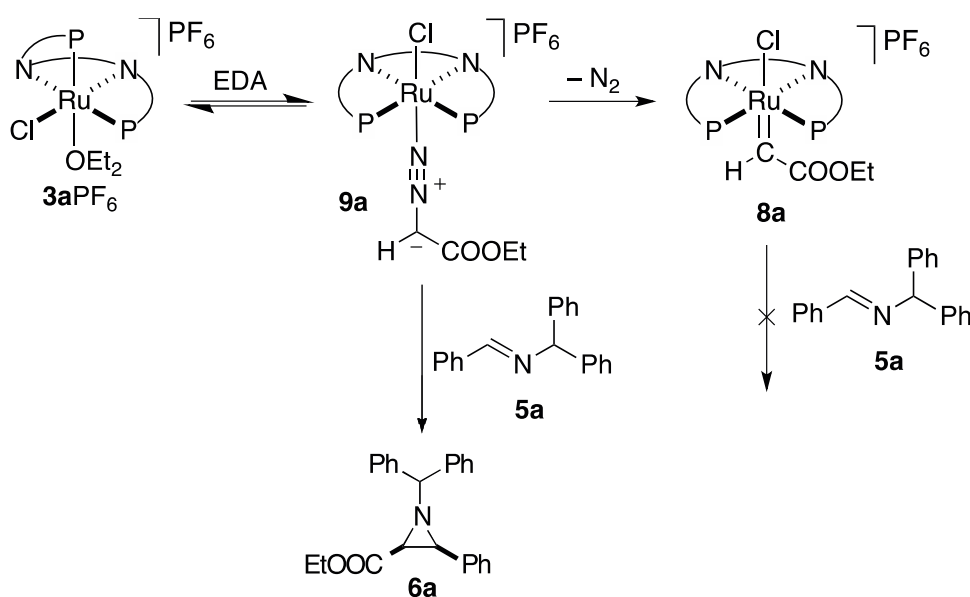


Figure 1.13 Open PNNP ligands containing bulky substituents on the phosphine groups.

The preliminary screening of the new ligands showed that complexes with ligands bearing substituents in the *meta* position of the aryl rings (**2b-2h**) give aziridine with high yields. The optimization of the most promising catalyst **2b** led to the discovery of the noninnocent role of the counterion, as it was found that the PF_6^- anion undergoes hydrolysis, as described in the next chapter. The use of a nonhydrolyzable anion, such as BF_4^- , which led to an increase of the yield and enantioselectivity of the aziridination, is discussed in Chapter 3, together with additional mechanistic investigations and the study of the substrate scope.

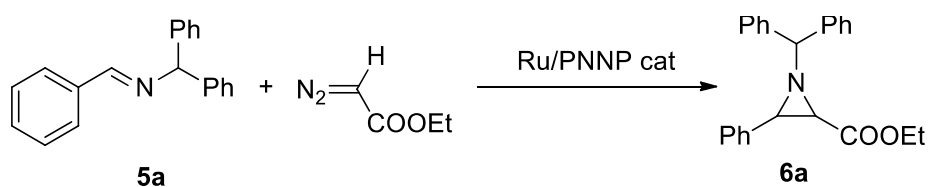
2. Substituted PNNP Ligands for Ru-Catalyzed Imine Aziridination

As discussed in paragraph 1.5, our group has investigated the possibility of using Ru(II)/PNNP cationic complexes in asymmetric imine aziridination. As a result of this study, a new aziridination mechanism was suggested,¹³⁹ in which the rate of decomposition of the diazoester adduct (**9a**) to the corresponding carbene complex (**8a**) controls the chemoselectivity of the reaction:



Scheme 2.1 Proposed mechanism for imine aziridination with Ru/PNNP catalysts.

As studies performed by Milstein^{149,150} showed that sterically hindered PNP ligands inhibit the decomposition of the diazoester complex into the carbene analogue, we decided to introduce bulky substituents on the phenyl rings of the phosphorus atoms of the open-chair PNNP ligands. This chapter will focus on the preparation of a new series of substituted PNNP ligands and on the use of their ruthenium complexes in the catalytic carbene transfer from a diazoester to an imine, such as **5a**. The aim was the study of the steric and electronic effects of differently substituted ligands on the yield and enantioselectivity of the aziridination reaction (Scheme 2.2).



Scheme 2.2 Aziridination reaction of imine **5a** with ethyl diazoacetate.

To this purpose, a new optimization of the catalytic conditions and some preliminary NMR spectroscopic studies were performed.

2.1 [RuCl(OEt₂)(PNNP)]PF₆ as Catalyst: New Substituted Ligands

2.1.1 Synthesis of the PNNP Ligands

The general synthetic method reported in Scheme 2.3 has been extensively used in our group for the preparation of different PNNP ligands such as the following:^{129,145,147}

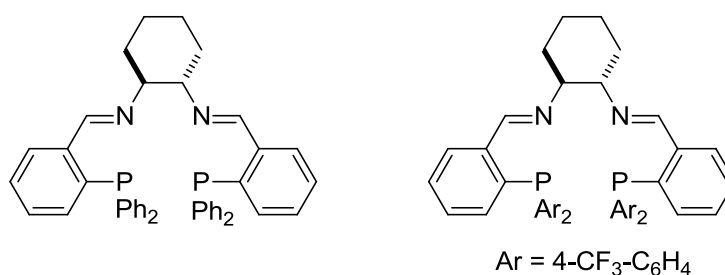
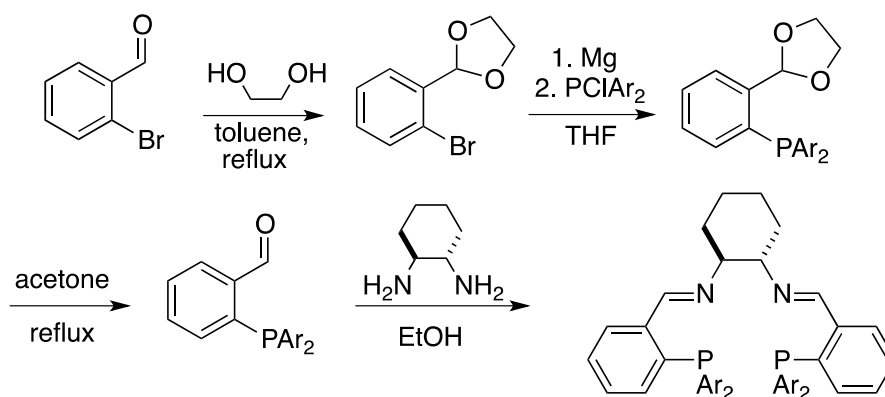


Figure 2.1 Examples of open-chain PNNP ligands.



Scheme 2.3 General method for the preparation of open-chain PNNP ligands.

This four-step procedure was used to prepare a series of open-chain PNNP ligands with different substituents on the phenyl rings of the phosphorus atoms (**1b-1h**):

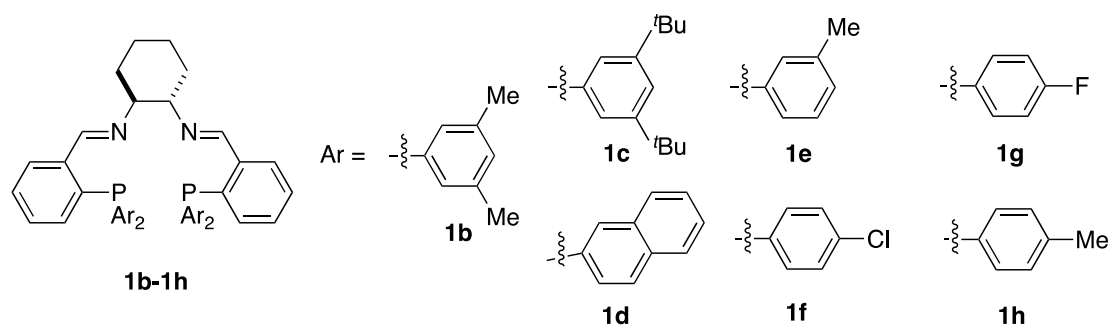
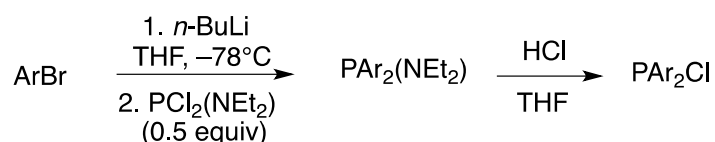


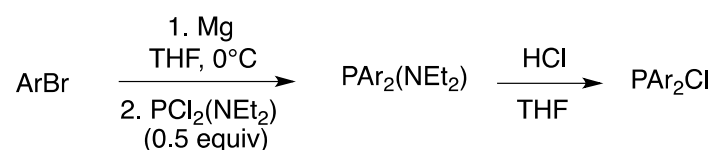
Figure 2.2 Open-chain PNNP ligands with substituents in the *meta* e *para* positions of the aryl groups.

The chlorodiarylyphosphines PClAr_2 used as starting material are, when commercially available, generally expensive. Therefore, they were often prepared from the corresponding cheap arylbromide by the following lithiation method:



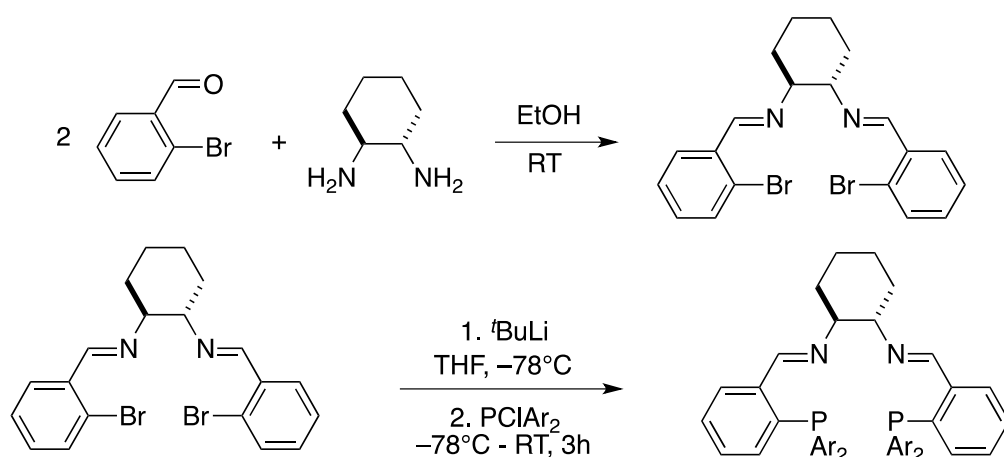
Scheme 2.4 General method for the preparation of chlorodiarylyphosphines via lithiation (See Figure 2.2 for the definition of Ar).

Other synthetic procedures might be combined to prepare the desired ligand. For instance, the diarylphosphine can be formed via a less sensitive Grignard route, which is, however, longer and requires an additional intermediate filtration:^{154,155}



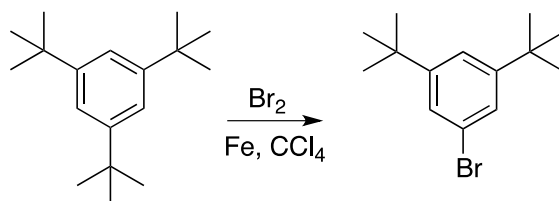
Scheme 2.5 General method for the preparation of PAR_2Cl via Grignard reagent.

A different synthetic approach exploits the dibromide intermediate shown in Scheme 2.6. This procedure is faster and limits the use of air-sensitive reagents to the very last step of the introduction of the PAr_2 moiety, which allows an easier manipulation. On the other hand, this step is very sensitive to air, water, and impurities. Therefore, it requires the use of highly pure PClAr_2 , which is not always easily accessible. Moreover, it is not suitable for scaling up. For these reasons, the synthetic approach presented in Scheme 2.3 was generally used.



Scheme 2.6 General method for the preparation of open-chain PNNP ligands.

In the case of the very bulky disubstituted 3,5-di-*tert*-butyl ligand (**1c**), a modified procedure was necessary. The 3,5-di-*tert*-butyl bromide was obtained easily from 1,3,5-tri-*tert*-butyl-benzene:



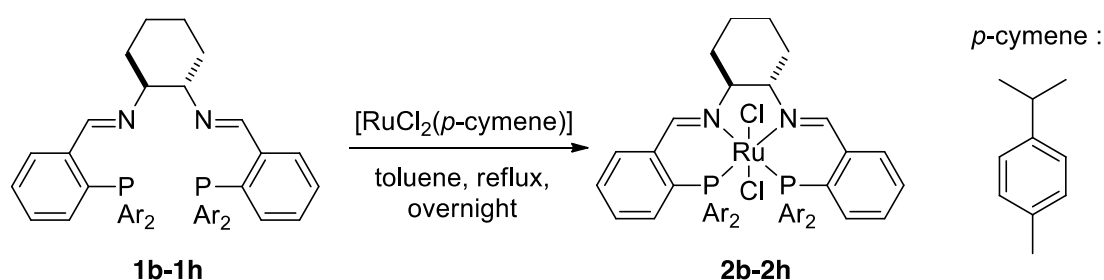
Scheme 2.7 Komen and Bickelhaupt synthesis of 3,5-di-*tert*-butyl bromide.

The bromination reaction reported by Komen and Bickelhaupt¹⁵⁴ worked properly, but involved the use of highly toxic tetrachloromethane and elemental bromine. 1-Bromo-3,5-di-*tert*-butylbenzene failed to form the corresponding Grignard reagent with magnesium, as already reported by RajanBabu,^{155,156} probably because

of the steric bulk of the *tert*-butyl groups. Therefore, the harsher lithiation procedure reported in Scheme 2.4 was used to prepare bis(3,5-di-*tert*-butylphenyl)chlorophosphine, which was then employed for the synthesis of ligand **1c** according to Scheme 2.6.

2.1.1 [RuCl₂(PNNP)] Complexes

The above ligands (**1b-1h**) were used to prepare the corresponding dichloro complexes [RuCl₂(**1b-1h**)] (**2b-2h**):



Scheme 2.8 Preparation of dichloro ruthenium complexes with open-chain PNNP ligands.

As ruthenium precursor, [RuCl₂(*p*-cymene)]₂ was used instead of [RuCl₂(PPh₃)₃], because of the easier removal of the *p*-cymene from the mixture in comparison to triphenylphosphine. No crystal structure analyses were performed, but the dichloro complexes (**2b-2h**) were otherwise completely characterized. Their ³¹P NMR spectra exhibited a singlet in agreement with the reported Ru/PNNP complexes.^{129,145} The multiplicity and chemical shifts of these signals support the *trans* configuration. The only exception was the 3,5-di-*tert*-butyl substituted complex (**2c**), which exhibited the signals of three species around δ 51, that is, two singlets at δ 51.1 and 51.5 and an AB system at δ 51.8 and 50.7 (²J_{P,P'} = 27.9 Hz) (Figure 2.3).

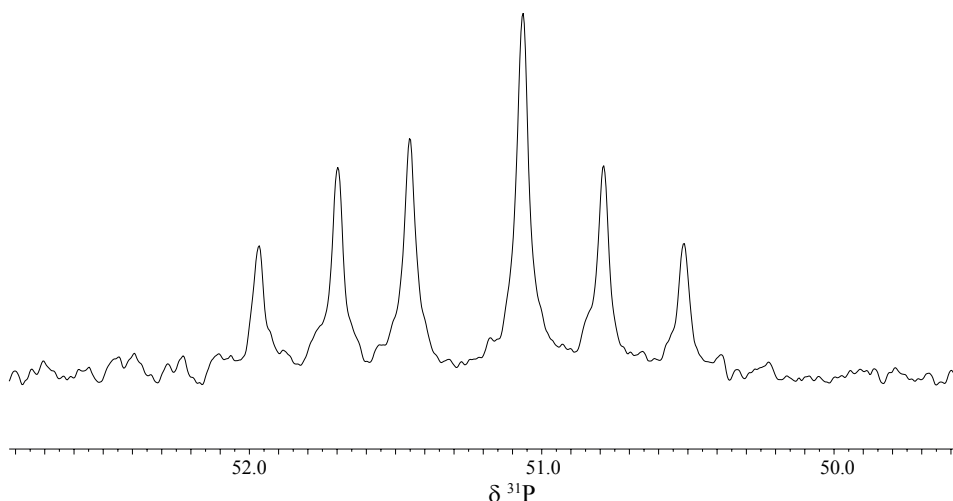
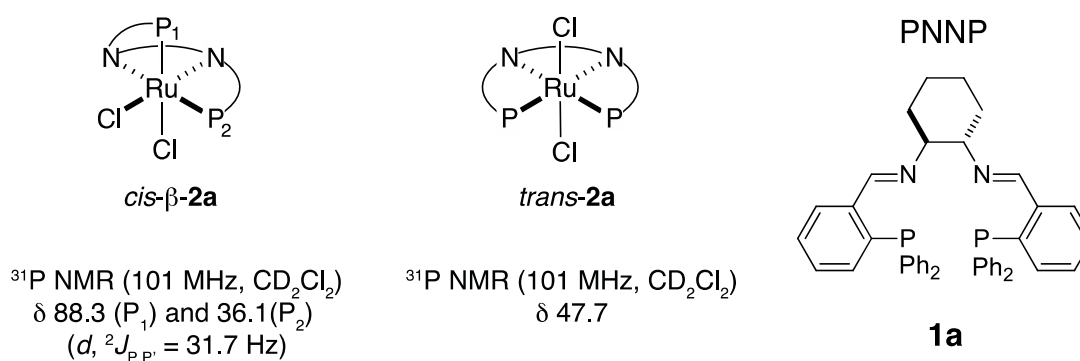


Figure 2.3 $^{31}\text{P}\{^1\text{H}\}$ spectrum (162.0 MHz, CDCl_3 , RT) of $[\text{RuCl}_2(\mathbf{1c})]$ (**2c**), exhibiting two singlets at δ 51.1 and 51.5 and an AB system at δ 51.8 and 50.7.

The multiplicity of these signals indicates the presence of two C_2 -symmetric and one C_1 -symmetric species. On the basis of the chemical shifts,^{128,140} the presence of *cis*- β isomers was ruled out and we excluded the *cis*- α isomers, too, as their formation is strongly energetically disfavored and was never observed.¹²⁸ In fact, the chemical shifts are in agreement with a phosphorus in *trans* position to a nitrogen atom:



Scheme 2.9 ^{31}P NMR chemical shift for *cis*- β and *trans* isomers of $[\text{RuCl}_2(\mathbf{1a})]$.

For a better understanding of the system in solution, an HMQC spectrum was measured (Figure 2.4).

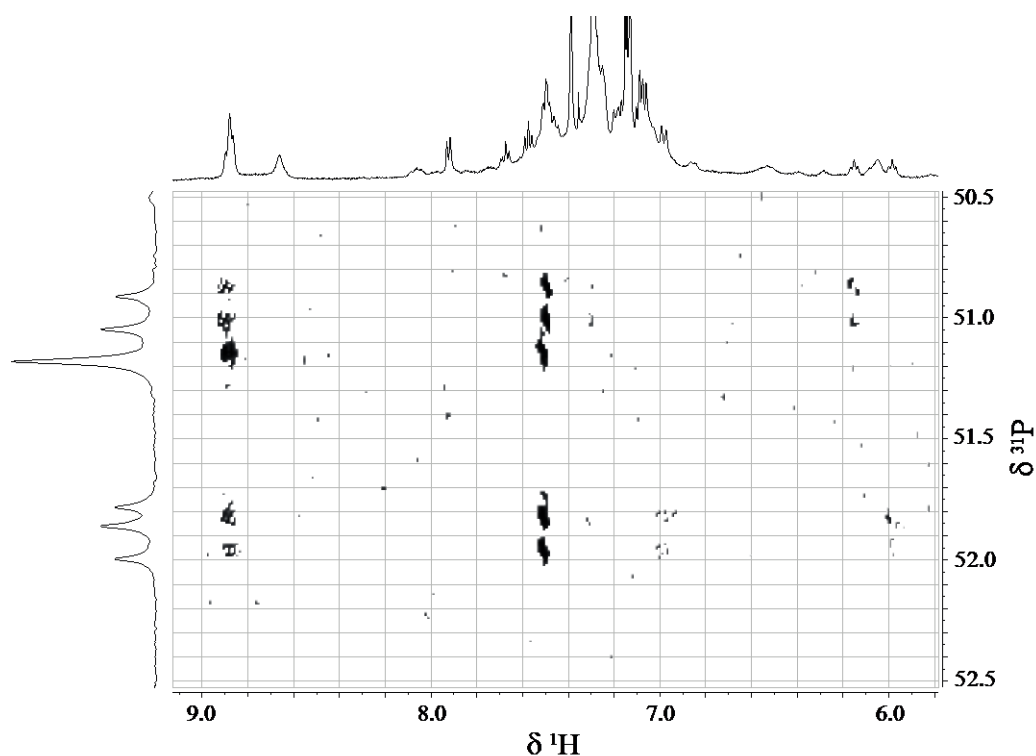
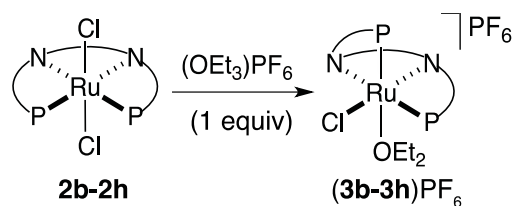


Figure 2.4 HMQC (500 MHz, CD_2Cl_2) of $[\text{RuCl}_2(\mathbf{1c})]$ ($\mathbf{2c}$).

In this 2D heteronuclear spectrum the imine protons of the ligand couple with all the phosphorus peaks, suggesting that the species in solution are rapidly exchanging at room temperature. On the basis of the above evidence, we suggest that the species observed are *trans* complexes, two of C_2 - and one of C_1 -symmetry. The loss of the C_2 -axis of symmetry can be caused by the 3,5-di-*tert*-butyl group on the phosphines. The distortion of the molecular geometry induced by the presence of substituents on the aryl groups of the phosphines has already been reported by Cristina Bonaccorsi in case of the 3,5-di-trifluoromethyl substituted ligand.¹²⁹

2.1.2 Activation of the Dichloro Complexes $[\text{RuCl}_2(\mathbf{1b-1h})]$ ($\mathbf{2b-2h}$)

As 18 electron species, the dichloro ruthenium complexes $[\text{RuCl}_2(\mathbf{1b-1h})]$ ($\mathbf{2b-2h}$) are coordinatively saturated and kinetically inert. The corresponding active complexes were obtained by single chloride abstraction with different chloride scavengers (1 equiv). The ether adducts $[\text{RuCl}(\text{OEt}_2)(\mathbf{1b-1h})]^+$ ($\mathbf{3b-3h}$) were typically formed by chloride abstraction from the dichloro complexes $\mathbf{2b-2h}$ with a triethyloxonium salt such as $(\text{Et}_3\text{O})\text{PF}_6$ (Scheme 2.10).

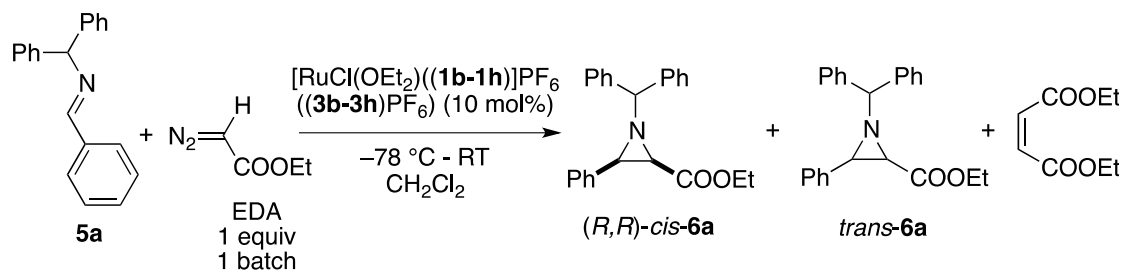


Scheme 2.10 Activation of ruthenium dichloro complexes by chloride abstraction with $(\text{Et}_3\text{O})\text{PF}_6$ to give the six-coordinate ether analogues.

In the case of $(\text{Et}_3\text{O})\text{PF}_6$ as scavenger, the chloride abstractor serves also as ether source. Chloroethane was formed as the only side product, in contrast to the activation with Tl(I) or Ag(I) salts, which formed insoluble TlCl or AgCl. The activation was usually performed overnight in dichloromethane as solvent at room temperature by using $(\text{Et}_3\text{O})\text{PF}_6$ (1 equiv) as chloride scavenger. A complete characterization of the monocationic complexes $[\text{RuCl}(\text{OEt}_2)(\mathbf{1b-1h})]\text{PF}_6$ (**(3b-3h)PF₆**) was not performed, but the reaction was assumed to proceed in analogy with the unsubstituted complex $[\text{RuCl}_2(\mathbf{1a})]$ (**2a**), where a change in the solution color from dark red to brown is observed. It has to be noted that the ether adduct $[\text{RuCl}(\text{OEt}_2)(\mathbf{1a})]^+$ (**3a**) dissociates at room temperature to give the corresponding five-coordinate $[\text{RuCl}(\mathbf{1a})]^+$ (**4a**), which is catalytically active (See 2.1.3.1 below).¹⁴²

2.1.3 Preliminary Catalytic Results in Imine Aziridination

The putative complexes $[\text{RuCl}(\text{OEt}_2)(\mathbf{1b-1h})]\text{PF}_6$ (**(3b-3h)PF₆**) were tested in the asymmetric aziridination of *N*-benzylidene-1,1-diphenylmethanamine (**5a**) with EDA. The reactions were performed under the optimized conditions discussed in the introduction (§ 1.5.4.2):



Scheme 2.11 Aziridination reaction for the screening of different ligands.

A CH₂Cl₂ solution of the catalyst was cooled to -78 °C, then imine **5a** and EDA were successively added in one batch. After 5 minutes, the reaction solution was warmed to room temperature and stirred for 4 h, during which it was monitored by TLC. Then, the solvent was removed, and 1,3,5-trimethoxybenzene was added in weighted amounts as internal standard. The ¹H NMR spectra of the reaction crude were recorded, and NMR yields were calculated on the basis of the internal standard. Afterwards, the crude mixture was purified by column chromatography, and the aziridine *cis*-**6a** was isolated as a crystalline solid, whose purity was confirmed by ¹H NMR spectroscopy. To establish the chemoselectivity of the reaction, the presence of side products was quantified by integration of the ¹H NMR spectra, as well. Maleate was found to be the prominent by-product, but also *trans*-aziridine (*trans*-**6a**) was detected. During the purification procedure, aziridine *trans*-**6a** was eluted with the unreacted imine **5a**, whereas *cis*-**6a** was obtained as an uncontaminated crystalline solid. The enantiomeric excess of *cis*-**6a** was measured by chiral HPLC and the retention times were compared with those measured by Marco Ranocchiari.¹³⁹ The results of this first screening of complexes **3b-3h** are summarized in Table 2.1.

Table 2.1 Imine Aziridination Catalyzed by [RuCl(OEt₂)(**1a-1h**)]PF₆ (**3b-3h**) (Temperature Gradient Method).

Entry	Ligand	conv. 5a (%)	maleate (%) (NMR)	<i>cis</i> - 6a (%) (NMR)	<i>cis</i> - 6a (%) (isolated)	ee (%) <i>cis</i> - 6a	<i>cis/trans</i> 6a (NMR)
1 ^a	1a (4-H)				26	84	100:0
2	1b (3,5-diMe)	100	19	84	80	3	85:15
3	1c (3,5-di ^t Bu)	40	13	18	13	1	-
4	1d (2-napht)	74	28	65	65	2	90:10
5	1e (3-Me)	95	9	72	70	3	87:13
6	1f (4-Cl)	19	91	3	-	-	-
7	1g (4-F)	10	82	4	-	-	-
8	1h (4-Me)	67	52	8	-	-	-
9	1i (4-CF ₃)	34	93	1	-	-	-

¹ Results reported by Marco Ranocchiari.¹³⁹

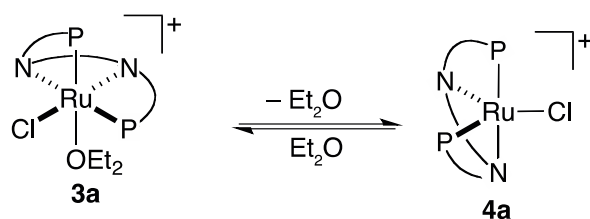
The introduction of substituents into the PPh₂ groups of the PNNP ligands led to drastic changes of the reaction outcome as compared to the results obtained with the unsubstituted ligand **1a** (entry 1).¹³⁹ The most striking common feature of the catalytic results with the substituted PNNP ligands is the nearly total loss of enantioselectivity for the formation of *cis*-**6a**. By increasing the steric bulk (entries 2-5), aziridine *cis*-**6a** was formed in higher yields, though. In particular, with ligands substituted in the *meta* position of the PAR₂ groups, *cis*-**6a** was obtained with high isolated yields (>65%) (entries 2, 4, and 5). The best result (80% isolated yield) was achieved with the 3,5-dimethyl substituted ligand **1b**. In runs 2 and 4, imine **5a** was almost quantitatively converted, but it was not possible to identify the other byproducts formed from the ¹H NMR spectra of the crude. On the other hand, ligands bearing substituents in the *para* position, such as *p*-Cl, *p*-F, *p*-Me, and *p*-CF₃, reduced drastically the yield (entries 7-11). In those catalytic runs, the presence of large amounts of unreacted **5a** was observed in the ¹H NMR spectra of the crude mixture. The very bulky ligand *tert*-butyl substituted **1c** (entry 3) gave low yields (18%), probably because of the extreme steric hindrance present on the complex.

With all ligands, the *cis*-stereoselectivity was maintained, with a *cis/trans* ratio of 85:15 in the worst case for ligand **1b**. These catalysts are less diastereoselective than **3a**PF₆, where no signals for the *trans* isomer were detected in the ¹H NMR spectra of the crude reaction mixture. On this topic, we note that apparent high diastereoselectivity has been reported for some Lewis acid catalysts^{157,158} that decompose stereospecifically the *trans* isomer, but this is not the case here, as *trans*-aziridine has been observed in the reaction crude (see above).

The high yields obtained with **1b**, **1d**, and **1e** were an encouraging result in spite of the absence of enantioselectivity. Therefore, different catalytic conditions were tested for a new optimization of the aziridination reaction with complexes **2b-2e** in order to reestablish the enantioselectivity.

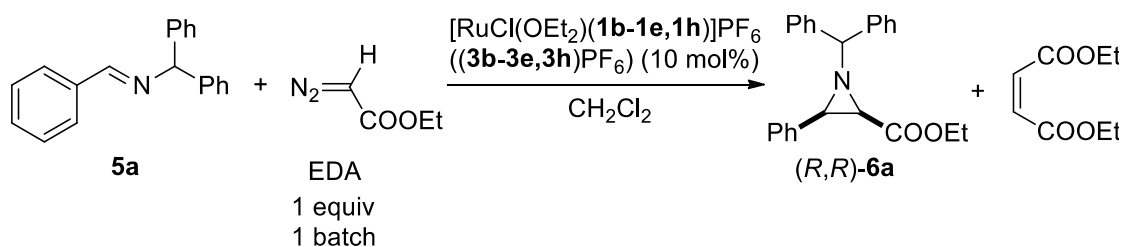
2.1.2.1 Temperature Effect

In our group, Christoph Schotes previously found out that the ether complex **3a** is in equilibrium with the five-coordinate system **4a** (Scheme 2.12).¹⁴² Upon decreasing the temperature, the equilibrium shifts towards the ether adduct and the exchange between the five- and the six-coordinate complex slows down.



Scheme 2.12 Equilibrium between the six-coordinate ether adduct and the five-coordinate complex.

Therefore, the change in the temperature influences the concentration of these active species in the catalytic solution. With the assumption that this behavior applies to the substituted complex **3b-3h**, too, we started to investigate the effect of the temperature on the reaction. Preliminary experiments showed that, at difference with the unsubstituted catalyst **3a**, which gave aziridine only with the temperature gradient, the new complexes $[\text{RuCl}(\text{OEt}_2)(\text{PNNP})]\text{PF}_6$ ($\text{PNNP} = \mathbf{3b-e,h}$) gave **6a** also at constant temperature. Therefore, to simplify the reaction protocol, we tested the new complexes **3b-e,h** at 25 and 0 °C. A longer reaction time (24 h) was used ensure the completion of the reaction:



Scheme 2.13 Aziridination reaction for the screening of several ligands under different temperature conditions.

The reaction mixture was analyzed as reported previously (Table 2.2). Under these conditions, the best yield was achieved with the 3,5-dimethyl substituted ligand (**1b**), which formed *cis*-**6a** with 55% isolated yield. The positive trend of yield in combination with bulky ligands was confirmed by the results obtained with the 3,5-di-*tert*-butyl- (**1c**) and the 2-naphthyl- (**1d**) substituted ligands (entries 3 and 4). In addition, the maleate yield was drastically reduced (entries 2-5). However, all reactions gave a very low enantioselectivity (0-13% ee). The temperature change did

not affect the chemoselectivity, but the *cis*-diastereoselectivity was lower (*cis/trans* ratio of 76:24 compared to 85:15) (Table 2.1, run 2).

Table 2.2 Results in Aziridination Catalyzed by [RuCl(OEt₂)(**1a-1e,1h**)]PF₆ (**3a-3e,3h**)PF₆ at Constant Temperature.

Entry	Ligand	T (°C)	conv. 5a (%)	maleate (%) (NMR)	<i>cis</i> - 6a (%) (NMR)	<i>cis</i> - 6a (%) (isol.)	ee (%) <i>cis</i> - 6a	<i>cis/trans</i> 6a (NMR)
1	1a (4-H) ^b	0				0	-	0
2	1a (4-H) ^b	25				0	-	0
3	1b (3,5-diMe)	0	65	20	57	55	13	76:24
4	1b (3,5-diMe)	25	100	11	51	50	2	85:15
5	1c (3,5-di ^t Bu)	0	66	21	36	32	3	75:25
6	1c (3,5-di ^t Bu)	25	49	12	24	20	0	76:24
7	1d (2-naphth)	0	65	14	40	37	13	73:27
8	1d (2-naphth)	25	78	6	51	45	0	70:30
9	1e (3-Me)	0	10	18	10	10	9	70:30
10	1h (4-Me)	0	17	78	6	-	-	-

^b Results reported by Marco Ranocchiari.¹³⁹

The best performing catalysts **3b-d** were tested at room temperature, too. The highest yield was obtained with the 3,5-dimethyl substituted ligand **1b**. However, at room temperature the enantioselectivity was drastically reduced, as essentially racemic aziridine *cis*-**6a** formed (entry 4).

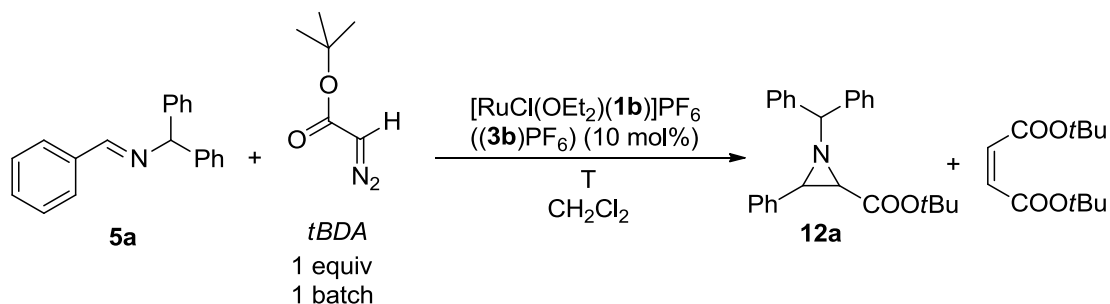
Nevertheless, we decided to proceed in the optimization of the reaction conditions with the most promising ligand, the 3,5-dimethylsubstituted (**1b**) one, which achieved the highest yields under each temperature condition.

2.2 Catalyst Optimization with [RuCl(OEt₂)(**1b**)]PF₆ (**3bPF**₆)

A thorough optimization of the most efficient system [Ru(**1b**)(OEt₂)Cl]PF₆ (**3bPF**₆) was performed, starting by testing a different carbene source and temperatures.

2.2.1 *Tert*-Butyl Diazoacetate as Carbenoid Source

As the steric hindrance on the ligands turned out to have a beneficial effect, at least on the aziridine yield, we tested a different diazoester as the carbene source, such as the extremely bulky *tert*-butyl diazoacetate (*t*BDA) (Table 2.3) in the catalytic reaction to give the *tert*-butyl substituted aziridine **12a**.



Scheme 2.14 Aziridination reaction with *tert*-butyl diazoacetate to give **12a**.

Table 2.3 Results in Aziridination Catalyzed by [RuCl(OEt₂)(**1b**)]PF₆ (**3bPF**₆) with *tert*-Butyl Diazoacetate as Carbenoid Source.

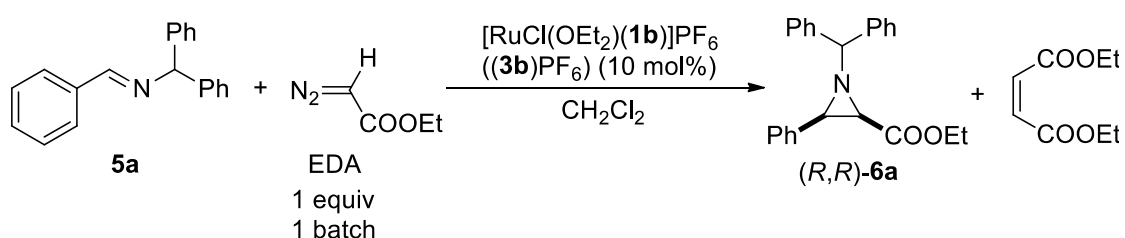
Entry	T	conv. 5a (%)	maleate (%) (NMR)	<i>cis</i> - 12a (%) (NMR)	<i>cis</i> - 12a (%) (isolated)	ee (%) <i>cis</i> - 12a	<i>cis/trans</i> 12a (NMR)
1	gradient	86	18	34	33	8	85:15
2	0 °C	26	7	9	6	0	-
3	RT	20	15	10	5	0	-

Moderate yields of *cis*-**12a** were achieved only with the gradient procedure, with a *cis/trans* ratio of 85:15, but the enantioselectivity was very low (8% ee) (entry 1). At constant temperature (entries 2 and 3), the yields were drastically reduced to 9% and 10% respectively, and the aziridine *cis*-**6a** was racemic. A possible

explanation for the reduced reactivity of the system is the extreme steric hindrance of the 3,5-di-*tert*-butyl substituted diazoacetate.

2.2.2 Temperature Screening

As the 3,5-dimethylsubstituted ligand **1b** gave the highest aziridine yield during the catalytic screening, a further investigation of the temperature condition was performed with the ether complex $[\text{RuCl}(\text{OEt}_2)(\mathbf{1b})]\text{PF}_6$ (**3bPF₆**). Different isothermal temperature conditions in the range between $-10\text{ }^\circ\text{C}$ and room temperature were applied with EDA as carbene source and the reproducibility of the results was tested.



Scheme 2.15 Aziridination reaction for the screening of the 3,5-dimethyl substituted ligand at different temperatures.

Table 2.4 Results in Aziridination Catalyzed by $[\text{RuCl}(\text{OEt}_2)(\mathbf{1b})]\text{PF}_6$ (**3bPF₆**) at Different Temperatures.

Entry	T	maleate (%)	<i>cis</i> - 6a (%)	ee (%) <i>cis</i> - 6a
1	gradient	10	84	3
2	RT	11	51	2
3	0 °C	20	57	13
4	0 °C ^c	15	28	0
5	-10 °C	9	32	0
6	-10 °C ^c	23	30	0

^c The reaction was performed a second time under the same conditions.

The results obtained with the gradient protocol are reported for comparison in entry 1. The highest yields (57%) were achieved under constant temperature (0 °C)

(entry 3). In this catalytic run, only 20% of maleate was formed, and the *cis/trans* ratio was 76:24. By performing the reaction at second time at $-10\text{ }^{\circ}\text{C}$ (entry 5), the yield was decreased to 32%, and no enantioselectivity was observed. Repeating the catalytic run at 0 and $-10\text{ }^{\circ}\text{C}$ (entries 4 and 6), a low reproducibility was observed. In particular, considering the reaction performed at $0\text{ }^{\circ}\text{C}$, the enantioselectivity was decreased, as only racemic *cis*-**6a** formed. On the other hand, the maleate yield was increased to 23% in entry 6.

2.2.3 Pressure Effect

As the results presented in Table 2.4 showed that the reaction is poorly reproducible, we carefully analyzed the experimental procedure. We realized that, depending on the operator, the reaction flask was either kept open to the argon line or closed for the whole reaction time. As dinitrogen is evolved upon EDA decomposition, a partial pressure of N_2 builds up in a closed system. Thus, to test whether the total pressure may affect the product distribution, a series of aziridination reactions was performed either in an open or in a closed Schlenk tube under identical temperature conditions (Table 2.5).

Table 2.5 Results in Aziridination Catalyzed by $[\text{RuCl}(\text{OEt}_2)(\mathbf{1b})]\text{PF}_6$ (**3bPF₆**) with Flask Open or Closed.

Run	T	maleate (%)	<i>cis</i> - 6a (%)	(<i>R,R</i>)- 6a ee (%)
1	RT (open)	11	51	2
2	RT (closed)	45	traces	-
3	$0\text{ }^{\circ}\text{C}$ (open)	20	55	13
4	$0\text{ }^{\circ}\text{C}$ (closed)	61	12	0

It was observed that the yields were strongly reduced by performing the reaction in a closed vessel. Approximating the volume of the Schlenk tube to an average of 20 mL and the temperature to $25\text{ }^{\circ}\text{C}$, the pressure generated by the decomposition of EDA to carbene and N_2 can be roughly calculated estimated to ca. 0.6 bar:

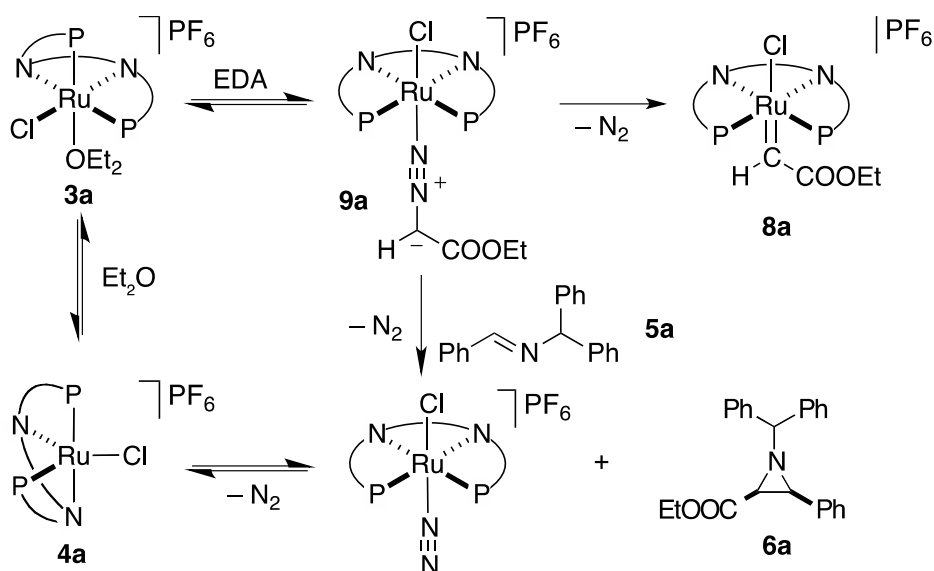
$$p \cdot V = n \cdot R \cdot T$$

$$V = 20 \cdot 10^{-3} \text{ L} \quad R = 0,082 \text{ L} \cdot \text{atm} \cdot \text{mol}^{-1} \cdot \text{K}^{-1}$$

$$n = 0.49 \cdot 10^{-3} \text{ mol} \quad T = 298 \text{ K}$$

$$p = \frac{n \cdot R \cdot T}{V} \approx 0,6 \text{ atm} \approx 0,61 \text{ bar}$$

The calculated value of the developed pressure (0.61 bar) is significant and only slightly diminishes to 0.55 bar by decreasing the temperature to 0 °C. When the reaction was carried out in a closed Schlenk tube with a Young valve, the pressure release was clearly perceived upon opening the vessel after completion of the reaction. A possible role of the reaction pressure can be discussed considering the following scheme (Scheme 2.16). Previous studies have shown that the reaction of the diazoester complex **9a** with the imine **5a** to give the aziridine **6a** results in the formation of a dinitrogen complex, which undergoes dissociation of the dinitrogen ligand to reform the ether adduct **3a**, possibly with the intermediacy of the five-coordinate complex **4a**.¹⁰⁵ The partial pressure of N₂ might influence the dissociation of the dinitrogen complex to the five-coordinate **4a**, and, hence, the distribution of the catalytic species in solution.

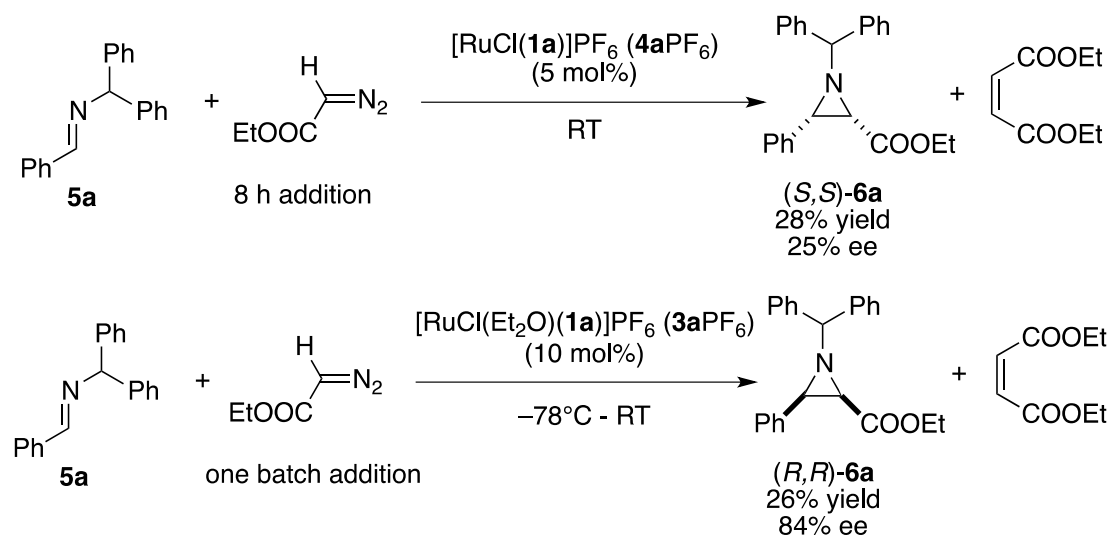


Scheme 2.16 The hypothesized mechanistic role of the dinitrogen molecule.

On the basis of this hypothesis, the higher partial pressure of N₂ reduces the concentration of the active species **4a**, which might explain the lower aziridine yields obtained when the reaction was performed in a closed vessel, as reported in Table 2.5.

2.2.4 Considerations on the Catalytic Activity of [RuCl(OEt₂)(**1b**)]PF₆

During the catalytic investigation performed with the six-coordinate ether complex [RuCl(OEt₂)(**1b**)]PF₆ (**3b**PF₆), we observed that all the experiments exhibited a low enantioselectivity (Table 2.4). It is known that the analogous complex with the unsubstituted ligand **1a** [RuCl(OEt₂)(**1a**)]⁺ (**3a**) is involved in an equilibrium with the five-coordinate complex [RuCl(**1a**)]⁺ (**4a**). Marco Ranocchiari reported that the latter species gives the opposite sense of induction in the asymmetric aziridination of **5a** with EDA as compared to **3a** (Scheme 2.17).¹³⁹ Therefore, the equilibrium between the five- and the six-coordinate complex might be responsible for the low enantioselectivity in case of the 3,5-dimethyl substituted ligand **1b**, as catalyst **4b**PF₆ and **3b**PF₆ might produce the opposite enantiomers.



Scheme 2.17 Best results obtained with the unsubstituted PNNP ligand **1a** under the optimized conditions for either **3a**PF₆ or **4a**PF₆.

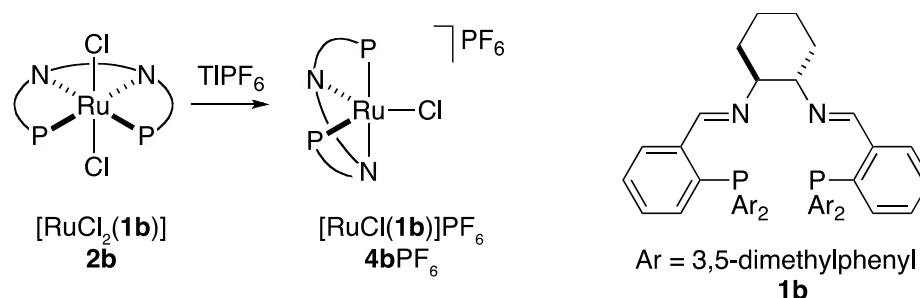
However, comparing the sense of induction of the two different systems under the same conditions is not possible, as aziridine **6a** is formed under different conditions with each system (Scheme 2.17).

As a second general observation, a poor reproducibility was exhibited with the six-coordinate **3bPF₆** (Table 2.5), for which no explanation was evident.

To cast some light on the above issues, we tested the five-coordinate **4bPF₆** under the same temperature and pressure conditions already used for the six-coordinate ether adduct **3bPF₆**.

2.3 Five-Coordinate [RuCl(**1b**)]PF₆ (**4aPF₆**) as Catalyst

The ruthenium complex [RuCl(**1b**)]PF₆ **4bPF₆** was formed by chloride abstraction from the dichloro complex **2b** with the thallium salt TlPF₆ (1 equiv), stirring overnight in dichloromethane at room temperature (Scheme 2.18).



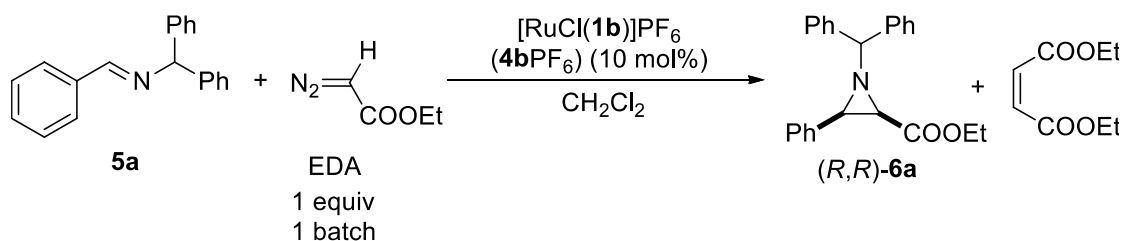
Scheme 2.18 The activation of the ruthenium dichloro complexes with the 3,5-dimethyl substituted ligand (**2b**) to give the five-coordinate **4bPF₆**.

The change of color from dark red to brown and the formation of a precipitate (TlCl) were taken as a confirmation for the successful activation. The greyish solid was not filtered off, as it was considered inactive for the reaction.

2.3.1 Temperature and Pressure Effects

We tested the five-coordinate complex **4bPF₆** under the same conditions already employed for the six-coordinate **3bPF₆**, in order to correlate the reactivity of

the two systems. Four different temperature conditions were applied to the reaction for its whole duration with the flask open to the argon line, while the imine and EDA were successively added in one batch. The catalytic runs under isothermal temperatures (0 °C, -10 °C, and RT) were repeated also in a closed Young Schlenk. Finally, to rationalize the pressure influence, further experiments were performed at constant temperature (-10 °C) under a nitrogen atmosphere instead of argon.



Scheme 2.19 Aziridination reaction with **4bPF₆** at different temperatures.

Table 2.6 Results in Aziridination Catalyzed by [RuCl(**1b**)]PF₆ (**4bPF₆**).

Entry	T	inert gas	flask	conv. 5a (%)	maleate (%) (NMR)	<i>cis</i> - 6a (%) (NMR)	ee (%) (<i>R,R</i>)- 6a
1	Gradient	Ar	Open	12	14	11	54
2	RT	Ar	Open	12	16	7	0
3	RT	Ar	Closed	<5%	21	8	0
4	0 °C	Ar	Open	52	58	24	0
5	0 °C	Ar	Closed	30	17	9	-29
6	-10 °C	Ar	Open	62	9	26	0
7	-10 °C	Ar	Closed	51	12	19	nd
8	-10 °C	N ₂	Open	41	13	12	0
9	-10 °C ^d	N ₂	Open	60	10	20	0
10	-10 °C	N ₂	Closed	63	8	33	0
11	-10 °C ^d	N ₂	Closed	58	10	28	0

^d The reaction was repeated a second time under the same conditions.

Under the gradient protocol (entry 1), the conversion was only 12% with the corresponding formation of *cis*-**6a** in 11% yield. The chemoselectivity of the reaction was low, as maleate was produced in 14% yield. Aziridine (*R,R*)-*cis*-**6a** was obtained with the enantioselectivity of 54% ee. Therefore, under the gradient protocol, catalyst **4b**PF₆ showed the same sense of induction with respect to the six-coordinate **3b**PF₆ (Table 2.4). At room temperature (entry 2), however, the aziridine yield decreased to 7% and, moreover, racemic product was formed. At 0 and –10 °C, aziridine was obtained in 20% and 26% yield, respectively, but without enantioselectivity (entries 4 and 6).

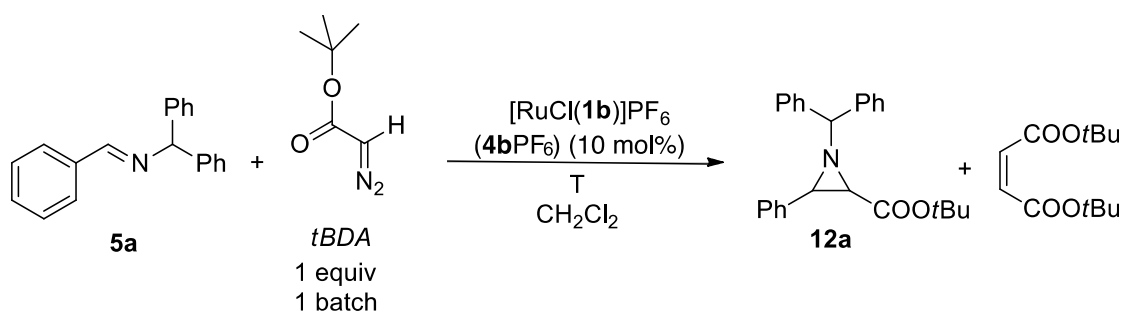
Performing the reaction under identical conditions but in a closed Young Schlenk led to different results depending on the temperature, in terms either of yield and enantioselectivity. At room temperature (entry 3), racemic *cis*-**6a** was obtained in 8% yield, giving similar aziridine yields with both protocols (open/closed). On the other hand, by decreasing the temperature to 0 °C (entry 5), the reaction showed an inverse sense of induction, as (*S,S*)-*cis*-**6a** was formed in 9% NMR yield with enantioselectivity of 29% ee in the closed system, whereas racemic **6a** was formed at constant pressure under argon.

The reactions at –10 °C are particularly interesting. Firstly, the yields of the reactions performed under nitrogen in a closed Schlenk (entries 10 and 11) were higher than those obtained in an open Schlenk under nitrogen (entries 8 and 9), and than those obtained in a closed Schlenk under argon atmosphere (entries 6 and 7), as well. These results are clearly contradicting the hypothesis that we proposed to explain the role of the pressure effect on the yield, as higher aziridine yields were obtained with higher nitrogen pressures. Secondly, the reproducibility of the reactions was poor, even after controlling the pressure conditions. In the case of the reaction performed in an open flask (entries 8 and 9), the difference between the two NMR aziridine yields (12 and 20% respectively) was significant.

Before searching for a different explanation, by means of NMR spectroscopic investigation of the catalytic system, we briefly examined *tert*-butyldiazoacetate as carbenoid source.

2.3.2 *Tert*-Butyl Diazoacetate as Carbenoid Source

For the sake of comparison with the six-coordinate system **3bPF₆**, the bulky *tert*-butyl diazoacetate was tested as carbenoid source as well (Table 2.7). As a general trend, upon decreasing the temperature from 25 °C (entry 2), to 0 °C (entry 3), to –10 °C (entries 4 and 5), the yield was enhanced up to 41% when the reaction was performed in an open flask connected to the argon line. A very low enantioselectivity (15%) was observed under the gradient protocol (entry 1), whereas under constant temperatures (entries 2-4) only racemic *cis*-**12a** was recovered.



Scheme 2.20 Aziridination reaction with *tert*-butyl diazoacetate.

Table 2.7 Results in Aziridination Catalyzed by $[\text{RuCl}(\mathbf{1b})]\text{PF}_6$ (**4bPF₆**) with *tert*-Butyl Diazoacetate as Carbenoid Source.

Run	T	Flask	5a conv. (%)	maleate (%)	<i>cis</i> - 12a (%)	<i>cis</i> - 12a ee (%)	12a <i>cis/trans</i>
1	gradient	open	30	30	16	15	-
2	RT	open	96	42	2	0	-
3	0 °C	open	68	12	25	0	86:14
4	–10 °C	open	82	12	41	4	89:11
5	–10 °C	closed	67	39	11	85	88:12

The results reported in entries 1-3 were comparable with those obtained with the six-coordinate $[\text{RuCl}(\text{OEt}_2)(\mathbf{1b})]\text{PF}_6$ **3bPF₆** (Table 2.3). As for **3bPF₆**, moderate yields and a very low enantioselectivity were obtained only under the gradient

conditions (entry 1), whereas by using an isothermal temperature protocol (RT and 0°C), only racemic product was recovered (entries 2 and 3).

In addition, the reaction at -10 °C (entry 4) was also repeated in a closed vessel (entry 5). The conversion of the imine was of 67% and maleate formation in 39% yield. Despite the high conversion of the imine, aziridine was isolated in only 11% yield, but from the crude spectra it was not possible to identify the other byproducts. However, a surprisingly high enantioselectivity of 85% was observed. For lack of reference of *tert*-butyl-substituted aziridines, the absolute configuration of the product was not established. Encouraged by this last promising result, we decided to perform some NMR spectroscopic studies for a better understanding.

2.3.3 NMR Spectroscopic Investigations

The above study of the temperature and pressure effects showed that several factors influence the catalytic performance of catalysts **3b**PF₆ and **4b**PF₆. However, the yield and the enantioselectivity of aziridine seem to vary without an apparent pattern. To disentangle these effects, we decided to perform some NMR spectroscopic studies with [Ru(**1b**)Cl₂] (**2b**) as precatalyst and TlPF₆ or (Et₃O)PF₆ as halide scavenger. To this respect, an intrinsic point is that the catalytic reactions run in an NMR tube had to be performed under protected atmosphere, which required the use of a closed system.

2.3.3.1 [RuCl(**1b**)]PF₆ (**4b**PF₆)

The dichlorocomplex **2b** was treated with TlPF₆ (1 equiv) in CD₂Cl₂ in an NMR tube under argon in an NMR tube equipped with a silicon septum. The mixture was stirred overnight at room temperature, and the ³¹P and ¹H NMR spectra of **4b**PF₆ were recorded at different temperatures. The ³¹P NMR spectrum at -40 °C shows an AX system (δ 59.6 and 50.1, ²J_{P,P'} = 29 Hz), which we assign to the five-coordinate complex [RuCl(**1b**)]⁺ (**4b**) on the basis of the spectroscopic data of the unsubstituted analogue [RuCl(**1a**)]PF₆, which shows signals at δ 59.5 and 49.6 (²J_{P,P'} = 29 Hz) (Figure 2.5).¹²⁹

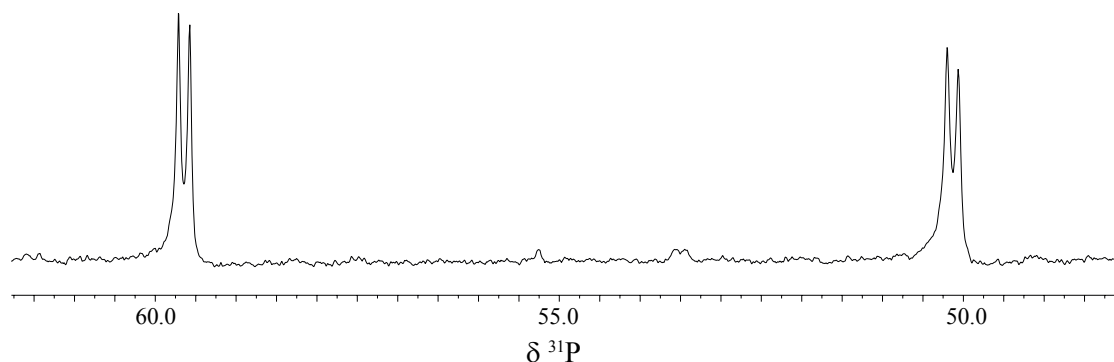


Figure 2.5 ^{31}P NMR spectrum (212 MHz, CD_2Cl_2) of $[\text{RuCl}_2(\mathbf{1b})]$ after activation with TlPF_6 (1 equiv) ($-40\text{ }^\circ\text{C}$).

The addition of imine **5a** (1, 5, and 10 equiv) to the reaction mixture did not result in any modification of the spectra. This confirmed that no coordination of **5a** to complex **4b** occurred, even in the presence of an excess of the imine.

The catalytic reaction was monitored by NMR spectroscopy, as well. To this purpose, the five-coordinate $\mathbf{4bPF}_6$ was prepared as described above. Then, **5a** and EDA were added at $0\text{ }^\circ\text{C}$ and the ^1H and ^{31}P NMR spectra were measured at $0\text{ }^\circ\text{C}$ every 10 minutes for 48 h:

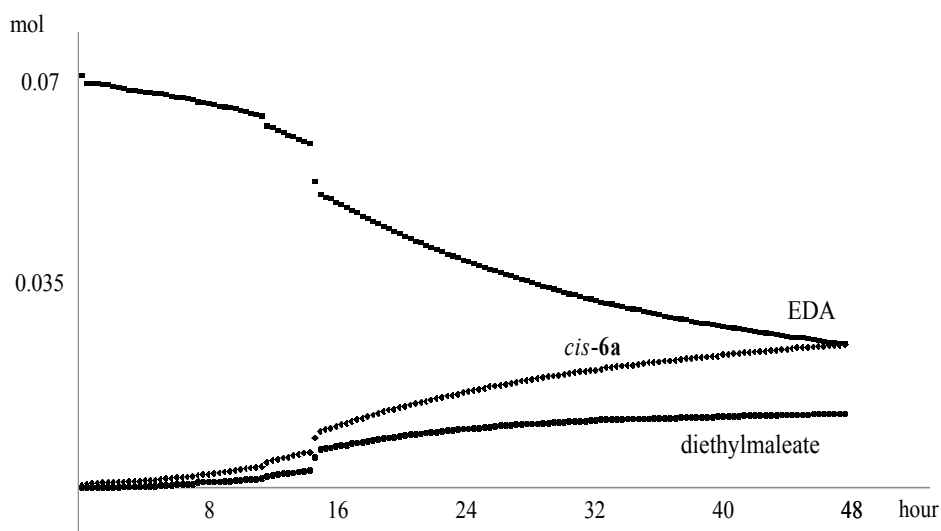


Figure 2.6 Reaction profile of the catalytic run performed with $\mathbf{4bPF}_6$ at $0\text{ }^\circ\text{C}$ as monitored by ^1H NMR spectroscopy (CD_2Cl_2 , 700 MHz) during 48 h. The ^1H NMR spectra were recorded every 10 min and the integration of the signals is plotted against time.

From the ^1H spectra, it was noted that the reaction was not quantitative after two days, even though the curve of the aziridine formation and the one of the EDA consumption started to flatten at this point. Finally, aziridine was formed in higher yield than maleate.

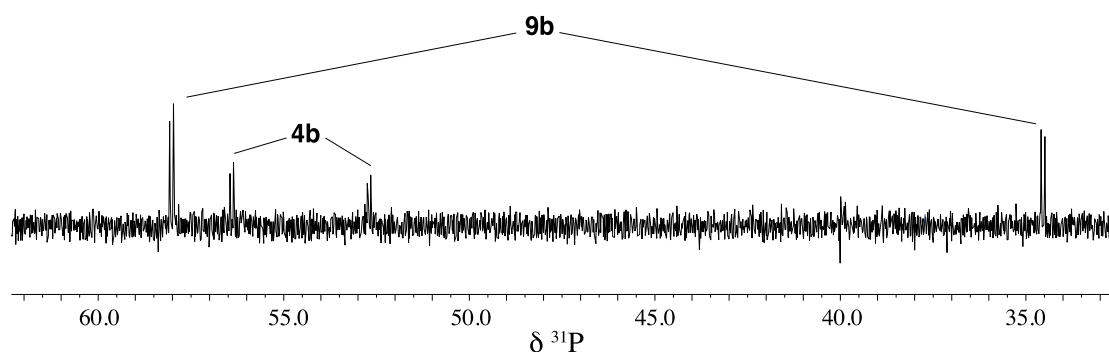


Figure 2.7 ^{31}P NMR spectrum (283 MHz, CD_2Cl_2) of $[\text{RuCl}(\mathbf{1b})]\text{PF}_6$ (10 mol%) recorded immediately after the addition of EDA (1 equiv) ($0\text{ }^\circ\text{C}$).

The ^{31}P NMR spectrum (Figure 2.7) at $0\text{ }^\circ\text{C}$ showed that the activated complex reacts with EDA to form a putative ruthenium diazoester adduct $[\text{RuCl}(\text{N}_2\text{C}(\text{H})\text{COOEt})(\mathbf{1b})]^+$ (**9b**). Two doublets at δ 58.0 and 34.5 ($^2J_{\text{P},\text{P}'} = 28\text{ Hz}$) were attributed to this latter species.

The presence of a phosphorus in *trans* position to a chloro atom can be excluded, since such systems exhibit signals at around δ 80, as in the case of the *cis*- β isomer of $[\text{RuCl}_2(\mathbf{1a})]$ (See scheme 2.9).^{128,140} On the other hand, the chemical shifts are not in agreement with a *trans*-diazoester adduct, which was observed and characterized by Marco Ranocchiari¹³⁹ with the unsubstituted ligand **1a**, as the ^{31}P NMR spectra of the diazoester adduct $[\text{RuCl}(\text{N}_2\text{C}(\text{H})\text{COOEt})(\mathbf{1a})]^+$ showed signals at δ 42.1 and 36.9 ($^2J_{\text{P},\text{P}'} = 24.2\text{ Hz}$) at room temperature. On the other hand, the chemical shifts are in agreement with a *cis*- β configuration of the diazoester adduct, in which the phosphorus atoms are both in *trans* position to a nitrogen. The signal at δ 58.0 might be assigned to a phosphorus in *trans* position to a weakly coordinated nitrogen, such as the one of the coordinated diazoester moiety (Figure 2.8).

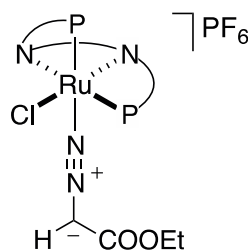


Figure 2.8 *Cis*- β configuration of the putative diazoester adduct.

It has to be noted that the spectrum of the unsubstituted catalyst $[\text{RuCl}(\text{N}_2\text{C}(\text{H})\text{COOEt})(\mathbf{1a})]^+$ exhibited signals at δ 42.4 (d , ${}^2J_{\text{P,P}'} = 25.3$ Hz), 41.1 (d , ${}^2J_{\text{P,P}'} = 25.3$ Hz), 35.8 (d , ${}^2J_{\text{P,P}'} = 25.2$ Hz), 34.8 (d , ${}^2J_{\text{P,P}'} = 25.4$ Hz) at -60 °C. This was attributed to the interconversion between the *s-cis* and *s-trans* isomers of the coordinate diazoester (Figure 2.9). However, no NMR spectrum of the analogous system with the 3,5-dimethylsubstituted ligand **1b** was recorded below 0 °C.

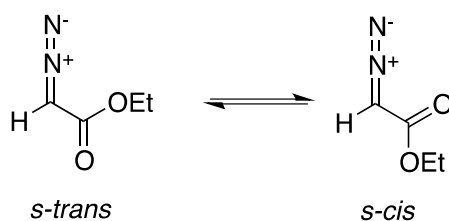


Figure 2.9 Interconversion between the *s-cis* and the *s-trans* isomers of EDA.

Finally, to exclude that the signals at δ 58.0 and 34.5 ppm belong to any aqua complex, the analogous aqua complex $[\text{RuCl}(\text{OH}_2)(\mathbf{1b})]^+$ (**7b**) was investigated, too. ${}^{31}\text{P}$ NMR spectra were recorded at different temperature after adding an excess of water (up to 10 equiv) to a CD_2Cl_2 solution of $\mathbf{4bPF}_6$. Two doublets at δ 63.6 and 46.3 (${}^2J_{\text{P,P}'} = 34$ Hz) corresponding to an AX pattern were observed at -40 °C and attributed to **7b**.

The formation of a *cis*- β -EDA complex as active species might explain the results obtained in the catalytic run performed under the same conditions (0 °C in a closed vessel), in which the enantiomer (*S,S*)-*cis*-**6a** was formed with an enantioselectivity of 29% ee (Table 2.6, entry 5).

By monitoring the reaction during 48 h, it was observed that the active five-coordinated complex **4bPF₆** is consumed within the first 8 h:



Figure 2.10 Reaction profile of a catalytic run performed with **4bPF₆** at 0 °C as monitored by ³¹P NMR spectroscopy (283 MHz, CD₂Cl₂) during 48 h. The ³¹P NMR spectra were recorded every 10 min and the integration of the signals is plotted against time.

2.3.3.2 [RuCl(OEt₂)(**1b**)]PF₆ (**3bPF₆**)

The next NMR study was focused on the ether adduct **3bPF₆**. The dichlorocomplex **2b** was treated with Et₃OPF₆ (1 equiv) in CD₂Cl₂ in an NMR tube equipped with a silicon septum under argon. After stirring at room temperature overnight, the ³¹P NMR spectra of **3bPF₆** were recorded in the range between 25 °C to –80 °C. At –80 °C, resolved signals consisting of a pseudo triplet at δ 67.9 ppm (²J_{P, P'} = 35 Hz) and a doublet at δ 48.8 (²J_{P, P'} = 32 Hz) were observed (Figure 2.11).

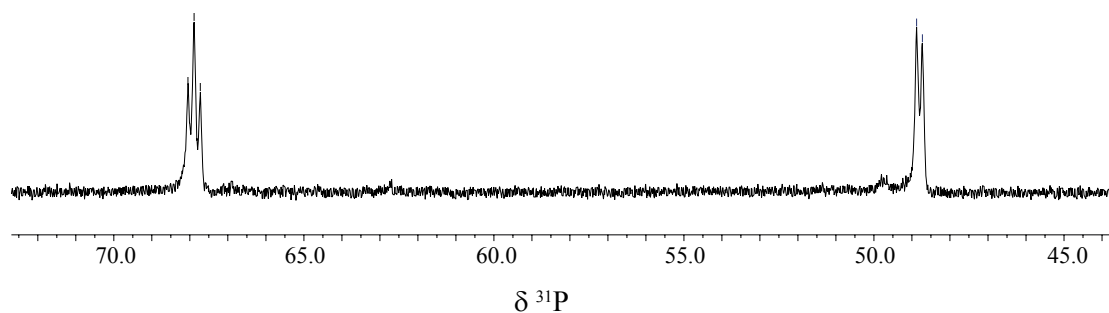


Figure 2.11 ^{31}P NMR spectrum (212 MHz, CD_2Cl_2) of $[\text{Ru}(\mathbf{1b})\text{Cl}_2]$ at $-40\text{ }^\circ\text{C}$ after activation with Et_3OPF_6 .

To our surprise, many other signals were present in the region of the spectrum between $\delta -15$ and -25 : a triplet at $\delta -19.3$ ($J = 1064$ Hz), a triplet at $\delta -18.6$ ($J = 1041$ Hz), a doublet of doublets at $\delta -16.1$, and a doublet of triplets at $\delta -16.6$ (Figure 2.12). We assign the biggest triplet at $\delta -19.3$ to PF_2O_2^- , which derives from the hydrolysis of PF_6^- , and the smaller signals to a monodentate coordinated anion.

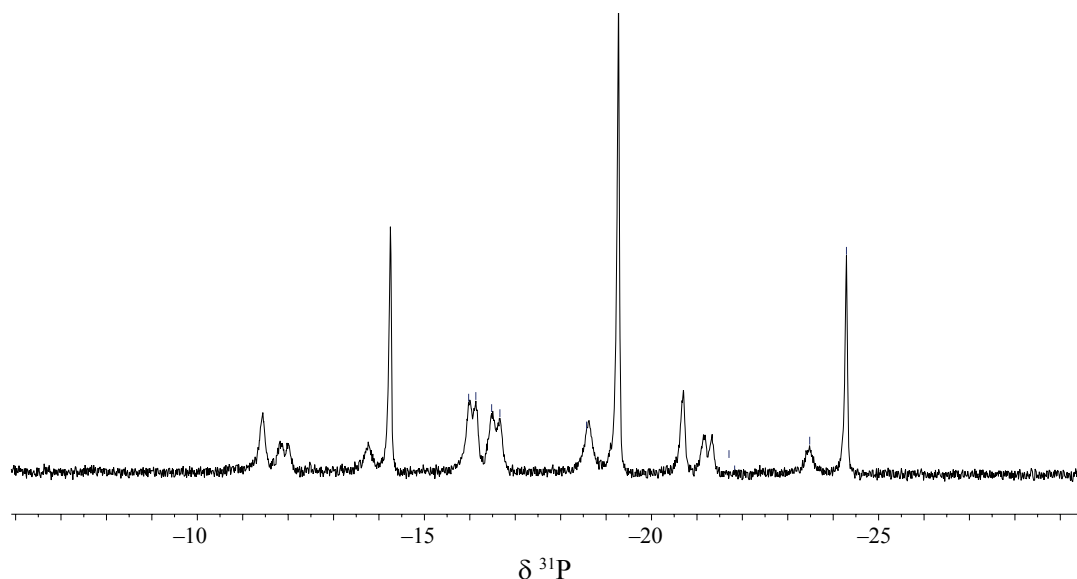


Figure 2.12 ^{31}P NMR spectrum (212 MHz, CD_2Cl_2) of $[\text{Ru}(\mathbf{1b})\text{Cl}_2]$ after activation with Et_3OPF_6 ($-80\text{ }^\circ\text{C}$).

The formation of difluorophosphates by hydrolysis of PF_6^- and their coordination to a variety of metals have been widely reported in the literature.¹⁵⁹⁻¹⁶³ Crystal structures and studies of the PO_2 stretching frequencies made clear that the

bidentate coordination mode via oxygen is preferred.^{164,166} Otero¹⁶⁷ reported that they are good ligands for transition metals, in particular for the highly oxophilic early transition metals. Webb¹⁶⁰ reported a rhodium(I) complex with a monodentate difluorophosphate anion, which exhibits a ³¹P NMR chemical shift $\delta -17.4$. Some examples of ruthenium complexes were published,¹⁶⁸⁻¹⁷⁰ as well, and Matsumoto observed similar values of chemical shifts ($\delta -15.86$) for the PF_2O_2^- anion in a bridged coordination to two ruthenium atoms.¹⁷⁰ On this basis, it is not surprising that the anionic oxygen of PF_2O_2^- is able to replace the labile molecule of coordinated ether of $[\text{RuCl}(\text{OEt}_2)(\mathbf{1b})]^+$. Therefore, we assigned the signals in Figure 2.12 to free and oxygen-coordinated anion PF_2O_2^- , whereas it was not possible to distinguish between a mono- and a bridged coordination. The signals depicted in Figure 2.11 were assigned to two different isomers, including rotamers, of a six-coordinate complex with difluorophosphate as ligand, such as $[\text{RuCl}(\text{PF}_2\text{O}_2)(\mathbf{1b})]$.

We were not able to prepare samples of the same species from **3b** and $(\text{Et}_3\text{O})\text{PF}_6$, therefore its characterization is not complete. We suggest that it is the ruthenium complex of the 3,5-dimethyl substituted ligand **1b** that catalyzes the hydrolysis of the PF_6^- , since with the unsubstituted PNNP ligand **1a** no hydrolysis was observed.

The presence of hydrolyzed (free and coordinated) acid species originated from the hydrolysis of PF_6^- present as counterion, might be responsible for aza-Darzens reactions, as Brønsted acids are reported to catalyze such reactions with high yield.¹⁷¹ Among the many examples, the most significant was published by Wulff. He reported initially¹¹⁷ a very efficient catalytic system based on the Lewis acid $\text{B}(\text{OPh})_3$ in combination with the chiral ligands VANOL or VAPOL:

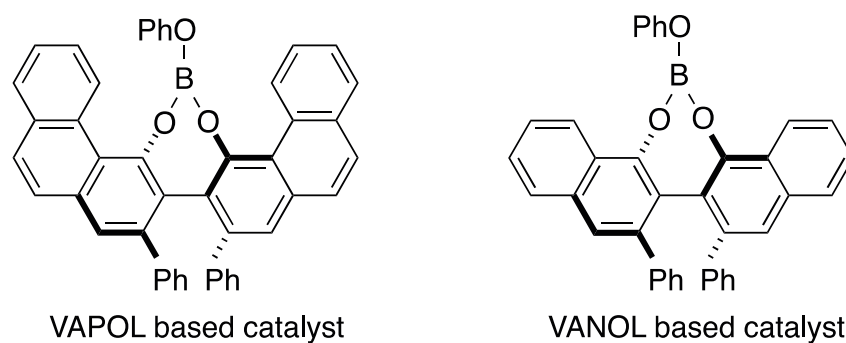


Figure 2.13 Wulff's first hypothesis of catalytic system.

During further studies on this system, his co-workers found some difficulties in reproducing the results achieved.¹⁷² For instance, the reaction of the phenyl-*N*-benzhydryl imine was originally reported to give aziridine with an enantioselectivity of 95% ee, but in later experiments the enantioselectivity was decreased to 89%. Then, it was found a similar reduction of the enantioselectivity also for other substituted *N*-benzhydryl imines, with differences up to 16%. Therefore, Wulff performed more investigations, in order to determine the structure of the active catalyst. NMR spectroscopic studies led to the proposal of the following chiral pyroborate derivatives as the active species:^{172,173}

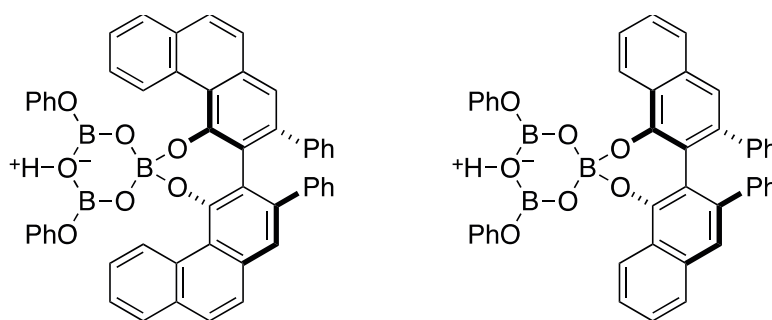
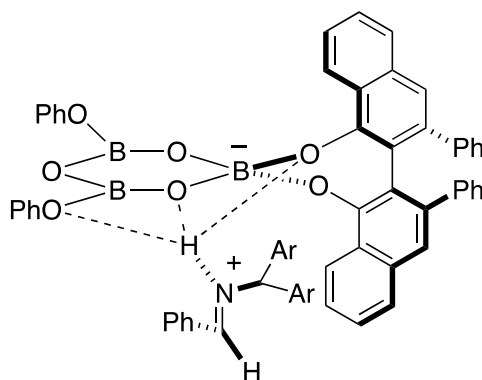


Figure 2.14 VAPOL- and VANOL based pyroborates.

In fact, these species act as chiral Brønsted acids, by forming with the imine the following adduct, which is determining the stereo- and enantioselectivity of the attack of the EDA molecule.¹¹⁹



Scheme 2.21 Imine activation by protonation with Wulff's catalytic system.

As the formation of pyroborates from VAPOL or VANOL and $B(OPh)_3$

requires an equivalent of water and the preparation of the catalyst was performed under moisture-free conditions, Wulff concluded that the water was coming from the commercially available B(OPh)₃.

Concerning the hydrolyzed [RuCl(OEt₂)(**1b**)]PF₆ (**3bPF₆**) system, we suggest that the hydrolysis of the PF₆⁻ originates a proton species, which activates the imine without forming any chiral adduct. This might explain the loss of enantioselectivity under all the different reaction conditions explored during the optimization presented.

2.4 Conclusion and Outlook

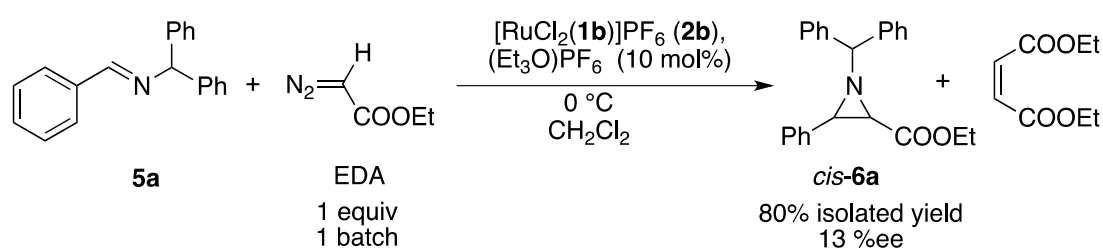
A preliminary catalytic screening in asymmetric imine aziridination of ruthenium/PNNP complexes with bulky the substituted PNNP ligands **2b-2h** was performed. The results showed that the introduction of sterically hindered groups such as 3,5-dimethyl (**2b**) or 2-naphthyl (**2d**) had beneficial effects on the yields of the aziridination reaction, which were increased up to 80% in case of the dimethylsubstituted ligand **1b**. As aziridine was obtained even when the reaction was performed under constant temperature, the reaction conditions were simplified. The role of the pressure was also investigated, as it was found that the reaction gave aziridine with different yields and enantioselectivity depending on the different pressure conditions. This was not surprising, as the aziridination is proposed to proceed via reaction of a diazoester complex, with subsequent formation of dinitrogen. Nevertheless, no clear pattern for the pressure influence was detected, and the experimental results contradicted the mechanistic hypothesis concerning the effect of the pressure.

As a major drawback, *cis*-aziridine was generally obtained with very low enantioselectivity (up to 13% ee). NMR spectroscopic investigations showed that the **3bPF₆** system was subject to the hydrolysis of the hexafluorophosphate anion to give free and coordinate PF₂O₂⁻ and Brønsted acid species. This latter catalyze a nonenantioselective aza-Darzens reaction, which is responsible of the low enantioselectivity observed with all the different reaction conditions presented. Moreover, the poor reproducibility might be explained by the changeable amount of adventitious water present. Eventually, the high yield obtained has to be attributed to the nonselective aza-Darzens reaction rather than to a ligand effect.

Therefore, we focused on preventing the hydrolysis in order to recover the enantioselectivity. Since the PF_6^- ion is so extensively reported to be subject to hydrolysis, we planned to use a different Meerwein salt with a non-hydrolyzable counterion, such as $(\text{Et}_3\text{O})\text{BF}_4$ or $(\text{Et}_3\text{O})\text{SbF}_6$, which are either commercially available or can be easily prepared. Further studies performed on the complex with the 3,5-dimethyl substituted ligand **1b** in combination with other chloride scavengers will be presented in the next chapter.

3. Enantioselective Imine Aziridination: a Breakthrough

The ligand screening described in the previous chapter has revealed that the high aziridine yield and the lack of enantioselectivity observed with **1b** is most probably caused by an acid species produced by the hydrolysis of the PF₆⁻ anion, which catalyzes a nonenantioselective aza-Darzens aziridination as a background reaction.



Scheme 3.1 Aziridination reaction of imine **5a** with EDA in the presence of [RuCl₂(**1b**)] upon treatment with Et₃OPF₆.

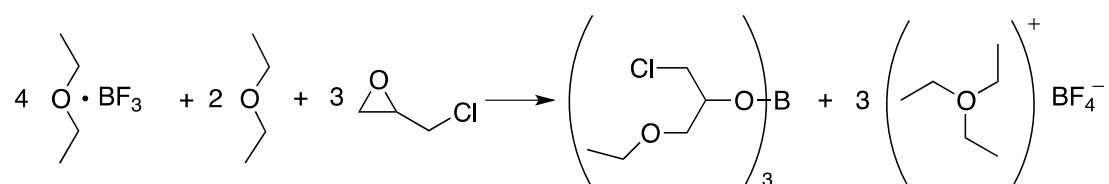
As the hydrolysis was not observed with the unsubstituted PNNP ligand **1a**, but was noticeable with the 3,5-dimethylsubstituted ligand **1b**, we suggested that complex **2b** is particularly prone to it. Moreover, attempts to characterize the hydrolyzed system failed, probably because of the variable amount of adventitious water present.

The strategies adopted to avoid such hydrolysis will be described in this chapter. We moved to chloride scavengers with nonhydrolyzable and non-coordinating anions, such as BF₄⁻ or SbF₆⁻. Finally, a substrate screening and competition experiments with different substituted imines were performed in order to investigate the role of the electronic effects on the chemo- and enantioselectivity.

3.1 [RuCl(OEt₂)(1b)]⁺ (3b) with Nonhydrolyzable Counterions

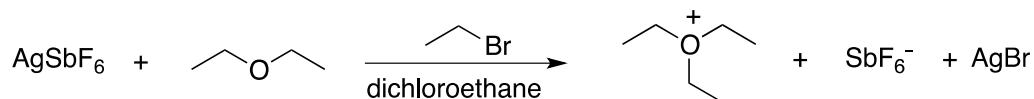
3.1.1 Synthesis of the Meerwein Salts

Hans Meerwein¹⁷⁴ reported the serendipitous preparation of (Et₃O)BF₄ in 1937 (Scheme 3.2). This general procedure was adapted for the synthesis of similar salts of type (Et₃O)X.



Scheme 3.2 Meerwein's first preparation of (Et₃O)BF₄.

Meerwein's salts with different counterions can be easily prepared and some of them are commercially available. As first choice, the commonly available triethyloxonium tetrafluoroborate (Et₃O)BF₄ salt was used. Then, triethyloxonium hexafluoroantimonate (Et₃O)SbF₆ was prepared following the reported procedure:¹⁷⁵



Scheme 3.3 Meerwein's procedure for the preparation of (Et₃O)SbF₆.

3.1.2 [RuCl(OEt₂)(1b)]BF₄ (3bBF₄)

The active catalyst was prepared as for **3bPF₆**, by treating the dichloro-complex [RuCl₂(**1b**)] (**2b**) with (Et₃O)BF₄ (1 equiv) in dichloromethane and stirring overnight at room temperature under argon. The solution color changed from dark red to brown during the activation, as expected, and no visible precipitate was observed. The ³¹P NMR spectra of **3bBF₄**, recorded at different temperatures, confirmed the successful activation (Figure 3.1).

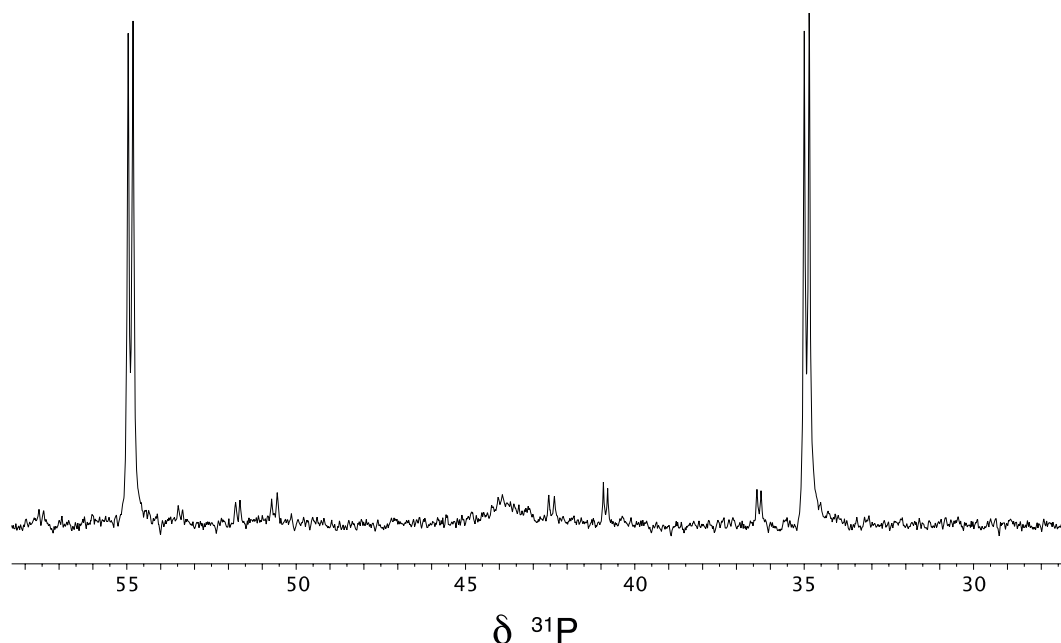
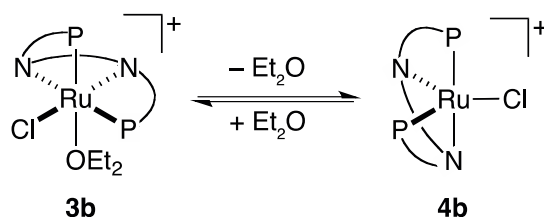


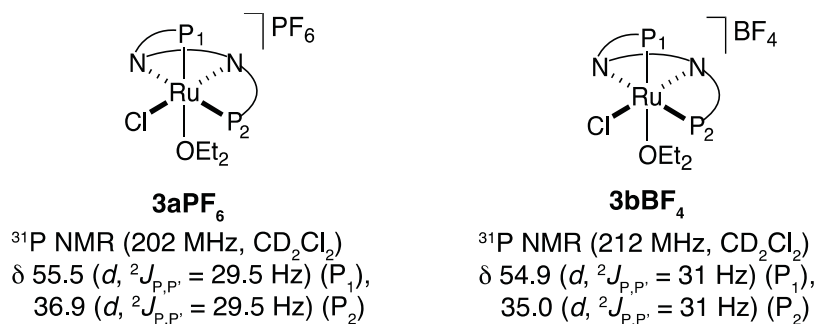
Figure 3.1 ^{31}P NMR spectrum (212 MHz, CD_2Cl_2) of $\mathbf{3bBF}_4$ at $-40\text{ }^\circ\text{C}$.

By analogy with *cis*- β - $[\text{RuCl}(\text{OEt}_2)(\mathbf{1a})]\text{PF}_6$, the ^{31}P NMR spectra are consistent with the formation of *cis*- β - $[\text{RuCl}(\text{OEt}_2)(\mathbf{1b})]\text{BF}_4$ ($\mathbf{3bBF}_4$). At room temperature, two broad signals were observed at δ 80.3 and 40.8. Upon gradually cooling to $-78\text{ }^\circ\text{C}$, the signals resolved to give an AX pattern (δ 54.9 and 35.0, $^2J_{\text{P,P}'} = 31\text{ Hz}$) at $-40\text{ }^\circ\text{C}$. This behavior confirms that the ether molecule is only weakly coordinated in $[\text{RuCl}(\text{OEt}_2)(\mathbf{1b})]^+$ ($\mathbf{3b}$) and readily dissociates to give the five-coordinate complex $\mathbf{4b}$ as observed for $\mathbf{3aPF}_6$:



Scheme 3.4 Dissociation of the ether ligand from the six-coordinate complex $\mathbf{3b}$ to give the five-coordinate $\mathbf{4b}$.

By comparison with the ^{31}P NMR chemical shifts of $[\text{RuCl}(\text{OEt}_2)(\mathbf{1a})]^+$ ($\mathbf{3a}$), it was assumed that the ether molecule is in *trans* position to one of the phosphorus atoms (Scheme 3.5).¹³⁹



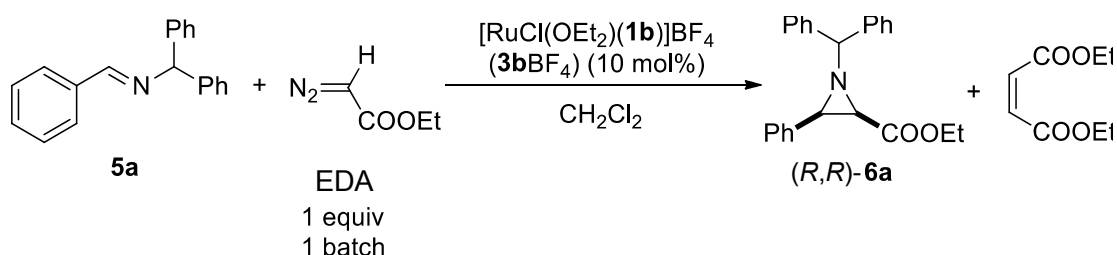
Scheme 3.5 ³¹P NMR data of **3aPF₆** and **3bBF₄**.

The other small signals observed in the spectrum belong to neither the five-coordinate complex [RuCl(**1b**)]⁺ (**4b**), nor to the aqua complex [RuCl(OH₂)(**1b**)] (**7b**) (See § 2.3.4.1).

3.1.3 Catalytic Aziridination with [RuCl(OEt₂)(**1b**)]BF₄

3.1.3.1 Preliminary Tests

The tetrafluoroborate derivative [RuCl(OEt₂)(**1b**)]BF₄ (**3bBF₄**) was tested in the asymmetric aziridination of *N*-benzylidene-1,1-diphenylmethanamine (**5a**) with EDA under different temperature conditions (Scheme 3.6). The temperature was kept constant with cooling baths, such as *i*-propanol/dry ice (−80 °C), acetonitrile/dry ice (−40 °C), and ice (0 °C) respectively. The reaction was performed at constant pressure to avoid the accumulation of N₂, as discussed previously.



Scheme 3.6 Screening of different temperature conditions for the aziridination reaction with **3bBF₄**.

The products of the reaction were analyzed by ^1H NMR spectroscopy after the addition of precise a weighted amount of 1,3,5-trimethoxybenzene as internal standard. The crude product was purified by column chromatography on silica gel, which gave pure *cis*-aziridine (*cis*-**6a**). We observed that the *trans* isomer (*trans*-**6a**) was eluted with the unreacted imine. The enantiomeric excess of *cis*-**6a** was determined with chiral HPLC on the isolated solid without further recrystallizations that might alter the enantiomeric excess.

Table 3.1 Results in Aziridination Catalyzed by $[\text{RuCl}(\text{OEt}_2)(\mathbf{1b})]\text{BF}_4(\mathbf{3bBF}_4)$.

Entry	T	conv. (%) 5a	maleate (%) (NMR)	<i>cis</i> - 6a (%) (NMR)	<i>cis</i> - 6a (%) (isolated)	ee (%) <i>cis</i> - 6a	6a <i>cis/trans</i> (NMR)
1	gradient	67	53	13	traces	92	81:19
2	-40 °C	43	61	19	18	0	79:21
3	0 °C	81	44	21	18	93	81:19

When the temperature gradient protocol was applied (Table 3.1, entry 1), aziridine *cis*-**6a** was formed in a very low yield. Traces of the (*R,R*)-product were isolated and presented a very high enantioselectivity (92%). The chemoselectivity of the reaction was very low, as maleate was formed in 53% yield. The reaction was repeated at constant temperature (-40 °C), and aziridine was isolated with low yield (18%), but without enantioselectivity (entry 2). Finally, performing the reaction at constant temperature (0 °C), (*R,R*)-**6a** was formed in slightly higher yield (21%). (*R,R*)-**6a** was isolated in 18% yield and enantioselectivity of 93% ee (entry 3). To the best of our knowledge, this is the highest enantioselectivity obtained in the imine aziridination catalyzed by transition metals.

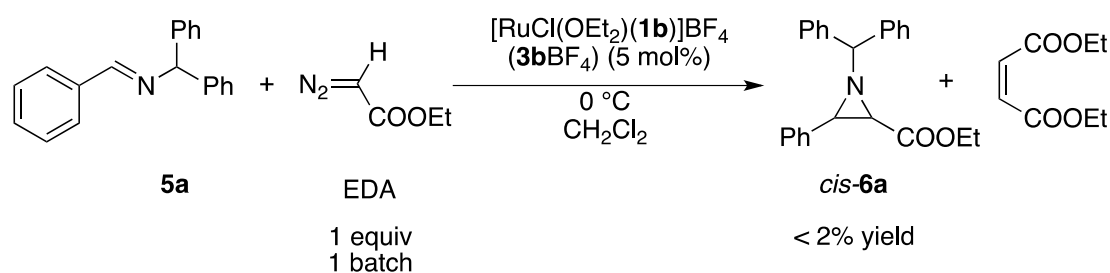
The conversion of the imine at 0 °C was high (up to 81%) and diethylmaleate was formed in 44% yield. By checking the mass balance, additional signals were observed in the ^1H NMR spectra, which might explain the high values of imine conversion, but it was not possible to identify the nature of such byproducts. However, no visible doublet signals corresponding to enaminoesters were found in the region between δ 8.60 and 10.30.¹⁰⁹ This spectroscopic evidence is relevant for

the mechanistic studies, as it is known that enaminoesters by-products are a clear indication that an acid catalyst is involved.¹⁰⁹

Catalyst **3b**BF₄ gave *trans* aziridine along with the *cis* isomer and is hence less diastereoselective than **3a**PF₆, where no signals for the *trans* isomer were detected in the ¹H NMR spectra of the crude reaction mixture.

3.1.3.2 Optimization of Catalyst **3b**BF₄.

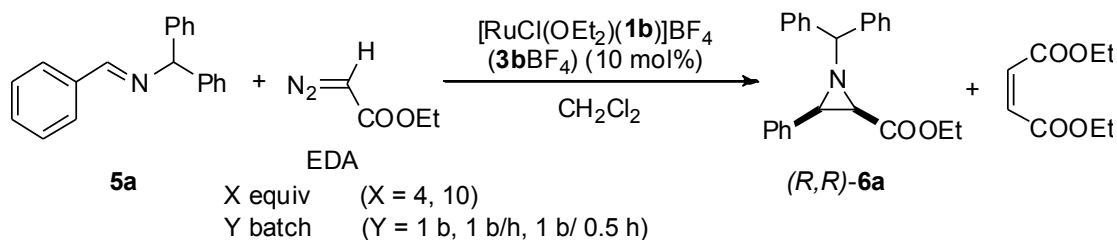
On the basis of these encouraging results, the amount of catalyst was reduced to 5% (Scheme 3.7). The imine conversion in this case was very low, as 89% of **5a** was recovered unreacted. The amount of aziridine formed was too small to be precisely quantified by ¹H NMR spectroscopy (less than 2%), and maleate was formed in traces (less than 1%), as well.



Scheme 3.7 Aziridination reaction with **3b**BF₄ (5 mol%).

Once established the new optimized temperature conditions (0 °C), type of chloride scavenger (Et₃OBF₄), and amount of catalyst (10 mol%), the mode of EDA addition was reinvestigated as well.

Previously, the addition of EDA in excess was performed either by adding EDA in one batch to [RuCl(OEt₂)**1a**]PF₆ (**3a**PF₆) or by a continuous addition to [RuCl(**1a**)]PF₆ (**4a**PF₆) of a dichloromethane solution of EDA during a period (4 h) shorter than the total reaction time (24 h) with the aid of a syringe pump. We decided to test both approaches with catalyst **3b**BF₄ and to perform a systematic screening of different procedures for the addition of an excess of EDA (Scheme 3.8, Table 3.2).



Scheme 3.8 Investigation of the mode of EDA addition.

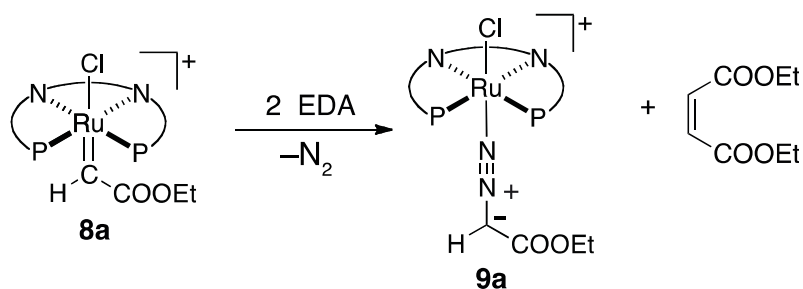
In the first catalytic run (entry 1), EDA was added in excess (4 equiv) during 4 h with the aid of a syringe pump. Racemic *cis*-**6a** was recovered in 7% isolated yield. *Trans*-**6a** was formed as well, with a *cis/trans* ratio of 75:25. When the same excess (4 equiv) was added in four single batches (1 batch/h), the yield increased up to 39%, but still racemic *cis*-**6a** was obtained. The diastereoselectivity was high, as a *cis/trans* ratio of 92:8 (entry 2) was observed. Then, a larger excess of EDA (10 equiv) was adopted, resulting in a reduction of the yield of aziridine to 26% (entry 3). When the excess of EDA (4 equiv) was added in one batch, (*R,R*)-*cis*-**6a** was isolated in 39% yield and with the enantioselectivity of 93% ee (entry 4). By adding a larger excess of EDA (10 equiv) in one batch, racemic *cis*-**6a** was recovered in 25% of isolated yield (entry 5). Considering the excellent results in terms of enantioselectivity observed in entry 4, by adding EDA (4 equiv) in one single batch, these conditions were adopted as optimized for the further studies.

Table 3.2 Results in Aziridination Catalyzed by $[\text{RuCl}(\text{OEt}_2)(\mathbf{1b})]\text{BF}_4$ ($\mathbf{3bBF}_4$) with Different Additions of EDA.

Entry	Addition of EDA (X/Y)	conv. (%) 5a	<i>cis</i> - 6a (%)	<i>cis</i> - 6a (%) (isolated)	ee (%) (<i>R,R</i>)- 6a	6a <i>cis/trans</i> (NMR)
1	4 equiv/4h ^a	31	12	7	0	75:25
2	4 equiv/3h/4 batches	71	39	22	0	92:8
3	10 equiv/5h/10 batches	51	26	24	0	70:30
4	10 equiv/1 batch	72	32	25	0	73:27
5	4 equiv/1 batch	100	44	39	93	78:22

^aEDA was dissolved in 1.5 mL of CH₂Cl₂ and added during 4 h with a syringe pump.

Previous studies in our group with the unsubstituted ligand **1a**¹³⁹ ascertained that the diazoester **9a** was the main species in solution when EDA was present in excess, as the carbene complex **8a** was formed in large amount only when EDA had completely reacted. As a possible explanation, it was proposed that, when EDA is present in excess, the carbene complex **8a** can react with EDA to give diethylmaleate and reform **9a**, as observed in a stoichiometric reaction between **8a** and ¹³C-EDA:¹³⁹

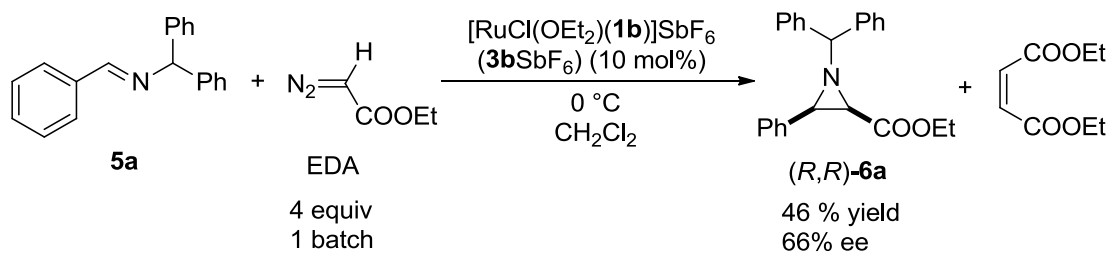


Scheme 3.9 Proposed reaction of **8a** with an excess of EDA.

The above results confirm that a reasonable excess of EDA is necessary to obtain high yields. When EDA is added slowly or in batches, its instantaneous concentration may be too low to form complex **9a** as major species in solution. Also, the formation of different isomers (such as a *cis*- β diazoester complex that transfers carbene with lower enantioselectivity) is conceivable, which would explain why no enantioselectivity is obtained upon slow or batchwise addition (entries 1-3). Finally, the lack of enantioselectivity in the presence of a large excess of EDA (entry 4) may be explained by the enhanced effect of impurities present in the diazoester. A similar effect has been observed with $[\text{RuCl}(\text{OEt}_2)(\mathbf{1a})]\text{BF}_4$ as catalyst (Table 3.3, entry 3).

3.1.4 $[\text{RuCl}(\text{OEt}_2)(\mathbf{1b})]\text{SbF}_6$ (**3bSbF₆**)

$(\text{Et}_3\text{O})\text{SbF}_6$ was also tested as chloride scavenger under the new optimized conditions. The reaction was performed with a catalyst loading of 10 mol% in dichloromethane at 0 °C by adding an excess of EDA (4 equiv) in one batch (Scheme 3.10).

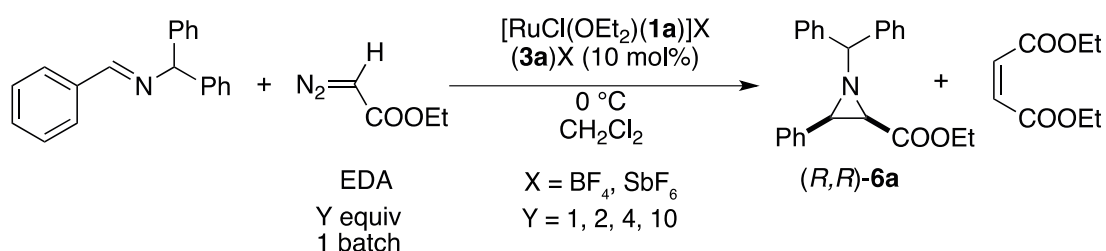


Scheme 3.10 Aziridination reaction with **3bSbF₆** under the optimized conditions.

No unreacted imine was recovered, and (*R,R*)-*cis*-**6a** was formed in 46% yield and 66% ee. Thus, the use of SbF_6^- as counterion has a beneficial effect on the aziridine yield, which increases from 39 to 46%. However, the enantioselectivity decreases significantly (from 93 to 66% ee), confirming the noninnocent role of the counterion in the aziridination reaction.

3.1.5 $[\text{RuCl}(\text{OEt}_2)(\mathbf{1a})]\text{X}$ (**3aX**) ($\text{X} = \text{BF}_4, \text{SbF}_6$)^b

The change of the anion turned out to play a beneficial effect on aziridination reaction, as $[\text{RuCl}(\text{OEt}_2)(\mathbf{1b})]\text{X}$ ($\text{X} = \text{BF}_4$ or SbF_6) gave high enantioselectivity and a reasonable aziridine yield even under isothermal condition (0 °C). Hence, we reinvestigated the catalytic activity of the system containing the unsubstituted ligand **1a**, $[\text{RuCl}(\text{OEt}_2)(\mathbf{1a})]^+$, in combination with $(\text{Et}_3\text{O})\text{BF}_4$ or $(\text{Et}_3\text{O})\text{SbF}_6$ as chloride scavengers:



Scheme 3.11 Investigation of the mode of EDA addition in the imine aziridination catalyzed by $[\text{RuCl}(\text{OEt}_2)(\mathbf{1a})]^+$.

^b The studies on the unsubstituted ligand **1a** were conducted by Mr. Joël Egloff and are reported in his Master thesis.

Table 3.3 Results in Aziridination Catalyzed by [RuCl(OEt₂)(**1a**)]X (**3aX**).

Run	X	EDA (Y equiv) one batch	conv. (%) 5a	<i>cis</i> - 6a (%) (NMR)	<i>cis</i> - 6a (%) (isolated)	ee (%) (<i>R,R</i>)- 6a	6a <i>cis/trans</i> (NMR)
1	BF ₄	1	50	32	24	78	78:22
2	BF ₄	4	92	53	20	78	81:19
3	BF ₄	10	85	38	37	0	76:24
4	PF ₆ ^{c,d}	1			26	84	100:0
5	PF ₆ ^c	1			0	-	-
6	PF ₆ ^{c,d}	2			18	35	100:0
7	SbF ₆	4	96	46	45	70	78:22

^c Results reported by Marco Ranocchiari¹³⁹

^d Reaction performed with the temperature gradient protocol.¹³⁹

In the presence of BF₄⁻ as counterion and by addition of 1 equivalent of EDA, *cis*-**6a** was formed with an NMR yield of 32% and enantioselectivity of 78% ee (Table 3.3, entry 1). The yield increased up to 53% when 4 equivalent of EDA were added, whereas the enantioselectivity remained unchanged (entry 2). When a larger excess of EDA (10 equiv) was added in one batch, the amount of aziridine formed was reduced to 38% (NMR yield) and only racemic product was recovered (entry 3). The lack of enantioselectivity in the presence of a large excess of EDA may be explained by the enhanced effect of impurities present in the diazoester. In fact, a similar effect has been observed with [RuCl(OEt₂)(**1b**)]BF₄ as catalyst (Table 3.2, entries 3 and 4).

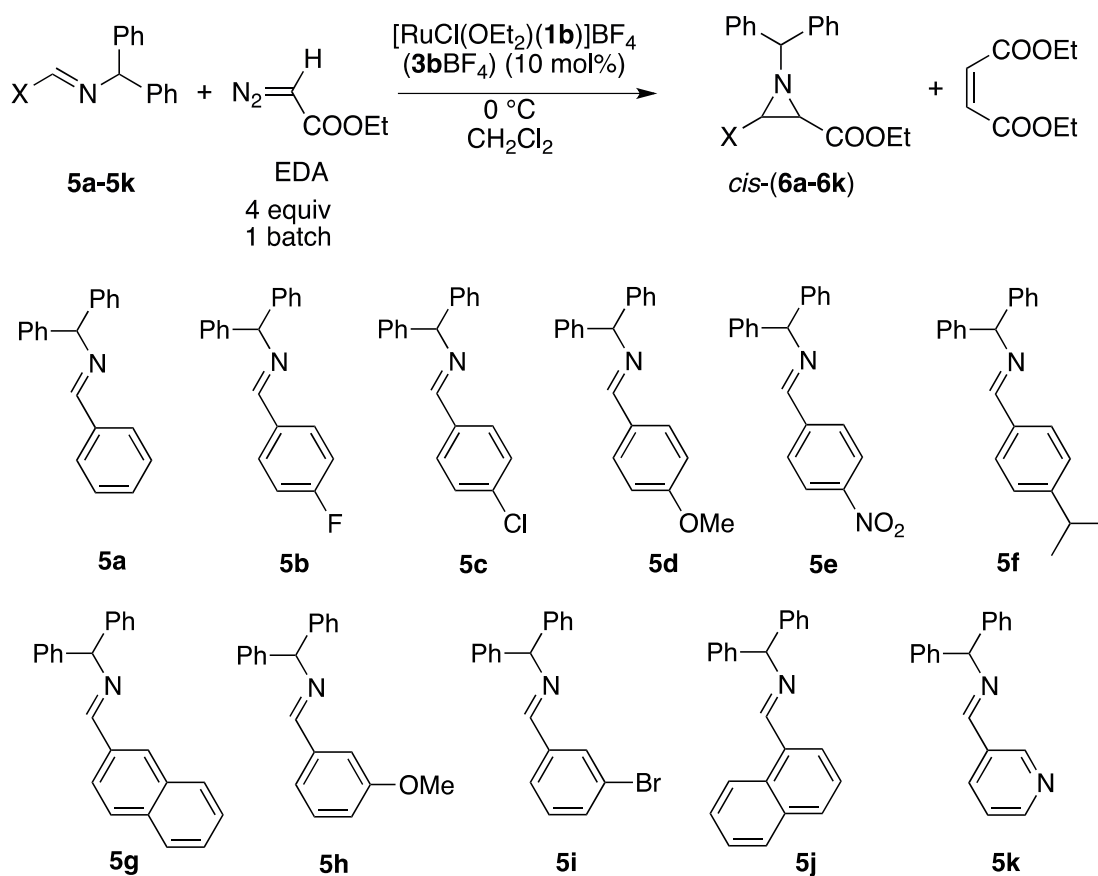
These results can be compared with those obtained with the **3a**PF₆ system studied by Marco Ranocchiari¹³⁹ (entries 4-6). With **3a**PF₆, a temperature gradient was necessary in order to obtain aziridine **6a** in 26% yield and enantioselectivity of 84% ee (entry 4). In contrast, no aziridine formation was observed by performing the reaction at constant temperature (0 °C) (entry 5). Moreover, the addition of an excess of EDA (2 equiv) led to a drastic reduction of the enantioselectivity from 84% to 35% ee even under the gradient temperature protocol (entry 6). Therefore, the change of the counterion has a beneficial effect, as it permitted a simplification of the

temperature conditions and allowed the use of a small excess of EDA, which has a positive influence on the yield. However, **3a**BF₄ is slightly less enantio- and diastereoselective than **3a**PF₆.

As a different anion, SbF₆⁻ was tested under the new optimized condition (0°C and 4 equiv of EDA) (entry 7). With **3a**SbF₆, aziridine was isolated with 45% yield, but the enantioselectivity was slightly lowered to 70% ee. Amounts of *trans*-**6a** were detected in the reaction mixture, as usual, with *cis/trans* ratios of around 78:22. Hence, BF₄⁻ gave the best results with the unsubstituted ligand **1a**, too.

3.1.6 Substrate Screening

Finally, to assess the substrate scope, we used the catalyst **3b**BF₄ containing the 3,5-dimethyl substituted ligand **1b** for a screening of the substituted benzaldimines **5b-5k** with the optimized protocol:



Scheme 3.12 Screening of different imines as substrate with **3b**BF₄.

The absolute configuration of the *cis*-aziridines (*cis*-**6b-k**) was assigned on the basis of the sign of the optical rotation and on the HPLC retention times by analogy with *cis*-**6a**.¹¹⁶ In the case of unreported aziridines, their racemates were prepared directly from the Brookhart-Templeton procedure,¹⁰⁹ fully characterized, and analyzed by chiral HPLC in order to find the best conditions for the separation of the enantiomers.

In general, the introduction of substituents affected the aziridine yield negatively (Table 3.4). As the only exception, the 4-MeO group (entry 4) contributed to enhance the yield to 37%. Nevertheless, the most noticeable effect was the drastic reduction of the enantioselectivity. Only the 4-fluoro- (**5b**) and the 4-chloro- (**5c**) substituted amines afforded aziridine in an enantioselective way, with 23% and 17% ee respectively (entries 2 and 3). When other substitution patterns were introduced, the enantioselectivity was completely lost.

Table 3.4 Substrate Screening of Substituted Imines in Aziridination Catalyzed by [RuCl(OEt₂)(**1b**)]BF₄ (**3b**BF₄).

Run	X	conv. (%) 5a	<i>cis</i> - 6a (%) (NMR)	<i>cis</i> - 6a (%) (isolated)	ee (%) (<i>R,R</i>)- 6a	6a <i>cis/trans</i>
1	H-C ₆ H ₄ (5a)	100	44	35	93	78:22
2	4-F-C ₆ H ₄ (5b)	58	29	28	17	83:17
3	4-Cl-C ₆ H ₄ (5c)	53	28	26	23	75:25
4	4-MeO-C ₆ H ₄ (5d)	nd	nd	37	0	73:27
5	4-NO ₂ -C ₆ H ₄ (5e)	65	18	17	0	90:10
6	4- <i>i</i> Pr-C ₆ H ₄ (5f)	63	18	15	0	nd
7	2-naphthyl- (5g)	44	14	16	0	82:18
8	3-MeO-C ₆ H ₄ (5h)	100	nd	36	0	nd
9	3-Br-C ₆ H ₄ (5i)	52	17	16	0	72:28
10	1-naphthyl (5j)	29	8	-	-	nd
11	3-pyridine (5k)	nd	-	-	0	nd

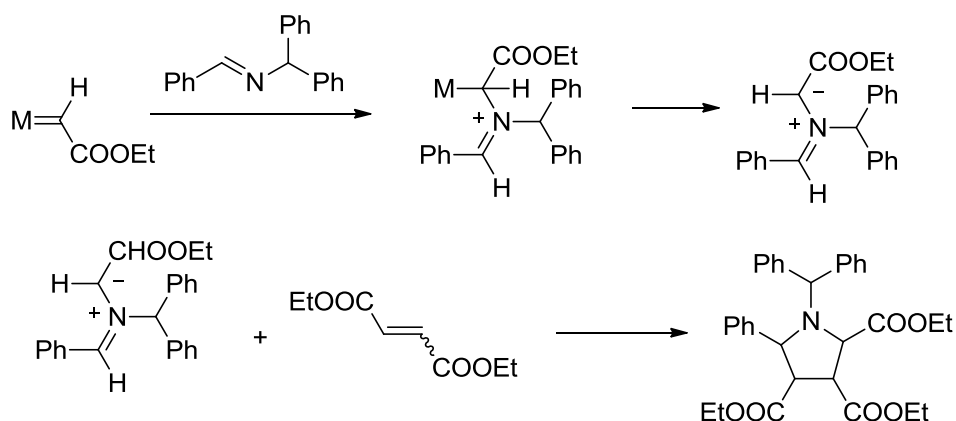
On the basis of these results, we assume that the most important effect was due to steric factors, as any hindrance increase to the system in comparison with **5a**

led to negative results. Considering the electronic influences, electron-withdrawing substituents are assumed to favor the nucleophilic attack of the diazoester complex to the imine (see below). On the other hand, electron-donating substituents, such as 4-MeO, are expected to disfavor this step. The reason for the drastic reduction of the enantioselectivity in both cases is not clear. More experiments recently performed in our laboratory by Joël Egloff show that the conditions used were optimal only for the unsubstituted imine **5a**. In particular, higher enantioselectivity was obtained for the substituted imines **5b-5k** when only 1 equivalent of EDA was used with the unsubstituted $[\text{RuCl}(\text{OEt}_2)(\mathbf{1a})]\text{BF}_4$ (**3aBF₄**) as catalyst at 0 °C. Therefore, the reactions with these substrates have to be reoptimized individually.

3.2 Mechanistic Investigations

3.2.1 Trapping Test with Diethyl Fumarate

To check whether an ylide intermediate is involved in the catalytic aziridination, a standard test for azomethine ylides was performed, as described by Jacobsen.¹²¹ By analogy with his work, we assumed that if the ylide is formed from the metal carbene complex, it should be trapped by diethylfumarate to give the pyrrolidine product:



Scheme 3.13 Jacobsen's trapping test for azomethine ylides.

An excess of diethylmaleate (10 equiv) or diethylfumarate (10 equiv) was added to the reaction solution containing $[\text{RuCl}(\text{OEt}_2)(\mathbf{1a})]\text{PF}_6$ (**3aPF₆**) (10 mol%),

imine **5a** (1 equiv), and EDA (1 equiv) under the temperature gradient conditions. The ^1H NMR spectrum of the crude reaction solution indicated that no pyrrolidine was formed, suggesting that no carbene was involved as intermediate in the reaction. The aziridine yield was slightly reduced from 26% to 23%, and only racemic *cis*-**6a** was recovered. This might be explained by the presence of either diethylfumarate or diethylmaleate, which is possibly deactivating the system by coordinating as oxygen donor the oxophylic ruthenium complex. These results are in agreement with our suggestion that the aziridination reaction with the Ru/PNNP catalysts does not proceed by nucleophilic attack of the imine onto a carbene complex.

3.2.2 Competition Experiments with $[\text{RuCl}(\text{OEt}_2)(\mathbf{1b})]\text{BF}_4$ (**3bBF₄**)

From the substrate screening performed on aryl-substituted imines **5a-5k** (Table 3.4), no clear trend correlating the electronic effect of the substituents was recognized. The yields decreased both with electron-withdrawing and with electron-donating substituents, and the enantioselectivity was similarly lowered.

In order to enhance the role of the electronic effects on the imine substrate, we planned competition experiments with the 4-substituted-*N*-benzylidene-anilines **5l-5p** (Figure 3.2), in which the aniline ring is substituted instead of the benzaldehyde one.

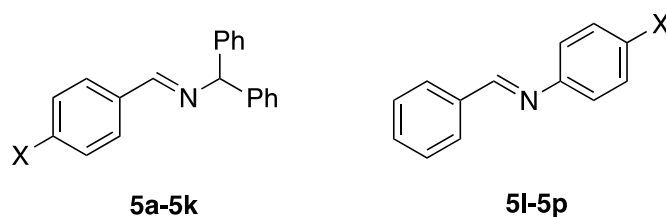


Figure 3.2 Different aldimines as substrate.

It has been reported¹⁷⁶ that coplanarity between the ring and the $\text{CH}=\text{N}$ plane is necessary in order to have the conjugation of the electrons of the two systems. Experimental evidence showed that, in the *trans*-*N*-benzylideneaniline (Figure 3.3), the benzaldehyde ring (A) is essentially coplanar with the imine double bond (θ is close to 0°), whereas the aniline ring (B) is twisted out of the $\text{PhCH}=\text{N}$ plane ($30^\circ < \phi < 55^\circ$).¹⁷⁷⁻¹⁷⁹

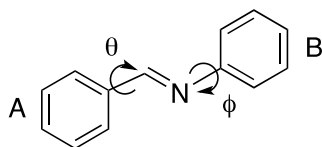


Figure 3.3 Twisting of the two aromatic rings in *trans*-*N*-benzylideneanilines.

Therefore, the conjugation between the aniline ring and $\text{CH}=\text{N}$ π -electrons is prevented by the twisting of the torsion angle ϕ . The ^1H NMR spectra of *N*-benzylideneanilines with *para* substituents on the benzaldehyde ring showed a correlation between the Hammett constant and the chemical shifts of the protons of the $\text{CH}=\text{N}$ groups. In contrast, there was no correlation for the *para* substituents on the aniline ring, as both electron-donating and electron-withdrawing groups did not affect the chemical shifts of the $\text{CH}=\text{N}$ protons.¹⁷⁶

In contrast, Echevarria¹⁸⁰ reported that the effects of substituents in *para* position of the benzaldehyde ring on imine carbon are surprisingly small. The ^{13}C NMR spectra showed that the chemical shifts of the $\text{CH}=\text{N}$ correlate with an inverse electronic effect as expected. On the contrary, the effects of the substituents on the aniline ring are larger and the ^{13}C NMR chemical shifts of the $\text{CH}=\text{N}$ correlate with the Hammett constants as expected. As an explanation, he proposed the resonance effect depicted in Figure 3.4, where X is an electron-withdrawing group. It should be noted that this conjugation through the nitrogen lone pair is compatible with the twisting of the aniline ring out of the imine plane. Therefore, we decided to perform the competition experiments with imines bearing the substituents on the aniline ring.

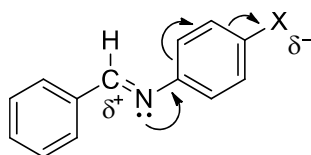
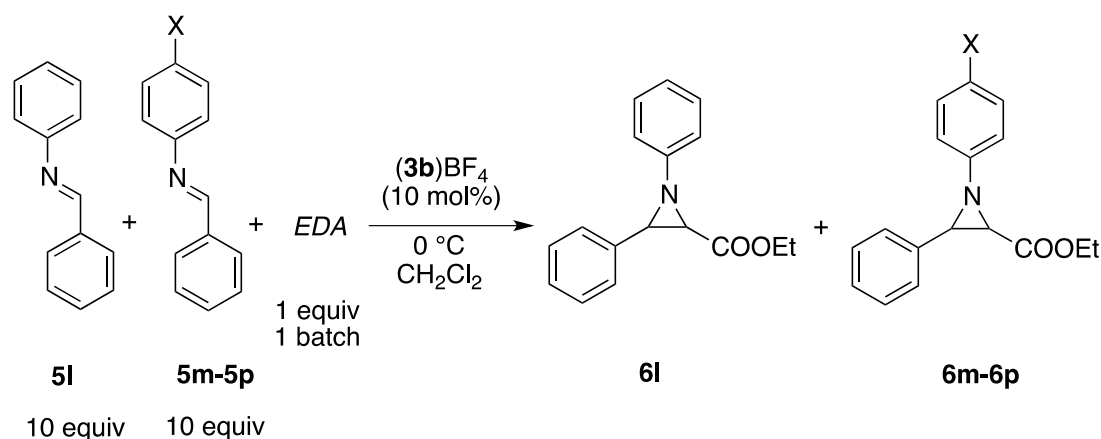


Figure 3.4 Resonance effect of a *para* substituted *N*-benzylideneaniline.

The competition experiments were performed under constant temperature (0°C) with an imine:EDA:catalyst ratio of 100:10:1, as summarized in the following scheme (Scheme 3.14)



Scheme 3.14 Competition experiments with *para* substituted *N*-benzylideneaniline.

In order to collect a larger data set, other imines were also tested in the competition experiments. Unfortunately, their manipulation and the analysis of the corresponding aziridine products were problematic. For instance, the *p*-CH₂CH₃ ($\sigma_p = -0.15$) and the *p*-CH₃ ($\sigma_p = -0.17$) substituted imines are poorly soluble in CH₂Cl₂ and were unsuitable for competition experiments, which require high imine concentrations. The *p*-N(CH₃)₂ ($\sigma_p = -0.15$) and the *p*-OMe ($\sigma_p = -0.27$) derivatives were prepared, as well, but proved to be unstable and decomposed spontaneously after a few hours at room temperature. Finally, the overlapping of the ¹H NMR signals of the crude mixture was problematic and limited the choice of the imines.

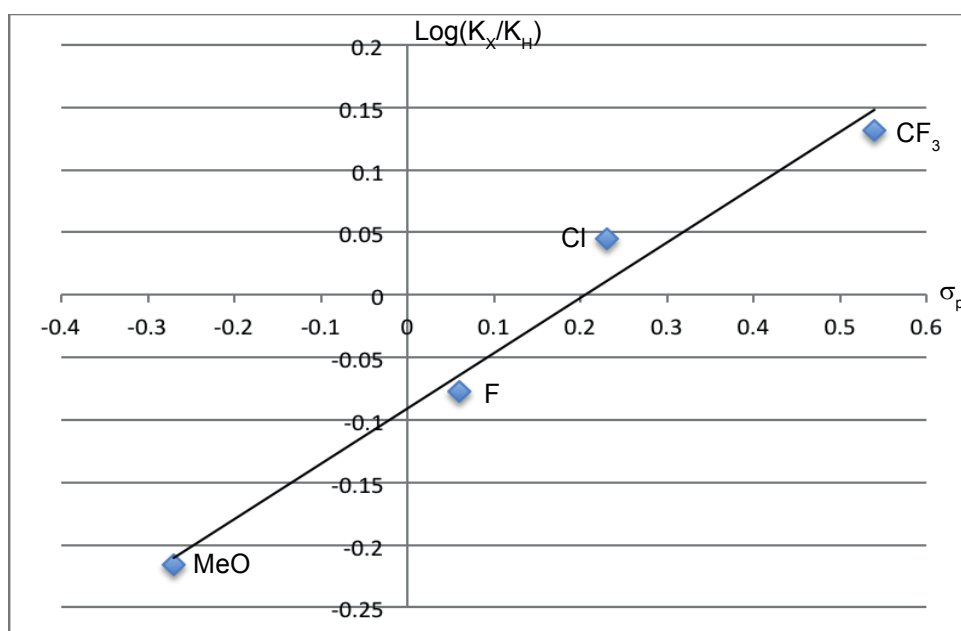
It was generally observed that such 4-substituted-*N*-benzylidene-anilines are less stable and have a lower tendency to crystallize than their benzhydryl-protected analogues. Also, the corresponding aziridines **6l-6p** decomposed during the HPLC analysis, even though such a problem had never been reported before.

After the addition of a weighted amount of trimethoxybenzene as internal standard, the yields of aziridines **6l-6p** were determined by ¹H NMR spectroscopy. Thus, the relative yield ratios K_{6l}/K_{6m-6p} were calculated. The logarithms of these values ($\log(K_{6l}/K_{6m-6p})$) and the σ_p values reported¹⁸¹ for each substituent are shown in Table 3.5.

Table 3.5 Results from the Competition Experiments

X	MeO (6m)	F (6n)	Cl (6o)	CF ₃ (6p)
σ_p	-0.27	0.06	0.23	0.54
$\log(K_X/K_H)$	-0.2156	-0.0769	0.0453	0.1319

The Hammett plot in Figure 3.5 shows that aziridines with electron-withdrawing substituents are formed faster than those bearing electron-donating groups. The ρ value was calculated to be +0.44 ($r^2 = -0.98$). Usually, when $0 < \rho < 1$, the reaction is less sensitive to substituents than the standard reaction with benzoic acid used as reference. Generally, reactions with a positive ρ value are considered to involve a transition state where its difference in energy from the reactants is diminished by a reduction of the electron density at the reactive site of the substrate.

**Figure 3.5** Hammett plot of the competition experiments.

The nice correlation with a +0.44 positive value for ρ supports a mechanism in which imines with electron-withdrawing substituents are reacting faster with EDA, as in the case of the attack of the nucleophilic metal coordinated EDA to the

electrophilic imine. This is in agreement with the proposed mechanism, in which EDA reacts as a nucleophile with the electrophilic imine, as discussed below in more detail.

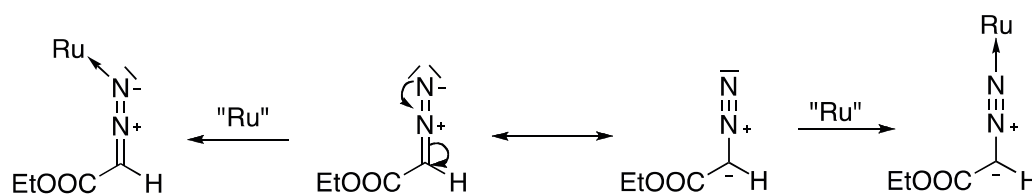
Two other examples of competition experiments have been described in the literature. The first one was reported by Jørgensen, who studied a SnCl₄-based catalyst for the aziridination of imines.¹⁸² He performed a series of competition experiments to investigate the effect of the substituents on the *para* position of the aniline ring of imines such as *p*-X-C₆H₄CH=NPh (X= CH₃, Cl, CN, NO₂). The reactions were carried out with an imine:EDA:SnCl₄ ratio of 100:50:1. He correlated the aziridine yields to the σ values of the substituents and found that imines with electron-donating substituents react faster than those with electron-withdrawing substituents. On the basis of these results, he proposed a two-step mechanism. The first step consists of the coordination of the imine to SnCl₄ and is favored for substrates bearing electron-donating groups. The second step is the nucleophilic attack of the ethyl diazoacetate onto the activated imine, which has the inverse electronic requirement. As the reaction exhibited a negative ρ correlation value of -1.2, indicating that electron-donating substituents have a beneficial effect on the reaction rate, he implicitly suggested that the rate of the reaction is determined by the first step, that is, the coordination of the imine to SnCl₄.

Che¹²⁴ investigated the mechanism of a Ru/porphyrin based catalyst. As already presented in the introduction (§1.4.2.3.2), he found out that the carbene complex [Ru(F₂₀-TPP)(CHCO₂Et)] failed to react with imines. To cast light on the mechanism, he performed competition experiments with substituted imines such as *p*-X-C₆H₄CH=NPh (X = OMe, Me, Br, Cl, NO₂) and observed a negative $\rho = -0.69$. On this basis, he proposed a mechanism in which imines with electron-donating substituents coordinate more efficiently to the ruthenium atom.

In contrast to these examples, previous NMR investigations performed in our laboratory¹³⁹ showed that, in case of ruthenium/PNNP systems, the imine does not coordinate to the metal. Instead, EDA to forms a diazoester complex, which was shown to react with imine **5a** to give aziridine **6a**. The results of the competition experiments are in agreement with the coordination of EDA to the metal and with the formation of the diazoester complex as the resting state of the catalyst. The reactivity of the diazoester complex is discussed in more detail below.

3.2.3 Considerations on the Diazoester Complex

To this point, it is important to note that the diazoester adduct *trans*-[RuCl(N₂CHCOOEt)(1a)]⁺ (9a) possesses a linear Ru–N–N–C moiety. The geometry of the Ru–EDA linkage may have an influence on the electronic properties of the carbenoid as the *end-on*, linear coordination of diazoalkanes to a transition metal stabilizes a limiting structure in which the α-C atom is nucleophilic, as discussed below:¹⁸³



Scheme 3.15 Coordination of ethyl diazoacetate to ruthenium.

Several examples of *end-on*, linear coordination have been reported.¹⁸³ One fully characterized example was published by Dartiguenave and co-workers.¹⁸⁴ The structure of [W(CO)₄(PPh₃)(N₂C(SiMe₃))] was confirmed by X-ray crystallography, with N–N and N–C bond lengths (1.165(15) Å and 1.34(1) Å) intermediate between double and triple, and single and double bond, respectively (Figure 3.6).¹⁸⁵ The presence of electron withdrawing groups, such as SiMe₃, is thought to stabilize the observed structure, in agreement with the formalism adopted.

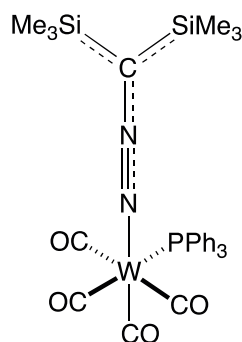


Figure 3.6 Structure of [W(CO)₄(PPh₃)(N₂C(SiMe₃))] as reported by Dartiguenave.

Many examples of diazoalkane complexes of d⁸ transition metals such as

iridium(I) and rhodium(I) have been reported, in particular by Werner.¹⁸⁶⁻¹⁸⁹ These complexes are quite stable, as they do not decompose by dissociation of dinitrogen to give the corresponding carbene complex, and were analyzed by X-ray crystallography (Figure 3.7).

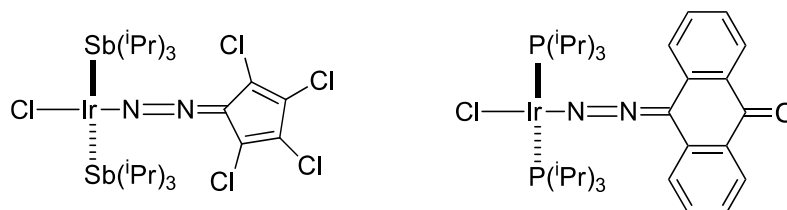


Figure 3.7 Structures of *trans*-[IrCl(N₂C₅Cl₄)(SbⁱPr₃)₂]¹⁸⁷ and *trans*-[RhCl(N₂CC₁₃H₈O)(PⁱPr₃)₂]¹⁸⁹.

Brookhart¹⁹⁰ reported the synthesis of a stable rhodium(I)-trimethylsilyldiazomethane complex (Figure 3.8), which possesses a linear, *end on* coordination, as confirmed by the crystal structure analysis.

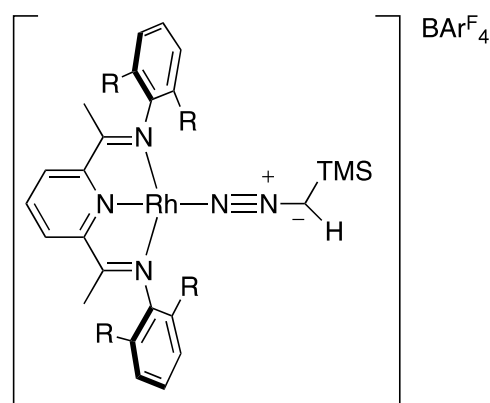


Figure 3.8 Rhodium(I)-trimethylsilyldiazomethane complex.

Diazoester complexes with d^6 transition metals, such as osmium^{191,192} and ruthenium,¹⁹³⁻¹⁹⁵ are known as well. In particular, several examples of diazoaryl complexes with ruthenium are reported, where the *end-on*, linear Ru–N=N=C coordination is supported by the ¹⁵N NMR spectra.¹⁹³⁻¹⁹⁵ Finally, some examples of ruthenium diazoalkane reported by Milstein^{149,150} have already been described in the introduction (§ 1.5.4.3), as they have a particular importance in the rationale of this thesis.

By considering the *end on*, linear ruthenium diazocomplex with the PNNP

ligand **9a** (Figure 3.9), it has to be noted that the d^6 ruthenium(II) ion features a set of fully occupied π -orbitals overlapping with the π -orbitals of the linearly coordinated diazoester. This permits the π back-donation from the metal to the EDA, which delocalizes the positive formal charge of the diazoacetate and increases its electron density.

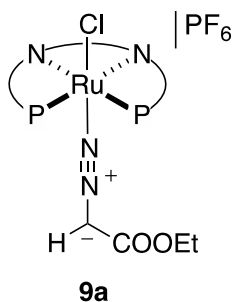
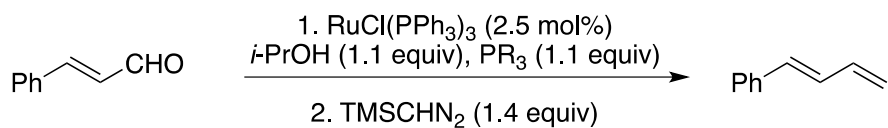


Figure 3.9 *Trans* ruthenium diazoester complex **9a**.

The significant role of the π -back donation from the metal to EDA in **9a**, is supported by the ^{15}N NMR spectroscopic observation of the corresponding ruthenium dinitrogen complex, in which the dinitrogen molecule is terminally coordinated to the metal, as reported by Marco Ranocchiari.¹³⁹ In this case, the π back donation stabilizes the coordination of the dinitrogen ligand, which is a weak π acceptor. This is in agreement with the ruthenium being a rare example of transition metal that binds dinitrogen.¹⁹⁷

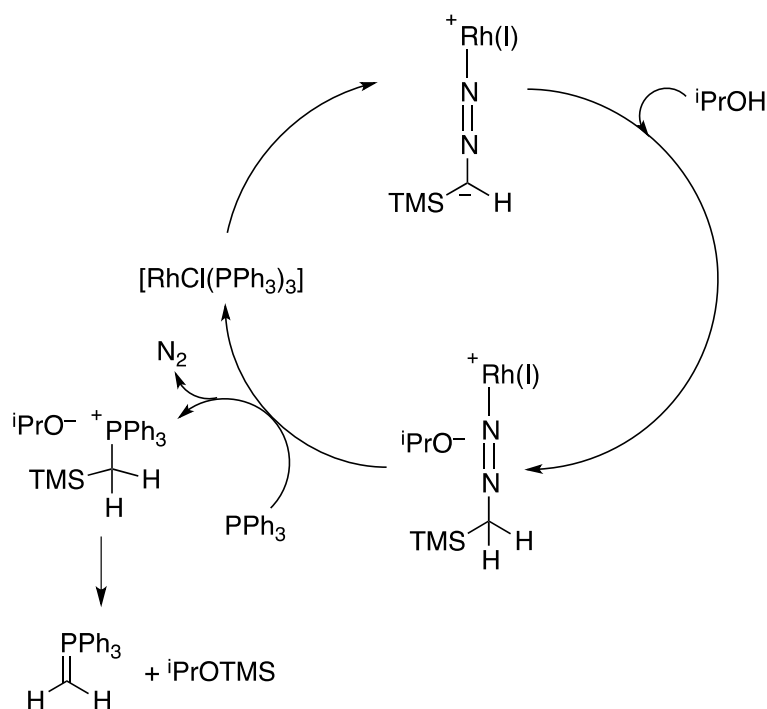
We suggest that the π -back donation from ruthenium to the coordinated diazoester plays a major role in the reactivity of the latter. In fact, the increase of electron density on the coordinated diazoester in **9a** reduces the double bond character of the carbenoid $\text{C}=\text{N}$ bond and supports a formal structure in which the carbon atom bears a localized negative charge (Scheme 3.15) and, thus, possesses an enhanced nucleophilicity.

With regard to this point, Lebel postulated an interesting mechanism for the transition metal catalyzed olefination of aldehydes with ethyl diazoacetate (Scheme 3.16).¹⁹⁶



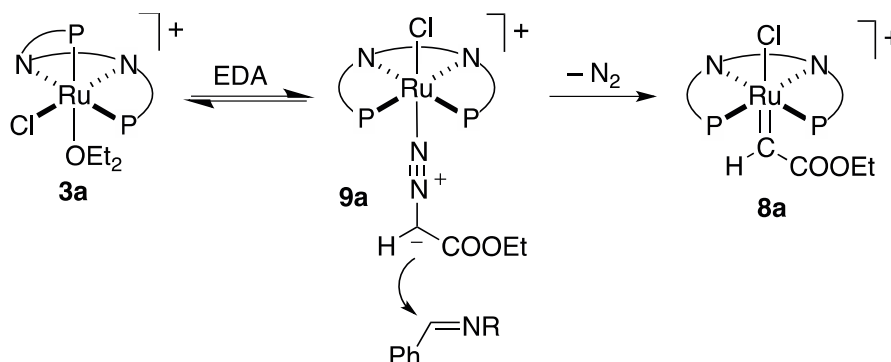
Scheme 3.16 Rhodium-catalyzed methylenation of aldehydes.

As NMR spectroscopic evidence ruled out the intermediacy of a rhodium carbene complex, a different mechanism was proposed, which involves a diazomethane complex. She suggested that the trimethylsilyldiazomethane coordinates to rhodium to give a rhodium(I)-TMS complex in analogy with the one proposed by Brookhart (Figure 3.8).¹⁹⁰ This species exhibits a nucleophilic character, as it is protonated by *i*-propanol before the attack of the phosphine with subsequently nitrogen extrusion:



Scheme 3.17 Lebel's catalytic cycle for rhodium(I)-catalyzed methylenation.

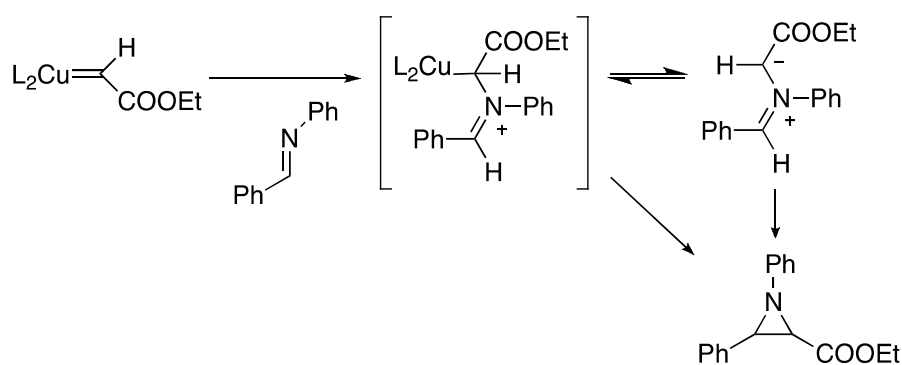
On the basis of these considerations, we suggest that the *end on*, linear coordination to ruthenium enhances the nucleophilicity of EDA and its reactivity toward the unactivated imine (Scheme 3.18).



Scheme 3.18 Scheme of the reactivity of the *trans* ruthenium diazoester complex **9a**.

3.2.4 The Role of Carbene Nucleophilicity

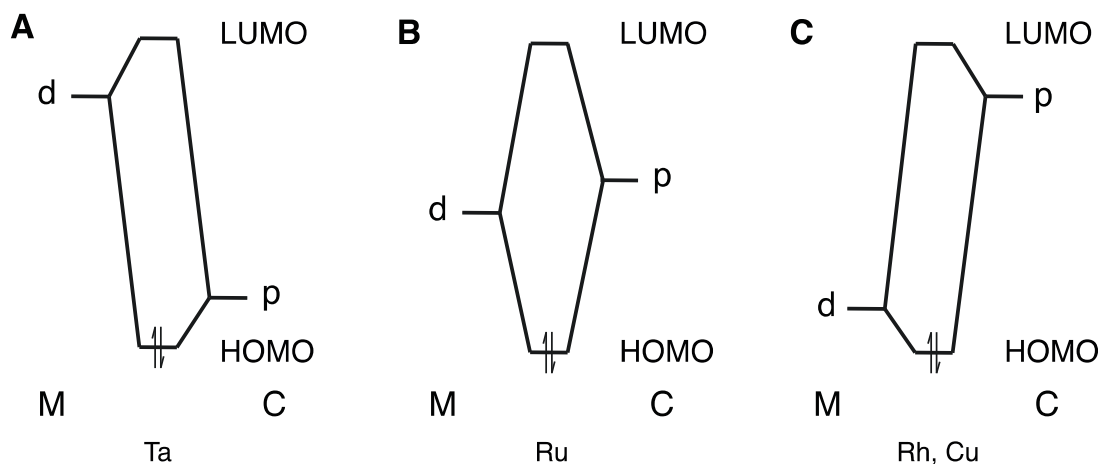
The reactivity of the carbene complex must be discussed as well, as our group observed that the ruthenium carbene complex does not react with the free imine, whereas a carbene complex is proposed to be the active species in the case of copper. For instance, Jacobsen¹²¹ obtained aziridine with moderate yields (27%) and enantioselectivity (67%) with a bis-oxazolines/copper (II) catalyst. On the basis of the analysis of the byproducts and of trapping test and by analogy with cyclopropanation, he suggested that the diazoester reacts with the metal to give a carbene complex, which undergoes nucleophilic attack by the imine. The resulting azomethine ylide can cyclize to give the aziridine product or dissociate to cyclize thereafter.



Scheme 3.19 Reactivity scheme of the azomethine ylide proposed by Jacobsen.

Moving from copper- to ruthenium- based systems, Che¹²⁴ reported an interesting observation in the case of a Ru/porphyrin catalyst. He noticed that the

ruthenium carbene complex does not react to give aziridine, suggesting a different mechanism from the one proposed by Jacobsen, in which the carbene complex was the active catalytic species. Che's observation concerning the failure of the ruthenium carbene complex to undergo nucleophilic attack by the imine is in agreement with our observation with the Ru/PNNP system. These results are explained considering the peculiarity of ruthenium in comparison with later transition metals, such as copper and rhodium. The energy of the *d* orbital involved in the π back donation to the coordinated carbene decreases considerably upon moving from early to later transition metals, which corresponds to moving from the A to the C type systems, as discussed by Nugent:^{197,198}

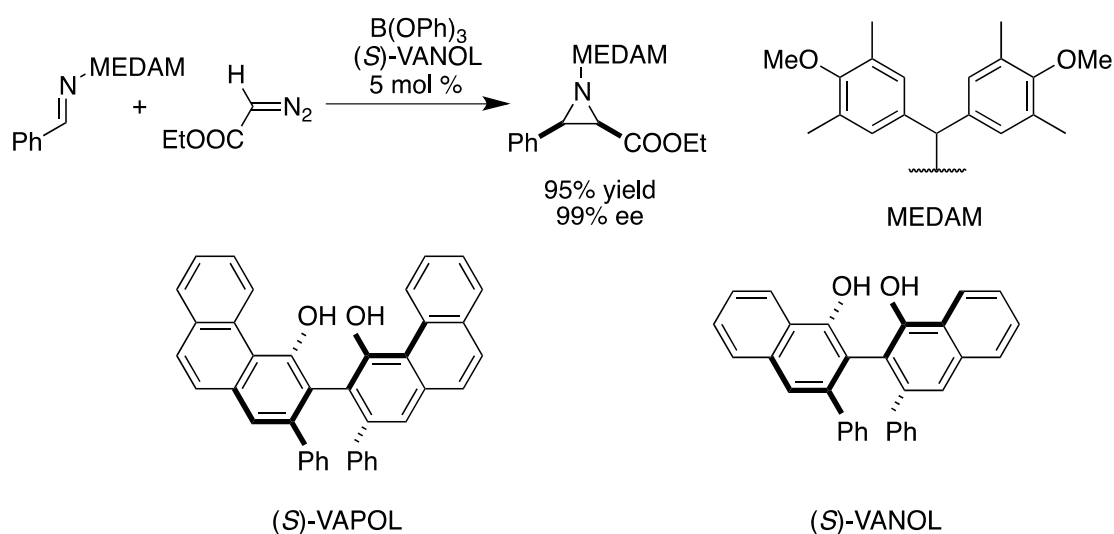


Scheme 3.20 Representation of energies of the HOMO and LUMO orbitals of carbene complexes with transition metals.

In the C type system, the energy of the 3*d* orbital is much lower than the energy of the *p* orbital of the carbenoid. The contribution to the LUMO of the metal-carbene bond is then bigger from the carbenoid C atom, which becomes more electrophilic. However, this is only true for frontier-orbital controlled reactions, that is, for soft molecules,¹⁹⁹ which is the case here. For this reason, late transition metals form particularly electrophilic carbene complexes. As a further consequence, the aziridination of imines catalyzed by copper and rhodium proceeds via nucleophilic attack of the imine to the metal carbene complex, whereas ruthenium carbene complexes are apparently not electrophilic enough to be attacked by the imine, which is a poor nucleophile.

3.3 Final Mechanistic Overview

The catalytic results illustrated in this chapter can be compared with those obtained using other catalytic systems for asymmetric aziridination of imines. Wulff¹¹⁶ reported the most efficient aziridination of imines in extremely high yields (up to 95%) and enantioselectivity (up to 99%) with a (*S*)-VAPOL/ BH_3 or (*S*)-VAPOL/ BH_3 catalyst:

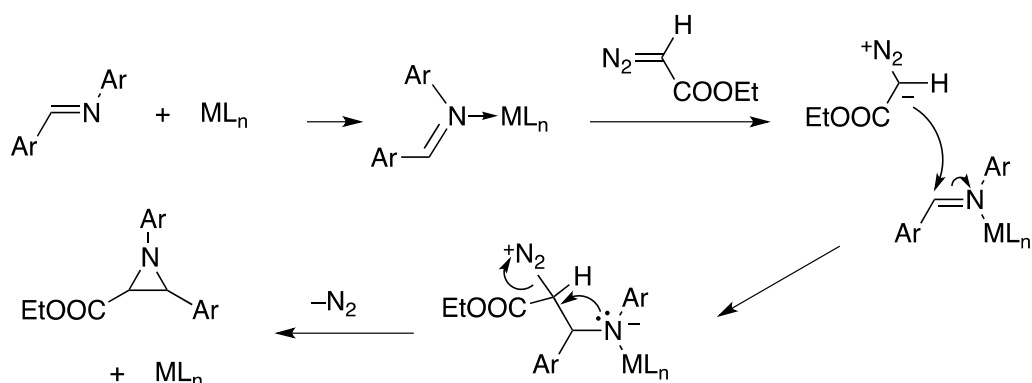


Scheme 3.21 Enantioselective imine aziridination as reported by Wulff.

The presence of a MEDAM (tetra-methyldianisylmethyl) as protecting group on the nitrogen turned out to be crucial for the excellent values of yields and enantioselectivity.¹⁵⁹ The deprotection from the MEDAM group was performed with triflic acid (5 equiv) in anisole, but was found to be problematic for aziridines bearing electron-rich *p*-substituents (such as MeO or Me), which limits the substrate scope. Concerning the mechanism, Wulff firstly proposed a Lewis acidic activation of the imine via coordination to the borane center. Only later, he found out that the active catalyst was the proton of a chiral Brønsted acid, originated from the borane/VANOL-based system (§ 2.3.4.2).¹¹⁹

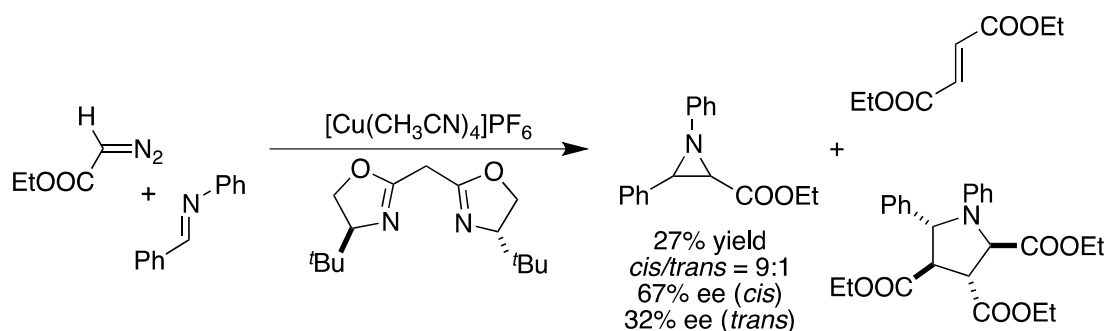
As an example of Lewis acid activation, Jørgensen¹¹⁰ tested SnCl_4 as achiral catalyst in the aziridination of imines. On the basis of the competition experiments performed,¹⁸² which showed that electron-donating imines react faster than electron-withdrawing ones, he proposed a mechanism that involves the nucleophilic attack of

the diazoacetate on the coordinated imine. The resulting species gives ring closure by intramolecular attack onto the imino carbon:



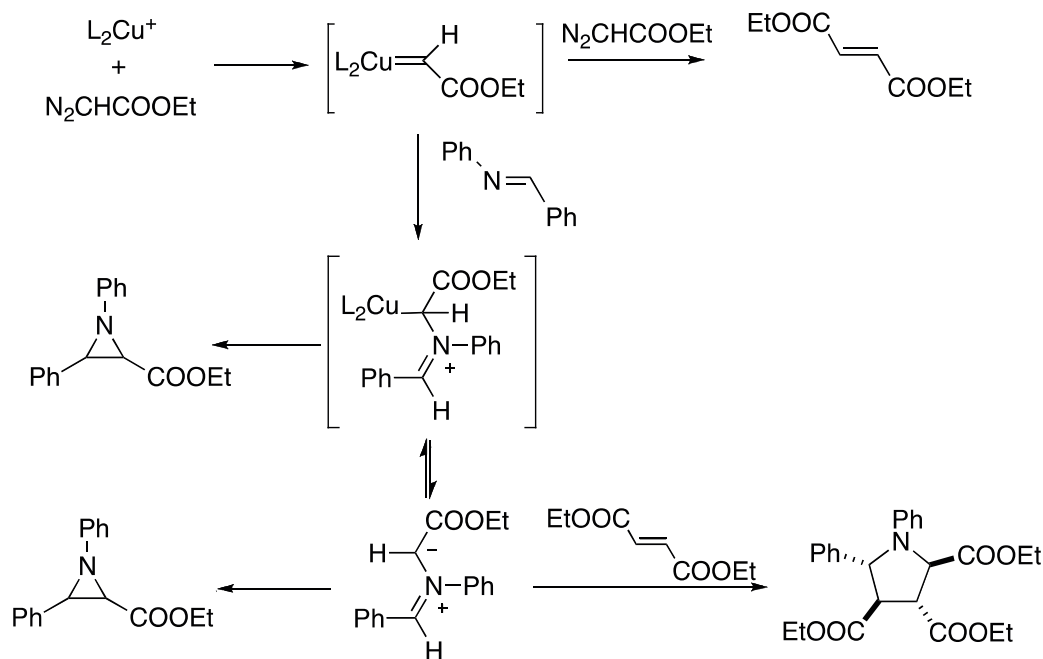
Scheme 3.22 Aziridination reaction mechanism by Lewis acid activation of the imine.

On the other hand, Jacobsen reported the asymmetric imine aziridination mediated by a copper carbene complex:¹²¹



Scheme 3.23 Jacobsen's imine aziridination with a Cu(I)-Box complex.

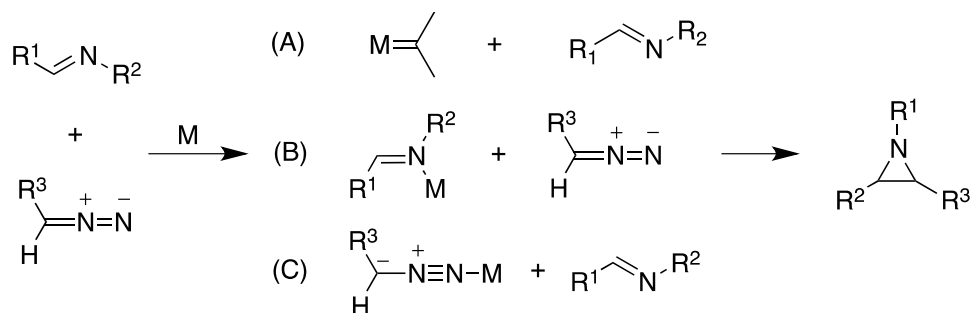
On the basis of the analysis of the byproducts and of trapping test, Jacobsen suggested that the formation of the aziridine involved a copper azomethine ylide complex as intermediate, generated by the nucleophilic attack of the imine onto a metal carbene complex (Scheme 3.24).



Scheme 3.24 Jacobsen's mechanism for imine aziridination catalyzed by copper.

In this context, we add to the above list a new mechanism proposed for Ru/PNNP based systems,¹⁰⁵ in which the carbene complex does not react and the active species is the ruthenium diazoester adduct.

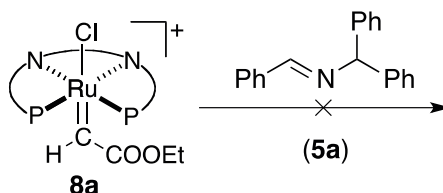
The following scheme summarizes the three possible mechanisms for imine aziridination (Scheme 3.25). The results presented in this thesis support the proposed mechanism (C) and contribute to rule out the other two paths (A) and (B). These evidences and the ones previously found in our group will be now briefly summarized.



Scheme 3.25 Reported mechanisms for catalytic imine aziridination with ethyl diazoacetate.

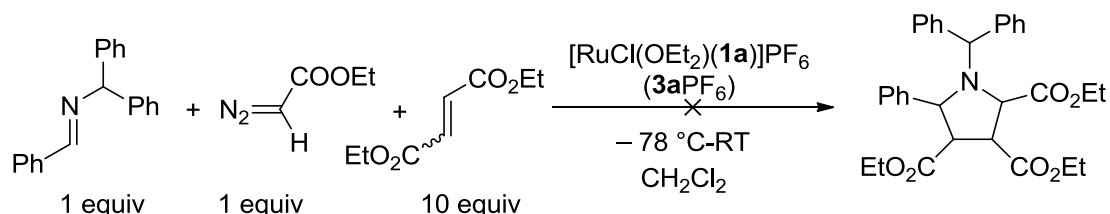
A) *Reaction of a metal carbene intermediate with a free imine.*

1. The carbene complex $[\text{RuCl}(\mathbf{1a})(\text{CHCOOEt})]$ **8a** was prepared by addition of EDA (1 equiv) to a solution of $\mathbf{3aPF}_6$ and characterized. It did not react with imine **5a** to give aziridine **6a**.¹³⁹



Scheme 3.26 Imine **5a** does not react with the carbene complex **8a**.

2. By analogy with Jacobsen's work,¹²¹ a standard test for azomethine ylides was performed. An excess of diethylmaleate (10 equiv) or diethylfumarate (10 equiv) was added to the reaction solution containing $[\text{RuCl}(\text{OEt}_2)(\mathbf{1a})]\text{PF}_6$ ($\mathbf{3aPF}_6$). The ^1H NMR spectrum of the crude reaction indicated that no pyrrolidine was formed, suggesting that no carbene was involved as intermediate in the reaction:

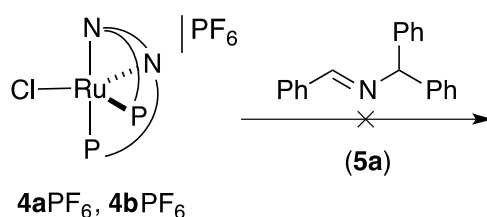


Scheme 3.27 Trapping test for azomethine ylides.

B) *Acidic activation of the imine and its reaction with the ethyl diazoacetate.*

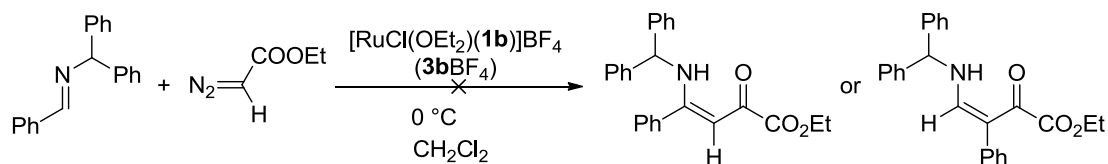
1. Previous NMR spectroscopic investigations performed in our group showed that imine **5a** did not react with the five-coordinate complex with the unsubstituted ligand $[\text{RuCl}(\mathbf{1a})]^+$ (**4a**).¹³⁹ Furthermore, the ^{31}P NMR spectra of the five-coordinate complex with the 3,5-dimethyl substituted ligand $[\text{RuCl}(\mathbf{1b})]^+$ (**4b**) recorded at different temperatures remained unchanged after the addition of imine **5a** (1, 5, and

10 equiv). This confirmed that no coordination of **5a** to complex **4b** occurred, even in the presence of an excess of the imine.



Scheme 3.28 Imine **5a** does not react with the five-coordinate complexes **4a** or **4b**.

2. Enaminoesters are known to be the typical byproducts of the aziridination reaction catalyzed by Lewis acidic activation of imine, as reported by Brookhart and Templeton.¹⁰⁹ By testing $[\text{RuCl}(\text{OEt}_2)(\mathbf{1b})]\text{BF}_4$ (**3bBF₄**) in the asymmetric aziridination of *N*-benzylidene-1,1-diphenylmethanamine (**5a**) with EDA under different temperature conditions at constant pressure, no signals that might be assigned to enaminoesters were found in the region between δ 8.60 and δ 10.30 of the ¹H NMR spectrum of the crude reaction mixture.



Scheme 3.29 Aziridination with $[\text{RuCl}(\text{OEt}_2)(\mathbf{1b})]\text{BF}_4$ does not give enaminoesters as byproducts.

C) *Carbene transfer from a diazoester complex to the free imine.*

1. The ¹⁵N NMR data of the diazoester complex *trans*- $[\text{RuCl}(\text{N}_2\text{CHCOOEt})(\mathbf{1a})]^+$ (**9a**) suggest a linear Ru–N–N–C moiety (Figure 3.10).¹³⁹ The geometry of the coordination is thought to influence the electronic properties of the carbenoid.¹⁸³ In particular *end-on*, linear coordination of diazoalkanes to a transition metal stabilizes a limiting structure of the diazoester in which the α -C atom is nucleophilic.

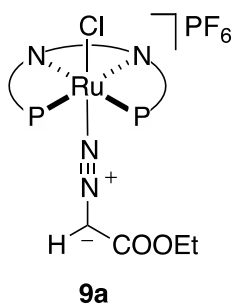


Figure 3.10 *Trans*-[RuCl(N₂CHCOOEt)(**1a**)]⁺ (**9a**).

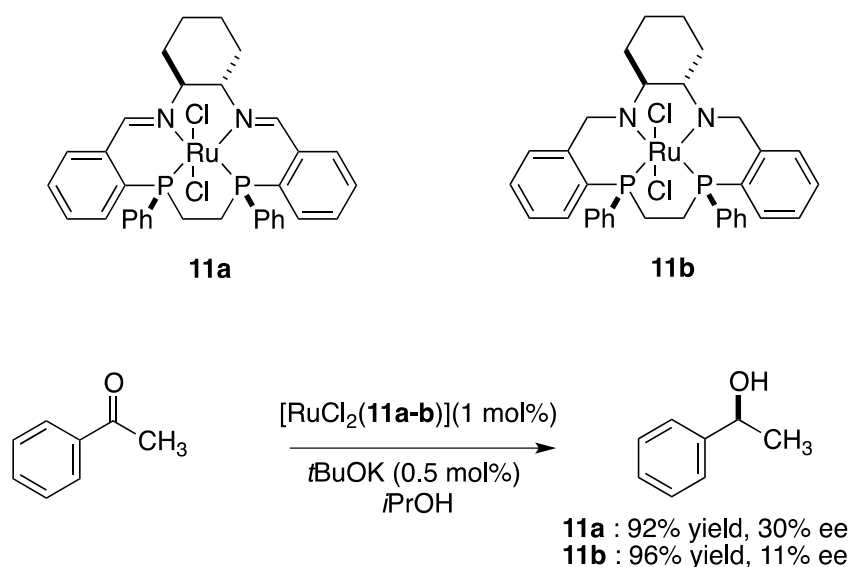
2. The competition experiments with 4-substituted-*N*-benzylidene-anilines showed that aziridines with electron-withdrawing substituents are formed faster than those bearing electron-donating groups (Figure 3.5). This supports a mechanism in which imines with electron-withdrawing substituents react faster with EDA, as in the case of the attack of the nucleophilic metal coordinated EDA to the electrophilic imine.

From the results presented in this chapter with the 3,5-dimethylsubstituted ligand **1b**, two conclusions can be drawn. First, the experimental evidences discussed above confirm a mechanism that involves the nucleophilic attack of a ruthenium diazoester complex to the free imine. Secondly, we found out that acid species present in traces are able to catalyze a nonenantioselective aza Darzens reaction to give racemic aziridine *cis*-**6a** with high yields and are therefore responsible for the low enantioselectivity. By using the nonhydrolyzable anion BF₄⁻ and by controlling the reaction conditions, in order to avoid the competing nonenantioselective aza-Darzens path, [RuCl(OEt₂)(**1b**)]⁺ catalyze the asymmetric aziridination of imine **5a** with an excess of EDA (4 equiv) to give aziridine (*R,R*)-*cis*-**6a** in good yields (39%) and high enantioselectivity (93%). This shows that it is possible to perform highly enantioselective imine aziridination also with a transition metal such as ruthenium.

4. Latest Studies on the Synthesis of New Chiral P_2N_2 Macrocycles of C_2 -Symmetry

Previous studies performed in our group suggested that, to increase the aziridine yield, the decomposition of the diazoester complex to carbene complex must be slowed down. As ruthenium complexes with conformationally rigid PNNP macrocyclic ligands seemed to be suitable to this purpose, we decided to test such complexes in asymmetric imine aziridination.

Our group has already investigated the possibility of using macrocyclic PNNP ligands in combination with ruthenium for asymmetric catalysis. The transfer hydrogenation of acetophenone performed with the C_1 -symmetric complex **11a** gave 1-phenylethanol with 92% yield and enantioselectivity of 30% ee, whereas higher yields (96%), but lower enantioselectivity (11% ee) were obtained with the diamine analogue **11b** (Scheme 4.1).¹⁵³ Considering the pseudo-*meso* relationship between the two phosphorus atoms, the low enantioselectivity of the reaction was not surprising. Therefore, we focused on the preparation of chiral C_2 -symmetric macrocycles.



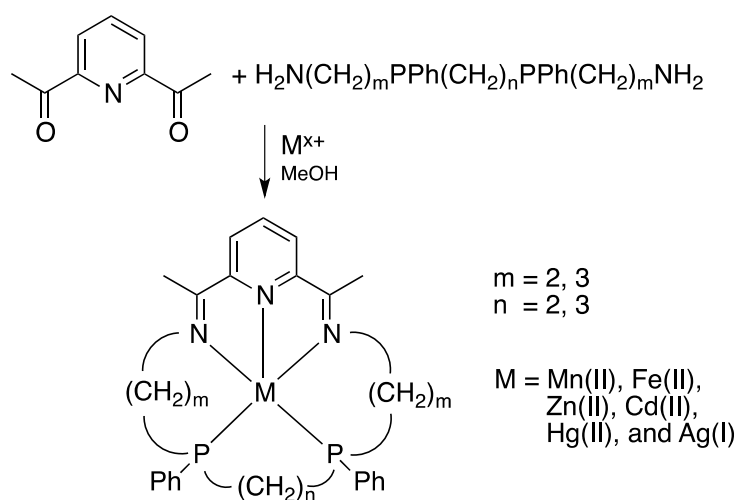
Scheme 4.1 Transfer hydrogenation of acetophenone catalyzed by ruthenium in combination with macrocyclic PNNP ligands.

After a general introduction on the reported synthetic methods for similar macrocyclic compounds or chiral phosphines with stereogenic phosphorus, our attempts of preparing C_2 -symmetric P_2N_2 macrocycles will be described.

4.1 Introduction

4.1.1 P_2N_2 Macrocycles

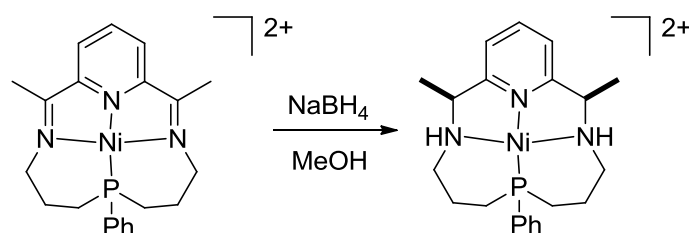
Before the 1980s, many macrocycles containing nitrogen donor atoms have been prepared by condensation of primary amines with aldehydes or ketones. A template effect, induced by the presence of metal ions, was exploited several times.²⁰⁰⁻²⁰² Later, phosphorus atoms were introduced in such cycles to modify their coordination properties.²⁰³ Cabral reported a synthesis that required refluxing 2,6-diacetylpyridine with the appropriate diphosphinodiamine and metal salt and was generally used for many years. The necessary ditertiaryphosphinodiamines were prepared in two steps from phenylphosphine and the corresponding chloroamines and dichlorides, as described by Issleib:²⁰⁴



Scheme 4.2 Cabral's template synthesis of macrocycles.

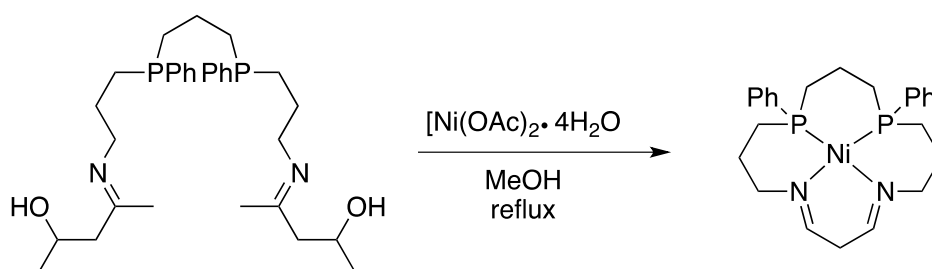
In 1974, Meek²⁰⁵ reported the synthesis of a tetradentate PN_3 -ligand containing phosphorus and nitrogen donor atoms in analogy with the one depicted in Scheme 4.2, with $\text{NiCl}_2 \cdot 6\text{H}_2\text{O}$ as the source of the templating Ni(II). The macrocycle

was then reduced by NaBH_4 in order to obtain the amine analogue:



Scheme 4.3 Nickel(II) complexes with macrocyclic PN_3 ligands.

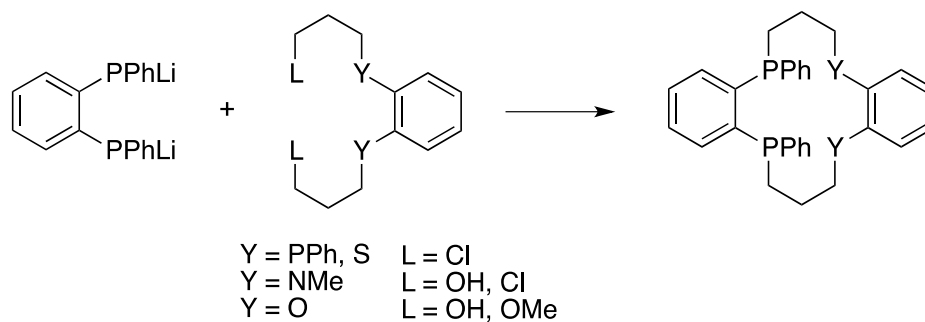
Macrocyclic ligands of the P_2N_2 type were published for the first time in 1980 by Cummings and Meek.²⁰⁶ They used a new approach for the templated synthesis of such molecules, since the method already reported for tetraaza systems²⁰⁷ was found ineffective. The key step was the formation of the following intermediate via Issleib's method,²⁰⁸ which was then cyclized with the aid of the templating nickel salt.



Scheme 4.4 Template synthesis of macrocyclic P_2N_2 ligands.

The ^{31}P NMR spectrum indicated the formation of only one type of phosphorus product, and X-ray diffraction confirmed the isolation of the *meso*-isomer. Interestingly, their synthesis was modulable for the preparation of macrocycles with different bridges between the nitrogen and the phosphorus atoms.¹⁹⁶ Since then, templating metals have been used to prepare many other ligands in a few steps and very high yields. More recent examples were found in the works of Edwards,²⁰⁹⁻²¹² Stelzer,²¹³⁻²¹⁵ and Morris.^{216,217}

A different approach was reported by Kyba and his group,²¹⁸ who published a nontemplate synthesis of tetradentate P_2N_2 macrocyclic ligands (Scheme 4.5).



Scheme 4.5 Kyba's nontemplate synthesis of macrocyclic P_2Y_2 ligands.

All the macrocyclizations described were carried out in boiling THF under high dilution conditions of all reagents. The products were obtained in around 20% yield. Because of the relatively low inversion barriers of the phosphines (32-35 kcal/mol), many isomers may form under such conditions. Nevertheless, they noted the exclusive formation of the *meso* isomer with the two phenyl rings in *cis* position with respect to the benzo bridge and occupying pseudoequatorial positions of the ring.

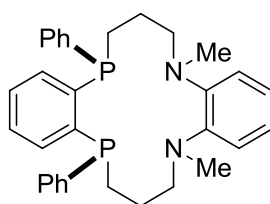
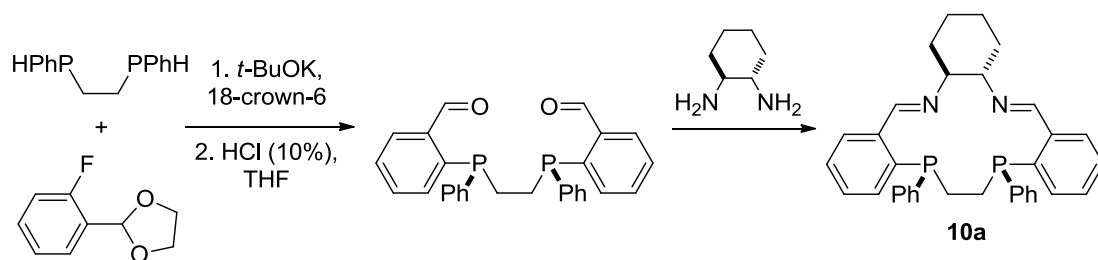


Figure 4.1 Kyba's 14 membered rings.

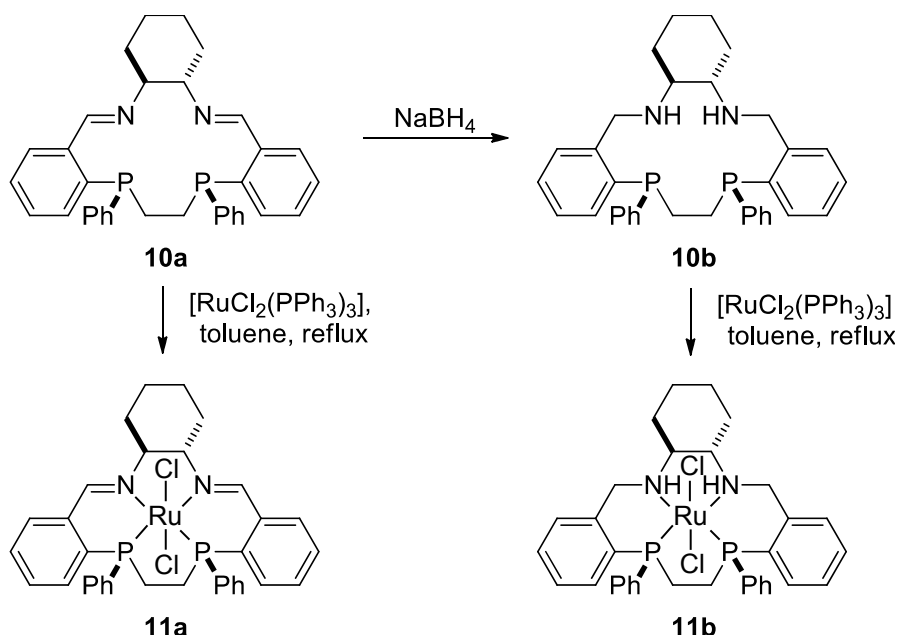
4.1.2 C_1 -Symmetric PNNP Macrocycles

In our group, the preparation of C_1 -symmetric macrocycles was performed in three steps without the introduction of any templating metal. This straightforward synthesis led to the formation of the first chiral macrocyclic PNNP (**10a**) (Scheme 4.6).¹⁵³



Scheme 4.6 General method for the preparation of chiral P₂N₂ macrocycles.

Ligand **10a** was easily reduced with NaBH₄ to its diamino analogue **10b** (Scheme 4.7). The complexation of **10a** and **10b** with a ruthenium precursor such as [RuCl₂(PPh₃)₃] gave the corresponding ruthenium(II) dichloro complexes (**11a**, **11b**):¹⁵³



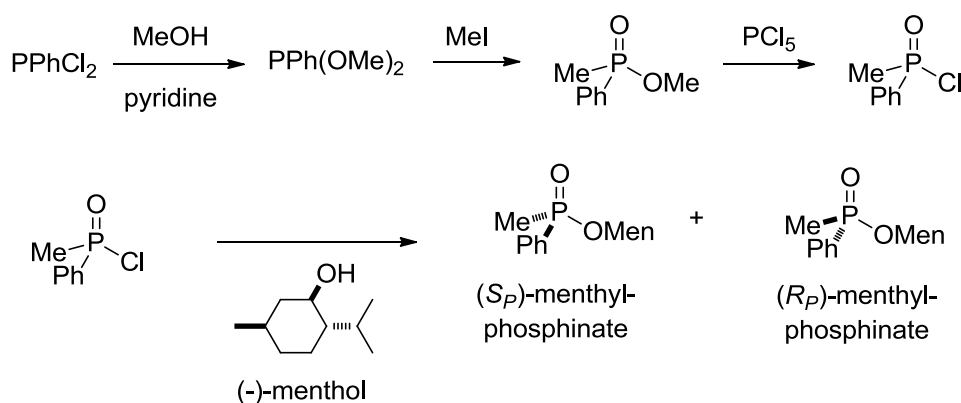
Scheme 4.7 Preparation of ruthenium(II) dichloro complexes with macrocyclic PNNP ligands.

4.1.3 Chiral Phosphines with Stereogenic Phosphorus

An attempt to reverse the tendency for the selective formation of the *meso*-isomer of the macrocycle reported by Kyba²¹⁸ may involve the stereoselective synthesis of chiral phosphines. In 1911, Meisenheimer and Lichtenstadt proved that

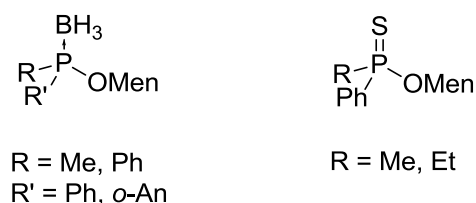
asymmetrically substituted phosphorus compounds can be resolved into two enantiomeric forms.²¹⁹ From then on, few reports have been published on the pyramidal instability of the phosphine at elevated temperatures. Mislow suggested that the effect of the substituents was mainly electronic, as electron-withdrawing substituents in the *para* position were found to lower the energy barrier to pyramidal inversion.^{220,221}

Concerning the preparation of enantiomerically pure phosphines, different procedures have been developed for their stereoselective synthesis besides the resolution of racemic mixtures. The first successful studies were performed by Nudelman and Cram²²² and by Mislow and co-workers,^{223,224} who reported the preparation of asymmetrically substituted menthyl phosphinates and the separation of the diastereoisomers by fractional crystallization:



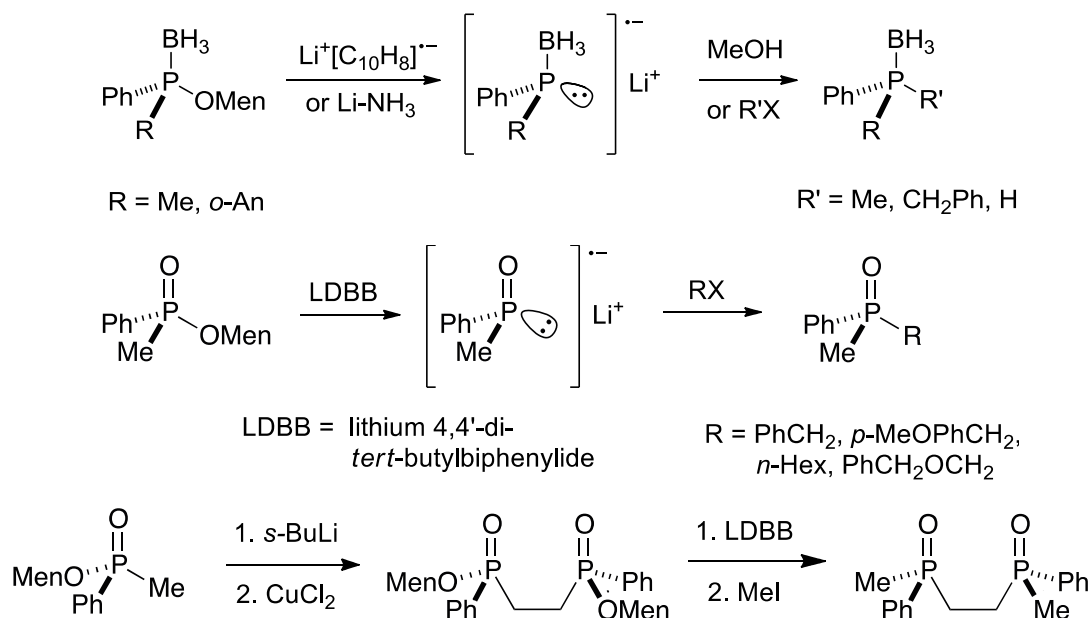
Scheme 4.8 Preparation of P-chirogenic menthyl phosphinates.

Alternative approaches were then developed, involving the formation of menthyl-phosphine boranes^{225,226} or menthyl-phosphine thioates.^{227,228}



Scheme 4.9 Preparation of P-chirogenic menthyl-phosphine borane and menthyl-phosphine thioates.

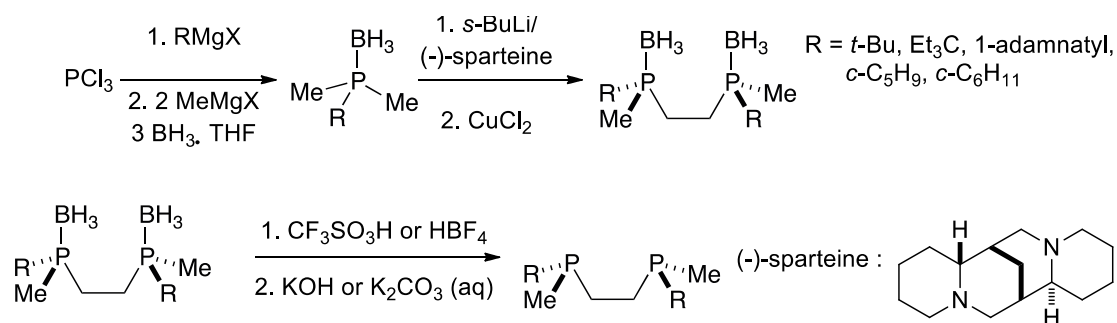
Imamoto and co-workers^{229,230} expanded the use of the menthyl phosphinates of oxides and boranes in combination with organometallic reagents and found that the ester P–O bond in menthylphosphinates can be selectively cleaved, to give a configurationally stable anionic tricoordinate phosphine borane intermediate:



Scheme 4.10 Imamoto's method for the preparation of P-chirogenic phosphine oxides and phosphine boranes.

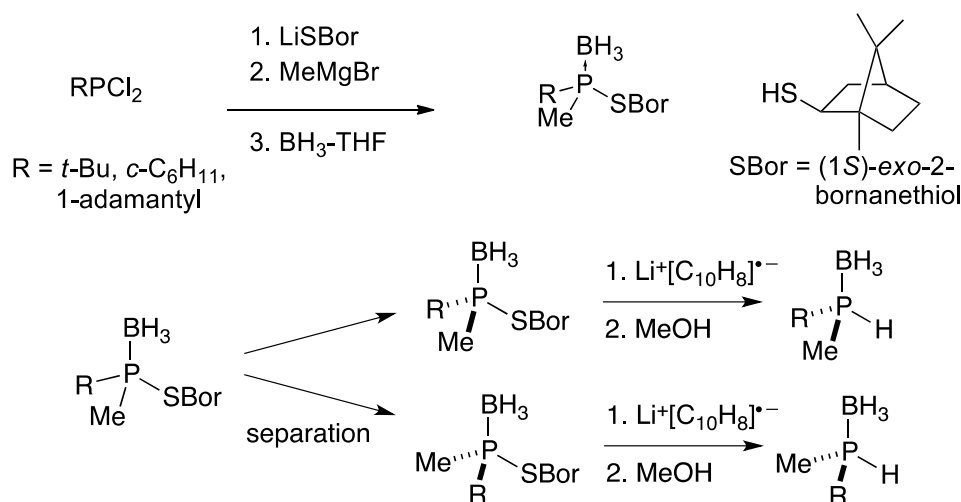
The lithiated phosphine borane derivatives react stereoselectively with organohalides to give precursors for interesting chiral phosphino derivatives.

Imamoto also²³¹ investigated the synthesis and reactivity of sterically hindered phosphineboranes, such as *tert*-butylmethyl-, cyclohexylmethyl-, and 1-adamantylmethylphosphine boranes. By using (–)-sparteine as the source of chirality, they performed an asymmetric enantioselective deprotonation with *s*-BuLi. On the basis of these achievements, they prepared new C_2 -symmetric *P*-chirogenic diphosphineboranes (Scheme 4.11).



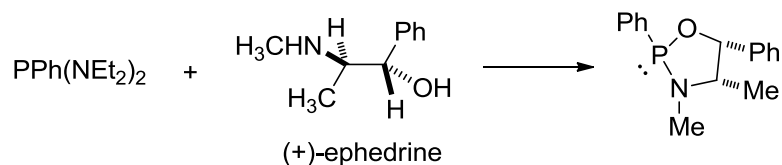
Scheme 4.11 Imamoto's preparation of C₂-symmetric diphosphines.

More recently, Imamoto²³² obtained chiral secondary phosphine boranes using (1*S*)-exo-2-bornanethiol (BorSH) as a chiral auxiliary.



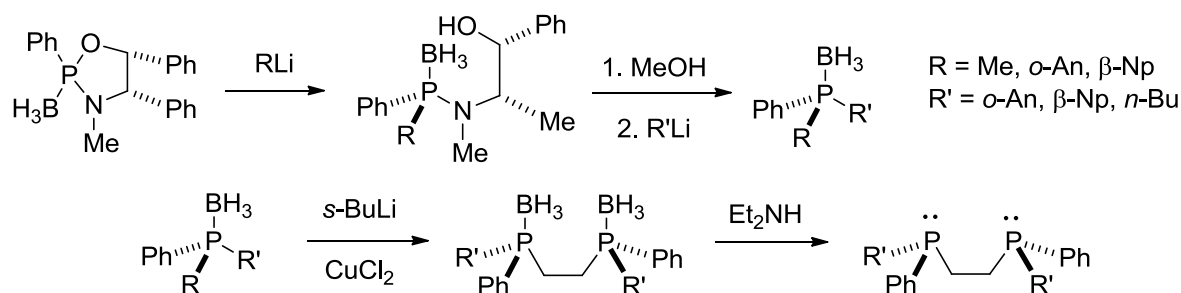
Scheme 4.12 Imamoto's synthesis of P-chirogenic secondary phosphine borane derivatives.

Jugé and Genet developed a synthesis of phosphinoboranes with a very high enantiomeric purity. They used a 1-phenyloxazaphospholidine obtained directly from (+)-ephedrine and PPh(NEt₂)₂.²³³



Scheme 4.13 Jugé's preparation of 1-phenyloxazaphospholidine.

Further studies²³⁴ performed on the corresponding phosphinamideboranes by the same group showed that the P–O bond was cleaved with retention of configuration (>92%) at the phosphorus atom.²³⁵ As a result, they developed a procedure for the synthesis of the largely employed PAMP and DIPAMP ligands (Scheme 4.14).



Scheme 4.14 Jugé's synthesis of P-chirogenic diphosphine boranes.

Some attempts¹³⁹ were performed in our group in order to exploit the methods developed by Jugé and Imamoto, aiming to the preparation of the following diphosphine borane intermediate:

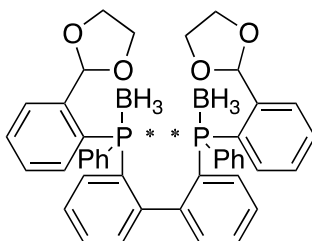
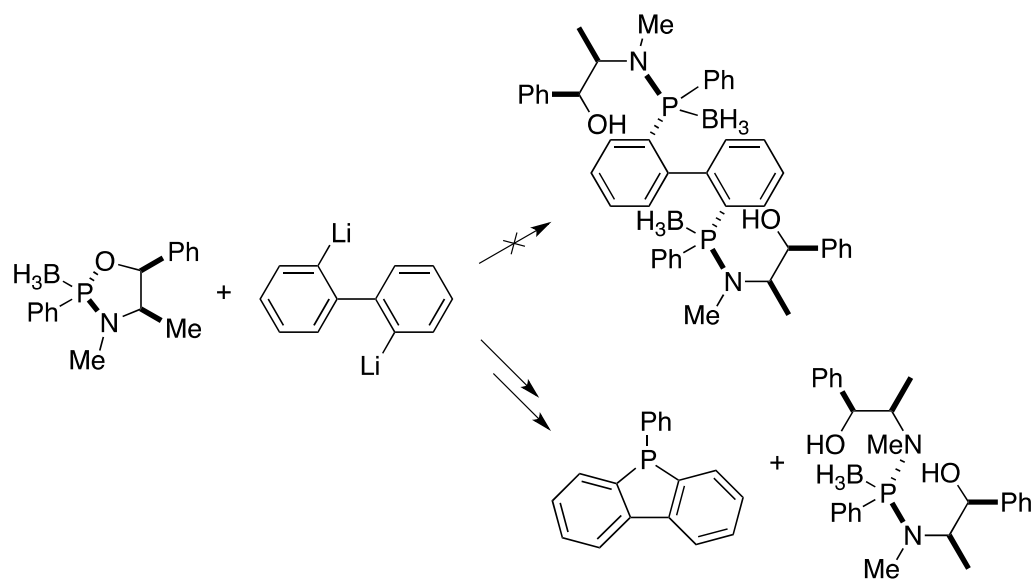


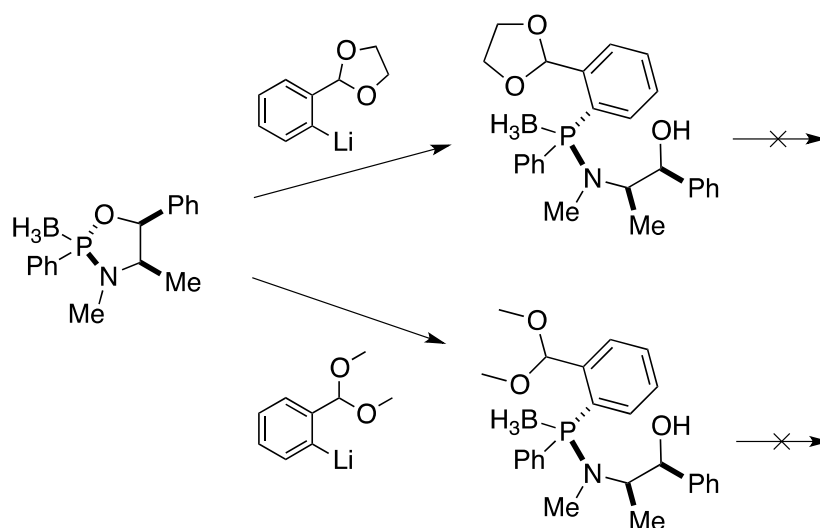
Figure 4.2 P-chirogenic diphosphine borane derivative as the synthetic target.

At first, the methodology developed by Jugé was tried in order to prepare the precursor depicted above by reacting 1-phenyloxazaphospholidine with dilithium biphenyl. The attempt failed, as the reaction gave undesired phenylphosphafluorene instead of the desired diphosphine (Scheme 4.15).



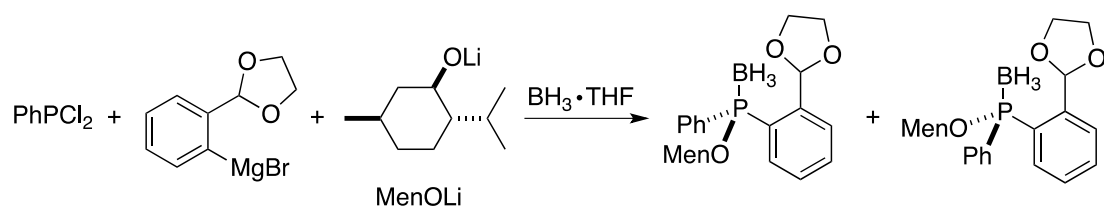
Scheme 4.15 Reaction of 1-phenyloxazaphospholidine with dilithium biphenyl.

A second attempt was unsuccessful because of the instability of the protecting group of the aldehyde under the conditions necessary to cleave the ephedrine residue to produce either the phosphinite borane or the chlorophosphine borane:



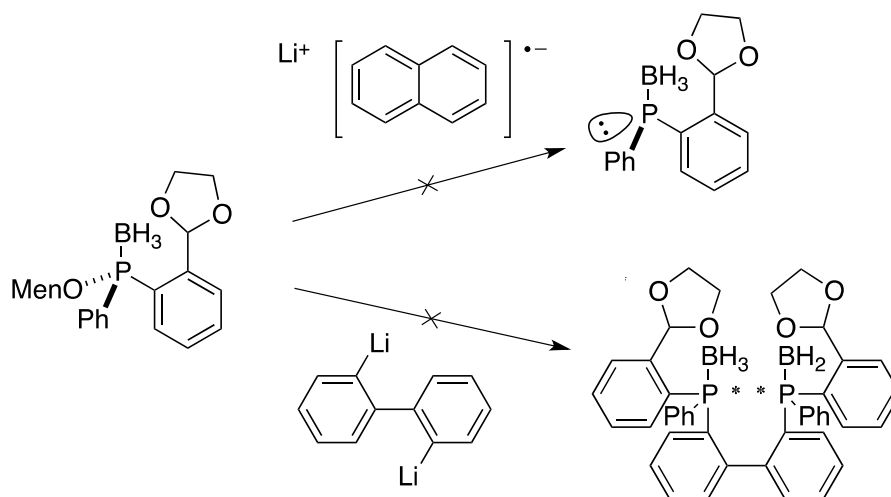
Scheme 4.16 Synthetic approach involving the formation of the two (aryl)(phenyl)-((methyl)amino-1-phenylpropan-1-ol)phosphine boranes .

Therefore, a different approach was tested, which was based on Imamoto's method for the synthesis of chiral borane derivatives with (-)-menthol as chiral auxiliary:



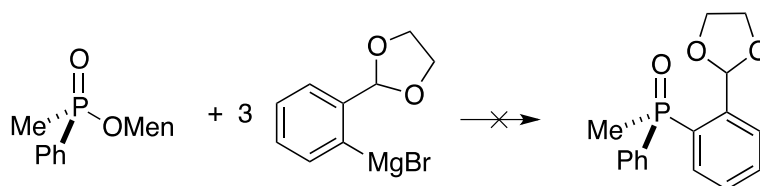
Scheme 4.17 Imamoto's synthetic approach for the preparation of the P-chirogenic (2-(1,3-dioxolan-2-yl)-phenyl)(menthyl)(phenyl)phosphine borane.

However, the reaction of the (2-(1,3-dioxolan-2-yl)-phenyl)(menthyl)(phenyl)-phosphine borane with lithium naphthalenide cleaved the P–C bond of the substituted aromatic ring instead of the P–O bond of the menthoxide moiety. On the other hand, the reaction with an excess of dilithium biphenyl gave a mixture of products, from which the desired diphosphine borane was not isolated:



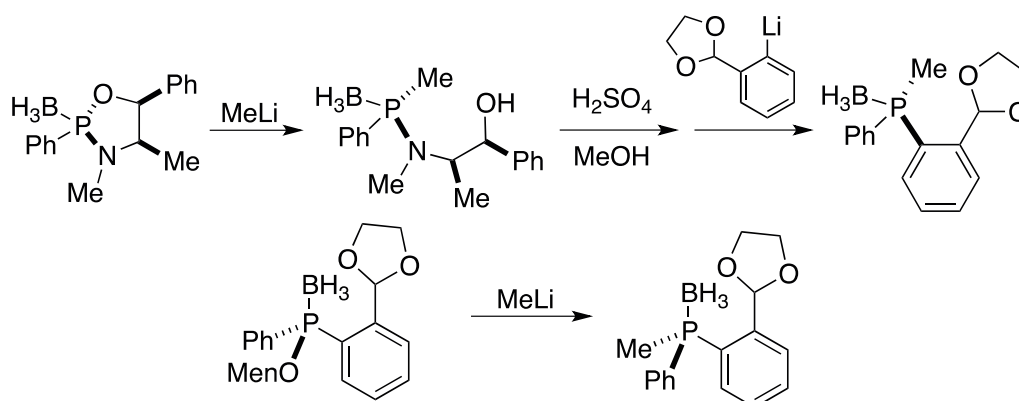
Scheme 4.18 The reaction of (2-(1,3-dioxolan-2-yl)-phenyl)(menthyl)(phenyl)-phosphine borane with lithium naphthalenide or dilithium biphenyl failed to give the desired P-chirogenic phosphine boranes.

As a further attempt, Mislow's approach involving the use of a phosphorus (V) intermediate and (-)-menthol as chiral auxiliary was tested, but failed to give the desired chiral phosphine oxide:

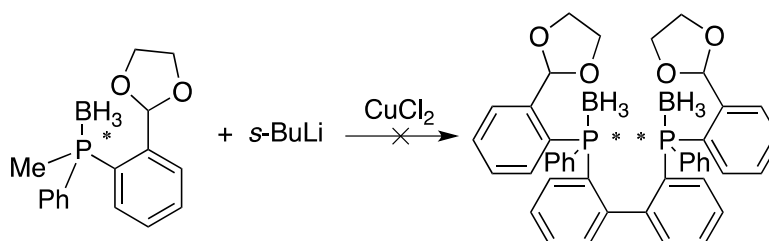


Scheme 4.19 Mislow's approach for the preparation of the P-chirogenic phosphine oxide.

Jugé and Imamoto's methods were successfully used for the preparation of (*R_p*)- and (*S_p*)-2-(1,3-dioxolan-2-yl)-phenyl(methyl)(phenyl)phosphine borane (Scheme 4.20), but this latter product did not give oxidative coupling in the presence of CuCl₂ to form the protected diphosphine:

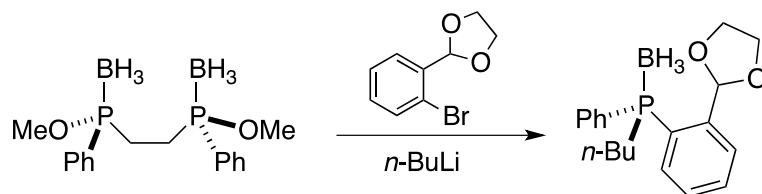


Scheme 4.20 Jugé's approach for the preparation of (*R_p*)- and (*S_p*)-2-(1,3-dioxolan-2-yl)-phenyl(methyl)(phenyl)phosphine borane.



Scheme 4.21 Reaction of (*R_p*)- and (*S_p*)-2-(1,3-dioxolan-2-yl)-phenyl(methyl)(phenyl)phosphine borane with CuCl₂

The last attempt involved a second method reported by Jugé to prepare DIPAMP derivatives. Unfortunately, the chiral diphosphinite did not react with 2-dioxolanophenyllithium to form the desired borane-protected chiral diphosphine, but gave instead the following phosphine:



Scheme 4.22 Reaction of P-chirogenic diphosphinite with 2-dioxolanophenyllithium.

Therefore, some completely different approaches toward the synthesis of C_2 -symmetric macrocycle had to be developed for the present study, which are described in the next paragraph.

4.2 C_2 -Symmetric Macrocycles: New Attempts

On the basis of the preliminary results achieved with the already described C_1 -symmetric ligands **10a**, we focused on the synthesis of chiral macrocyclic PNNP ligands of C_2 -symmetry:

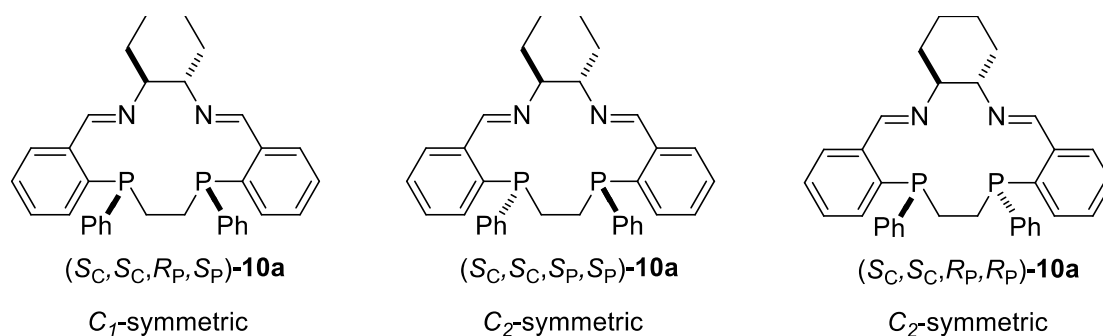
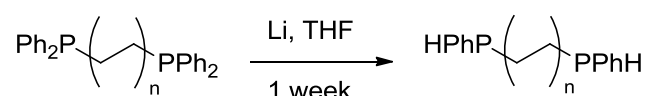


Figure 4.3 C_1 - and C_2 - symmetric macrocycles.

To this purpose, the most challenging issue was the control of the stereochemistry at the two stereogenic phosphorus atoms. Hence, three different approaches to the synthesis of chiral C_2 -symmetric macrocycles were explored.

4.2.1 Cyclization by Condensation

We decided to extend the same procedure used for the C_1 -symmetric macrocycles to the C_2 -symmetric target. Therefore, we prepared the secondary diphosphines 1,2-bis(phenylphosphino)ethane (mppe) and 1,2-bis(phenylphosphino)propane (mppp) from 1,2-bis(diphenylphosphino)ethane (dppe) and 1,2-bis(diphenylphosphino)propane (dppp), by Kimpton method.²³⁶

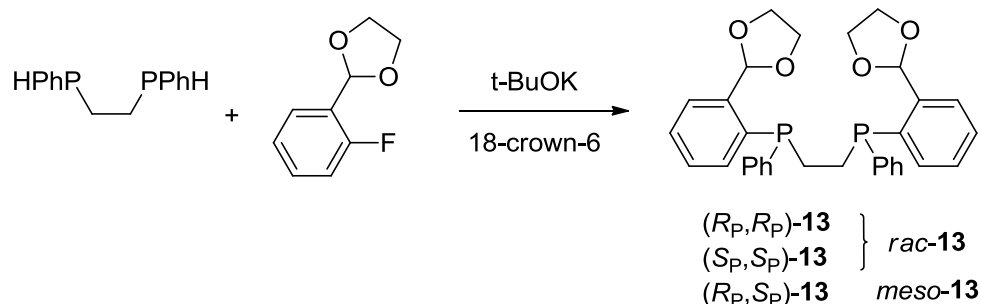


Scheme 4.23 Kimpton's preparation of secondary diphosphines with metallic lithium.

The above procedure is more efficient than other procedures involving the reduction of the tertiary diphosphine with LiAlH_4 ^{237,238} or the reaction of either NaPPhH or KPPhH ²³⁹⁻²⁴¹ with the appropriate n -dihaloalkane. In this method, a P-aryl bond of a ditertiary phosphines, $\text{Ph}_2\text{P}(\text{CH}_2)_n\text{PPh}_2$, is cleaved with metallic lithium to give $\text{PhLiP}(\text{CH}_2)_n\text{PLiPh}$, which is then hydrolyzed to the desired disubstituted phosphine.

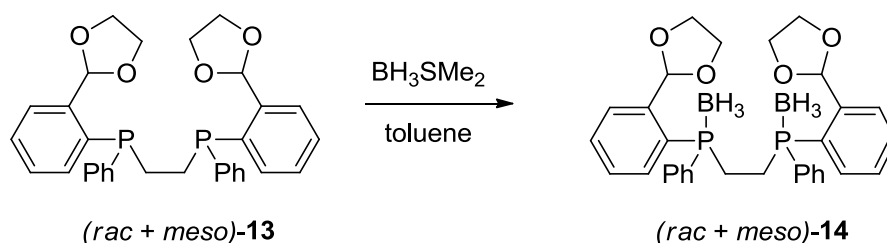
Kimpton reported that the competing cleavage of a P- CH_2 bond gave large amounts of alternative products owing to, but also that this was strongly reduced under suitable conditions. For instance, the reaction between dppe and metallic lithium in THF reached completion within 24 h at 300 K, but significant cleavage of P- CH_2 bonds occurred so that the yield of the desired mppe was low. In contrast, by reducing the temperature to 0 °C, the P-C bond cleavage was more selective, and the formation of $\text{PhLiPCH}_2\text{CH}_2\text{PLiPh}$ was favored, although the reaction times were significantly longer (200 h). The same procedure at low temperature (<0 °C) gave good yields also in case of other α,ω -bis(diphenylphosphino)alkanes, such as dppp. For these reasons, we prepared mppe and mppp by stirring the reaction mixture at 0 °C for 16 days. The secondary diphosphines were isolated by distillation under high vacuum at high temperatures, as they have are reported to have boiling points of 90 °C/4.0 mmHg and 147 °C/0.09 mmHg, respectively.²⁴²

Freshly distilled mppe was used in the aromatic substitution with the protected *o*-fluorobenzaldehyde after deprotonation of the phosphine with potassium *tert*-butoxide in presence of 18-crown-6 ether. A mixture of the *rac* and *meso* isomers was obtained:



Scheme 4.24 Preparation of (*rac* + *meso*)-**13**.

Attempts of separation of the *rac*-**13** and *meso*-**13** isomers by crystallization failed, as *rac*-**13** was an oil, which always resulted contaminated with the *meso* isomer. Therefore, in order to purify and separate the mixture of diastereoisomers of **13**, the phosphine were protected by preparing the borane adducts **14**, which are air-stable and often crystalline:

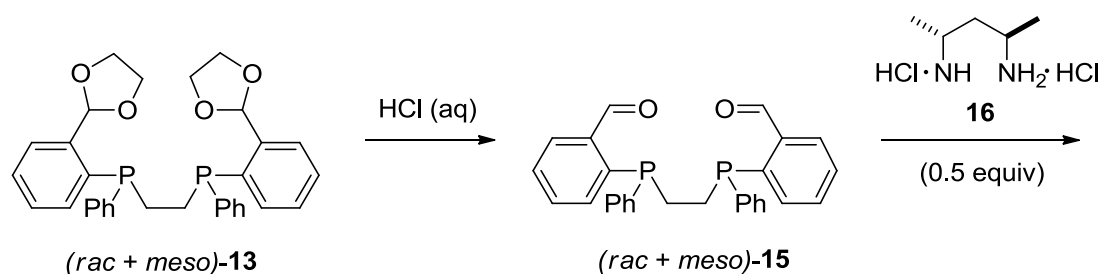


Scheme 4.25 Preparation of (*rac* + *meso*)-**14**.

A mixture of **13** was treated with $\text{BH}_3\cdot\text{SMe}_2$ in toluene at room temperature while monitoring the reaction by TLC. The reaction reached completion after 12 h and was quenched with water. The successful formation of a P–borane adduct was confirmed by ^{31}P NMR spectroscopy. Then, the organic layer was separated and the product was isolated as a white solid after evaporation of the solvent under reduced pressure. Repeated attempts to crystallize **14** in methanol by warming the solution at 35 °C revealed that the borane adduct was not as stable as expected. Finally, the separation of the borane adduct (*R,R*)-**14** and (*S,S*)-**14** isomers with preparative chiral

HPLC failed on several columns (OJ, OD-H, AD-H) under different solvent and flow rate conditions.

Therefore, we decided to use the mixture of the diastereoisomers **14** for the further step, that is, the deprotection of the carbonyl groups with aqueous HCl (5%). As expected, the borane adduct **14** was not stable in the presence of the acid and, hence, the protection on the phosphorus atoms was removed as well. For the last condensation step, (*S,S*)-2,4-diaminopentane dihydrochloride (**16**) (0.5 equiv), prepared as reported by Harries and Haga,^{243,244} was refluxed for 4 h in the presence of an excess of K₂CO₃ (2 equiv) in an EtOH/H₂O (2:1) solution. Then, the *rac*- and *meso*-2,2'-(ethane-1,2-(phenylphosphinediyl)dibenzaldehyde (*rac*- and *meso*-**15**) was dissolved in ethanol (20 mL), added to the reaction mixture, and refluxed for 48 h.



Scheme 4.26 Preparation of (*rac* + *meso*)-**15** and subsequent reaction with **16**.

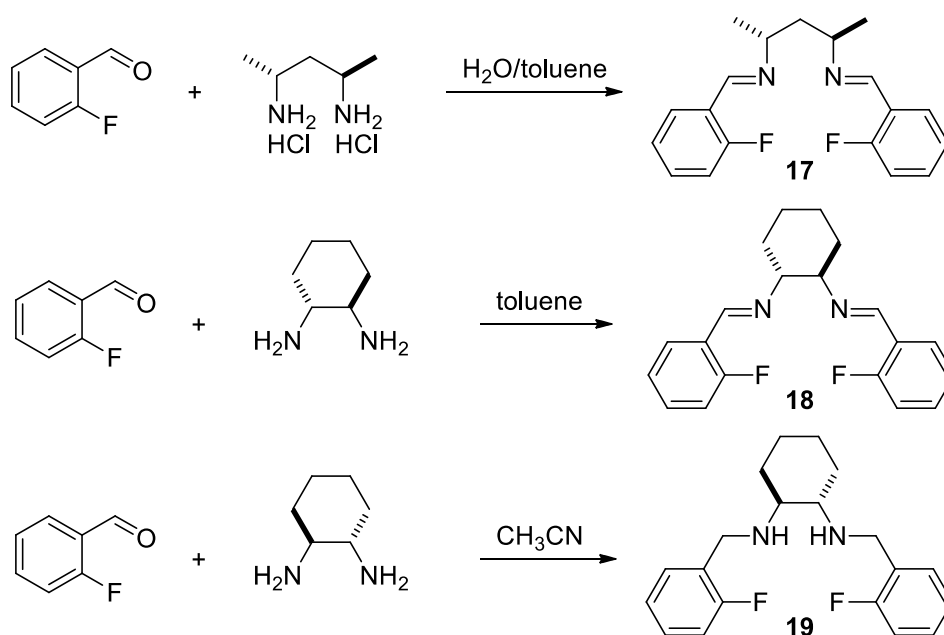
During the reaction, whose course was monitored by ³¹P NMR spectroscopy, the solution turned from yellow to colorless. In the ³¹P NMR spectrum, many different signals were observed, probably due to oligomerization or decomposition of the products. Upon repeating the same experiment under milder conditions and stirring at room temperature for 96 h, the aldehyde reacted quantitatively. The ³¹P NMR spectrum of the reaction solution showed two doublets at δ -8.9 and -29.5 (²J_{P,P'} = 41 Hz) and a singlet at δ -26.4. These signals were in agreement with the formation of both *C*₁- and *C*₂- symmetric macrocycles, and their integration indicated approximately a 40:60 ratio. Moreover, it has to be noted that only one singlet was observed in the ³¹P NMR spectra. This is an indication that only one of the two possible *C*₂-symmetric isomers was formed.

MM calculation (Cerius²) for the three isomers with the configuration on the iminic atoms fixed at (*R,R*) suggested that the (*R,R,R_P,R_P*) diastereoisomer was 10.2

kcal/mol more stable than the corresponding (*R,R,S_P,S_P*) one. This might imply that the formation of only one of the two possible *C*₂-symmetric cycles is energetically favored. All the attempts to separate the products via chromatographic column and preparative HPLC failed, as the compounds proved to be air sensitive and were oxidized during the purification, even though degassed solvents and an argon flow were employed.

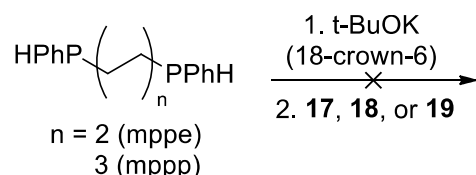
4.2.2 Cyclization by Substitution

Due to the difficulties encountered in the separation of the diastereomeric ligands, a different approach was explored, in which a stereogenic element was introduced into the diimine before the cyclization step to enforce the formation of the *C*₂-symmetric cycle. Thus, the condensation between the chiral diamine and the *o*-fluorobenzaldehyde was performed as first step, leaving the aromatic substitution and the formation of the bridge between the phosphines at the end. This approach also offered the advantage of reducing the number of the air-sensitive steps to one, although it maintained the possibility of isolating the intermediate products. Compounds **17** - **19** were therefore prepared by condensation of *o*-fluorobenzaldehyde (2 equiv) with the corresponding dimine (1 equiv) and isolated as crystalline solids.



Scheme 4.26 Synthesis of **17**, **18**, **19**.

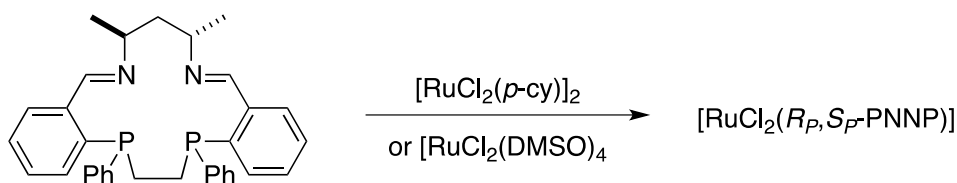
In the attempted cyclization, the secondary diphosphine (mppe or mppp) was deprotonated with *t*-BuOK, either in presence of 18-crown-ether, as reported in the original synthesis (Schemes 4.6), or in the absence of any additive, in order to exploit a possible templating effect induced by the potassium ion. Various reaction conditions were tested, such as different temperatures ($-10\text{ }^{\circ}\text{C}$, $0\text{ }^{\circ}\text{C}$, or reflux) and solvents (tetrahydrofuran and diethyl ether):



Scheme 4.27 Reaction of deprotonated mppe or mppp with **17**, **18**, or **19**.

The reaction with 1,2-bis(phenylphosphino)ethane mppe, which was monitored by ^{31}P NMR spectroscopy, exhibited a very poor selectivity. Many different signals were observed in the ^{31}P spectra of the crude reaction mixture, whose assignment to the C_2 -symmetric macrocycles on the basis of multiplicity failed also because such compounds were less than 20% of the total species present. In the best cases, the diastereomeric ratio between the C_1 and the C_2 -symmetric cycles was of 1:1, but the isolation of the products was not possible.

As a further step, we decided to complex the diastereomeric ligands to ruthenium and to try to separate the air stable diastereoisomeric dichloro complexes. To this aim, $[\text{RuCl}_2(\text{p-cymene})]_2$ was added to the crude ligand mixture in toluene, and the resulting suspension was refluxed overnight. In the ^{31}P NMR spectra, the signals corresponding to the C_1 -symmetric ligand were shifted from -8.9 and -29.5 to δ 91.3 and 90.4, indicating complexation, whereas the signals assigned to the C_2 -symmetric diastereoisomer remained unchanged. A different ruthenium precursor, $[\text{RuCl}_2(\text{DMSO})_4]$, was also tested, but the same results were obtained (Scheme 4.28).



Scheme 4.28 Complexation with different ruthenium precursors gave the C_1 -symmetric complex $[\text{RuCl}_2(R_P, S_P\text{-PNNP})]$.

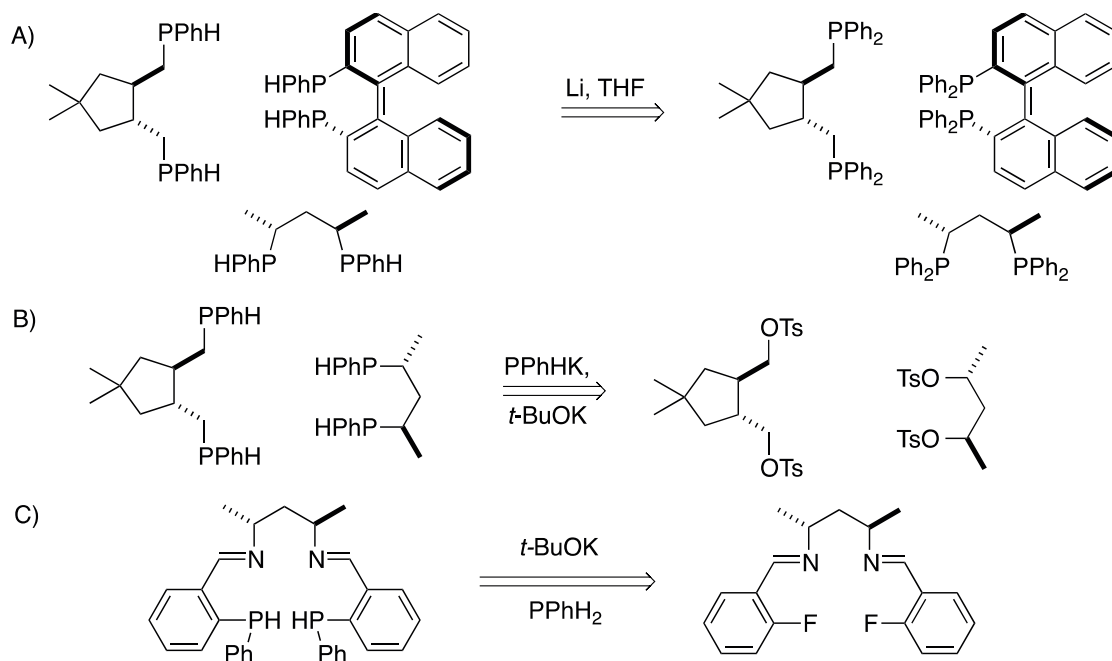
Eventually, we concluded that the complexation of the diastereoisomers with ruthenium was possible only for the C_1 -symmetric macrocycle, whereas the C_2 -symmetric isomer was too hindered to coordinate to the metal.

The reaction with 1,2-bis(phenylphosphino)propane (mppp) was even less selective in comparison to the one performed with mppe. Many signals were observed in the ^{31}P NMR spectrum, and their assignment was not possible. Moreover, any attempt to separate the reaction mixture failed.

However, we planned to introduce longer bridges for the further attempts, as suggested by the results obtained with mppe, where the complexation was successful only for the R_P, S_P -PNNP ligand.

4.2.3 Secondary Diphosphines With a Chiral Backbone

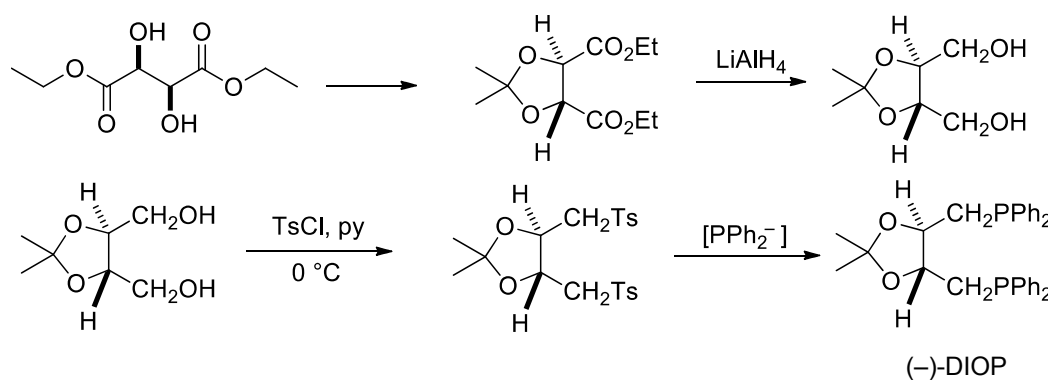
As further approach, we decided to introduce an additional stereogenic element into the diphosphine to enforce the formation of the C_2 -symmetric cycle. Previous studies in our group investigated the possibility of preparing chiral phosphines with stereogenic phosphorus atoms¹³⁹ by preparing P -stereogenic phosphine boranes precursors with the methods established by Jugé and Imamoto (§ 4.1.3). Due to the difficulties encountered, the present work focused on a different route, which involved the synthesis of secondary diphosphines with chiral backbones. The different approaches to the synthetic strategy are summarized in Scheme 4.29. The first one is based on the cleavage of tertiary diphosphines with lithium metal (A), the second one involves the reaction of the very reactive species KPHPh with a chiral tosyl derivative (B), and the last one exploits the nucleophilic aromatic substitution of the deprotonated primary phosphine PPhH_2 onto a chiral diimine backbone (C).



Scheme 4.29 Retrosynthetic approach for the preparation of secondary diphosphines with a chiral backbone.

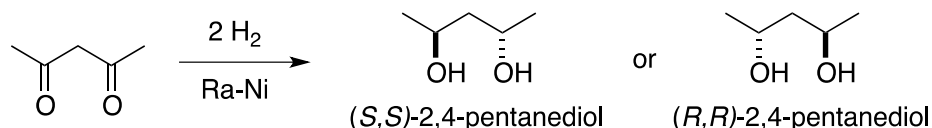
4.2.3.1 Cleavage of the P–Ph Bond with Lithium Metal

The chiral tertiary diphosphines were prepared by reaction of the tosyl derivative with lithium diphenylphosphide, according to the procedure reported for their first preparation. (–)-DIOP ((–)-2,3-*O*-isopropylidene-2,3-dihydroxy-1,4-bis-(diphenylphosphino)butane) was synthesized by Kagan and Dang in 1972²⁴⁵ from (+)-tartaric acid, which is easily accessible from the chiral pool. The PPh₂ groups are introduced by nucleophilic attack of sodium diphenylphosphine:



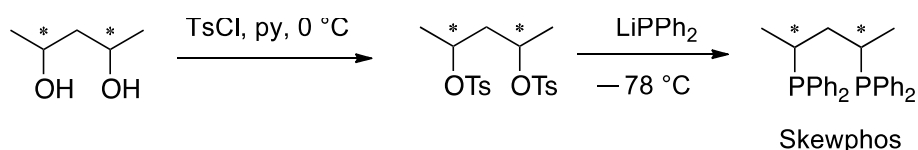
Scheme 4.30 Kagan and Dang's synthesis of (–)-DIOP.

Skewphos was synthesized from pentanediol with the procedure reported by Bakos in 1985,²⁴⁶ similarly to the preparation of Chiraphos (bis(diphenylphosphinobutane) published by Fryzuk and Bosnich in 1977.²⁴⁷ The *R,R* and *S,S* enantiomers of 2,4-pentanediol are commercially available, but they can be prepared starting from acetylacetone and using asymmetric heterogeneous hydrogenation over Raney-nickel modified with a mixture of tartaric acid and NaBr.



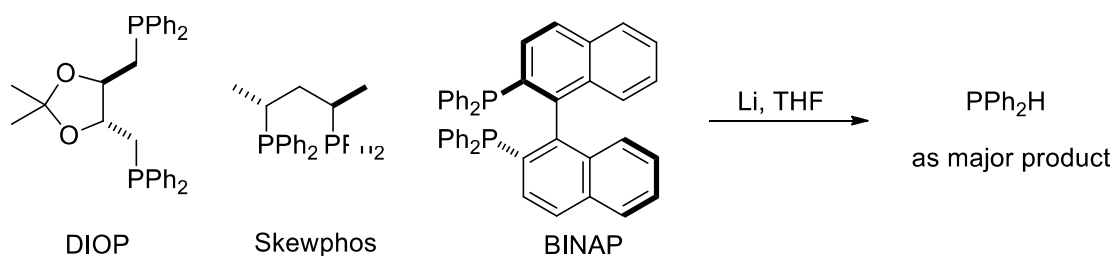
Scheme 4.31 Enantioselective preparation of 2,4-pentanediol.

The reaction of 2,4-pentanediol with TsCl in pyridine at 0 °C gave quantitatively the ditosyl derivative, which was then treated with lithium diphenylphosphide at lower temperature:



Scheme 4.32 Preparation of Skewphos.

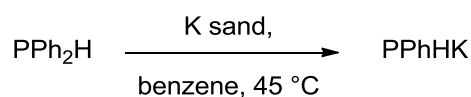
With the same procedure reported by Kimpton,²³⁶ the chiral tertiary diphosphines DIOP, Skewphos, and BINAP were treated with lithium metal in THF to cleave the P–Ph bond. It is known that the selectivity of the reaction strongly depends on the temperature conditions (see paragraph 4.2.1). Therefore, different temperatures (–78 °C, –10 °C, room temperature and reflux) were tested. Nevertheless, instead of the P–Ph bond, the bond between the phosphorus and the aliphatic chiral backbone was preferentially cleaved with almost complete conversion to diphenylphosphine (Scheme 4.33).



Scheme 4.33 Reaction of chiral tertiary diphosphine with metallic lithium.

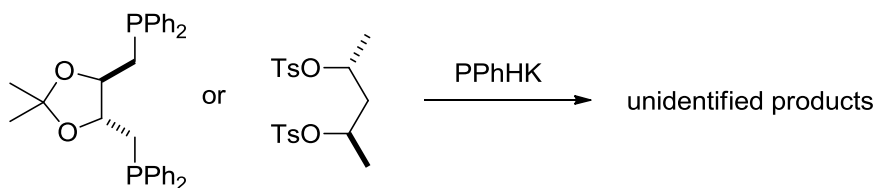
4.2.3.2 Reaction of KPhH with the Corresponding Tosyl Derivative

A different approach to chiral secondary diphosphine involved the use of KPhH , by modification of the method developed by Issleib.²⁴⁰ This is a very reactive nucleophile, which can be prepared by deprotonating the secondary diphenylphosphine with potassium metal (Scheme 4.34). Freshly made potassium sand was added to a solution of phenylphosphine in benzene under an argon atmosphere. The suspension was heated under vigorous stirring at 45 °C until the development of H_2 stopped. After washing several times with diethylether, the product was obtained by removing the solvent under reduced pressure as a light yellow solid, flammable and very sensitive to air.



Scheme 4.34 Preparation of PPhHK .

The reaction of KPhH with the tosyl derivative gave several unidentified products, even when the reaction occurred at very low temperatures (−78 °C):

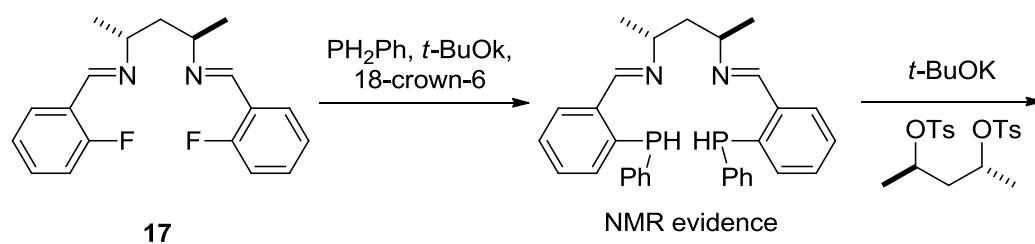


Scheme 4.35 Reaction of PPhHK with chiral tosylate derivatives.

This was not surprising considering the high reactivity of KPHPh. As the temperature was already low, no room for the optimization of the reaction conditions was left and, therefore, no further attempts were performed.

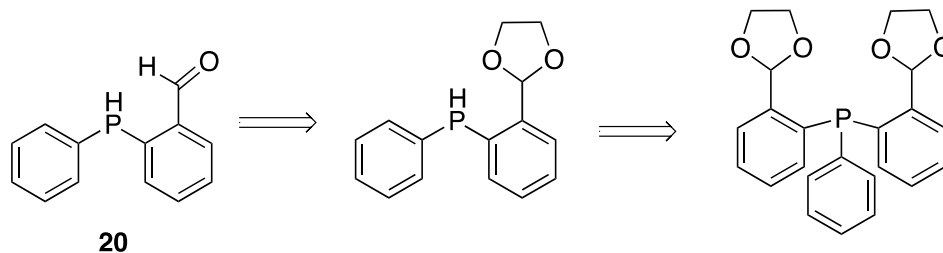
4.2.3.3 Reaction of the Deprotonated Primary Diphosphine with a Chiral Tosyl Derivative

As an additional approach, we decided to introduce two secondary phosphine groups on the chiral diimine and to perform the cyclization by reaction with a chiral tosyl derivative. A solution of PH_2Ph in THF was deprotonated by treatment at -78°C with *t*-BuOK and 18-crown-6 ether. Then, the fluoroderivative **17** was added to the mixture that was stirred at -78°C for 3 h, during which the dark red of the phosphide color disappeared. The ^{31}P NMR spectrum of the reaction crude showed along with unidentified products, signals in agreement with the formation of a secondary PNNP, as two doublets at δ 48.9 and 51.1 ($J = 37.0$ and $J = 36.6$ Hz) were observed in the H-coupled ^{31}P NMR spectrum. Since the attempts of isolation of the products failed, the mixture was directly treated at -78°C with *t*-BuOK and then (*R,R*)-2,4-ditosylpentane was added, as reported in Scheme 4.36. Unfortunately, only a very complex mixture of byproducts was obtained.



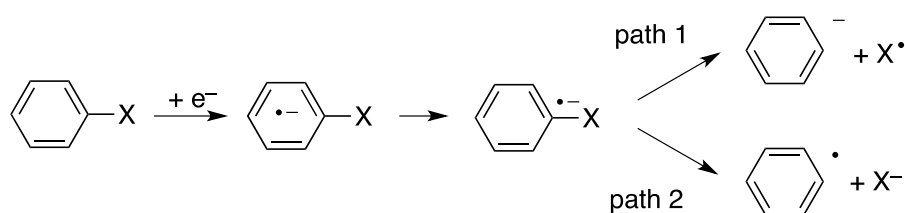
Scheme 4.36 Reaction of deprotonated diphenylphosphine with **17**.

As a modification of the approach described above, we tried to prepare a building block bearing a secondary phosphine and a formyl group by Birch reduction of mixed arylphosphines, such as **20** (Scheme 4.37).



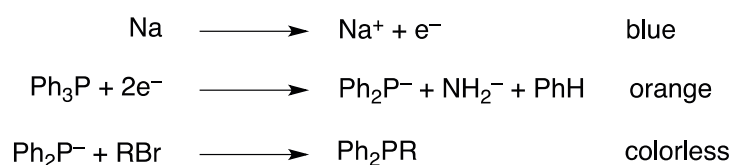
Scheme 4.37 Retrosynthetic approach for the preparation of **20**.

Triphenylphosphine can be easily cleaved by Birch reduction with sodium in liquid ammonia at $-78\text{ }^{\circ}\text{C}$. This is a very simple one pot reaction that allows an easy isolation of the final product.²⁴⁸ Moreover, the stages of the reaction are clearly indicated by color changes.²⁴⁹ The by-product, sodium amide, can be destroyed by addition of protons, for example from NH_4Cl . The mechanistic aspects of the reductive cleavage of Ar-P bond, in particular the effect of the substituents, have been studied.²⁵⁰⁻²⁵⁵ The reductive cleavage of the Ar-X bond is considered as a two-step process,^{256,257} as depicted in Scheme 4.38.



Scheme 4.38 Reductive cleavage of the Ar-X bond.

Transfer of an electron from a reducing agent to the LUMO (π^* orbital) of an aryl ring leads to a radical anion.²⁵⁵ Then, the electron is transferred to the σ^* orbital of the Ar-P bond to produce a radical anion that can easily dissociate. Finally, the Ar-P bond breaks to form a radical and an anion. Every step is indicated by the following changes in the color:

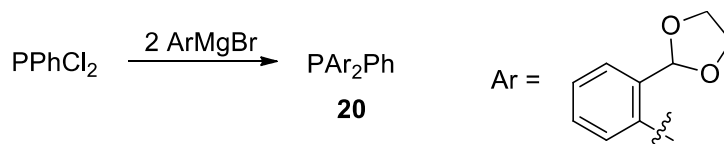


Scheme 4.39 Reaction steps shown by color changes.

In the mechanism presented, the π^* orbital plays a crucial role. If the energy of this orbital is too high, no reduction will take place. Similarly, if there is a large energy gap between the π^* and the σ^* orbitals, the rate of the cleavage is low. Unfortunately, the energy levels and coefficients of the π^* orbital of functionalized triarylphosphines are not known. From *ab initio* calculations on functionalized phosphines ($\text{P}(\text{C}_6\text{H}_4\text{X})_3$), it was found that electronegative substituents, such as halogens (*m*-fluoro, *p*-fluoro, *p*-chloro, *o*-fluoro, and *o*-bromo), are cleaved from the phenyl group and that the resulting compound is able to subsequently undergo further reactions. In contrast, when strongly electron-donating substituents are present, the compound is not reduced by Na/NH_3 , and no cleavage occurs. Experimental evidence shows that, with 4-(CH_3)₂N-, 2,4-(CH_3O)₂, and 2,4,6-(CH_3O)₃, the functionalized triphenylphosphine is not reduced by Na/NH_3 at -78°C .²⁵⁵

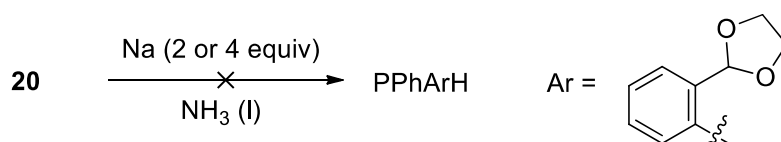
On the other hand, when a mixed phosphine PAr_2Ph is reduced, the electron can be captured either in the aryl or in the phenyl group orbital, depending on the lowest LUMO energy. When the aryl group bears electron-donating substituents, the π^* orbital of the phenyl will be the LUMO of the molecule. Besides, it can overlap with the σ^* orbital of the C–P bond. Thus, the phenyl anion will be more stable than the corresponding Ar^- . Electron-withdrawing substituents may decrease the energy of the π^* orbital of the aryl group. In that case, the π^* orbital of the aryl group is the LUMO of the molecule and the Ar–P bond is expected to break preferentially. When the energy of the π^* orbital of the aryl and phenyl groups are about the same, mixtures of products are formed. Experimentally, it was found that the cleavage of *ortho*-substituted mixed phosphines was generally very selective and proceeded in high yields. In most cases, the aryl groups were cleaved from the phosphorus atom with 100% selectivity. This allowed the synthesis of the mixed secondary phosphines ArPhPH from the cleavage of Ar_2PhP bearing a substituent on the *ortho* position of the aryl ring.²⁵⁴

We prepared the following mixed tertiary phosphine by reaction of the corresponding chlorophosphine with the Grignard reagent of the *o*-bromophenyl-dioxolane (Scheme 4.40).



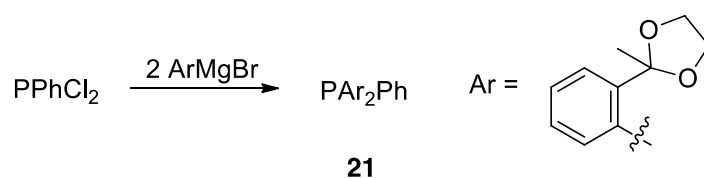
Scheme 4.40 Preparation of **20**.

We applied the Birch protocol to compounds **20** by treating it with sodium metal (2 equiv) in liquid ammonia. A clear change in the reaction color was observed, but, after quenching with NH_4Cl , the starting material was recovered unreacted. The same results were achieved using a larger excess of sodium (4 equiv):



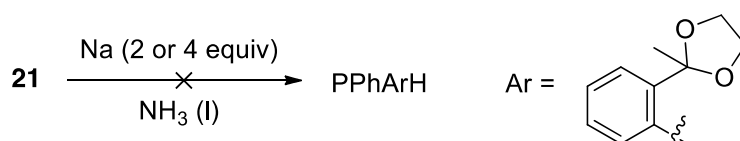
Scheme 4.41 Reaction of **20** under Birch conditions.

As we realized that the deprotonation of the acetal carbon may occur instead of the Ar–P cleavage, we prepared the following ketone derivative:



Scheme 4.42 Preparation of **21**.

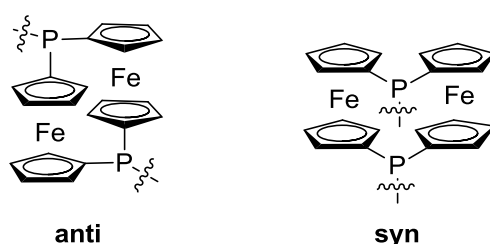
However, also **21** did not react under the same Birch reaction conditions without apparent reason.



Scheme 4.43 Reaction of **21** under Birch conditions

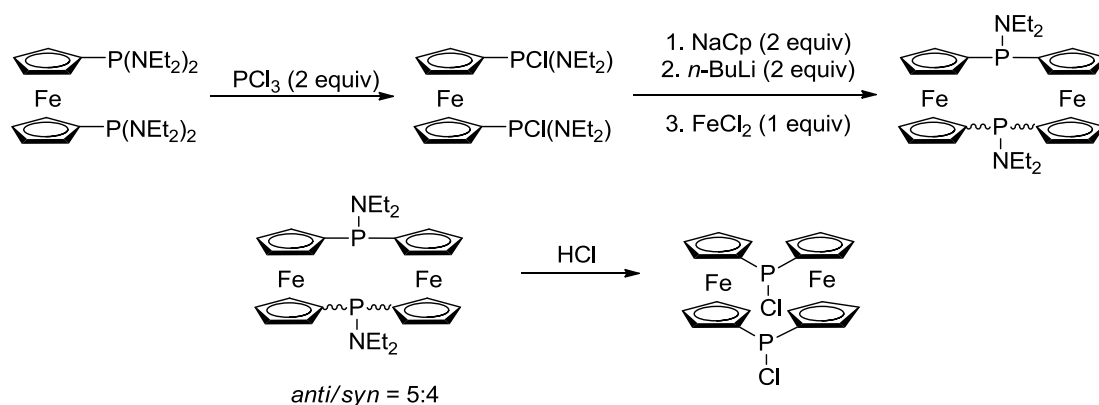
4.2.4 Doubly Bridged Diphosphines

Since the control of the stereoselectivity at the phosphorus atoms is the crucial issue, a last approach to the synthesis of C_2 -symmetric macrocycles implied the elimination of the phosphorus stereogenicity itself. This might be performed by replacing the two phenyl rings of the secondary diphosphine with a second identical bridge between the two phosphorus atoms. To this purpose, the following *syn*-ferrocenophane derivative might be a suitable backbone:



Scheme 4.44 [1.1]ferrocenophane as backbone for doubly bridged diphosphines.

Miyoshi²⁵⁸ reported in 2005 the synthesis of the corresponding chloro phosphine. It has to be noted that the deprotection with HCl was proposed to catalyze the isomerization of the *anti*- into the *syn*-isomer, as only *syn* dichlorodiphosphine was formed from a mixture of *anti* and *syn* isomers (5:4) of the protected bis(diethylamine)diphosphine:



Scheme 4.45 Miyoshi's method for the preparation of the phosphorus-bridged [1.1]ferrocenophane with *syn* conformation.

The preference of [1.1]ferrocenophane for one of the two conformations strictly depends on the balance of two intramolecular steric repulsions. The first one, which develops between the chlorine atoms is small and present only in the *syn* conformation. The second repulsion is between the two hydrogens in α and α' position and can be relieved by twisting only in case of the more flexible *syn* isomer.²⁵⁹ Preliminary attempts to prepare the above compounds according to the reported procedure²⁵⁸ failed. Due to lack of time, this strategy was not further pursued. Thus, this approach might still be explored in the future.

4.3 Conclusion and Outlook

To summarize, all the synthetic strategies aiming to the synthesis of macrocycles of C_2 -symmetry were not successful. Firstly, attempts to separate the diastereoisomers of the diphosphine **13** and the borane adduct **14** (Figure 4.4) failed.

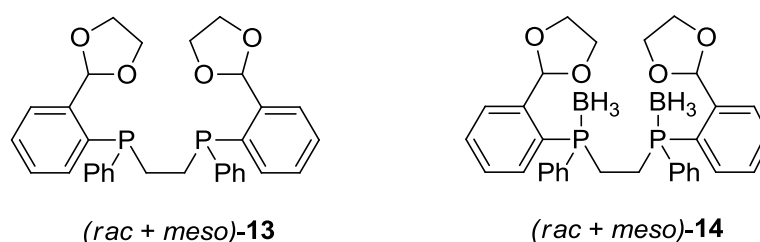


Figure 4.4 Diastereoisomeric mixtures of **13** and its protected analogue **14**.

In addition, the cyclization performed by reacting the mixture of the isomers with a chiral diamine, such as the (*R,R*)-2,4-diaminopentane, was not stereoselective. Finally, it was not possible to separate the diastereoisomers of the macrocycle.

The second approach consisted in the introduction of a stereogenic element on the diimine moiety before the last cyclization step in order to enforce the selective formation of the C_2 -symmetric cycle. However, the reactions of **16**, **17**, or **18** with deprotonated 1,2-bis(phenylphosphino)ethane (mppe) and 1,2-bis(phenylphosphino)propane (mppp) were not selective.

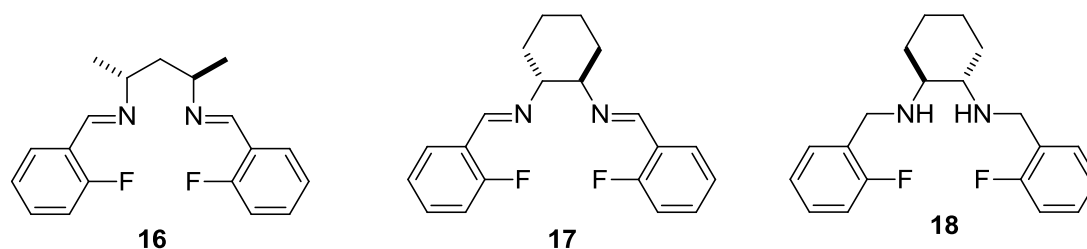


Figure 4.5 Chiral diimine derivatives.

Moreover, by refluxing the crude mixture of isomers of the mppe-based ligand with different ruthenium precursors, the corresponding ruthenium complex was formed only with the pseudo-*meso* isomer. We proposed that the other isomers were too hindered to coordinate to the metal atom. Therefore, we decided to enlarge the macrocycle by using in the further attempts longer bridges between the phosphorus and the nitrogen atoms, respectively. However, as we tried to add more stereogenic elements, by introducing a chiral backbone also between the phosphorus atoms, every synthetic strategy to prepare the chiral secondary diphosphine failed.

For the future, further synthetic possibilities can still be investigated. Firstly, the approach described in § 4.2.4 was not fully explored, as the following diphosphine can be prepared and tested (Figure 4.6).

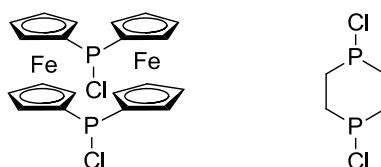


Figure 4.6 Doubly bridged diphosphines.

Secondly, a structural modification into the macrocyclic backbone can be introduced. To this aim, a diphosphine with a bridge presenting a different flexibility in comparison with α,ω -bis(diphenylphosphino)alkanes can be used, such as the one depicted in Figure 4.7.

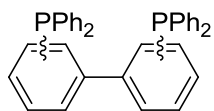
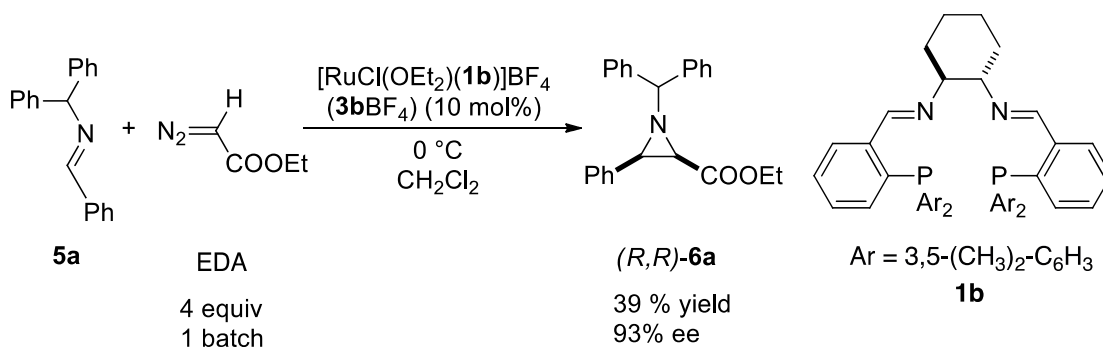


Figure 4.7 Bis(diphenylphosphino)-1,1'-biphenyl as a different bridge between the phosphorus.

5. Conclusion and Outlook

In the light of the results exposed in this thesis, some general considerations can be made on the transition metal-based catalysts for asymmetric imine aziridination reported in the literature. Whereas the aziridination via nitrene transfer to olefins turned out to be a very successful reaction, the alternative approach via carbene transfer to imines showed a limited success. In particular, this latter was generally considered an inconvenient route for enantioselective aziridination since Jacobsen's report of Cu(II)-catalyzed imine aziridination, which involves the nucleophilic attack of the imine onto a highly electrophilic metal carbene complex. As the resulting ylide is relatively stable and can dissociate from the chiral catalyst, the enantio- and chemoselectivity is low. From his report on, few mechanistic studies were performed on system based on different transition metal, as it was assumed that the metal-carbene path was generally operative.

The project of this thesis started from the previous observation made in our group that Ru/PNNP catalysts aziridinate imines with the intermediacy of an EDA rather than a carbene complex. On this basis, we investigated the possibility to control the chemoselectivity of the imine aziridination reaction by exploiting the effect of conformationally rigid macrocycles as ligand. However, all the synthetic attempts for the preparation of C_2 -symmetric macrocycles were not successful, mainly because of the difficult control of the stereogenicity at the phosphorus. Therefore, we tested a second approach, which involves the use of bulky substituted open-chain PNNP ligands. Eventually, high enantioselectivity (93% ee) and improved yield (39%) were obtained with $[\text{RuCl}(\text{OEt}_2)(\mathbf{1b})]^+$ in the aziridination of imine **5a** to aziridine (*R,R*)-**6a**. The optimized conditions include the use of the nonhydrolyzable, noncoordinating anion BF_4^- .



The study of the electronic effects with **3b**BF₄ as catalyst and 4-substituted-*N*-benzylidene-anilines suggests the nucleophilic attack of a metal-bound diazoester onto the noncoordinated imine. Such a mechanism is suitable for metals that form less electrophilic carbenes such as ruthenium(II), as already discussed in § 3.2.4.

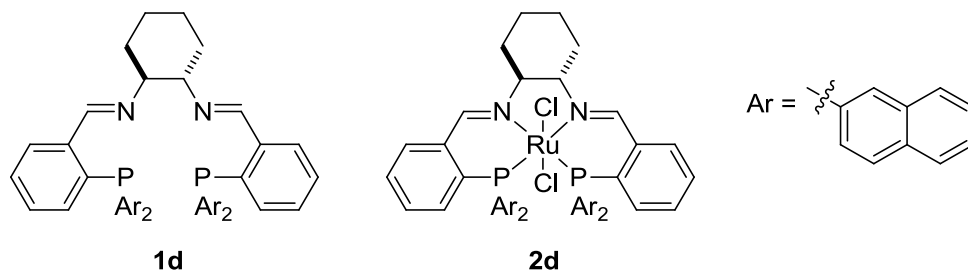
On the basis of the proposed mechanism, two conclusions can be drawn about the enantioselectivity of the reaction. Firstly, the nucleophilic attack of the diazoester on the imine occurs far from the chiral metal center, which reduces the efficiency of the transfer of the chiral information in the transition state of the aziridine formation. This might explain the good, but not excellent enantioselectivity observed in combination with the unsubstituted ligand (**1a**), which gave aziridine (*R,R*)-*cis*-**6a** with enantioselectivity of around 80% ee. Secondly, we found out that acid species present in traces are able to catalyze a nonenantioselective aza Darzens reaction to give racemic aziridine *cis*-**6a** with high yields. This species might be HPF₂O₂, generated by the hydrolysis of the PF₆⁻ anion by the presence of adventitious water, or traces of impurities, as in the case of the addition of an excess of EDA (10 equiv). The efficiency of this competing reaction is so high, that even small amounts of acids overwhelm the metal catalyzed path and reduce drastically the enantioselectivity.

In conclusion, we showed that it is possible to perform highly enantioselective imine aziridination with a transition metal such as ruthenium, provided that the steric property of the ligands and the reaction conditions are carefully controlled, in order to avoid the competing nonenantioselective aza-Darzens mechanism. It might also be interesting to reinvestigate the mechanism for catalytic systems based on transition metals different from copper, such as Che's ruthenium-based one.

On the other hand, it is possible that the acid catalyzed aza-Darzens aziridination is operating as a background reaction in the case of catalysts that show a poor enantioselectivity. Our experience is that it is not easy to detect the competing aza-Darzens path, as the presence of diagnostic byproduct, such as enaminoesters, is not always evident from the analysis of the crude reaction mixture. To the best of our knowledge there are no examples of systems in which the acid aza-Darzens has been systematically investigated as a possible competing reaction that might be responsible for the low enantioselectivity, although it is well known to be a highly efficient catalytic reaction for imine aziridination.

Some possible future developments may be taken into consideration. Firstly, the opportunity to test other bulky ligands, such as the 2-naphthyl substituted ligand

(**1d**), which gave results similar to those obtained with **1b** during the preliminary screening, but have not been tested with nonhydrolyzable anions because of lack of time.



Secondly, additional experiments recently performed in our laboratory by Joël Egloff showed that the conditions used were optimal only for the unsubstituted imine **5a**. In particular, higher enantioselectivity was obtained for substituted imines when only 1 equivalent of EDA was used with the unsubstituted $[\text{RuCl}(\text{OEt}_2)(\mathbf{1a})]\text{BF}_4$ (**3aBF₄**) catalyst at 0 °C. Therefore, the reactions with **3bBF₄** with these substrates have to be reoptimized individually.

Thirdly, more NMR spectroscopic studies must be carried out, in order to perform a complete characterization of the active species, such as the diazoester adduct, in combination with the 3,5-dimethyl substituted ligand **1b**.

Finally, as the bulky substituents proved to have a beneficial effect on both yield and enantioselectivity, the conformationally rigid macrocyclic PNNP ligands remain a possible interesting approach, which is still worth to investigate in the future, despite the difficulty posed by their synthesis.

6. Experimental Part

6.1 General

6.1.1 Techniques and Instrumentation

Reactions with air- or moisture-sensitive materials were carried out under an argon atmosphere using Schlenk techniques or in a glove box under nitrogen. All solvents used for synthetic and crystallization purposes were of “puriss p.a.” quality (Fluka AG, Riedel-de Häen, or Merck, Sigma Aldrich) and were distilled from an appropriate drying agent under argon prior to use (CH_2Cl_2 , MeOH, and EtOH from CaH_2 ; toluene, hexane, THF, and Et_2O from Na/benzophenone). CH_2Cl_2 , MeOH, and EtOH were also degassed after distillation for the synthesis of oxygen-sensitive molecules. For flash chromatography, technical grade solvents were generally used. Deuterated solvents for NMR analysis of sensitive compounds were dried over molecular sieves and degassed prior to use (3 × freeze/pump/thaw cycles).

TLC: Silica: Merck 60-F254; Alumina: Macherey-Nagel co N/UV254; detection: UV-light (254 nm), mostaine for borane-protected phosphines (10g $(\text{NH}_4)_6[\text{Mo}_7\text{O}_{24}] \cdot 4\text{H}_2\text{O}$, 12 mL H_2SO_4 conc., 190 mL H_2O , 0.4 g $\text{Ce}(\text{SO}_4) \cdot n\text{H}_2\text{O}$), or $\text{KMnO}_4/\text{H}_2\text{SO}_4$ for 2-carboxyaziridines.

Flash Chromatography: Silica: Fluka Silica Gel 60; Alumina: ICN Alumina Act. 1.

NMR Spectroscopy: ^1H , $^{13}\text{C}\{^1\text{H}\}$, $^{31}\text{P}\{^1\text{H}\}$, $^{15}\text{N}\{^1\text{H}\}$ spectra were recorded on Bruker AVANCE 250, 300, and DPX 500 spectrometers. Multidimensional NMR spectra were recorded on a Bruker AVANCE 300 and DPX 500 spectrometer. ^1H and ^{13}C positive chemical shifts in ppm are downfield from tetramethylsilane. ^{31}P NMR spectra are referenced to external 85% H_3PO_4 . ^{15}N NMR spectra are referenced to external CH_3NO_2 (neat).

Mass Spectroscopy: Routine EI-MS and MALDI-MS measurements were performed by the MS-service of the Laboratory of Organic Chemistry (ETH Zürich). The signals are given in m/z and the intensity in % of the base peak.

EA: Elemental analyses were carried out by the Laboratory of Microelemental Analysis (ETH Zürich).

IR: Thermo Scientific Pike.

HPLC: Agilent Series 1100 or HP 150 with UV-detector (DAD); flow in mL/min, eluent (hexane:2-PrOH) and wavelength are given in each experiments. Columns: Chiralcel AD-H (4.6 × 250 mm, 5 μm particle), OD-H (4.6 × 250 mm, 5 μm particle), AM (4.6 × 250 mm, 5 μm particle), OJ (4.6 × 250 mm, 5 μm particle).

GC-MS: Thermo Finnigan TraceMS, EI-M; column: Zebron ZB-5 (30m × 0.25mm × 0.25μm).

Polarimeter: Optical rotations were measured using an Anton Paar MCP 200 polarimeter with a 1 dm cell.

Calculations: Molecular Modeling Calculations were performed with the program Cerius2 for Linux (Accelrys Studio).

Chemicals

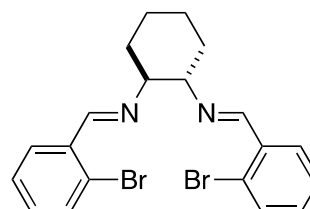
Ethyl diazoacetate (Fluka) was distilled and stored over molecular sieves.

6.2 Catalyst

6.2.1 Precursors

(1S,2S)-N,N'-Bis(2-bromo-benzylidene)cyclohexane-1,2-diamine.

(1S,2S)-(+)-1,2-Diaminocyclohexane (4.6 g, 40.5 mmol, 1 equiv) and 2-bromobenzaldehyde (15.0 g, 81.1 mmol, 2 equiv) were dissolved in freshly distilled toluene (250 mL). The solution was refluxed in a Dean-Stark apparatus for 12 h. The solvent was evaporated under high vacuum



and the pure product was obtained as a white solid upon recrystallization from EtOH at low temperature (4 °C). Yield: 14.3 g (80%).

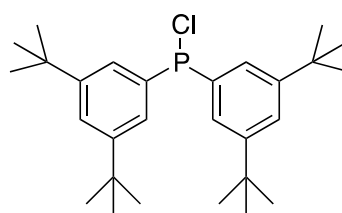
¹H NMR (300 MHz, CDCl₃): δ 8.58 (s, 2H, N=CH), 7.94-7.91 (m, 2H, H_{arom}), 7.50-7.47 (m, 2H, H_{arom}), 7.30-7.17 (m, 4H, H_{arom}), 3.57-3.48 (m, 2H, NCH), 1.91-1.82 (m, 6H, CH₂), 1.57-1.50 (m, 2H, CH₂). NMR data in agreement with the published values.¹²⁹

Chlorophosphines Ar₂PCl: General Method.

ⁿBuLi (1.6 M in hexane, 2.2 equiv) was added to a solution of ArBr (2.0 equiv) in THF at -78 °C during 5 min. After 5 min, PCl₂NEt₂ (1 equiv) was added dropwise. After 5 min from the addition, the reaction mixture was warmed to 0 °C, and then stirred for 30 min. The resulting (Et₂N)PAr₂ was treated with HCl (2 M in Et₂O, 2 equiv) at 0 °C to give the desired Ar₂PCl. The reaction mixture was analyzed by ³¹P NMR to ascertain complete conversion. The mixture was then filtered through celite, dried *in vacuo* and the product was used without further purification.

Bis(3,5-di-tert-butylphenyl)chlorophosphine.

ⁿBuLi (1.6M, 9.57 ml, 15.32 mmol, 2.1 equiv) was added dropwise during 5 min to a stirred solution of 1-bromo-3,5-di-tert-butylbenzene (3.93 g, 14.59 mmol, 2 equiv) in dry THF (10 mL) at -78 °C. After 5 min *N,N*-diethylphosphoramidous dichloride (1.27 g, 1.08 mL,

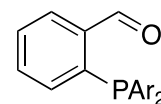


(7.29 mmol, 1 equiv) was added slowly to the mixture. After 5 min, the reaction solution was warm up and stirred at 0 °C for 30 min.

Then, a solution of HCl in diethylether (2.0 M, 10.93 mL, 21.86 mmol, 3 equiv) was added slowly at 0 °C and the reaction mixture was stirred overnight at room temperature. The mixture was filtered under argon over celite and washed with dry THF (4 x 10 mL). The solvent was removed under reduced pressure, and a white solid was obtained. ³¹P NMR (101 MHz, CDCl₃): δ 87.51 (s).

2-(Bisarylphosphino)benzaldehyde: General Method.

A solution of ArMgBr in THF was prepared *in situ* by adding magnesium turnings (12 mmol, 1.2 equiv) to a solution of 2-(2-bromophenyl)-1,3-dioxolane (11 mmol, 1.1 equiv) in THF (200 mL) at



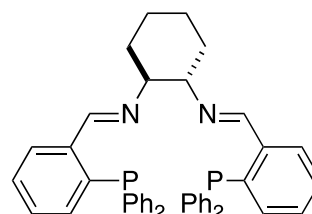
0 °C and by refluxing the mixture for 6 h. Then, PClAr₂ was added dropwise at 0 °C and the reaction solution was heated to reflux for 6 h. The reaction was quenched with a 10% solution of aqueous NH₄Cl and the organic phase was extracted with saturated aqueous NaCl. The organic phase was separated and the solvent was removed by reduced pressure. The resulting [2-(1,3-dioxolane-2-yl)phenyl]bisarylphosphine was dissolved in degassed acetone (200 mL) with a catalytic amount of *p*-toluenesulfonic acid monohydrate, and the mixture was heated to reflux overnight, during which the

solution turned yellow. The desired 2-(bisarylphosphino)benzaldehyde was isolated as a yellow solid from crystallization from MeOH.

6.2.2 PNNP Ligands

(1S,2S)-N,N'-Bis{2-[bisphenylphosphino]benzylidene}-cyclohexane-1,2-diamine (1a).

2-(diphenylphosphino)benzaldehyde (5.0 g, 17.2 mmol, 2 equiv) was added to a solution of (1*S*,2*S*)-(+)-1,2-diaminocyclohexane (0.98 g, 8.6 mmol, 1 equiv) in EtOH (250 mL). The reaction solution was stirred at room temperature overnight, during which the solution turned



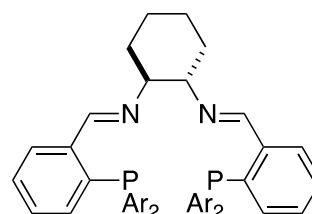
colorless. The solvent was removed under reduced pressure, and the product was obtained as a white solid from crystallization from MeOH at low temperature.

¹H NMR (400 MHz, CDCl₃): δ 8.72 (*d*, 2H, HC=N, *J*_{P,H} = 3.6 Hz), 7.82-6.82 (*m*, 28H, *H*_{arom}), 3.15 (*m*, 2H, N-CH), 1.70 (*m*, 2H, NCH-CHH'), 1.48-1.27 (*m*, 6H, CH₂).

³¹P NMR (162 MHz, CDCl₃) δ -12.5 (*s*, 2P).

(1S,2S)-N,N'-Bis{2-[bis(3,5-dimethylphenyl)phosphino]benzylidene}-cyclohexane-1,2-diamine (1b).

2-(Bis(3,5-dimethylphenylphosphino)benzaldehyde (2.0 g, 5.8 mmol, 2 equiv) was added to a solution of (1*S*,2*S*)-(+)-1,2-diaminocyclohexane (0.33 g, 2.9 mmol, 1 equiv) in EtOH (100 mL). The reaction solution was stirred at room temperature overnight, during which the solution turned colorless. The solvent was removed under reduced

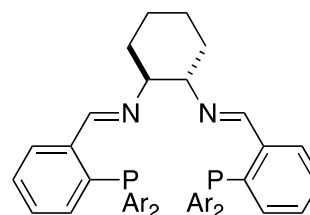


Ar = 3,5-dimethyl-phenyl

pressure and the product was obtained as a white solid from crystallization from MeOH at low temperature. ¹H NMR (300 MHz, CDCl₃): δ 8.83 (*d*, 2H, HC=N, *J*_{P,H} = 4.5 Hz), 6.84-7.83 (*m*, 20H, *H*_{arom}), 3.23 (*m*, 2H, NCH), 2.29-2.21 (*m*, 24H, CH₃), 1.90-1.28 (*m*, 8H, CH₂). ³¹P NMR (121.5 MHz, CDCl₃) δ -14.6 (*s*, 2P).

(1*S*,2*S*)-*N,N'*-Bis{2-[bis(3,5-ditertbutylphenyl)phosphino]benzylidene}-cyclohexane-1,2-diamine (**1c**).

(1*S*,2*S*)-*N,N'*-Bis(2-bromobenzylidene)cyclohexane-1,2-diamine (0.2g, 0.45 mmol) was dissolved in THF (15 mL) and cooled to $-80\text{ }^{\circ}\text{C}$, and a 1.7 M pentane solution of ^tBuLi (0.53 mL, 0.90 mmol, 2 equiv) was added dropwise thereto. The resulting dark red solution was stirred at $-80\text{ }^{\circ}\text{C}$ for 1 h, then a solution of bis(3,5-di-*tert*-

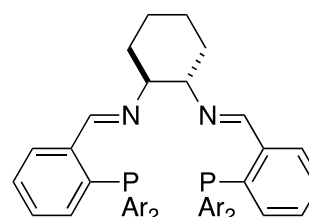


Ar = 3,5-di-*tert*-butyl-phenyl

butylphenyl)chlorophosphine (0.89 mmol, 2 equiv) in THF was added dropwise. The reaction solution was allowed to reach room temperature during 3 h, during which the solution turned pale yellow. The solvent was evaporated under reduced pressure to give a crystalline solid, which was used without further purification. ³¹P NMR (162 MHz, CDCl₃): $\delta -10.39$ (*s*, 2P).

(1*S*,2*S*)-*N,N'*-Bis{2-[bis(2-naphthyl)phosphino]benzylidene}-cyclohexane-1,2-diamine (**1d**).

(1*S*,2*S*)-*N,N'*-Bis(2-bromobenzylidene)cyclohexane-1,2-diamine (0.2g, 0.45 mmol) was dissolved in THF (15 mL) and cooled to $-80\text{ }^{\circ}\text{C}$, and a 1.7 M pentane solution of ^tBuLi (0.53 mL, 0.90 mmol, 2 equiv) was added dropwise thereto. The resulting dark red solution was stirred at $-80\text{ }^{\circ}\text{C}$ for 1 h, then bis(2-naphthyl)chlorophosphine (0.89

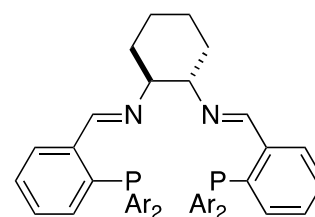


Ar = 2-naphthyl

mmol, 2 equiv) was added dropwise. The reaction solution was allowed to reach room temperature during 3 h, during which the solution turned pale yellow. The solvent was evaporated under reduced pressure to give a yellow solid, which was used without further purification. ¹H NMR (700 MHz, CDCl₃): δ 8.73 (*d*, 2H, HC=N, $J_{\text{P,H}} = 4.1$ Hz), 7.88-6.93 (*m*, H_{arom}), 3.09 (*m*, 2H, NCH-CHH'), 1.13-1.51 (*m*, 6H, CH₂). ³¹P NMR (283 MHz, CDCl₃) $\delta -12.6$ (*s*, 2P).

(1*S*,2*S*)-*N,N'*-Bis{2-[bis(3-methylphenyl)phosphino]benzylidene}-cyclohexane-1,2-diamine (**1e**).

(1*S*,2*S*)-*N,N'*-Bis(2-bromobenzylidene)cyclohexane-1,2-diamine (0.2g, 0.45 mmol) was dissolved in THF (15 mL) and cooled to $-80\text{ }^{\circ}\text{C}$, and a 1.7 M pentane solution of $t\text{BuLi}$ (0.53 mL, 0.90 mmol, 2 equiv) was added dropwise thereto. The resulting dark red solution was stirred at $-80\text{ }^{\circ}\text{C}$ for 1 h, then bis(3-methylphenyl)chlorophosphine (0.89

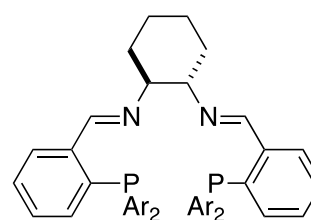


Ar = 3-methylphenyl

mmol, 2 equiv) was added dropwise. The reaction solution was allowed to reach room temperature during 3 h, during which the solution turned pale yellow. The solvent was evaporated under reduced pressure to give a yellow solid, which was used without further purification. ^{31}P NMR (162 MHz, CDCl_3) δ -12.5 (s, 2P).

(1*S*,2*S*)-*N,N'*-Bis{2-[bis(4-chlorophenyl)phosphino]benzylidene}-cyclohexane-1,2-diamine (**1f**).

(1*S*,2*S*)-*N,N'*-Bis(2-bromobenzylidene)cyclohexane-1,2-diamine (0.2g, 0.45 mmol) was dissolved in THF (15 mL) and cooled to $-80\text{ }^{\circ}\text{C}$, and a 1.7 M pentane solution of $t\text{BuLi}$ (0.53 mL, 0.90 mmol, 2 equiv) was added dropwise thereto. The resulting dark red solution was stirred at $-80\text{ }^{\circ}\text{C}$ for 1 h, then bis(4-chlorophenyl)chlorophosphine (0.89

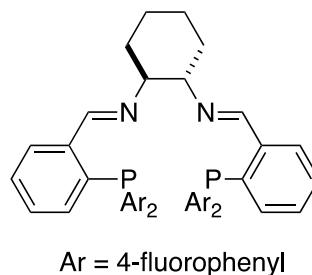


Ar = 4-chlorophenyl

mmol, 2 equiv) was added dropwise. The reaction solution was allowed to reach room temperature during 3 h, during which the solution turned pale yellow. The solvent was evaporated under reduced pressure to give a yellow solid, which was used without further purification. ^1H NMR (300 MHz, CDCl_3): δ 8.44 (d, 2H, $\text{HC}=\text{N}$, $J_{\text{P,H}} = 3.8$ Hz), 7.69-6.77 (m, H_{arom}), 3.06 (m, 2H, $\text{NCH-CHH}'$), 1.89-1.28 (m, 8H, CH_2). ^{31}P NMR (121.5 MHz, CDCl_3) δ -14.1 (s, 2P).

(1*S*,2*S*)-*N,N'*-Bis{2-[bis(4-fluorophenyl)phosphino]benzylidene}-cyclohexane-1,2-diamine (**1g**).

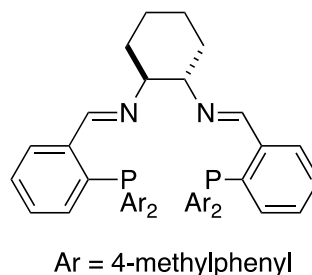
(1*S*,2*S*)-*N,N'*-Bis(2-bromobenzylidene)cyclohexane-1,2-diamine (0.2 g, 0.45 mmol) was dissolved in THF (15 mL) and cooled to $-80\text{ }^{\circ}\text{C}$, and a 1.7 M pentane solution of $t\text{BuLi}$ (0.53 mL, 0.90 mmol, 2 equiv) was added dropwise thereto. The resulting dark red solution was stirred at $-80\text{ }^{\circ}\text{C}$ for 1 h, then bis(4-fluorophenyl)chlorophosphine (0.89



mmol, 2 equiv) was added dropwise. The reaction solution was allowed to reach room temperature during 3 h, during which the solution turned pale yellow. The solvent was evaporated under reduced pressure to give a yellow solid, which was used without further purification. ^{31}P NMR (101 MHz, CDCl_3) δ -14.0 (s, 2P).

(1*S*,2*S*)-*N,N'*-Bis{2-[bis(4-methylphenyl)phosphino]benzylidene}-cyclohexane-1,2-diamine (**1h**).

(1*S*,2*S*)-*N,N'*-Bis(2-bromobenzylidene)cyclohexane-1,2-diamine (0.2 g, 0.45 mmol) was dissolved in THF (15 mL) and cooled to $-80\text{ }^{\circ}\text{C}$, and a 1.7 M pentane solution of $t\text{BuLi}$ (0.53 mL, 0.90 mmol, 2 equiv) was added dropwise thereto. The resulting dark red solution was stirred at $-80\text{ }^{\circ}\text{C}$ for 1 h, then bis(4-methylphenyl)chlorophosphine (0.89



mmol, 2 equiv) was added dropwise. The reaction solution was allowed to reach room temperature during 3 h, during which the solution turned pale yellow. The solvent was evaporated under reduced pressure to give a yellow solid, which was used without further purification. ^1H NMR (400 MHz, CDCl_3): δ 8.44 (d, 2H, $\text{HC}=\text{N}$, $J_{\text{P,H}} = 4.28$ Hz), 7.78-6.82 (m, H_{arom}), 3.17 (m, 2H, $\text{NCH-CHH}'$), 2.37-2.30 (m, 12H, CH_3), 1.88-1.28 (m, 6H, CH_2). ^{31}P NMR (162 MHz, CDCl_3) δ -14.7 (s, 2P).

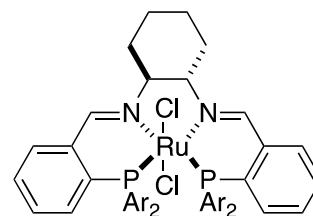
6.2.3 Ru/PNNP Complexes

[RuCl₂((1S,2S)-N,N'-Bis{2-[bis(3,5-dimethylphenyl)phosphino]benzylidene}cyclohexane-1,2-diamine) (2b) as General Method for the preparation of complexes 2b-2h.

*[RuCl₂(*p*-cymene)]₂ (1 equiv) was added to a toluene solution of (1S,2S)-N,N'-bis{2-[bis(3,5-dimethylphenyl)phosphino]benzylidene}cyclohexane-1,2-diamine (1*

equiv), and the resulting solution was heated to reflux for 10 h. The toluene was evaporated under reduced pressure, and the resulting dark red solid was crystallized from

CH₂Cl₂/hexane. Overall yield 40% (based on the corresponding 3,5-dimethylbromide). ¹H NMR (500 MHz, CDCl₃): δ 8.91 (d, 2H, HC=N, J_{P,H} = 4.0 Hz), 7.62-6.79 (m, 20H, H_{arom}), 4.18 (m, 2H, N-CH), 2.73 (d, 2H, NCH-CHH', J = 10.17 Hz), 1.95-2.38 (m, 24H, CH₃), 1.26-1.54 (m, 6H, CH₂). ³¹P NMR (162.0 MHz, CDCl₃) δ 47.0 (s, 2P). Anal. Calcd. for C₄₈H₄₈N₂P₂Cl₂ Ru: C, 66.24; H, 5.99; N, 2.97. Found C, 66.11; H, 5.56; N, 2.70. [α]_D²⁰ = -138 (c = 0.25, CHCl₃). MS (ESI): Calcd. m/z 907.2656, found m/z 907.2656. IR (ATR, cm⁻¹): 1626 (ν_{C=N}).

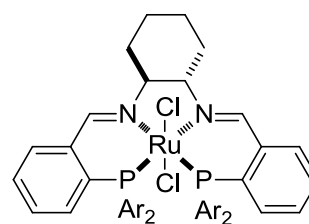


Ar = 3,5-dimethyl-phenyl

[RuCl₂((1S,2S)-N,N'-bis{2-[bis(2-naphthylphenyl)phosphino]benzylidene}cyclohexane-1,2-diamine) (2c).

Overall yield 31% (based on the corresponding 3,5-di-*tert*-butylbromide).

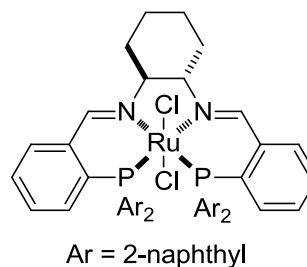
³¹P NMR (101 MHz, CDCl₃): δ 52.94 (d, J = 27 Hz), 52.57 (s), 52.18 (s), 51.78 (d, J = 27 Hz). MS (MALDI) calcd. 1243.6413. Found m/z 1243.6419. Anal. calcd. for C₇₆H₁₀₄N₂P₂Cl₂Ru: C, 71.34; H, 8.19; N, 2.19. Found: C, 62.50; H, 8.10, N, 1.53. The presence of grease explains the deviation.



Ar = 3,5-di-*tert*-butylphenyl

[RuCl₂((1S,2S)-N,N'-Bis{2-[bis(2-naphthyl)phosphino]benzylidene}cyclohexane-1,2-diamine)] (2d).

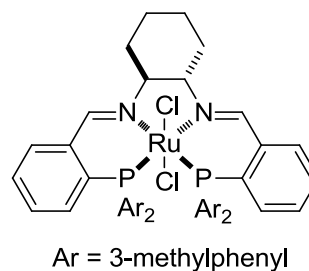
Yield: 23% (based on the corresponding bis(2-naphthyl)-chlorophosphine. ¹H NMR (400 MHz, CDCl₃): δ 9.01 (*m*, 2H, HC=N), 7.75–6.85 (*m*, 20H, H_{arom}), 4.28 (*m*, 2H, N-CH), 2.79 (*d*, 2H, NCH-CHH', J_{P,H} = 11.6 Hz), 2.12 (*m*, 2H, CH₂), 2.04 (*m*, 2H, CH₂), 1.47 (*m*, 2H, CH₂). ³¹P NMR (162.0 MHz, CDCl₃) δ 49.0 (*s*, 2P). Anal. Calcd for



C₆₀H₄₈N₂P₂Cl₂ Ru: C, 69.90; H, 4.69; N, 2.72. Found C, 69.23; H, 4.82; N, 2.51. [α]_D²⁰ = -138 (c = 0.50). MS (ESI): *m/z* 995.2 (M⁺). IR (ATR, cm⁻¹): 1625 (ν_{C=N}).

[RuCl₂((1S,2S)-N,N'-bis{2-[bis(3-methylphenyl)phosphino]benzylidene}-cyclohexane-1,2-diamine)] (2e).

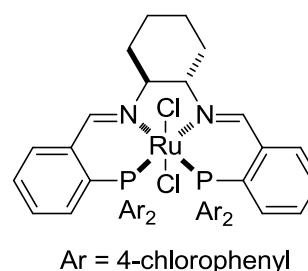
Yield: 34%. ¹H NMR (250 MHz, CDCl₃): δ 8.89 (*m*, 2H, HC=N), 7.62-6.90 (*m*, H_{arom}), 4.19 (*m*, 2H, N-CH), 2.75-2.70 (*m*, 2H, NCH-CHH'), 2.30-2.20 (*m*, 2H, N-CH), 2.06 (*s*, CH₃), 1.98 (*s*, CH₃), 1.41 (*m*, 2H, CH₂). ³¹P NMR (101.2 MHz, CDCl₃) δ 47.1 (*s*, 2P). Anal. Calcd for



C₄₈H₄₈N₂P₂Cl₂ Ru: C, 65.01; H, 5.46; N, 3.16. Found C, 64.72; H, 5.74; N, 3.01. [α]_D²⁰ = -174 (c = 0.50). MS (ESI): *m/z* 851.2032 (M⁺).

[RuCl₂((1S,2S)-N,N'-bis{2-[bis(4-chlorophenyl)phosphino]benzylidene}-cyclohexane-1,2-diamine)] (2f).

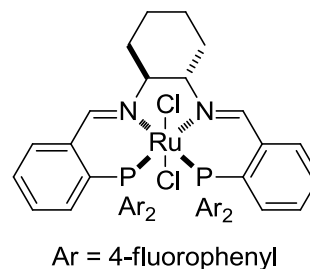
Yield: 40%. ¹H NMR (250 MHz, CDCl₃): δ 8.91 (*m*, 2H, HC=N), 7.70-6.96 (*m*, H_{arom}), 4.16 (*m*, 2H, N-CH), 2.76-2.74 (*m*, 2H, NCH-CHH'), 2.13 (*m*, 2H, N-CH) 2.00 (*m*, CH₂), 1.46 (*m*, 2H, CH₂). ³¹P NMR (101.2 MHz, CDCl₃) δ 48.3 (*s*, 2P). Anal. Calcd for C₄₄H₃₆N₂P₂Cl₆ Ru: C, 54.57; H, 3.75; N, 2.89. Found C, 53.61; H, 3.87; N, 2.73. The presence of grease explains the deviation. MS (ESI): *m/z* 851.2 (M⁺).



IR (ATR, cm⁻¹): 1626 (ν_{C=N}).

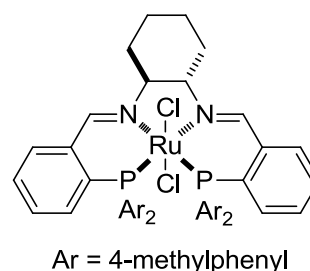
[RuCl₂((1S,2S)-N,N'-bis{2-[bis(4-fluorophenyl)phosphino]benzylidene}-cyclohexane-1,2-diamine) (2g).

Yield 60%. ¹H NMR (500 MHz, CDCl₃): δ 8.91 (*m*, 2H, HC=N, *J*_{P,H} = 4.0 Hz), 7.38-6.73 (*m*, 24H, H_{arom}), 4.16 (*m*, 2H, N-CH), 2.77-2.72 (*m*, 2H, NCH-CHH'), 2.12 (*m*, 2H, CH₂), 2.00 (*m*, 2H, CH₂), 1.45 (*m*, 2H, CH₂). ³¹P NMR (162.0 MHz, CDCl₃) δ 46.55 (*s*, 2P). ¹⁹F NMR (188 MHz, CDCl₃): δ 110.9 (*m*, 4F). Anal. Calcd for C₄₄H₃₆N₂F₄P₂Cl₂Ru: C, 58.54; H, 4.02; N, 3.10. Found C, 58.63; H, 4.23; N, 2.96. [α]_D²⁰ = -280.0 (c = 0.45). MS (ESI): *m/z* 867.1024 (M⁺). IR (ATR, cm⁻¹): 1629 (ν_{C=N}).



[RuCl₂((1S,2S)-N,N'-bis{2-[bis(4-methylphenyl)phosphino]benzylidene}-cyclohexane-1,2-diamine) (2h).

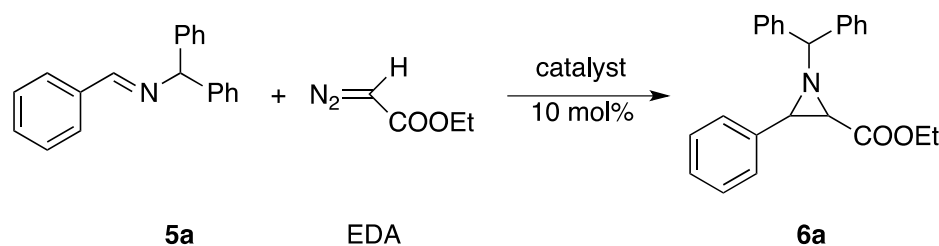
Yield: 60%. ¹H NMR (300 MHz, CDCl₃): δ 8.88 (*m*, 2H, HC=N), 7.62-6.74 (*m*, H_{arom}), 4.16 (*m*, 2H, N-CH), 2.72 (*m*, 2H, NCH-CHH'), 2.44-2.19 (*m*, 24H, CH₃), 2.10-2.06 (*m*, 2H, CH₂), 2.00-1.94 (*m*, 2H, CH₂). ³¹P NMR (121.5 MHz, CDCl₃): δ 46.32 (*s*, 2P). Anal. Calcd for C₄₈H₄₈N₂P₂Cl₂Ru: C, 65.01; H, 5.46; N, 3.16. Found C, 64.42; H, 5.53; N, 3.00. [α]_D²⁰ = -170 (c = 0.50). MS (ESI): *m/z* 851.2031 (M⁺). IR (ATR, cm⁻¹): 1626 (ν_{C=N}).



6.3 Ru/PNNP Catalyzed Asymmetric Imine aziridination

6.3.1 Imine aziridination

General Procedure for the Catalytic Aziridination of N-Benzylidene-1,1-diphenylmethanamine with Ethyldiazoacetate at Constant Temperature (0 °C).



[RuCl₂(**1b-1h**)] (**2b-2h**) (0.049 mmol) and the appropriate chloride scavenger (0.049 mmol) were dissolved in freshly distilled CH₂Cl₂ (3 mL), and the solution was stirred at room temperature overnight. The mixture was then cooled at 0 °C, and imine **5a** (0.49 mmol) and EDA (1.96 mmol) were added under argon. The mixture was stirred at 0°C for 24 h, leaving the argon inlet open. The yield was determined by ¹H NMR spectroscopy by adding a known amount of 1,3,5-trimethoxybenzene as internal standard to the crude mixture at the end of the reaction. The crude was purified by column chromatography over silica using hexane/ethyl acetate 95:5 mixture as eluent.

General Procedure for the Catalytic Aziridination of N-Benzylidene-1,1-diphenylmethanamine with Ethyldiazoacetate with the Gradient Temperature Protocol.

[RuCl₂(**1b-1h**)] (**2b-2h**) (0.049 mmol) and proper chloride scavenger (0.049 mmol) were dissolved in freshly distilled CH₂Cl₂ (3 mL), and the solution was stirred at room temperature overnight. The mixture was then cooled at -78 °C, and imine **5a** (0.49 mmol) and EDA (1.96 mmol) were added under argon. The mixture was stirred at -78 °C for 5 min, then it was warmed to room temperature in an *i*-propanol bath, and stirred for 24 h at room temperature, leaving the argon inlet open. The yield was determined by ¹H NMR spectroscopy by adding a known amount of 1,3,5-trimethoxybenzene as internal standard to the crude mixture at the end of the reaction. The crude was purified by column chromatography over silica using hexane/ethyl

acetate 95:5 mixture as eluent.

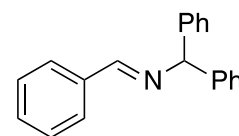
General Procedure for the Competition Experiments.

[RuCl₂(**1b**)] (**2b**) (46.3 mg, 0.049 mmol) and Et₃OBF₄ (9.3 mg, 0.049 mmol) were dissolved in freshly distilled CH₂Cl₂ (3 mL), and the solution was stirred at room temperature overnight. The mixture was then cooled at 0 °C, imine **5l** (4.9 mmol, 10 equiv), imine **5m-5p** (4.9 mmol, 10 equiv) and EDA (0.49 mmol, 1 equiv) were added under argon. The mixture was stirred at 0 °C for 24 h, leaving the argon inlet open. The yield was determined by ¹H NMR spectroscopy by adding a known amount of 1,3,5-trimethoxybenzene as internal standard to the crude mixture at the end of the reaction. The crude was purified by chromatographic column using hexane/ethyl acetate 95:5 mixture as eluent.

6.3.2 Synthesis of Imines

N-Benzylidene-1,1-diphenylmethanamine (5a).

A mixture of benzaldehyde (8.5 g, 80 mmol), diphenylmethanamine (4.7 g, 80 mmol), and ZnCl₂ (223 mg, 1.74 mmol) in toluene (500 mL) was refluxed overnight in a

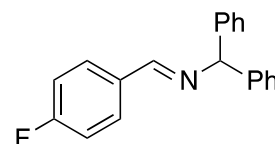


Dean-Stark apparatus. Thus, the salts were filtered off, the solvent was evaporated under reduced pressure, and the crude product was recrystallized from ethanol at low temperature to give white crystals.

Yield: 18.1 g (83%). ¹H NMR (CDCl₃, 300 MHz): δ 8.53 (s, 1H, NCHPh), 7.96 – 7.33 (m, 15H, H_{arom}), 5.71 (s, 1H, NCHPh₂). NMR data in agreement with the published values.²⁶⁰

N-(4-Fluorobenzylidene)-1,1-diphenylmethanamine (5b).

Similarly to **5a**, **5b** was obtained as a white solid using 4-fluorobenzaldehyde (5.34 g, 43 mmol), diphenylmethanamine (7.9 g, 43 mmol), ZnCl₂ (110 mg, 0.80 mmol), and toluene (250 mL).

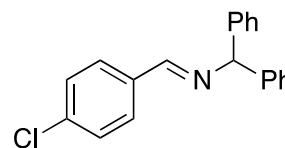


Yield: 7.2 g (79%). ¹H NMR (CDCl₃, 250 MHz): δ 8.39 (s, 1H, NCHAr), 7.60 – 7.23 (m, 14H, H_{arom}), 5.59 (s, 1H, NCHPh₂). NMR data in agreement with the published

values.²⁶¹

N-(4-Chlorobenzylidene)-1,1-diphenylmethanamine (**5c**).

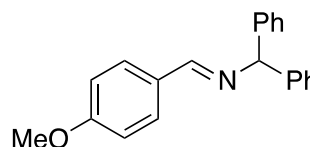
Similarly to **5a**, **5c** was obtained as a white solid using 4-chlorobenzaldehyde (2.42 g, 17 mmol), diphenylmethanamine (3.16 g, 17.2 mmol), ZnCl₂ (98 mg, 0.72 mmol), and toluene (100 mL).



Yield: 3.4 g (85%). ¹H NMR (CDCl₃, 250k MHz): δ 8.38 (s, 1H, NCHAr), 7.78 – 7.23 (m, 14H, H_{arom}), 5.60 (s, 1H, NCHPh₂). NMR data in agreement with the published values.²⁶⁰

N-(4-Methoxybenzylidene)-1,1-diphenylmethanamine (**5d**).

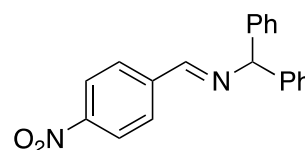
Similarly to **5a**, **5d** was obtained as a white solid using 4-methoxybenzaldehyde (2.0 g, 14.7 mmol), diphenylmethanamine (2.7 g, 14.7 mmol), ZnCl₂ (100 mg, 0.73 mmol), and toluene (100 mL).



Yield: 2.7 g (61%). ¹H NMR (CDCl₃, 300 MHz): δ 8.36 (s, 1H, NCHAr), 7.86-7.21 (m, 14H, H_{arom}), 5.57 (s, 1H, NCHPh₂), 3.83 (s, 3H, CH₃). NMR data in agreement with the published values.²⁶⁰

N-(4-Nitrobenzylidene)-1,1-diphenylmethanamine (**5e**).

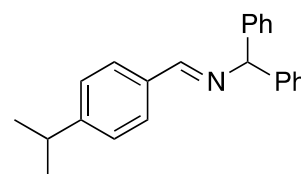
Similarly to **5a**, **5e** was obtained as a white-yellow solid using 4-nitrobenzaldehyde (3.0 g, 19.9 mmol), diphenylmethanamine (3.6 g, 19.9 mmol), ZnCl₂ (50 mg, 0.37 mmol), and toluene (100 mL).



Yield: 4.90 g (78%). ¹H NMR (CDCl₃, 300 MHz): δ 8.42 (s, 1H, NCHAr), 8.21-7.18 (m, 14H, H_{arom}), 5.67 (s, 1H, NCHPh₂). NMR data in agreement with the published values.¹⁷²

N-(4-Isopropylbenzylidene)-1,1-diphenylmethanamine (**5f**).

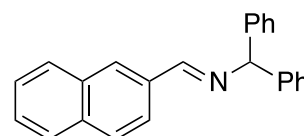
Similarly to **5a**, **5f** was obtained as a white solid using 4-isopropylbenzaldehyde (1.21 g, 8.2 mmol), diphenylmethanamine (1.50 g, 17.2 mmol), ZnCl₂ (50 mg, 0.37 mmol), and toluene (50 mL).



Yield: 1.05 g (54%). ¹H NMR (CDCl₃, 300 MHz): δ 8.43 (*s*, 1H, NCHAr), 7.82-7.13 (*m*, 14H, H_{arom}), 5.62 (*s*, 1H, NCHPh₂), 2.96 (*sept*, 1H, CH(CH₃)₂), 1.31 (*d*, 6H, (CH₃)₂ *J* = 11.1 MHz). NMR data in agreement with the published values.¹⁶²

N-(2'-Naphthylbenzylidene)-1,1-diphenylmethanamine (**5g**).

Similarly to **5a**, **5g** was obtained as a white solid using 2-naphthaldehyde (0.85 g, 5.5 mmol), diphenylmethanamine (1.0 g, 5.5 mmol), ZnCl₂ (50 mg, 0.37 mmol), and methanol

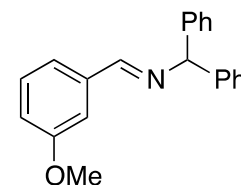


stirring at room temperature (20 mL) for 30 min. Solid obtained from recrystallization from methanol at low temperature.

Yield: 1.56 g (89%). ¹H NMR δ 8.60 (*s*, 1H, NCHAr), 7.90–7.25k (*m*, 17H, H_{arom}), 5.71 (*s*, 1H, NCHPh₂). NMR data in agreement with the published values.¹⁶³

N-(3-Methoxybenzylidene)-1,1-diphenylmethanamine (**5h**).

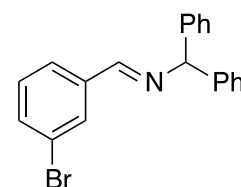
Similarly to **5e**, **5h** was obtained as a white solid using 3-methoxybenzaldehyde (0.74 g, 5.5 mmol), diphenylmethanamine (1.0 g, 5.5 mmol), and methanol stirring at room temperature (20 mL) for 30 min.



Yield: 1.24 g (75%). ¹H NMR (CDCl₃, 200 MHz): δ 8.32 (*s*, 1H, NCHAr), 7.50-7.26 (*m*, 14H, H_{arom}), 5.74 (*s*, 1H, NCHPh₂), 3.85 (*s*, 3H, CH₃). NMR data in agreement with the published values.¹⁶⁴

N-(3-Bromobenzylidene)-1,1-diphenylmethanamine (**5i**).

Similarly to **5e**, **5i** was obtained as a white solid using 3-bromobenzaldehyde (1.0 g, 5.5 mmol), diphenylmethanamine (1.0 g, 5.5 mmol), and methanol stirring at room temperature (10 mL) for 30 min.

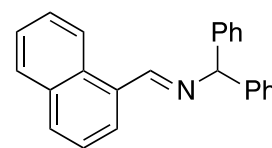


Yield: 1.51 g (79%). ¹H NMR (CDCl₃, 300 MHz): δ 8.38 (*s*, 1H, NCHAr), 7.44-7.28

(*m*, 14H, H_{arom}), 5.63 (*s*, 1H, NCHPh₂).

N-(1'-Naphthylbenzylidene)-1,1-diphenylmethanamine (**5j**).

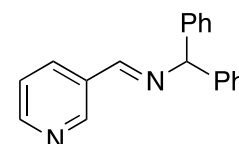
Similarly to **5e**, **5j** was obtained using 1-naphthaldehyde (0.85 g, 5.5 mmol), diphenylmethanamine (1.0 g, 5.5 mmol), ZnCl₂ (50 mg, 0.37 mmol), and methanol stirring at room temperature (20 mL) for 30 min. A white solid was obtained by crystallization from methanol at low temperature.



Yield: 2.45 g (90%). ¹H NMR (CDCl₃, 300 MHz): δ 8.46 (*s*, 1H, NCHAr), 7.90-7.24 (*m*, 17H, H_{arom}), 5.64 (*s*, 1H, NCHPh₂).

N-(3-Pyridine)-1,1-diphenylmethanamine (**5k**).

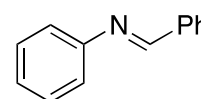
Similarly to **5a**, **5k** was obtained using 3-pyridine-carbaldehyde (1.1 g, 5.5 mmol), diphenylmethanamine (1.0 g, 5.5 mmol), and methanol stirring at room temperature (10 mL) for 30 min. A white solid was obtained by crystallization from methanol at low temperature.



Yield: 1.11 g (75%). ¹H NMR (400 MHz, CDCl₃): δ 8.65 (*d*, *J* = 4.84 Hz, 1H, H_{arom}), 8.56 (*s*, 1H, H_{arom}), 8.26 (*d*, *J* = 7.9 Hz, 1H, H_{arom}), 7.78 (*t*, *J* = 7.6 Hz, 4H, H_{arom}), 7.40 (*d*, *J* = 7.1 Hz, 4H, H_{arom}), 7.37-7.31 (*m*, 4H, H_{arom}), 7.31-2.24 (*m*, 2H), 5.72 (*s*, 1H, NCHPh₂). NMR data in agreement with the published values.²⁶⁵

N-Benzylideneaniline (**5l**).

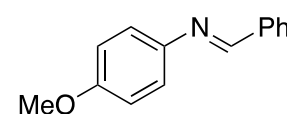
Similarly to **5e**, **5l** was obtained using benzaldehyde (1.00 g, 9.4 mmol), aniline (0.88 g, 9.4 mmol), and methanol stirring overnight at room temperature (10mL). A white solid obtained was obtained by crystallization from methanol at low temperature.



Yield: 0.84 g (9%). ¹H NMR. (CDCl₃, 200 MHz): δ 8.57 (*s*, 1H, NCH), 8.06-7.40 (*m*, 10H, H_{arom}).

N-Benzylidene-4-methoxyaniline (**5m**).

Similarly to **5e**, **5m** was obtained using benzaldehyde (1.00 g, 9.4 mmol), 4-methoxyaniline (1.16 g, 9.4 mmol), and methanol stirring overnight at room temperature (10mL). A white solid

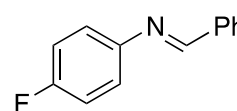


was obtained by crystallization from methanol at low temperature.

Yield: 0.88 g (42%). $^1\text{H NMR}$ (CDCl_3 , 400 MHz): δ 8.51 (*s*, 1H, NCH), 7.93-6.95 (*m*, 9H, H_{arom}), 3.85 (*s*, 3H, CH_3O).

N-Benzyldine-4-fluoroaniline (**5n**).

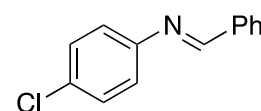
Similarly to **5e**, **5n** was obtained using benzaldehyde (2.09 g, 19.7 mmol), 4-fluoroaniline (2.19 g, 19.7 mmol), and methanol stirring overnight at room temperature (10mL). A white solid was obtained by crystallization from methanol at low temperature.



Yield: 2.4 g (61%). $^1\text{H NMR}$ (CDCl_3 , 200 MHz): δ 8.55 (*s*, 1H, NCH), 8.07-7.22 (*m*, 9H, H_{arom}).

N-Benzyldine-4-chloroaniline (**5o**).

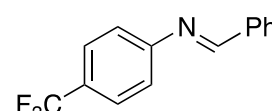
Similarly to **5e**, **5o** was obtained using benzaldehyde (2.0 g, 18.9 mmol), 4-chloroaniline (2.4 g, 18.9 mmol), and methanol stirring overnight at room temperature (20mL). A white solid was obtained by crystallization from methanol at low temperature.



Yield: 2.84 g (72%). $^1\text{H NMR}$ (CDCl_3 , 200 MHz): δ 8.48 (*s*, 1H, NCH), 7.96-6.99 (*m*, 9H, H_{arom}).

N-Benzyldine-4-trifluoromethylaniline (**5p**).

Similarly to **5e**, **5p** was obtained using benzaldehyde (2.0 g, 18.9 mmol), 4-trifluoroaniline (2.4 g, 18.9 mmol), and methanol stirring overnight at room temperature (20mL). A white solid was obtained by crystallization from methanol at low temperature.



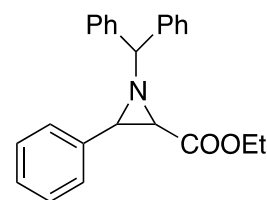
Yield: 1.36 g (34%). $^1\text{H NMR}$ (CDCl_3 , 200 MHz): δ 8.47 (*s*, 1H, NCH), 7.99-7.18 (*m*, 9H, H_{arom}).

5.3.3 Aziridines

(2R,3R)-Ethyl 1-benzhydryl-3-phenylaziridine-2-carboxylate (*cis*-**6a**).

Product obtained as a white solid.

¹H NMR (CDCl₃, 300.2 MHz): δ 7.18-7.64 (*m*, 14H, H_{arom}), 3.99 (*s*, 1H, CHPh₂), 3.96 (*q*, 2H, *J* = 7.14 Hz, COOCH₂), 3.25 (*d*, 1H, *J* = 6.84 Hz, NCHCOOEt), 2.71 (*d*, 1H, *J* = 6.84 Hz,

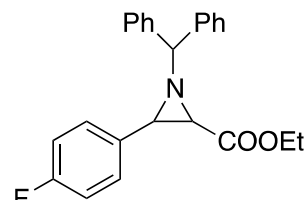


NCHPh), 1.00 (*t*, 3H, *J* = 7.11 Hz, CH₃). ¹³C NMR (CDCl₃, 125.8 MHz): δ 14.0, 46.5, 48.1, 60.6, 77.8, 127.3–128.6, 135.1, 134.0, 142.5, 142.6, 167.8. ¹H NMR and ¹³C NMR spectroscopic data are in agreement with published values.¹¹⁶ Chiral HPLC: AM column, eluent: hexane/2-propanol (99:1), flow rate 0.5 mL/min, *R*_t (min) = 34.4 (major, (*2R,3R*)-**6a**), 41.8 (minor, (*2S,3S*)-**6a**). [α]_D²⁰ = 22.9 ± 1 (*c* = 1.5, CHCl₃) @ 93% ee. Absolute configuration assigned on the basis of the sign of the optical rotation reported.¹¹⁶ HRMS (MALDI): Calcd. for C₂₄H₂₄N O₂ *m/z* 358.1802 found *m/z* 358.1801.

(2R,3R)-Ethyl 1-Benzhydryl-3-(4-fluorophenyl)aziridine-2-carboxylate (*cis*-**6b**).

Product obtained as a white solid.

¹H NMR (CDCl₃, 500.2 MHz): δ 7.64-6.96 (*m*, 14H, H_{arom}), 3.99 (*q*, 2H, *J* = 6.60 Hz, COOCH₂), 3.97 (*s*, 1H, CHPh₂), 3.22 (*d*, 1H, *J* = 6.85 Hz, NCHCOOEt), 2.71 (*d*, 1H, *J* = 6.80 Hz, NCHPh), 1.05 (*t*, 3H, *J* = 7.10 Hz, CH₃).



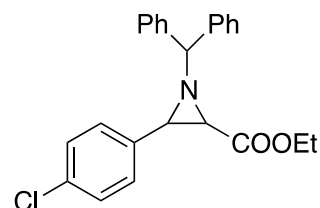
¹³C NMR (CDCl₃, 125.8 MHz):

δ 14.4, 46.8, 47.7, 61.1, 78.1, 115.0, 115.2, 127.9129.0, 142.7, 142.9, 161.7, 163.6, 168.0. Chiral GC: AD-H column; eluent: hexane/2-propanol (99:1); flow rate: 0.5 mL/min; *R*_t (min) = 27.0 (major, (*2R,3R*)-**6b**); 45.2 (minor, (*2S,3S*)-**6b**) @ 17% ee. HRMS (MALDI): Calcd. for C₂₄H₂₃F N O₂ *m/z* 376.1707 found *m/z* 376.1707.

(2R,3R)-Ethyl 1-benzhydryl-3-(4-chlorophenyl)aziridine-2-carboxylate (*cis*-**6c**).

Product obtained as a white solid.

¹H NMR (CDCl₃, 500.2 MHz): δ 7.62-7.22 (*m*, 14H, H_{arom}), 3.99 (*q*, 2H, *J* = 6.55 Hz, COOCH₂), 3.97 (*s*, 1H, CHPh₂), 3.20 (*d*, 1H, *J* = 6.45 Hz, NCHCOOEt), 2.72 (*d*,

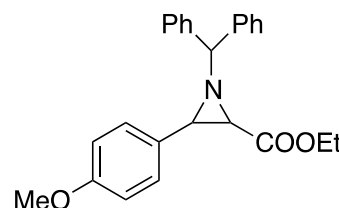


1H, $J = 6.35$ Hz, NCHPh), 1.06 (*t*, 3H, $J = 6.95$ Hz, CH₃). ¹³C NMR (CDCl₃, 125.8 MHz): δ 14.4, 46.9, 47.7, 61.1, 78.1, 127.6–129.6, 133.6, 134.0, 142.6, 142.8, 167.9. ¹H NMR and ¹³C NMR spectroscopic data are in agreement with the published values. Chiral GC: AD-H column; eluent: hexane/2-propanol (99:1); flow rate: 0.5 mL/min; R_t (min) = 21.6 (major, (2*R*,3*R*)-**6c**), 31.4 (minor, (2*S*,3*S*)-**6c**) @ 23% ee. **HRMS (MALDI)**: Calcd. for C₂₄H₂₃Cl N O₂ m/z 392.1412 found m/z 392.1412.

Cis-Ethyl 1-benzhydryl-3-(4-methoxyphenyl)aziridine-2-carboxylate (cis-6d).

Product obtained as a white solid.

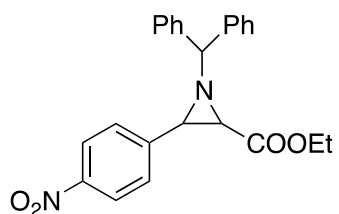
¹H NMR (CDCl₃, 300.1 MHz): δ 7.86-7.14 (*m*, 14H, H_{arom}), 4.11 (*q*, 2H, $J = 7.14$ Hz, COOCH₂), 4.06 (*s*, 1H, CHPh₂), 3.77 (*s*, 3H, OCH₃), 3.17 (*d*, 1H, $J = 6.72$ Hz, NCHCOOEt), 2.63 (*d*, 1H, $J = 6.75$ Hz, NCHPh), 1.01 (*t*, 3H, $J = 7.08$ Hz, CH₃). ¹H NMR in agreement with the published values.¹⁷² Chiral GC: AD-H column; eluent: hexane/2-propanol (98:2); flow rate: 0.5 mL/min; R_t (min) = 51.3, (2*R*,3*R*)-**6d**); 55.4, (2*S*,3*S*)-**6d** @ 0% ee.



Cis-Ethyl-1-benzhydryl-3-(4-nitrophenyl)aziridine-2-carboxylate (6e).

Product obtained as a yellow solid.

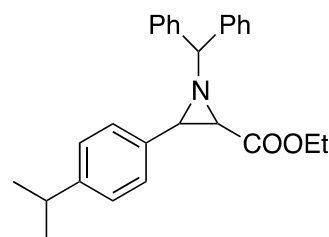
¹H NMR (CDCl₃, 500.2 MHz): δ 7.64-6.96 (*m*, 14H, H_{arom}), 3.99 (*q*, 2H, $J = 6.6$ Hz, COOCH₂), 3.97 (*s*, 1H, CHPh₂), 3.22 (*d*, 1H, $J = 6.9$ Hz, NCHCOOEt), 2.71 (*d*, 1H, $J = 6.80$ Hz, NCHPh), 1.05 (*t*, 3H, $J = 7.10$ Hz, NCHPh). ¹³C NMR (CDCl₃, 125.8 MHz): δ 14.4, 46.8, 47.7, 61.1, 78.1, 115.0, 115.2, 127.9–129.0, 142.7, 142.9, 161.7, 163.6, 168.0. Chiral GC: AD-H column; eluent: hexane/2-propanol (99:1); flow rate: 0.5 mL/min; R_t (min) = 27.0 ((2*R*,3*R*)-**6e**); 45.2 ((2*S*,3*S*)-**6e**) @ 0 ee. **HRMS (MALDI)**: Calcd. for C₂₄H₂₃F N O₂ m/z 403.1652 found m/z 403.1652.



Cis-Ethyl-1-benzhydryl-3-(4-isopropylphenyl)aziridine-2-carboxylate (cis-6f).

Product obtained as a white solid.

¹H NMR (CDCl₃, 500.2 MHz): δ 7.64-7.13 (m, 14H, H_{arom}), 3.99 (q, 2H, J = 7.3 Hz, COOCH₂), 3.97 (s, 1H, CHPh₂), 3.23 (d, 1H, J = 6.85 Hz, NCHCOOEt), 2.88 (sept, 1H, J = 6.90, CHCH₃), 2.67 (d, 1H, J = 6.75 Hz,

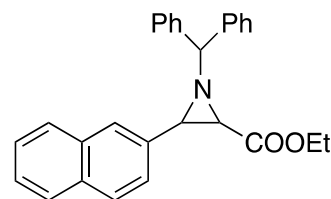


NCHPh), 1.24 (d, 6H, J = 6.95, CH₃), 0.99 (t, 3H, J = 6.95 Hz, NCHPh). ¹³C NMR (CDCl₃, 125.8 MHz): δ 14.4, 46.8, 47.7, 61.1, 78.1, 115.0, 115.2, 127.9–129.0, 142.7, 142.9, 161.7, 163.6, 168.0. Chiral GC: AD-H column; eluent: hexane/2-propanol (99:1); flow rate: 0.5 mL/min; R_t (min) = 27.0 ((2R,3R)-6f); 45.2 ((2S,3S)-6f), 0% ee. HRMS (MALDI): Calcd. for C₂₄H₂₃F N O₂ m/z 400.2271 found m/z 400.2271.

Cis-Ethyl-1-benzhydryl-3-(2-naphthyl)aziridine-2-carboxylate (cis-6g).

Product obtained as a white solid.

¹H NMR (CDCl₃, 500.2 MHz): δ 7.19-7.92 (m, 17H, H_{arom}), 4.06 (s, 1H, CHPh₂), 3.94 (q, 2H, J = 7.50 Hz, COOCH₂), 3.40 (d, 1H, J = 6.80 Hz, NCHCOOEt), 2.80 (d, 1H, J = 6.85 Hz, NCHPh), 0.98 (t, 3H, J = 7.4 Hz,

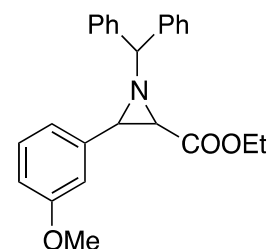


NCHPh). ¹³C NMR (CDCl₃, 125.8 MHz): δ 14.1, 46.9, 48.4, 60.8, 77.9, 125.8–128.7, 132.8, 133.0, 133.1, 142.5, 142.6, 167.9. Chiral GC: AD-H column; eluent: hexane/2-propanol (99:1); flow rate: 0.5 mL/min; R_t (min) = 61.4 ((2R,3R)-6g); 67.0 ((2S,3S)-6g), 0% ee. HRMS (MALDI): Calcd. for C₂₄H₂₃F N O₂ m/z 408.1958 found m/z 408.1958.

Cis-Ethyl-1-benzhydryl-3-(3-methoxyphenyl)aziridine-2-carboxylate (cis-6h).

Product obtained as a colorless oil.

¹H NMR (CDCl₃, 300.1 MHz): δ 7.52-6.64 (m, 14H, H_{arom}), 3.88 (q, 2H, J = 7.11 Hz, COOCH₂), 3.86 (s, 1H, CHPh₂), 3.87 (s, 3H, OCH₃), 3.10 (d, 1H, J = 6.84 Hz, NCHCOOEt), 2.58 (d, 1H, J = 6.87 Hz, NCHPh), 0.93 (t, 3H, J = 7.11 Hz,



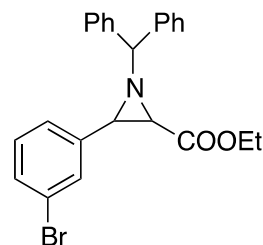
NCHPh). ¹³C NMR (CDCl₃, 125.8 MHz): δ 14.4, 47.3, 47.5, 61.4, 78.0, 123.5–129.2, 142.2, 142.5, 142.9, 147.8, 167.4. Chiral GC: AD-H column; eluent: hexane/2-propanol (99:1); flow rate: 0.5 mL/min; R_t

(min) = 36.9 ((2*R*,3*R*)-**6e**); 41.5 (2*S*,3*S*)-**6e**). **HRMS (MALDI)**: Calcd. for C₂₄H₂₃ N₂ O₄ *m/z* 403.1652 found *m/z* 403.1652.

Cis-Ethyl-1-benzhydryl-3-(3-bromophenyl)aziridine-2-carboxylate (**6i**).

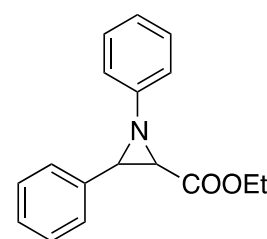
Product obtained as a white solid.

¹H NMR (CDCl₃, 300.1 MHz): δ 7.82-7.10 (*m*, 14H, H_{arom}), 3.99 (*q*, 2H, *J* = 6.93 Hz, COOCH₂), 3.97 (*s*, 1H, CHPh₂), 3.18 (*d*, 1H, *J* = 6.78 Hz, NCHCOOEt), 2.72 (*d*, 1H, *J* = 6.87 Hz, NCHPh), 1.06 (*t*, 3H, *J* = 6.93 Hz, NCHPh).



Cis-Ethyl 1,3-Diphenylaziridine-2-carboxylate (**6l**).

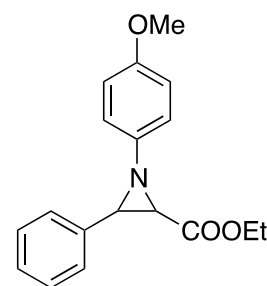
¹H NMR (CDCl₃, 500 MHz): δ 7.56-6.89 (*m*, H_{arom}), 4.19 – 3.99 (*m*, 2H, *J* = 6.8 Hz, COOCH₂), 3.63 (*d*, 1H, *J* = 6.75 Hz, NCHCOOEt), 3.24 (*d*, 1H, *J* = 6.7 Hz, NCHPh), 1.03 (*t*, 3H, *J* = 7.0 Hz, CH₃). NMR data in agreement with literature values.²⁶⁶



Trans-**6m**: ¹H NMR (CDCl₃, 500 MHz): δ 7.55–6.89 (*m*, H_{arom}), 4.08 (*q*, 2H, *J* = 7.1 Hz, COOCH₂), 3.85 (*m*, 1H, NCHCOOEt), 3.28 (*m*, 1H, NCHPh), 1.20 (*t*, 3H, *J* = 7.2 Hz, CH₃).

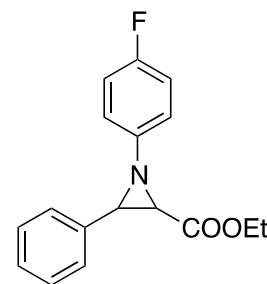
Cis-Ethyl 1-(4-Methoxyphenyl)-3-phenylaziridine-2-carboxylate (*cis*-**6m**).

¹H NMR (CDCl₃, 400 MHz): δ 7.92-6.44 (*m*, H_{arom}), 3.76 (*s*, 3H, OCH₃), 3.17 (*d*, 1H, *J* = 6.8 Hz, NCHPh), 1.02 (*t*, 3H, *J* = 7.1 Hz, CH₃). The NCHCOOEt and the COOCH₂ signals overlap with other signals of **13e**, diethylmaleate, and trimethoxybenzene used as internal standard and was not assigned. NMR data in agreement with literature values.²⁶⁶



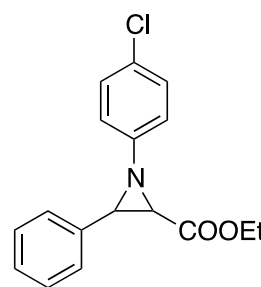
Cis-Ethyl 1-(4-Fluorophenyl)-3-phenylaziridine-2-carboxylate (*cis*-**6n**).

¹H NMR (CDCl₃, 500 MHz): δ 7.53-6.88 (*m*, H_{arom}), 4.12-3.98 (*m*, 2H, COOCH₂), 3.20 (*d*, 1H, *J* = 6.8 Hz, NCHPh), 3.58 (*d*, 1H, *J* = 6.8 Hz, NCHCOOEt), 1.03 (*t*, 3H, *J* = 7.2 Hz, CH₃). NMR data in agreement with the published values.²⁶⁶



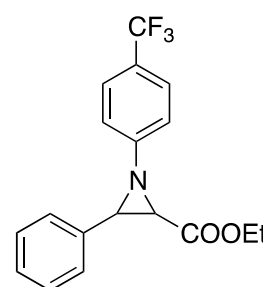
Cis-Ethyl 1-(4-Chlorophenyl)-3-phenylaziridine-2-carboxylate (cis-6o).

$^1\text{H NMR}$ (CDCl_3 , 300 MHz): δ 7.94-6.83 (*m*, H_{arom}), 4.11-3.96 (*m*, 2H, COOCH_2), 3.59 (*d*, 1H, $J = 6.8$ Hz, NCHCOOEt), 3.21 (*d*, 1H, $J = 6.8$ Hz, NCHPh), 1.03 (*t*, 3H, $J = 7.1$ Hz, CH_3). *trans-6u*: $^1\text{H NMR}$ (CDCl_3 , 300 MHz): δ 7.94 – 6.83 (*m*, H_{arom}), 4.18 (*q*, 2H, $J = 7.2$ Hz, COOCH_2), 3.81 (*br s*, 1H, NCHCOOEt), 3.27 (*br s*, 1H, NCHPh), 1.23 (*t*, 3H, $J = 7.0$ Hz, CH_3). NMR data in agreement with the published values.²⁶⁶



Cis-Ethyl 1-(4-Trifluoromethylphenyl)-3-phenylaziridine-2-carboxylate (cis-6p).

$^1\text{H NMR}$ (CDCl_3 , 300 MHz): δ 7.58-6.96 (*m*, H_{arom}), 4.18-4.02 (*m*, 2H, COOCH_2), 3.66 (*d*, 1H, $J = 6.8$ Hz, NCHCOOEt), 3.28 (*d*, 1H, $J = 6.8$ Hz, NCHPh), 1.03 (*t*, 3H, $J = 7.1$ Hz, CH_3).



6.3.3 NMR experiments

General considerations

The reactions described below were run under argon in NMR tubes fitted with serum septa and were monitored by NMR spectroscopy as detailed below. Reagents were added by microsyringe. A 2-PrOH/dry-ice bath was used to keep the sample temperature at the values indicated below during all the manipulations and transfer from and to the spectrometer.

Ethyl 2- ^{13}C -Glycine hydrochloride.

Ethyl 2- ^{13}C -Glycine Ethyl 2- ^{13}C -Glycine (98% 2- ^{13}C , 0.51 g, 6.66 mmol) was suspended in ethanol, and the mixture was cooled to -20 °C (ice-salt bath). SOCl_2 (0.58 mL, 8.00 mmol) was added, the mixture was warmed to room temperature, and another equivalent of solid 2- ^{13}C -glycine (0.51 g, 6.66 mmol) was slowly added. The mixture was refluxed for 2 h. After cooling the colorless solution to room temperature, and the solvent was evaporated under reduced pressure. The resulting white solid was dried in high vacuum for 2 h and recrystallized from ethanol.

Yield: 85%.

Ethyl 2-¹³C-diazoacetate (¹³C-EDA).

Ethyl 2-¹³C-glycine hydrochloride (1.20 g, 7.2 mmol) was mixed with H₂O (2 mL) and CH₂Cl₂ (4mL) in a two-necked flask equipped with septum, argon inlet, and internal thermometer. The colorless mixture was cooled down to -5 °C, and an ice-cold solution of NaNO₂ (0.71, 10.2 mmol) in H₂O (2mL) was added. The resulting mixture was cooled to -10 °C, and a 5% (w/w) H₂SO₄ solution (0.815 g) was slowly added. As higher temperatures might decrease the yield, the solution was never let to warm above 0 °C, during the addition. Thereafter, the mixture was stirred for 20 min between -10 °C and 0 °C, and then poured into an ice-cold separating funnel. The yellow organic layer was recovered, and the aqueous phase was extracted with CH₂Cl₂ (2 x 3 mL). The combined organic phase was dried over Na₂SO₄, filtered, and the solvent was removed under reduced pressure. The resulting yellow oil was dried in vacuum for 15 min, and the product distilled with cold distillation under high vacuum.

Yield: 0.65 g, 66%. ¹H NMR (500 MHz, CD₂Cl₂, 298 K): δ 4.80 (d, 1H, ¹J_{C,H} = 205 Hz, N₂ 13CH), 4.23 (q, ²J_{H,H} = 7.1, 2H, OCH₂CH₃), 1.30 (t, ²J_{H,H} = 7.1 3H, OCH₂CH₃). ¹³C NMR (126 MHz, CD₂Cl₂, 298 K): δ 46.3 (s, N₂CH).

Ethyl 2-⁵³N-diazoacetate (¹³C-EDA).

¹⁵N-EDA was prepared analogously to ¹³C-EDA from ethyl glycine hydrochloride and Na¹⁵NO₂.

[RuCl(OEt₂)](1b)]BF₄ (3bBF₄).

[RuCl₂(1b)] (2b) (46 mg, 0.049 mmol) was activated with Et₃OBF₄ (9.3 mg, 0.049 mmol) in CD₂Cl₂ (0.5 mL) at room temperature overnight. ³¹P NMR (212 MHz, CD₂Cl₂, 313 K): δ 54.9 (d, ²J_{P,P'} = 30.7 Hz), 35.0, (d, ²J_{P,P'} = 30.5 Hz).

[RuCl(1b)]PF₆ (4bPF₆).

[RuCl₂(1b)] (2b) (46 mg, 0.049 mmol) was activated with TlPF₆ (17.1 mg, 0.049 mmol) in CD₂Cl₂ (0.5 mL) at room temperature overnight. ³¹P NMR (212 MHz, CD₂Cl₂, 313 K): δ 59.6 (d, ²J_{P,P'} = 29.0 Hz), 50.1 (d, ²J_{P,P'} = 29.3 Hz).

[RuCl(OH₂)(1b)]PF₆ (7bPF₆).

A solution of *[RuCl(1b)]PF₆* (**4bPF₆**) (0.049 mmol) in CD₂Cl₂ (0.5 mL) was prepared as described above. Then, water (0.024, 1 equiv.) was added at 273 K. ³¹P NMR (212 MHz, CD₂Cl₂, 313 K): δ 63.6 (*d*, ²J_{P,P'} = 34.0 Hz), 46.3 (*d*, ²J_{P,P'} = 34.9 Hz). Upon successively addition of water (4 + 5 equiv) at 273 K, no significant changes were observed in the ³¹P NMR spectra.

[RuCl(1b)]PF₆ (4bPF₆) + imine (1: 1-10).

[RuCl₂(1b)] (2b) (22 mg, 0.024 mmol) was activated with TIPF₆ (9.1 mg, 0.023 mmol) in CD₂Cl₂ (0.5 mL) at room temperature overnight. After stirring the solution at room temperature overnight, the formation of **4bPF₆** was confirmed by the ³¹P NMR spectra. Then imine **5a** (1 equiv) was added. The ³¹P NMR spectra remained unchanged. ³¹P (202 MHz, -40 °C): δ 59.7 (*d*, ²J_{P,P'} = 28 Hz), 50.5 (*d*, ²J_{P,P'} = 28 Hz). Upon successively addition of imine (4 + 5 equiv) at 273 K, no significant changes were observed in the ³¹P NMR spectra.

6.4 PNNP Macrocycles

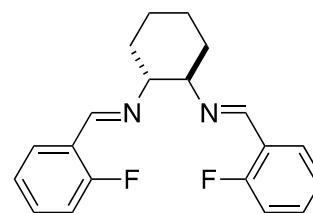
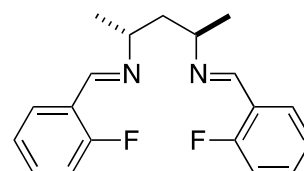
(R,R)-bis(2-fluorobenzylidene)pentane-2,4-diamine (17).

A solution of (2*R*,4*R*)-diaminopentane hydrochloride (0.54 mmol), and K₂CO₃ (2.2 mmol) in a toluene/H₂O 2:1 mixture (30 mL) was refluxed for 4 h. Then, 2-fluorobenzaldehyde (1.1 mmol) was added, and the reaction solution was refluxed overnight in a Dean-Stark apparatus. The mixture was washed with water (10 mL) and the organic layer was separated and dried over Na₂SO₄. The product was obtained as a white solid by crystallization with EtOH. Yield 48%.

¹H NMR (CDCl₃, 250 MHz): δ 8.48 (s, 2H, N=CH), 8.04-7.05 (*m*, 8H, H_{arom}), 1.99 (*m*, 2H, CH₂), 1.27 (s, CH₃), 1.25 (s, CH₃).

(R,R)-bis(2-fluorobenzylidene)cyclohexane-1,2-diamine (18).

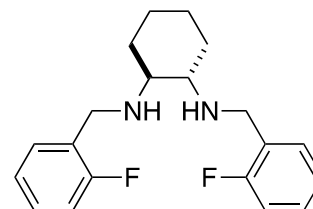
A solution of (*R,R*)-1,2-diaminocyclohexane (3.5 mmol) and 2-fluorobenzaldehyde (7.9 mmol) in 20 mL of toluene was refluxed overnight in a Dean Stark apparatus. The



solvent was evaporated under low pressure, and the product was obtained as a slightly yellow solid. Yield 82%. $^1\text{H NMR}$ (CDCl_3 , 250 MHz): δ 8.54 (*s*, 2H, $\text{N}=\text{CH}$), 7.91–6.96 (*m*, 8H, H_{arom}), 3.48 (*m*, 2H, NCH), 1.87 (*m*, 6H, CH_3), 1.52 (*m*, 2H, CH_2).

(S,S)-bis(2-fluorobenzyl)cyclohexane-1,2-diamine (**19**).

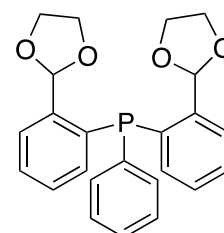
A solution of (*S,S*)-diaminocyclohexane (1.94 mmol), 2-fluorobenzylbromide (3.86 mmol), and K_2CO_3 (2.04 mmol) in CH_3CN (10 mL) was stirred overnight at room temperature. The solvent was removed under reduced



pressure and the product was purified by column chromatography over silica with hexane/EtOAc 95:5 as eluent. Product obtained as a white solid. $^1\text{H NMR}$ (CDCl_3 , 300 MHz): δ 7.58–6.91 (*m*, 8H, H_{arom}), 3.90 (*d*, $J = 13.3$, 2H, ArCH_2N), 3.76 (*d*, $J = 13.4$, 2H, ArCH_2N), 2.26 (*m*, 2H, NH), 2.08 (*m*, 4H, CH_2), 1.68 (*m*, 2H, CH), 1.27–1.01 (*m*, 4H, CH_2).

Bis(2-(1,3-dioxolan-2-yl)phenyl)(phenyl)phosphine (**20**).

A solution of 2-(2-bromophenyl)1,3-dioxolane (8.8 mmol) in dry THF (1.8 mL) was added dropwise to a stirred suspension of Mg turnings (9.8 mmol) in THF (12 mL) and a crystal of elemental iodine. The reaction mixture was refluxed for 1h, during which it turned brownish. Then, PPhCl_2 (4.4 mmol) dissolved in THF (5

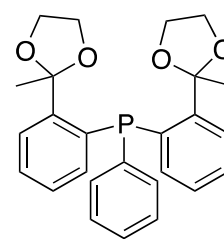


mL) was added dropwise to the filtered solution at $-5\text{ }^\circ\text{C}$ (ice/salt bath). During the addition, the reaction mixture turned yellow and cloudy and was then refluxed overnight. Then, it was quenched with a saturated NH_4Cl aqueous solution (15 mL). The THF was removed under reduced pressure and the solid was extracted with toluene (3 x 15 mL) and dried over Na_2SO_4 . The resulting crude was crystallized at low temperature from toluene and MeOH. The product was obtained as a white solid. Yield 72%.

$^1\text{H NMR}$ (CDCl_3 , 250 MHz): δ 7.73–6.93 (*m*, H_{arom}), 6.40 (*d*, 2H, $J = 5.1$ Hz, CH), 4.13–3.91 (*m*, 8H $\text{O}-\text{CH}_2-\text{CH}_2-\text{O}$). $^{31}\text{P NMR}$ (101.3 MHz) -16.3 (*s*, 1P).

Bis-(2-acetylphenyl)(phenyl)phosphine (21).

A solution of 2-(2-bromophenyl)-2-methyl-1,3-dioxolane (8.2 mmol) in dry THF (1.8 mL) was added dropwise to a stirred suspension of Mg turnings (9.1 mmol) in THF (12 mL) and a crystal of elemental iodine. The reaction mixture was refluxed for 1h, during which it turned brownish. Then, PPhCl₂ (4.4 mmol)



dissolved in THF (5 mL) was added dropwise to the filtrated solution at -5 °C (ice/salt bath). During the addition, the reaction mixture turned yellow and cloudy and was then refluxed overnight. Then, it was quenched with a saturated NH₄Cl aqueous solution (15 mL). The THF was removed under reduced pressure and the solid was extracted with toluene (3 x 15 mL) and dried over Na₂SO₄. The resulting crude was crystallized at low temperature from toluene and MeOH. Product was obtained as a white solid. Yield 64%.

¹H NMR (CDCl₃, 250 MHz): δ 7.70-6.93 (*m*, H_{arom}), 4.12-3.90 (*m*, 8H, O-CH₂-CH₂-O), 2.04 (*s*, 6H, CH₃). ³¹P NMR (101.3 MHz) -15.5 (*s*, 1P).

7. References

1. Hu, X. E. *Tetrahedron* **2004**, 2701.
2. Fürmeier, S.; Metzger, J. O. *Eur. J. Org. Chem.* **2003**, 649.
3. Kasai, M.; Kono, M. *Synlett* **1992**, 778.
4. Johnson, R. D.; Myers, R. J.; Gwinn, W. D. *J. Chem. Phys.* **1953**, 21, 1425.
5. Allen, F. H.; Kennard, O.; Watson, D. G. *J. Chem. Soc. Perkin Trans. 2* **1987**, S1-19.
6. Tanner, D. *Angew. Chem. Int. Ed. Engl.* **1994**, 33, 599.
7. McCoull, W.; Davis, F. A. *Synth.* **2000**, 10, 1347.
8. Sweeney, J. B. *Chem. Soc. Rev.* **2002**, 31, 247.
9. Wu, J.; Hou, X.-L.; Dai, L.-X. *J. Chem. Soc., Perkin Trans. 1* **2001**, 1314.
10. Stamm, H. *J. Prakt. Chem.* **1999**, 341, 319.
11. Wade, T.N. *J. Org. Chem.* **1980**, 45, 5328.
12. Meguro, M.; Yamamoto, Y. *Heterocycles*, **1996**, 43, 2473.
13. Meguro, M.; Asso, N.; Yamamoto, Y. *Tetrahedron Lett.* **1994**, 35, 7395.
14. Ibuka, T.; Nakai, K.; Habashita, H.; Fujii, N.; Garrido, F.; Mann, A.; Chouan, Y.; Yamamoto, Y. *Tetrahedron Lett.* **1993**, 34, 7421.
15. Mao, H.; Joly, G.J.; Peeters, K.; Hoorneart, G. J.; Compernelle, F. *Tetrahedron* **2001**, 57, 6955.
16. Katagiri, T.; Takahashi, M.; Fujiwara, Y.; Ihara, H.; Uneyama, K. *J. Org. Chem.* **1999**, 64, 7323.
17. Matsubara, S.; Kodama, T.; Utimoto, K. *Tetrahedron Lett.* **1990**, 31, 6379.
18. Ungureanu, I.; Klotz, P.; Mann, A. *Angew. Chem., Int. Ed.* **2000**, 41, 4615.
19. Karimova, N. M.; Teplenicheva, Y. L.; Kolomiets, A. F.; Fokin, A. V. *Russ. Chem. Bull.* **1997**, 46, 1136.
20. Stankovic, S.; D'hooghe, M.; Catak, S.; Eum, H.; Waroquier, M.; Van Speybroeck, V.; De Kimpe, N.; Ha, H.-J. *Chem. Soc. Rev.* **2012**, 41, 643.
21. Mall, T.; Stamm, H. *Chem. Ber.* **1988**, 121, 1353.
22. Bornholdt, J.; Felding, J.; Kristensen, J. L. *J. Org. Chem.* **2010**, 75, 7454.
23. Bornholdt, J.; Felding, J.; Clausen, R. P.; Kristensen, J. L. *Chem. Eur. J.* **2010**, 16, 12474.
24. Ghorai, M. K.; Tiwari, D. P. *J. Org. Chem.* **2010**, 75, 6173.

25. Ghorai, M. K.; Kumar, A.; Tiwari, D. P. *J. Org. Chem.* **2010**, *75*, 137.
26. Osborn, H. M. I.; Sweeney, J. D.; Howson, B. *Synlett.* **1993**, 676.
27. Wu, J.; Hou, X.-L.; Dai, L.-X. *J. Org. Chem.* **2000**, *65*, 1344.
28. Meguro, M.; Asao, N.; Yamamoto, Y. *Tetrahedron Lett.* **1994**, *35*, 7395.
29. Righi, G.; Franchini, T.; Bonini, C. *Tetrahedron Lett.* **1998**, *39*, 2385.
30. Watson, I. D. G.; Yu, L.; Yudin, A. K. *Acc. Chem. Res.* **2006**, *39*, 194.
31. Nenajdenko, V. G.; Karpov, A. S.; Balenkova, E. S. *Tetrahedron: Asymmetry* **2001**, *12*, 2517.
32. Hayes, J. F.; Shipman, M.; Slawin, A. M. Z.; Twin, H. *Heterocycles* **2002**, *58*, 243.
33. Hedley, S. J.; Moran, W. J.; Prenzel, A. H. G. P.; Price, D. A.; Harrity, J. P. A. *Synlett.* **2001**, 1596.
34. Cardillo, G.; Gentilucci, L.; Tolomelli, A.; Tomasini, C. *Tetrahedron Lett.* **1997**, *38*, 6953.
35. Cardillo, G.; Gentilucci, L.; Tolomelli, A. *Chem. Commun.* **1999**, 167.
36. Cardillo, G.; Gentilucci, L.; Tolomelli, A. *Tetrahedron* **1999**, *55*, 15151.
37. Eastwood, F. W.; Perlmutter, P.; Yang, Q. *J. Chem. Soc., Perkin. Trans. 1* **1997**, *35*, 159.
38. Eastwood, F. W.; Perlmutter, P.; Yang, Q. *Tetrahedron Lett.* **1994**, *35*, 2039.
39. Gabriel, S. *Ber. Dtsch. Chem. Ges.* **1888**, *21*, 1049.
40. Wenker, H. *J. Am. Chem. Soc.* **1935**, *57*, 2328.
41. Hoch, J.; *Compt. Rend.* **1934**, *198*, 1865.
42. Campbell, K. N.; McKenna, J. F. *J. Org. Chem.* **1939**, *4*, 198.
43. Campbell, K. N.; Campbell, B. K.; Chaput, E. P. *J. Org. Chem.* **1943**, *8*, 103.
44. Zalkow, L. H.; Oehlschlager, A. C. *J. Org. Chem.* **1963**, *28*, 3303.
45. Abramovitch, R. A.; Roy, J.; Uma, V. *Canadian J. Chem.* **1965**, *43*, 3407.
46. Kwart, H.; Khan, A. A. *J. Am. Chem. Soc.* **1967**, *89*, 1951.
47. Evans, D. A.; Worpel, K. A.; Hinman, M. M.; Faul, M. M. *J. Am. Soc. Chem.* **1991**, *113*, 726.
48. Evans, D. A.; Faul, M. M.; Bilodeau, M. T. *J. Org. Chem.* **1991**, *56*, 6744.
49. Evans, D. A.; Faul, M. M.; Bilodeau, M.; Anderson, T. B. A.; Barnes, D. M. *J. Am. Chem. Soc.* **1993**, *115*, 5328.
50. Evans, D. A.; Faul, M. M.; Bilodeau, M. T. *J. Am. Chem. Soc.* **1994**, *116*, 2742.

51. Lowenthal, R.; Abiko, A.; Masamune, S. *Tetrahedron Lett.* **1990**, *31*, 6005
52. Lowenthal, R. E.; Masamune, S. *Tetrahedron Lett.* **1991**, *32*, 7373.
53. Fritschi, H.; Leutenegger, U.; Siegmann, K.; Pfaltz, A.; Keller, W.; Kratky, C. *Helv. Chim. Acta.* **1988**, *71*, 1541.
54. Li, Z.; Conser, K. R.; Jacobsen, E. N. *J. Am. Chem. Soc.* **1993**, *115*, 5326.
55. Li, Z.; Quan, R. W.; Jacobsen, E. N. *J. Am. Chem. Soc.* **1995**, *117*, 5889.
56. Sanders, C. J.; Gillespie, K. M.; Bell, D.; Scott, P. *J. Am. Chem. Soc.* **2000**, *122*, 7132.
57. Gillespie, K. M.; Sanders, C. J.; O'Shaughnessy, P.; Westmoreland, I.; Thickitt, C. P.; Scott, P.; *J. Org. Chem.* **2002**, *67*, 3450.
58. Xu, J.; Ma, L.; Jiao, P. *J. Chem. Soc., Chem. Comm.* **2004**, 1616.
59. Wang, X.; Ding, K. *Chem.-Eur. J.* **2006**, *12*, 4568.
60. Chang, W. W.; Ton, T. M. U.; Zhang, Z.; Xu, Y.; Chan, P. W. H. *Tetrahedron Lett.* **2009**, *50*, 161.
61. Gök, Y.; Noël, T.; Van der Eycken, J. *Tetrahedron: Asymm.* **2010**, *21*, 2275.
62. Müller, P.; Baud, C.; Jacquier, Y. *Tetrahedron* **1996**, *52*, 1543.
63. Liang, J.-L.; Yuan, S.-X.; Chan, P. W. H.; Che, C.-M. *Org. Lett.* **2002**, 4507.
64. Liang, J.-L.; Yuan, S.-X.; Chan, P. W. H.; Che, C.-M. *Tetrahedron Lett.* **2003**, *44*, 5917.
65. Guthikonda, K.; When, P. M.; Caliendo, B. J.; Du Bois, J. *Tetrahedron* **2006**, *62*, 11331.
66. Lebel, H.; Spitz, C.; Leogane, O.; Trudel, C.; Parmentier, M. *Org. Lett.* **2011**, 5460.
67. Kim, C.; Uchida, T.; Katsuki, T. *Chem. Comm.* **2012**, *48*, 7188.
68. Kawabata, H.; Omura, K.; Uchida, T.; Katsuki, T. *Chem.-Asian J.* **2007**, *2*, 248.
69. Noda, K.; Hosoya, N.; Irie, R.; Ito, Y.; Katsuki, T. *Synlett* **1993**, 469.
70. Nishikori, H.; Katsuki, T. *Tetrahedron Lett.* **1996**, *37*, 9245.
71. Mansuy, D.; Mahy, J.-P.; Dureault, A.; Bedi, G.; Battioni, P. *Chem. Comm.* **1984**, 1161.
72. Mahy, J.-P.; Bedi, G.; Battioni, P.; Mansuy, D. *Tetrahedron Lett.* **1988**, *29*, 1927.
73. Mahy, J.-P.; Bedi, G.; Battioni, P.; Mansuy, D. *J. Chem. Soc., Perkin Trans. 2* **1988**, *29*, 1517.
74. Breslow, R.; Gellman, S. H. *Chem. Commun.* **1982**, 1400.

75. Breslow, R.; Gellman, S. H. *J. Am. Chem. Soc.* **1983**, *105*, 6728.
76. Liang, J.-L.; Yuan, S.-X.; Huang, J.-S.; Che, C.-M. *J. Org. Chem.* **2004**, *69*, 3610.
77. Lai, T.-S.; Kwong, H.-L.; Che, C.-M.; Peng, S.-M. *Chem. Commun.* **1997**, 2373.
78. Fantauzzi, S.; Gallo, E.; Caselli, A.; Piangiolino, C.; Ragaini, F.; Cenini, S. *Eur. J. Org. Chem.* **2007**, 6053.
79. Fantauzzi, S.; Caselli, A.; Gallo, E. *Dalton Tran.* **2009**, 5434.
80. Piangiolino, C.; Gallo, E.; Caselli, A.; Fantauzzi, S.; Ragaini, F.; Cenini, S. *Eur. J. Org. Chem.* **2007**, 743.
81. Intrieri, D.; Caselli, A.; Ragaini, F.; Macchi, P.; Casati, N.; Gallo, E. *Eur. J. Inorg. Chem.* **2012**, 569.
82. Caselli, A.; Gallo, E.; Fantauzzi, S.; Morlacchi, S.; Ragaini, F.; Cenini, S. *Eur. J. Inorg. Chem.* **2008**, 3009.
83. Jones, J. E.; Ruppel, J.V.; Gao, G.Y.; Moore, T.M.; Zhang, X.P. *J. Org. Chem.* **2008**, *73*, 7260.
84. Subbarayan, V.; Ruppel, J. V.; Zhu, S.-F.; Perman, J. A.; Zhang, X. P. *Chem. Comm.* **2009**, 4266.
85. Ruppel, J. V.; Gauthier, T. J.; Snyder, N. L.; Perman, J. A.; Zhang, X. P. *Org. Lett.* **2009**, *11*, 2273.
86. TcesN₃ is reported to be stable until 100 °C.
87. Rosen, T. *Comprehensive Organic Synthesis*, Pergamon Press, Oxford, vol. 2, p. 428.
88. Deyrup, J. A. *J. Org. Chem.* **1969**, *34*, 2724.
89. Cainelli, G.; Panunzio, M.; Giacomini, D. *Tetrahedron Lett.* **1991**, *32*, 121.
90. Fujisawa, T.; Hayakawa, R.; Shimizu, M. *Tetrahedron Lett.* **1992**, *33*, 7903.
91. Davis, F. A.; Zhou, P.; Reddy, G. V. *J. Org. Chem.* **1994**, *59*, 3243.
92. Davis, F. A.; Zhou, R.; Liang, C.-H.; Reddy, R. E. *Tetrahedron: Asymmetry* **1995**, *6*, 1511.
93. Li, A.-H.; Dai, L.-X.; Hou, X.-L. *Chem. Commun.* **1996**, 491.
94. Li, A.-H.; Dai, L.-X.; Hou, X.-L. *J. Chem. Soc., Perkin Trans. 1* **1996**, 867.
95. Li, A.-H.; Dai, L.-X.; Hou, X.-L.; Chen, M.-B. *J. Org. Chem.* **1996**, *61*, 4641.
96. Li, A.-H.; Dai, L.-X.; Hou, X.-L. *J. Chem. Soc., Perkin Trans. 1* **1996**, 2725.
97. Li, A.-H.; Zhou, Y.-G.; Dai, L.-X.; Hou, X.-L.; Xia, L.-J.; Lin, L. *Angew. Chem.*

- Int. Ed.* **1997**, *36*, 1317.
98. Liao, W.-W.; Deng, X.-M.; Tang, Y. *Chem. Commun.* **2004**, 1516.
 99. Aggarwal, V. K.; Abedl-Rahman, H.; Jones, R. V. H.; Lee, H. Y.; Reid, B. D. *J. Am. Chem. Soc.* **1994**, *116*, 5793.
 100. Aggarwal, V. K.; Thompson, A.; Jones, R. V. H.; Standen, M. *Tetrahedron Asymm.* **1995**, *6*, 2557.
 101. Aggarwal, V. K.; Alonso, E.; Fang, G.; Ferrara, M.; Hynd, G.; Porcelloni, M. *Angew. Chem. Int. Ed.* **2001**, *40*, 1430.
 102. Aggarwal, V. K.; Charmant, J. P. H.; Ciampi, C.; Hornby, J. M.; O'Brien, C. J.; Hynd, G.; Parsons, R. *J. Chem. Soc., Perkin Trans. 1*, **2001**, 3159.
 103. Bisol, T. B.; Sa, M. M. *Quim. Nova* **2007**, *30*, 106.
 104. Muller, P.; Fruit, C. *Chem. Rev.* **2003**, *103*, 2905.
 105. Ranocchiari, M.; Mezzetti, A. *Organometallics* **2009**, *28*, 3611.
 106. Bartnik, R.; Mloston, G. *Synthesis* **1983**, 924.
 107. Bartnik, R.; Mloston, G. *Tetrahedron*, **1984**, *40*, 2569.
 108. Jephcote, V. J.; John, D. I.; Williams, D. J. *J. Chem. Soc., Perkin Trans. 1* **1986**, 2195.
 109. Casarrubios, L.; Pérez, J. A.; Brookhart, M.; Templeton, J. L. *J. Org. Chem.* **1996**, *61*, 8358.
 110. Juhl, K.; Hazell, R. G.; Jørgensen, K. A. *J. Chem. Soc., Perkin Trans. 1* **1999**, 2293.
 111. Mayer, M. F.; Hossain, M. M. *J. Organom. Chem.* **2002**, 202.
 112. Mayer, M. F.; Hossain, M. M. *J. Org. Chem.*, **1998**, *20*, 6841.
 113. Williams, A. L.; Johnston, J. N. *J. Am. Chem. Soc.* **2004**, *126*, 1612.
 114. Hashimoto, T.; Uchiyama, N.; Maruoka, K. *J. Am. Chem. Soc.* **2008**, *130*, 14380.
 115. Akayima, T.; Suzuki, T.; Mori, K. *Org. Lett.* **2009**, *11*, 2445.
 116. Antilla, J. C.; Wulff, W. D. *J. Am. Chem. Soc.* **1999**, *121*, 5099.
 117. Antilla, J. C.; Wulff, W. D. *Angew. Chem. Int. Ed.* **2000**, *39*, 4518.
 118. Huang, L.; Wulff, W. D. *J. Am. Chem. Soc.* **2011**, *133*, 8892.
 119. Veticatt, M. J.; Desai, A. A.; Wulff, W. D. *J. Am. Chem. Soc.* **2010**, *132*, 13104.
 120. Baret, P.; Buffet, H.; Pierre, J. L. *B. Soc. Chim. Fr.* **1972**, 825.
 121. Hansen, K. B.; Finney, N. S.; Jacobsen, E. N. *Angew. Chem., Int. Ed.* **1995**, *34*,

676.

122. Padwa, A. *Arc. Chem. Res.* **1991**, *24*, 22.
123. Padwa, A.; Hornbuckle, S. F. *Chem. Rev.* **1991**, *91*, 263.
124. Li, Y.; Chan, P. W. H.; Zhu, N.-Y.; Che, C.-M.; Kwong, H.-L. *Organometallics* **2004**, *23*, 54.
125. Marxen, T. L.; Johnson, B. J.; Nilsson, P. V.; Pignolet, L. H. *Inorg. Chem.* **1984**, *23*, 4663.
126. Gao, J.-X.; Ikariya, T.; Noyori, R. *Organometallics* **1996**, *15*, 1087.
127. Mezzetti, A. *Dalton Trans.* **2010**, *39*, 7851.
128. Stoop, R. M.; Bachmann, S.; Valentini, M.; Mezzetti, A. *Organometallics* **2000**, *19*, 4117.
129. Bonaccorsi, C. ETH, Ph. D. Thesis, no 16352, Zürich, Switzerland, 2005.
130. Toullec, P. Y.; Bonaccorsi, C.; Mezzetti, A.; Togni, A. *Proc. Natl. Acad. Sci. USA* **2004**, *101*, 5810.
131. Bonaccorsi, C.; Althaus, M.; Becker, C.; Togni, A.; Mezzetti, A. *Pure Appl. Chem.* **2006**, *78*, 391.
132. Althaus, M.; Becker, C.; Togni, A.; Mezzetti, A.; *Organometallics* **2008**, *27*, 3866.
133. Althaus, M. ETH, Ph. D. Thesis, no 17673, Zürich, Switzerland, 2008.
134. Santoro, F. ETH, Ph. D. Thesis, no 17024, Zürich, Switzerland, 2007.
135. Althaus, M.; Bonaccorsi, C.; Mezzetti, A.; Santoro, F. *Organometallics* **2006**, *25*, 3108.
136. Santoro, F.; Althaus, M.; Bonaccorsi, C.; Gischig, S.; Mezzetti, A. *Organometallics* **2007**, *26*, 5902.
137. Schotes, C.; Mezzetti, A. *J. Am. Chem. Soc.* **2010**, *132*, 3652.
138. Schotes, C.; Mezzetti, A. *Angew. Chem. Int. Ed.* **2011**, *50*, 3072.
139. Ranocchiaro, M. ETH, Ph. D. Thesis, no 18613, Zürich, Switzerland, 2009.
140. Stoop, R. M. ETH, Ph. D. Thesis, no 13394, Zürich, Switzerland, 2000.
141. Bonaccorsi, C.; Bachmann, S.; Mezzetti, A. *Tetrahedron: Asymmetry* **2003**, *14*, 845.
142. Schotes C.; Ranocchiaro, M.; Mezzetti, A. *Organometallics* **2011**, *30*, 3596.
143. Schotes, C. ETH, Ph. D. Thesis, no 19959, Zürich, Switzerland, 2011.
144. Stoop, R. M.; Mezzetti, A. *Green Chem.* **1999**, *1*, 39.
145. Bachmann, S. ETH, Ph. D. Thesis, no 14882, Zürich, Switzerland, 2002.

146. Bachmann, S.; Furler, M.; Mezzetti, A. *Organometallics* **2001**, *20*, 2102.
147. Bonaccorsi, C.; Mezzetti, A. *Organometallics* **2005**, *24*, 4953.
148. Bachmann, S.; Mezzetti, A. *Helv. Chim. Acta* **2001**, *84*, 3063.
149. Zhang, J.; Gandelman, M.; Shimon, L. J. W.; Milstein, D. *Organometallics*, **2008**, *27*, 3526.
150. Cohen, R.; Rybtchinski, B.; Gandelman, M.; Rozenberg, H.; Martino, J. M. L.; Milstein, D. *J. Am. Chem. Soc.* **2003**, *125*, 6532.
151. Sui-Seng, C.; Haque, F. N.; Hazdovic, A.; Pütz, A. M.; Reuss, V.; Meyer, N.; Lough, A. J.; Zimmer-De Iulii, M.; Morris, R. H. *Inorg. Chem.* **2009**, *48*, 735.
152. Caminade, A. M.; Majoral, J. P. *Chem Rev.* **1994**, *94*, 1183.
153. Ranocchiaro, M.; Mezzetti, A. *Organometallics*, **2009**, *28*, 1286.
154. Komen, C. M. D.; Bickelhaupt, F. *Synthetic Comm.* **1996**, *26*, 1693.
155. RajanBabu, T. V.; Casalnuovo, A. L. *Pure Appl. Chem.* **1994**, *66*, 1535.
156. RajanBabu, T. V.; Ayers, T. A.; Casalnuovo, A. L. *J. Am. Chem. Soc.* **1994**, *116*, 4101.
157. Mayer, M. F.; Wang, Q.; Hossain, M. M. *J. Organom. Chem.* **2001**, *630*, 78.
158. Mazumdar, A.; Xue, Z.; Mayer, M. F. *Synlett.* **2007**, 2025.
159. Thompson, S. J.; Bailey, P.M.; White, C.; Maitlis, P. M. *Angew. Chem. Int. Ed. Engl.* **1976**, *15*, 490.
160. Branam, D. M.; Hoffmann, N. W.; McElroy, E. A.; Prokopuk, N.; Salazar, A. B.; Robbins, M. J.; Hill, W. E.; Webb, T. R. *Inorg. Chem.* **1991**, *30*, 1200.
161. White, C.; Thompson, S. J.; Maitlis, P. M. *J. Organomet. Chem.* **1977**, *134*, 319.
162. Wimmer, F. L.; Snow, M. R. *Aust. J. Chem.* **1978**, *31*, 267.
163. Chen, L.; Khan, M.A.; Richter-Addo, G. B. *Inorg. Chem.* **1998**, *37*, 533.
164. Dove, M. F. A.; Hibbert, R. C.; Logan, N. *J. Chem. Soc. Dalton Trans.* **1985**, 707.
165. Dehnicke, K.; Shihada, A. F. *Struct. Bonding (Berlin)*, **1976**, *28*, 51.
166. Toy, A. D. F. *Comprehensive Inorganic Chemistry*, Pergamon Press, London, **1973**, *2*, 536.
167. Fernandez-Galan, R.; Manzano, B. R.; Otero, A. *J. Organom. Chem.* **1999**, 271.
168. Abkayeva, D. N.; Di Vaira, M.; Costantini, S. S.; Peruzzini, M.; Stoppioni, P. *J. Chem. Soc. Dalton. Trans.* **2006**, 389.
169. Smith, G.; Cole-Hamilton, D. J.; Gregory, A. C.; Gooden, N. G.; *Polyhedron*

- 1982**, *1*, 97.
170. Matsumoto, K.; Sano, Y.; Kawano, M.; Uemura, H.; Mutsunami, J. Sato, T.; *Bull. Chem. Jpn.* **1997**, *70*, 1239.
171. Johnston, J. N.; Muchalski, H.; Troyer, T. L. *Angew. Chem. Int. Ed.* **2010**, *49*, 2290.
172. Zhang, Y.; Desai, A.; Lu, Z.; Hu, G.; Ding, Z.; Wulff, W. D. *Chem - Eur. J.* **2008**, *14*, 3785.
173. Mukherjee, M.; Gupta, A. K.; Lu, Z.; Zhang, Y.; Wulff, W. D. *J. Org. Chem.* **2010**, *75*, 5643.
174. Meerwein, H.; Hinz, G.; Hofmann, P.; Kroning, E.; Pfeil, E. *J. Prakt. Chem.* **1937**, *147*, 17.
175. Meerwein, H.; Hederich, V.; Wunderlich, K. *Archiv der Pharmazie* **1958**, *291*, 541.
176. Odian, G.; Yang, N.-L.; Wei, Y. *Magn. Reson. Chem.* **1985**, *23*, 908.
177. Burgi, H. B.; Dunitz, J. D. *Helv. Chim. Acta* **1970**, *53*, 1747.
178. Akaba, R.; Tokumaru, K.; Kobayashi, T. *Bull. Chem. Soc. Jpn.* **1980**, *53*, 1993.
179. Lewis, J. W.; Sandorfy, C. *Can. J. Chem.* **1982**, *60*, 1720.
180. Echevarria, A.; Miller, J.; Nascimento, M. G. *Magn. Reson. Chem.* **1985**, *23*, 809.
181. Hansch, C.; Leo, A. *Substituent Constants for Correlation Analysis in Chemistry and Biology*, Wiley-Interscience, NY, 1979.
182. Rasmussen, K. G.; Juhl, K.; Hazell, R. G.; Jørgensen, K. A. *J. Chem. Soc., Perkin Trans. 2* **1998**, 1347.
183. Dartiguenave, M.; Menu, M. J.; Deydier, E.; Dartiguenave, Y.; Siebald, H. *Coord. Chem. Rev.* **1998**, *180*, 623.
184. Menu, M. J.; Crocco, G.; Dartiguenave, M.; Dartiguenave, Y.; Bertrandt, G. J. *Chem. Soc., Chem. Commun.* **1988**, 1598.
185. *Structural Inorganic Chemistry*, 3rd Ed., Oxford, 1962.
186. Brandt, L.; Wolf, J.; Werner, H. *J. Organom. Chem.* **1993**, *444*, 235.
187. Ortmann, D. A.; Weberndörfer, B.; Ilg, K.; Laubender, M.; Werner, H. *Organometallics* **2002**, *21*, 2369.
188. Werner, H.; Schneider, M. E.; Bosch, M.; Wolf, J.; Teuben, J. H.; Meetsma, A.; Troyanov, S. I. *Chem. Eur. J.* **2000**, 3052.
189. Werner, H.; Mahr, N.; Wolf, J.; Fries, A.; Laubender, M.; Bleuel, E.; Garde, R.;

- Lahuerta, P. *Organometallics* **2003**, *22*, 3566.
190. Dias, E. L.; Brookhart, M.; White, P. S. *J. Am. Chem. Soc.* **2001**, *123*, 2442.
191. Werner, H.; Stüer, W.; Wolf, J.; Laubender, M.; Weberndörfer, B.; Herbst-Irmer R.; Lehmann, C. *Eur. J. Inorg. Chem.* **1999**, 1889.
192. Albertin, G.; Antoniutti, S.; Bordignon, E.; Carrera, B. *Inorg. Chem.* **2000**, *39*, 4646.
193. Albertin, G.; Antoniutti, S.; Pelizzi, G.; Vitali, F.; Bordignon, E. *Inorg. Chem.* **1988**, *27*, 829.
194. Albertin, G.; Antoniutti, S.; Bortoluzzi, M.; Castro-Fojo, J.; Garcia-Fontan, S. *Inorg. Chem.* **2004**, *43*, 4511.
195. Fan, L.; Einstein, F. W. B.; Sutton, D. *Organometallics* **2000**, *19*, 684.
196. Lebel, H.; Paquet, V. *J. Am. Chem. Soc.* **2004**, *126*, 320.
197. Nugent, W. A.; Mayer, J. M. *Metal-ligand multiple bonds*, Wiley, 1988.
198. Nugent, W. A.; McKinney, R. J. Kasowski, R. V.; Vancatledge, F. A. *Inorg. Chim. Acta* **1982**, *65*, L91.
199. Klopman, G. J. *Am. Chem. Soc.* **1968**, *90*, 223.
200. Busch, D. H. *Helv. Chim. Acta*, Fasciculus Extraordinarius, **1967**, 174.
201. Curtis, N. F. *Coordin. Chem. Rev.* **1968**, *3*, 3.
202. Newkome, G. R.; Sauer, J. D.; Roper, J. M.; Hager, D. C. *Chem. Rev.* **1977**, *77*, 513.
203. Cabral, J. O.; Cabral, M. F.; Drew, M. G. B.; Nelson, S. M.; Rodgers, A. *Inorg. Chim. Acta* **1977**, *25*, L77.
204. Isslieb, K.; Oehme, H.; *Chem. Ber.* **1967**, *100*, 2695.
205. Riker-Nappierand, J.; Meek, D. W. *J. Chem. Soc., Chem. Commun.* **1974**, 442.
206. Scanlon, L. G.; Taso, Y. Y.; Cummings, S. C.; Toman, K.; Meek, D. W. *J. Am. Chem. Soc.* **1980**, *102*, 6849.
207. Cummings, S. C.; Sievers, R. E. *Inorg. Chem.* **1970**, *9*, 1133.
208. Scanlon, L. G.; Tsao, Y.-Y.; Toman, K.; Cummings, S. C.; Meek, D. *Inorg. Chem.* **1982**, *21*, 1215.
209. Edwards, P. G.; Newman, P. D.; Hibbs, D. E. *Angew. Chem., Int. Ed.* **2000**, *39*, 2722.
210. Edwards, P. G.; Newman, P. D.; Malik, K. M. A. *Angew. Chem., Int. Ed.* **2000**,

- 39, 2922.
211. Edwards, P. G.; Haigh, R.; Li, D.; Newman, P. D. *J. Am. Chem. Soc.* **2006**, *128*, 3818.
212. Battle, A. R.; Edwards, P. G.; Haigh, R.; Hibbs, D. E.; Li, D.; Liddiard, S. M.; Newman, P. D. *Organometallics* **2007**, *26*, 377.
213. Brauer, D. J.; Lebbe, T.; Stelzer, O. *Angew. Chem., Int. Ed. Engl.* **1988**, *27*, 438.
214. Lebbe, T.; Machnitzki, P.; Stelzer, O.; Sheldrick, W. S. *Tetrahedron* **2000**, *56*, 157.
215. Bartsch, R.; Hietkamp, S.; Morton, S.; Peters, H.; Stelzer, O. *Inorg. Chem.* **1983**, *22*, 3624.
216. Mikhailine, A.; Kim, E.; Dingels, C.; Lough, A. J.; Morris, R. H. *Inorg. Chem.* **2008**, *47*, 6587.
217. Mikhailine, A.; Lough, A. J.; Morris, R. H. *J. Am. Chem. Soc.* **2009**, *131*, 1394.
218. Kyba, E. P.; Davis, R. E.; Hudson, C. W.; John, A. M.; Brown, S. B.; McPhaul, M. J.; Liu, L.-K.; Glover, A. C. *J. Am. Chem. Soc.* **1981**, *103*, 3868.
219. Meisenheimer, J.; Lichtenstadt, L. *Chem Ber.* **1911**, *44*, 456.
220. Baechler, R. D.; Mislow, K. *J. Am. Chem. Soc.* **1970**, 3090.
221. Baechler, R. D.; Mislow, K. *J. Am. Chem. Soc.* **1971**, 773.
222. Nudelman, A.; Cram, D. J. *J. Am. Chem. Soc.* **1968**, *90*, 3869.
223. Korpiun, O.; Lewis, R. A.; Chickos, J.; Mislow, K. *J. Am. Chem. Soc.* **1968**, *90*, 4842.
224. Korpiun, O.; Mislow, K. *J. Am. Chem. Soc.* **1967**, *89*, 4784.
225. Imamoto, T.; Kusumoto, T.; Suzuki, N.; Sato, K. *J. Am. Chem. Soc.* **1985**, *107*, 5301.
226. Imamoto, T.; Oshiki, T.; Onozawa, T.; Kusumoto, T.; Sato, K. *J. Am. Chem. Soc.* **1990**, *112*, 5244.
227. Mikołajczyk, M.; Omelanczuk, J.; Perlikowska, W. *Tetrahedron* **1979**, *35*, 1531.
228. De'ath, N. J.; Ellis, K.; Smiths, D. H. J.; Trippet, S. *J. Chem. Soc., Chem. Commun.* **1971**, 714.
229. Oshiki, T.; Hirosaka, T.; Imamoto, T. *Tetrahedron Lett.* **1991**, *32*, 3371.
230. Koide, Y.; Sakamoto, A.; Imamoto, T. *Tetrahedron Lett.* **1991**, *32*, 3375.
231. Imamoto, T.; Watanabe, J.; Wada, Y.; Masuda, H.; Yamada, H.; Tsuruta, H.; Matsukawa, S.; Yamaguchi, K. *J. Am. Chem. Soc.* **1998**, *120*, 1635.
232. Miura, T.; Yamada, H.; Kikuchi, S.; Imamoto, T. *J. Org. Chem.* **2000**, *65*, 1877.

233. Jugé, S.; Genet, J. P. *Tetrahedron Lett.* **1989**, *30*, 2783.
234. Jugé, S.; Stephan, M.; Laffitte, J. A.; Genet, J. P. *Tetrahedron Lett.* **1990**, *31*, 6357.
235. Jugé, S.; Stephan, M.; Merdes, R.; Genet, J. P.; Halut-Desportes, S. *J. Chem. Soc., Chem. Commun.* **1993**, 531.
236. Kimpton, B. R.; Mcfarlane, W.; Muir, A. S.; Patel, P. G.; Bookham, J. L. *Polyhedron*, **1993**, *12*, 2525.
237. Issleib, K.; Weichmann, H. Z. *Chem. Ber.* **1968**, *101*, 2197.
238. Issleib, K.; Weichmann, H. Z. *Anorg. Allg. Chem.* **1968**, *362*, 33.
239. Issleib, K.; Staudtke, K. *Chem. Ber.* **1963**, *96*, 279.
240. Issleib, K.; Jacob, D. *Chem. Ber.* **1961**, *94*, 107.
241. Issleib, K.; Krech, F. *Chem. Ber.* **1961**, *94*, 2656.
242. Patel, P. G. PhD Thesis, City of London Polytechnic, **1989**.
243. Harries, H.; Haga, T. *Ber.* **1898**, *31*, 550.
244. Harries, H.; Haga, T. *Ber.* **1899**, *32*, 1192.
245. Kagan, H. B.; Dang, T.-P. *J. Am. Chem. Soc.* **1972**, *94*, 6429.
246. Bakos, J.; Tóth, I.; Heil, B.; Markó, L. *J. Organom. Chem.* **1985**, *23*.
247. Fryzuk, M. D.; Bosnich, B. *J. Am. Chem. Soc.* **1977**, *99*, 6262.
248. Andrieux, C. P.; Saveant, J. M.; Zann, D. *Nouveau Journal de Chimie* **1984**, *8*, 107.
249. Horner, L.; Heupt, W. *Phosphorus* **1975**, *5*, 139.
250. Thornton, T. A.; Woolsey, N. F.; Bartak, D. E. *J. Am. Chem. Soc.* **1986**, *108*, 6497.
251. Francisco, M. A.; Kurs, A.; Katritzky, A. R.; Rasala, D.; *J. Org. Chem.* **1988**, *53*, 596.
252. Fish, R. H.; Dupon, J. W. *J. Org. Chem.* **1988**, *53*, 5320.
253. Thornton, T. A.; Ross, G. A.; Patil, D.; Mukaida, K.; Warwick, J. O.; Woolsey, N. F.; Bartak, D. E. *J. Am. Chem. Soc.* **1989**, *111*, 2434.
254. Van Doorn, J. A.; Frijns, J. H.; Meijboom, N. *Recl. Trav. Chim. Pays-Bas* **1991**, *110*, 441.
255. Budzelaar, P. H. M.; van Doorn, J. A.; Meijboom, N. *Recl. Trav. Chim. Pays-Bas* **1991**, *110*, 420.
256. Villar, H. O.; Castro, E. A.; Rossi, R. A. *Z. Naturforsch.* **1984**, *39A*, 49.
257. Rossi, R. A.; Bunnett, J. F. *J. Am. Chem. Soc.* **1974**, *112*, 96.

258. Imamura, Y.; Mizuta, T.; Miyoshi, K. *Organometallics* **2005**, *24*, 990.
259. Mizuta, T.; Imamura, Y.; Miyoshi, K.; Yorimitsu, H.; Oshima, K. *Organometallics* **2005**, *24*, 990.
260. Devendra, J. V.; Frölich, R.; Oestreich, M. *Org. Lett.* **2011**, *13*, 2094.
261. Brunner, B.; Stogaitis, N.; Lautens, M. *Org. Lett.* **2006**, *8*, 3473.
262. Hudson, H. R.; Lee, R. J.; Matthews, R. W. Phosphorus, Sulfur and Silicon and the Related Elements **2004**, *179*, 1691.
263. Ishihara, K.; Miyata, M.; Hattori, K.; Tada, T.; Yamamoto, H. *J. Am. Chem. Soc.* **1994**, *116*, 10520.
264. Wuennemann, S.; Froehlich, R.; Hoppe, D. *Eur. J. Org. Chem.* **2008**, *4*, 684.
265. Seayad, A. M.; Ramalingam, B.; Chai, C. L. L.; Yoshinaga, K.; Nagata, T. *Org. Lett.* **2010**, *12*, 264.
266. Yadav, J. S.; Reddy, B. V. S.; Rao, M. Shesha; Reddy, P. N. *Tetrahedron Lett.* **2003**, *44*, 5275.

Curriculum Vitae

First Name Amata
Family Name Schira
Date of Birth 6th of June 1985
Citizenship Swiss - Italian

- 12.2008 - 02.2013 **Laboratory of Inorganic Chemistry, ETH Zürich, Switzerland.** Ph. D. Thesis under the supervision of Prof. Dr. Antonio Mezzetti. Title of the thesis: 'Enantioselective Imine Aziridination with Ru/PNNP Catalysts: a Breakthrough'. Examiner Prof. Dr. Antonio Mezzetti, co-examiner Prof. Dr. Christophe Copéret, co-examiner Prof. Dr. Antonio Togni. Laboratory teaching assistant for first semester chemistry students during two years. Supervision of one undergraduate student and of one master student.
- 10.2006 - 10/2008 **Università degli Studi di Milano, Italy.** Master degree under the supervision of Prof. Fabio Ragaini. Title of the thesis: 'Sintesi di nanoparticelle magnetiche per il recupero di catalizzatori'. Final mark 108/110.
- 10.2003 - 10.2006 **Università degli Studi di Milano, Italy.** Bachelor Degree under the supervision of Prof. Fabio Ragaini. Title of the thesis: 'Sintesi di leganti della classe ARBIAN aventi sostituenti diversi sugli atomi di azoto'. Final mark 110/110.
- 09.1998 – 06.2003 **Liceo Diocesano - Collegio Pio XII, Lugano, Switzerland.** Federal Matura type A (classic). Final Mark 88/90.

Scientific Publications

Egloff, J; Ranocchiari, M.; Schira, A.; Schotes, C.; Mezzetti, A. "Highly Enantioselective Ruthenium/PNNP-Catalyzed Imine Aziridination: Evidence of Carbene Transfer from a Diazoester Complex", *Organometallics*, **2013**, Accepted.

Conferences and Poster Presentation

IUPAC Symposium on Organometallic Chemistry Directed Towards Organic Synthesis (OMCOS 15), 2009, Glasgow, Scotland, '*Chiral Macrocyclic PNNP Ligands for Asymmetric Catalysis*' Marco Ranocchiari, Amata Schira, Antonio Mezzetti.

Swiss Chemical Society (SCS) Fall Meeting 2009, Lausanne, Switzerland, '*Chiral Macrocyclic PNNP Ligands for Asymmetric Catalysis*' Marco Ranocchiari, Amata Schira, Antonio Mezzetti.

Swiss Chemical Society (SCS) Fall Meeting 2010, Zürich, Switzerland, '*Chiral Macrocyclic PNNP Ligands*', Amata Schira, Antonio Mezzetti.

EuCheMS Conference on Organometallic Chemistry (EuCOMC XIX), 2011, Toulouse, France, '*Asymmetric Imine Aziridination with Ru/PNNP Complexes*', Amata Schira, Joël Egloff, Antonio Mezzetti.

Swiss Chemical Society (SCS) Fall Meeting 2011, Lausanne, Switzerland, '*Asymmetric Imine Aziridination with Ru/PNNP Complexes*', Amata Schira, Joël Egloff, Antonio Mezzetti.

International Conference: Catalysis in Organic Synthesis (ICCOS-2012), 2012, Moscow, Russia, '*Ru/PNNP Catalyzed Asymmetric Aziridination: Recent Progress*' Amata Schira, Joël Egloff, Antonio Mezzetti.

Swiss Chemical Society (SCS) Fall Meeting 2012, Zürich, Switzerland, '*Asymmetric Imine Aziridination with Ru/PNNP: Ligand Tuning*', Amata Schira, Joël Egloff, Antonio Mezzetti (oral presentation).